Regulation of Herpes Simplex Virus-1 Latent Infection and Reactivation by Facultative Heterochromatin and Neuronal Stress Signaling determined using a Novel Primary Neuronal Model

Sara Anna Dochnal
Chicago, IL

Bachelor of Science in Animal Sciences with a Concentration in Pre-veterinary Studies
University of Illinois, Urbana-Champaign, IL
2018

A Dissertation Presented to the Graduate Faculty of the University of Virginia in Candidacy for the Degree of Doctor of Philosophy

Department of Microbiology, Immunology, and Cancer Biology
University of Virginia School of Medicine
November 2023

Anna R. Cliffe, PhD (Advisor)
Lucy F. Pemberton, PhD (Committee Chair)
M. Mitchell Smith, PhD
Jeffrey S. Smith, PhD
Daniel A. Engel, PhD
Christopher D. Deppmann, PhD

Abstract

Herpes simplex virus-1 (HSV-1) establishes a latent infection in peripheral neurons, during which repressed lytic viral gene promoters associate with cellular heterochromatin. Periodically following stress, the viral genome can re-initiate lytic viral gene expression, reactivate, and cause serious clinical disease. The molecular events which mediate the repression and reactivation of lytic viral genes directly from the viral genome remain unresolved, and this study is complicated by heterogeneous ability of an individual neuron to undergo latency or reactivation. We developed a new model in primary neurons to preserve the heterogenous nature of these processes, which we use to explore how 1) neuronal stress signaling and 2) Polycomb silencing contribute to HSV-1 latency establishment, latency maintenance, and reactivation.

Neuronal stress kinases dual leucine zipper kinase (DLK) and c-Jun N-terminal kinase (JNK) mediate initial viral gene expression during reactivation. However, how downstream host factors work with JNK to stimulate reactivation remains unclear. We find that c-Jun, the primary target downstream of physiological neuronal DLK/JNK signaling, functions on the viral genome during reactivation to permit the transition to full HSV-1 reactivation initiated by multiple stressors. We also find that this stress signaling pathway critical for reactivation becomes activated upon *de novo* neuronal infection and promotes the formation of more reactivation-competent genomes.

We further discover a predominant role for Polycomb repressor complex 1 (PRC1) and its associated histone modification, the mono-ubiquitination of histone H2A (H2AK119ub), for silencing a population of HSV-1 genomes in a manner that is amenable to later reactivation. Our data also suggest that a viral long noncoding RNA

may mediate PRC1 recruitment to the HSV-1 genome. We altogether propose that events during initial HSV-1 infection and acquisition modify the type of latency HSV-1 establishes at the level of the viral genome, characterized by how amenable to reactivation it may be. Our work provides compelling evidence for the heterogenous nature of HSV-1 latent infection and reactivation and introduces new methods to study these processes at a higher biological resolution to create more targeted, accurate therapeutic interventions.

Dedication

It has been a privilege to take this scientific journey and to continue a path where I am able to learn and discover each day. However, the completion of this dissertation has not been an easy feat and would not have been possible to achieve without the overwhelming support of my mentors, colleagues, friends, and family.

First, I would like to thank Dr. David Miller, Rebecca Winters, Dr. Momal Sharif, and Dr. Ryan Dilger, who warmly welcomed me into the world of scientific research during my undergraduate studies. They are exceptional people and accessible mentors who took very active roles to incorporate me into their scientific community and to prepare me technically and intellectually to pursue my PhD.

Next, I am grateful for my advisor and mentor Dr. Anna Cliffe, who invested a great deal of time in my growth into a confident person and an independent scientist. Anna has fostered my enthusiasm for science and has encouraged me to move outside of my intellectual and technical comfort zone throughout my entire PhD. I am thankful for the opportunities for professional growth Anna has granted me, as she has supported me to pursue and publish multiple projects, author reviews, and present at (inter)national conferences. Anna opened and encouraged every avenue to becoming a productive research scientist, and she has connected me to some of my other favorite scientific mentors, including Dr. Ben Gewurz and Dr. David Knipe.

In addition to Anna, I am thankful for my committee members: Dr. Lucy Pemberton, Dr. Jeffrey Smith, Dr. Mitchell Smith, Dr. Christopher Deppmann, and Dr. Daniel Engel. They have provided constant, direct, and reliable scientific feedback and support, as well as professional guidance outside of formal committee meetings. Many other

students, fellows, and faculty in the MIC department, including Dr. Lou Hammarskjöld, Dr. David Rekosh, Dr. David Kashatus, Dr. Alison Criss, and Dr. Drew Dudley, have similarly done so.

I thank my fellow past and present lab members, who have been reliable and scientifically engaging peers, including Sean, Alison, Patryk, Abigail, Matt, and Matthew, among others. With you all, I have shared many hypotheses, hours, disappointments, achievements, tears, and laughs. Past members Austin and Jon introduced me to the technical and conceptual fundamentals of the lab and inspired me with their work ethic and organization.

This endeavor also could not have been completed without the encouragement of my friends including Daniel, Jasleena, Monica, Zoe, Nicole (and new baby Jack), Tyler, Sima, Herman, Sean, Jeb, Sarah, Patryk, Caroline, and others, some of whom have been cheering me on for over a decade now.

Finally, I am filed with gratitude towards my family. I thank my parents Agata and Krzysztof, who worked extremely hard to give me the opportunity to pursue an education in the USA. My mother has also been my number one fan throughout my entire academic journey and life. I thank my sister Michelle, who makes me laugh and inspires me with her mental strength; my niece Penny and nephew Gage, who bring me so much joy and the desire to be creative; as well as my Dziadziuś, who emphasized the value of a formal education. I am grateful for my in-laws, Debbie, Jeff, and Emily, who remind me that joy is very important in anything you do and who have helped me navigate my next professional steps. I thank my husband and best friend, Brian, for intellectually challenging and emotionally supporting me. Thank you for listening to and

engaging in my crazy scientific theories that were so great in length and number, and for loving me and our little family (including Redford the dog and Cleopatra the cat) so well.

Finally, I write this dissertation in loving memory of my Baba, to whom I am indebted. Baba raised me into who I am and set forward the example of who I aspire to be, and she instilled in me a love of learning that I hope is reflected in the pages of this dissertation.

Table of Contents

Chapter 1: Introduction to Herpes Simplex Virus Infection

Parts of this chapter have been adapted from:

Dochnal, SA, Francois, AK, & Cliffe, AR. De Novo Polycomb Recruitment: Lessons from Latent Herpesviruses. *Viruses*, 27;13(8):1470 doi: 10.3390/v13081470. (2021)

Herpes Simplex Virus-1 (HSV):

Viral infection is often acute in nature, resulting in the eventual clearance of the virus, although long term sequalae attributed to inflammatory tissue damage may remain. Herpesviruses are large, double-stranded DNA viruses characterized by their insidious ability to establish a lifelong latent infection, from which they can periodically reactivate to cause disease and transmit infectious virus to new hosts. Human Herpesviruses are categorized into three groups by genetic composition, and each fashions a unique cellular tropism with which the virus can establish a latent infection; the gamma herpesviruses persist primarily in lymphocytes (and additionally epithelial, endothelial, and natural killer cells) (1-4), the beta herpesviruses within hematopoietic lineage cells (5-7), and the alpha herpesviruses can establish a latent infection within neurons of the peripheral nervous system (PNS) (8).

Herpes simplex virus-1 (HSV-1) is the most prevalent human alpha herpesvirus, present in over 60% of the global population aged 0-49 according to the latest World Health Organization (WHO) estimates (9). HSV-1 can be found in one of three modes of infection, with the potential for the virus to transition from one another (10): lytic replication, latent infection, or reactivation. Following lytic infection on the body's surface, HSV-1 can infect innervating peripheral ganglia. HSV-1 lytic replication occurs within a broad range of host cells (including neurons) (11-13), but latent infection and reactivation from latent infection are restricted to peripheral neurons, frequently within sensory or autonomic ganglia (14-17). HSV-1 is associated with a wide range of pathologies.

Clinical Significance

HSV-1 is acquired by most through sexual contact and can also transmit in a vertical fashion from mother to newborn during vaginal delivery (18). A majority of infected persons present as asymptomatic (19) but nonetheless contribute significantly to viral shedding and transmission to new hosts (20-22). When symptoms manifest clinically, HSV-1 is most often associated with recurrent, painful lesions on oral or genital mucosa (23). Importantly, HSV-1 is also the causative agent of ocular keratitis, the leading cause of blindness in the developed world (23-25).

The neurotropism of HSV-1 also lends itself to a spectrum of neuronal disease. HSV-1 can cause post-herpetic neuralgia, where painful sensations persist and transmit through the PNS despite the resolution of acute infection and associated clinical symptoms. This finding is supported by clinical case reports (26-28), as well as experimental data gathered from mouse models (29-33). The link between HSV-1 infection and neuropathic pain may in part be attributed to chronic inflammation in response to HSV-1 within sites of latency (34), as this response has been linked with neuronal hyper-excitability and sensitivity to non-painful stimuli. Ironically, the attenuated HSV-1 backbone is commonly used as a genetic vector for neuropathic pain due its ability to penetrate neurons. From the attenuated HSV-1 backbone, exogenous expression of proteins which modify neuronal current generation and hyper-excitability can be manipulated for therapy (35).

Following reactivation from latently infected peripheral ganglia, new infectious virus can traffic anterograde through peripheral axons to the central nervous system (CNS) (36). It is also possible for HSV-1 infection to proceed directly into the CNS through the olfactory route or rarely through the umbilical vein from mother to fetus (37). HSV-1 infection in the CNS can then propagate throughout the frontal cortex, hippocampus, and cerebellum. Active replication of HSV-1 in the brain, termed herpetic simplex encephalitis /HSE, results in the death of neurons and support cells (38). This acute infection also leads to immune cell recruitment and inflammatory cytokine release, and therefore pervasive inflammation elicits further degeneration (39). Despite receiving antiviral treatment at the time of active replication, encephalitic patients demonstrate neuronal sequalae which can persist for years (40, 41).

Notably, there is accumulating epidemiological and experimental evidence linking HSV-1 infection with the development of late-onset dementia and Alzheimer's disease (AD) (42-47). The presence of the APOE-E4 allele variant alone confers a high risk of developing AD, but the addition of HSV-1 infection to this APOE-E4 allele phenotype further exacerbates risk (48, 49). It has also been demonstrated in mouse models that HSV-1 infection and recurrent *in vivo* reactivation leads to the accumulation of AD hallmarks, including Aβ42 oligomers, amyloid-B protein, tau hyperphosphorylation, and neuroinflammation markers (50-53).

An extensive summary of human epidemiological data also linking HSV-1 infection and chronic psychiatric illness was recently published (54). Conditions

mediated through the CNS such as depression, suicidal behavior, and schizophrenia are proposed to accelerate due to chronic neuroinflammation in response to recurrent HSV-1 reactivation events. In one clinical study, the treatment of schizophrenic and HSV-1 seropositive patients with antiviral valacyclovir demonstrated improvements in several cognitive parameters (55).

There is no vaccine nor cure for HSV-1, nor any human herpesvirus apart from varicella zoster virus (VZV). The primary antiviral agents for HSV-1 are nucleoside derivatives (which can easily be identified through the suffix “clovir”) that interfere with lytic infection by perturbing viral DNA replication (recently reviewed in (56)). However, 1) these agents can exhibit extensive renal toxicity (57-59) and long-term use has been associated with neurotoxicity *in vitro* (60), 2) antiviral resistance to these therapies is building (61, 62), and 3) nucleoside derivatives only target the lytic phase of infection. Therefore, elucidating the molecular mechanisms behind how a latent infection is established and reactivation is initiated in a neuron is integral to identifying new therapeutic targets to relieve clinical burden.

Lytic Replication:

Host Cell Entry

At the nanometer resolution, an HSV-1 virion consists of a double enveloped particle coated with viral glycoproteins which facilitate host cell entry and infection. These particles contain an epigenetically naïve 152 kB dsDNA genome compacted into an icosahedral capsid surrounded by viral tegument proteins (63).

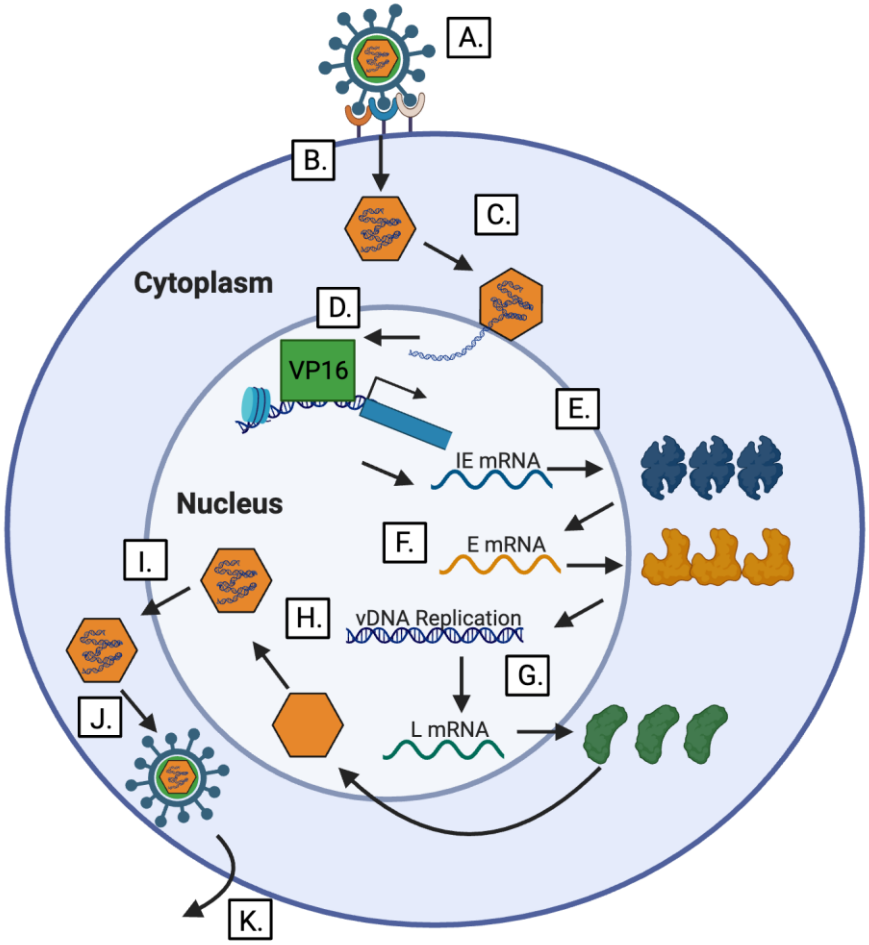

Figure 1. HSV Lytic Replication: A) Viral glycoproteins bind one of three host cell entry receptors, leading to B) the fusion of the viral envelope and host membrane. Viral tegument proteins (green in virion) and the viral capsid containing the viral DNA genome are released into the cytoplasm. C) The viral capsid is trafficked to the nucleus, into which epigenetically naïve viral DNA (vDNA) is released. D) Viral DNA is assembled into transcriptionally permissive chromatin, from which viral tegument protein VP16 initiates transcription of IE (immediate early) mRNA. E) In the cytoplasm, IE mRNA is translated into IE proteins (blue), which traffic to the nucleus to mediate transcription of E (early) mRNA. F) E mRNA is translated into E proteins (orange), which facilitate vDNA replication and L (late) gene transcription in the nucleus. G) In response to vDNA replication, L mRNA is translated into L proteins in the cytoplasm, which traffic to the nucleus to assemble the viral capsid. H) vDNA is packaged into the viral capsid. I) The viral capsid egresses from the nucleus. J) The viral capsid is re-enveloped in the cytoplasm by membrane containing viral glycoproteins. K) The new infectious virus particle is released from the host cell.

HSV-1 transmission to a new host begins with an acute, lytic replicating infection at the body's surface, littered with epithelial cells and other susceptible host cells,

carrying at least one of three entry receptors: nectin-1, herpes virus entry meditator (HVEM), or 3-O-sulfated-heparan sulfate (3-OS-HS) (Fig 1A). Depending on the cell, HSV-1 can enter through fusion, endocytosis, or both processes as recently reviewed (64). An abundance of viral glycoproteins coats the double-membrane envelope of an HSV-1 virion, but only four are essential to viral entry (64-66): glycoprotein D (gD) binds one of three cellular entry receptors, triggering a conformational change and binding to a heterodimer composed of gH and gL, which in turn activates fusogen gB to merge the HSV-1 lipid envelope and facilitate entry of the viral capsid into the cytoplasm (Fig 1B). The 11 additional glycoproteins have been proposed to play roles in mediating alternative routes of host cell entry, but this is superficially understood in the case of HSV-1. Following host cell entry, HSV-1 tegument proteins (UL36, UL137) co-opt host motor proteins kinesin and dynein to enable movement along cellular microtubules (67, 68). The viral capsid is translocated via these microtubules to the host's nuclear pore complex (NPC), through which HSV-1 will inject its genomic material into the nucleus using a combination of viral and host factors (69-74) (Fig 1C).

Transcriptional Initiation

When Herpesvirus genomes first enter the nucleus, they are not associated with cellular histone proteins and are therefore epigenetically naïve (75-80). However, the HSV-1 genome rapidly becomes chromatinized by an undefined chromatin structure composed of unstable nucleosomes as well as cellular histones with transcriptionally permissive modifications (81-85). Apart from one human herpesvirus (86), the viral genomes persist as extrachromosomal episomes, remaining unintegrated from the host

cell's own genomic material. HSV-1 lytic genes are classified into three sets: immediate early (IE) genes, early (E) genes, and late (L) genes, and viral gene expression during a new lytic infection occurs in an ordered cascade (63). Gene expression is initiated from the viral genome by viral transactivator and tegument protein VP16 (Fig 1D), which forms a complex with cellular factors involved in transcriptional activation, including general transcription factors, ATP-dependent chromatin remodelers, and histone-modifying enzymes to promote expression of immediate early (IE) genes (87). Synthesis of the IE proteins is required for early (E) mRNA transcription (Fig 1E), and early viral proteins enable viral DNA (vDNA) replication, which is carried out in replication compartments (Fig 1F). vDNA replication is a prerequisite for true-late (TL) mRNA transcription, likely due to a shift in genome accessibility which enables the increased binding of host transcriptional machinery including the preinitiation complex (88). The L genes largely encode structural viral proteins involved in capsid assembly and egress, as well as the eventual budding and binding of new infectious virus to surrounding host cells.

De Novo Virus Exit

Individual viral capsid proteins, while produced in the cytoplasm, are translocated into the nucleus where they assemble with newly replicated virus into a herpesvirus capsid (89) (Fig 1G-H). Subsequently, viral capsids egress from the nucleus through envelopment and de-envelopment at the inner and outer nuclear membranes respectively, a process mediated by viral proteins UL31 and UL34 (together known as the nuclear export complex) (90, 91) (Fig 1I). Following exit into the cytoplasm, the viral

capsid associates with viral tegument proteins, some of which mediate the cytoplasmic trafficking of the capsid via microtubules. Viral glycoproteins are processed through the endoplasmic reticulum and unite with capsids in endosomal particles, which are subsequently trafficked to the cell surface through host microtubules (89) (Fig 1J). Like other herpesviruses, HSV-1 co-opts the host endosomal sorting complex (ESCRT) for release of enveloped virions (92) (Fig 1K).

Modeling HSV-1 Latent Infection and Reactivation:

Before discussing the molecular mechanisms behind HSV-1 latency and reactivation, a summary of current model systems is required due to their extensiveness, synergy, advantages, and caveats. Given the post-mitotic nature of the neuron, *in vitro* and *in vivo* modeling is carried out largely using non-human animal hosts. Other alpha herpesviruses, like VZV, which display a strict human tropism, are likely for this reason under-studied.

The study of HSV-1 *in vivo* is broad, where animal species (rabbit, guinea pig, rat, mouse), inoculation route (corneal, footpad, flank), virus strain and related pathogenicity, and method as well as potency of reactivation (where applicable) vary significantly (93). The most common animal model is the mouse, where latency can be established in both the sensory and autonomic ganglia following inoculation and a period of acute, lytic replication at the body's surface and ganglia. In the mouse, reactivation can be triggered from latently infected ganglia by hormone modulation (94, 95), hyperthermia (96), and UV irradiation (97). Animal models provide a more robust

reactivation output using an *ex vivo* method of reactivation, wherein latently infected ganglia are removed and stimulated to reactivate by axotomy alone or in combination with anti-NGF antibody or PI3 Kinase inhibition (98-101).

In Vitro Models

In vivo models most accurately recapitulate the processes of HSV-1 latency establishment and reactivation during a natural infection. However, the use of *in vitro* models is also required in complement. *In vitro* models provide a robust latent reservoir and reactivation output, and they can be easily manipulated for functional studies using small molecule inhibitors or RNA-mediated depletions. *In vitro* systems also enable the contribution of individual host (immune) or viral factors on HSV-1 infection to be interrogated.

An *in vitro* system that employs primary human peripheral neurons has been established using post-mortem material from human donors (102). However, access to these samples is irregular, and these neurons may already be naturally infected with other alpha herpesviruses. Therefore, the mouse and the rat serve as the primary species of study *in vitro*. Primary neurons from peripheral ganglia, including dorsal root ganglia (DRG), trigeminal ganglia (TG), and superior cervical ganglia (SCG) from fetal, neonatal, or adult mice or rats are dissected and cultured using anti-mitotic agents (aphidicolin/APH or fluorodeoxyuridine/FUdR) to eliminate non-neuronal cells (99, 103-106). Following the establishment of a latent infection, reactivation can be elicited through the activation of several signaling pathways, including the loss of neurotrophic

factor support (99, 103, 106-108), enhanced neuronal hyper-excitability (109-111), perturbation of the DNA damage response (112), and heat stress (113).

Recently, several groups have attempted to establish a cultured human neuronal model for HSV-1 latency and reactivation. Several *in vitro* models of human origin have been developed from embryonic cells that can be differentiated into human neurons and latently infected, including neural stem cell (NSC) rosettes (114), HD10.6 cells (115), and Lund human mesencephalic (LUHMES) (116). These systems carry species-specificity, as well as the ability to provide substantial cellular material for experimental assays as the cells can be propagated prior to differentiation. However, these models also come with disadvantages.

Reactivation in LUHMES has been reported by one group using nonspecific PI3K inhibitor wortmannin, but multiple other groups (including our own) have reported immense difficulty in achieving reactivation (116). Further, the group that reports achieving reactivation in LUHMES also documented detectable infectious virus in culture prior to reactivation, drawing into question if latency is truly established in this system or if the “reactivation” readout is cell-to-cell spread of infectious virus from lytically infected neurons. Reactivation has also not been achieved in HD10.6 cells without superinfection with live or UV-inactivated virus (115). These cells are also derived from fetal tissue, which is problematic as HSV-1 does not infect fetal neurons and most infections are acquired during early adulthood, where the transcriptional and epigenetic nature of the cell is markedly different as discussed later. Further,

proliferation prior to differentiation is regulated by a v-myc transgene, and therefore a low level of Myc expression persists even following differentiation. Lastly, the clonal nature of these passaged cells cannot accurately recapitulate the heterogeneity demonstrated in mature, *in vivo* differentiated neurons within individual ganglia which may contribute to the heterogeneity witnessed during latent infection and reactivation as described in later paragraphs.

Upon initial HSV-1 infection of neurons, only a subpopulation of infected neurons enters a latent state, whereas other neurons become lytic infected; this phenomenon is also observed in animal models. In the absence of the immune system, lytic infected neurons transmit new infectious virus, superinfect the culture, and eliminate the possibility of establishing a latent infection (117). Therefore, *in vitro* cultures (both murine and human) are often quiescently infected with HSV-1 in the presence of viral DNA replication inhibitors, primarily acyclovir (ACV) and less frequently phosphonoacteic acid (PAA), to interfere with viral DNA replication and new virus production and ultimately promote the establishment of a latent infection *in vitro*. However, in the presence of ACV, the process of viral DNA replication and subsequent late gene expression cannot be studied in lytic neurons during latency establishment (117). Moreover, the fate of any genomes that incorporate ACV is unknown, and there is some neurotoxicity associated with its use (60). There are groups that have periodically promoted HSV-1 latent infection and suppressed lytic infection *in vitro* in the absence of ACV or PAA by using a low multiplicity of infection (MOI)/inoculating amount of infectious virus (making reactivation difficult to achieve) (118) or immune system

components such as interferon (introducing host immune components which may muddle the biology of the virus) (99). In addition, even in systems where ACV is used, there can be low levels of spontaneous reactivation after removal of ACV from cultures, and initial molecular reactivation events cannot be discerned from downstream cell-to-cell spread.

HSV-1 Latent Infection:

HSV-1 latent infection in neurons is defined by the persistence of viral DNA in the absence of detectable infectious virus with the ability to reactivate following a stimulus. Latency resembles a state of viral dormancy as lytic gene transcription and viral DNA replication are largely repressed, although there is a low level of promiscuous lytic expression associated with a latent infection (8). During latency, there is also a collection of long noncoding RNAs, collectively known as the latency-associated transcripts (LATs), that are pervasively transcribed. During a latent infection, repressed lytic genes are bound by multiple forms of cellular heterochromatin (119). Constitutive chromatin characterized by the di/tri-methylation of lysine 9 on histone H3, or H3K9me2/3, displays enrichment on the latent HSV-1 viral genome (120). The enrichment of another common constitutive mark, H4K20me3, was investigated but not found to be significantly enriched on the viral genome when compared to host heterochromatin (121). Facultative heterochromatin (fHC), which is also known as Polycomb silencing, is also enriched on repressed lytic gene promoters during HSV-1 latent infection (121-124). Polycomb silencing is a form of heterochromatin defined by its ability to convert to active euchromatin. Therefore, it is unsurprising that latent

herpesvirus genomes that are capable of reactivation associate with this reversible form of heterochromatin.

Polycomb Silencing:

Polycomb silencing is deposited by two major protein-complexes: the polycomb repressive complex 1 (PRC1) and PRC2. PRC1 can deposit H2A lysine 119 monoubiquitination (H2AK119ub1) and PRC2 can deposit H3 lysine 27 methylation (H3K27me). The study of mammalian Polycomb repression comes with many intricacies as the composition of Polycomb silencing can vary on different regions of DNA and in different cell types (125-127), which can modify the mechanisms of PRC1/2 recruitment (128) and mechanisms to maintain transcriptional repression (129, 130).

Polycomb Repressor Complex 2

PRC2, which can deposit the mono-, di-, or tri-methylation of histone H3 lysine 27 (H3K27me1, H3K27me2, H3K27me3) (131-133), is composed of three core components: enhancer of Zeste 1 or 2 (EZH1/2), suppressor of Zeste 12 (SUZ12), and embryonic ectoderm development (EED) (Fig 1.2). EZH1/2 is catalytically active, but the full trimeric core is required for *in vitro* H3K27 methylation activity (133-135). PRC2 core proteins also include retinoblastoma associated proteins 46 and 48 (RbAp46/48; also known as RBBP4/7). The formation and function of K27 methylation has been most extensively studied in mouse embryonic stem cells (mESCs) and human induced pluripotent stem cells (iPSCs). In these systems, H3K27me2 exists across 50-70% of total histone H3, predominately at intergenic regions (136). H3K27me1 and H3K27me3

are each found on approximately 10-15% of total H3 (137, 138). H3K27me3 is found centered around CpG islands of transcriptionally silent genes, and is the only methylation state to which PRC2 stably binds (136). Therefore, these CpG islands can act as nucleation sites for facultative heterochromatin formation and propagation (136).

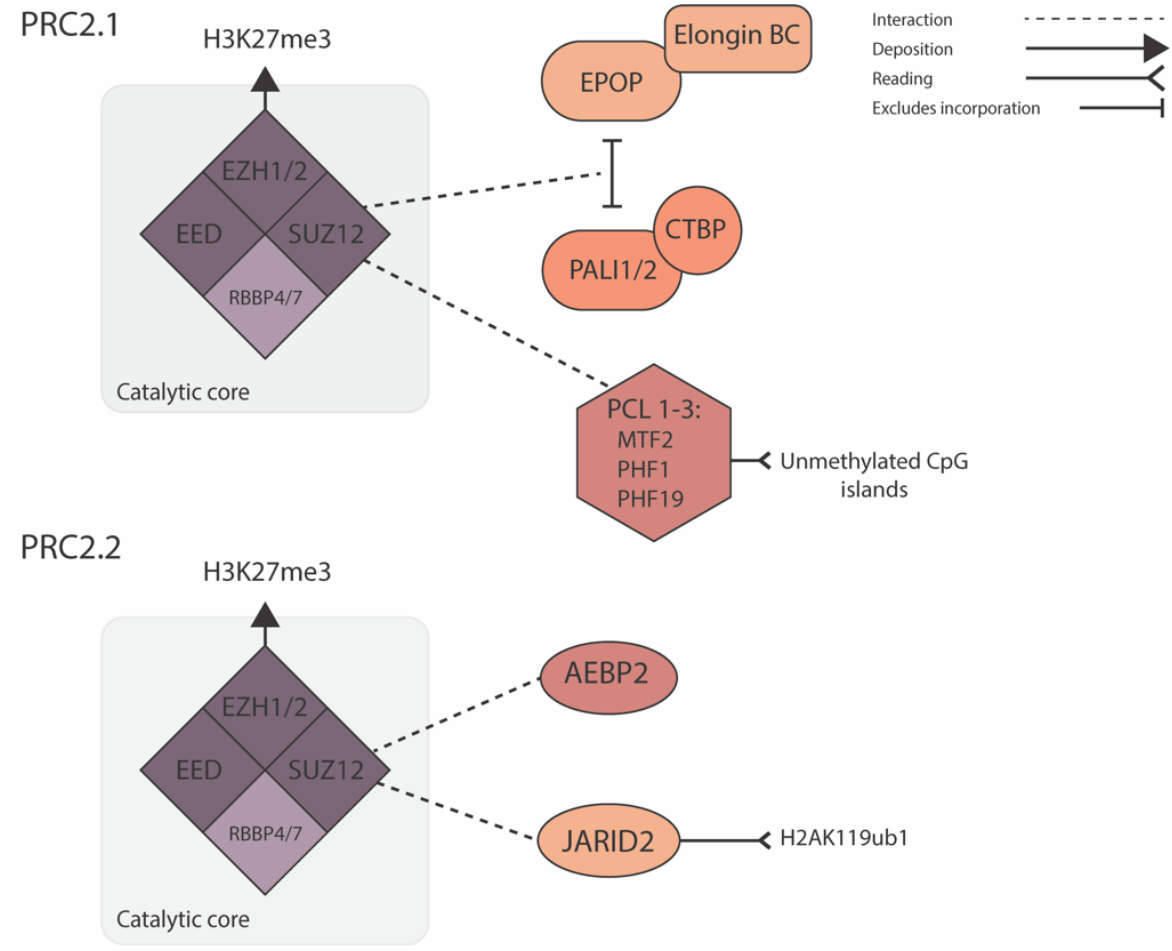

Figure 1.2 The Composition of PRC2.1 and PRC2.2 Complexes: Polycomb repressive complex 2 (PRC2) has a catalytic core of EED, EZH1/2 and SUZ12 along with RBBP4/7. PRC2 carries out all three methylation states of H3K27, but H3K27me3 is the only one stably bound by the complex. To form the PRC2.1 complex, the core can interact with either PALI1/2 and CTBP or EPOP and Elongin BC. One pair excludes the other from joining the complex. SUZ12 in PRC2.1 also interacts with one of three PCL proteins, but this interaction does not compete for the interacting pairs. PCL proteins enable binding to unmethylated CpG islands. PRC2.2 forms by SUZ12 in the same catalytic core interacting with JARID2 and AEBP2. Unlike PRC2.1, JARID2 enables PRC2.2 recruitment to sites of H2AK119ub1. Figure was executed by Alison Francois.

PRC2 also associates with a variety of accessory proteins, resulting in two distinct complex variants: PRC2.1 and PRC2.2 (139) (Fig 1.2). The PRC2.1 complex includes one of three Polycomb-like (PCL) proteins (PCL1/2/3), also known as PHF1, MTF2 and PHF19 respectively, which enable PRC2.1 binding to unmethylated CpG islands (139). PRC2.1 also contains Elongin BC and Polycomb repressive complex 2-associated protein (EPOP) or PRC2-associated LCOR isoform 1 (PALI1/2) (140-143). PRC2.2 instead contains Jumonji and AT-rich interaction domain 2 (JARID2), and adipocyte enhancer-binding protein 2 (AEBP2) which together recruit PRC2.2 to the H2AK119ub1 modification and permit the PRC2 methyltransferase activity to overcome the repressive effects of active histone modifications H3K4me3 and H3K36me3 (144-147). Therefore, the differential activities of PHF1/PHF19/MTF2 and JARID2 contribute to PRC2.1 and 2.2 recruitment to different regions of chromatin. PRC2 occupancy is also significantly higher for PRC2.1 target regions than PRC2.2 bound regions, at least in human iPSCs (148). However, ultimately the inhibition of both PRC2.1 and PRC2.2 is required for full inhibition of PRC2 activity in pluripotent cells (149).

PRC2 recruitment and function can change upon differentiation and in distinct differentiated cell types. For example, PRC2.2 appears important for *de novo* silencing during differentiation whereas MTF2-containing PRC2.1 is required to maintain high amounts of H3K27me3 at already repressed CpG dense promoters (126). Further, as cells become more differentiated, they reduce EZH2 expression and enhance levels of EZH1 (150, 151), which is believed to be predominant in the maintenance of H3K27me3 in terminally differentiated cells (146). Studies in mESCs indicate that EZH1/2 use

different mechanisms to repress chromatin, with EZH2 largely catalyzing H3K27me2/3 and EZH1 contributing to chromatin compaction (150). Further, PRC2-EZH2 but not EZH1 displays allosteric activation by H3K27me3 and PRC2-EZH1 activity is inhibited by free DNA whereas PRC2-EZH2 is unaffected by non-nucleosomal DNA (150). This may explain why PRC2-EZH2 is the major methyltransferase in ES cells as the chromatin structure is more open and higher levels of H3K27me3 favor allosteric activation. In contrast, the more compact chromatin structure in differentiated cells would result in less inhibition of EZH1.

Forms of Polycomb-associated proteins may also change with differentiation. For example, full length JARID2 is down-regulated with differentiation and replaced by a cleaved protein lacking the PRC2-interacting domain (DelN-JARID2), at least in differentiated keratinocytes. This shorter form of JARID2 negatively regulates PRC2 function and may release PRC2-mediated repression of differentiation genes (152). Even post-differentiation, as cells undergo maturation, the expression patterns of Polycomb group proteins change. Neurons, for example, undergo an intense maturation from the postnatal to adult period, during which time EZH2 and EED are down-regulated, and EZH1 levels remain unchanged (153).

Polycomb Repressor Complex 1

The composition of PRC1 complexes can be categorized into canonical (cPRC1) and non-canonical/variant (vPRC1) (129, 130) (Fig 1.3). The PRC1 core contains dimerized RING1A or B, which interact with one of six possible PCGF proteins (PCGF1-

6). cPRC1 complexes contain either PCGF2/MEL18 or PCGF4/BMI1 together with one of five chromobox (CBX2, 4, 6, 7 and 8) proteins (154). The CBX subunit of cPRC1 directly binds H3K27me3 for recruitment to chromatin; therefore, the activity of cPRC1 is dependent on PRC2 (155-157). vPRC1 complexes can contain any of the six PCGF proteins but lack CBX proteins and instead contain RYBP or YAF2 (128, 154, 158). Therefore, vPRC1 complexes cannot bind H3K27me3 and are recruited to chromatin independently of PRC2 (128, 159). Recruitment of vPRC1 can occur through direct DNA binding activities, for example KDM2B-containing vPRC1 directs the complex to non-methylated CpG islands (160). vPRC1 can also interact with and facilitate recruitment through sequence-specific DNA binding proteins such as E2F6, REST and RUNX1 (Fig 1.3) or RNA (Fig 1.5) (161).

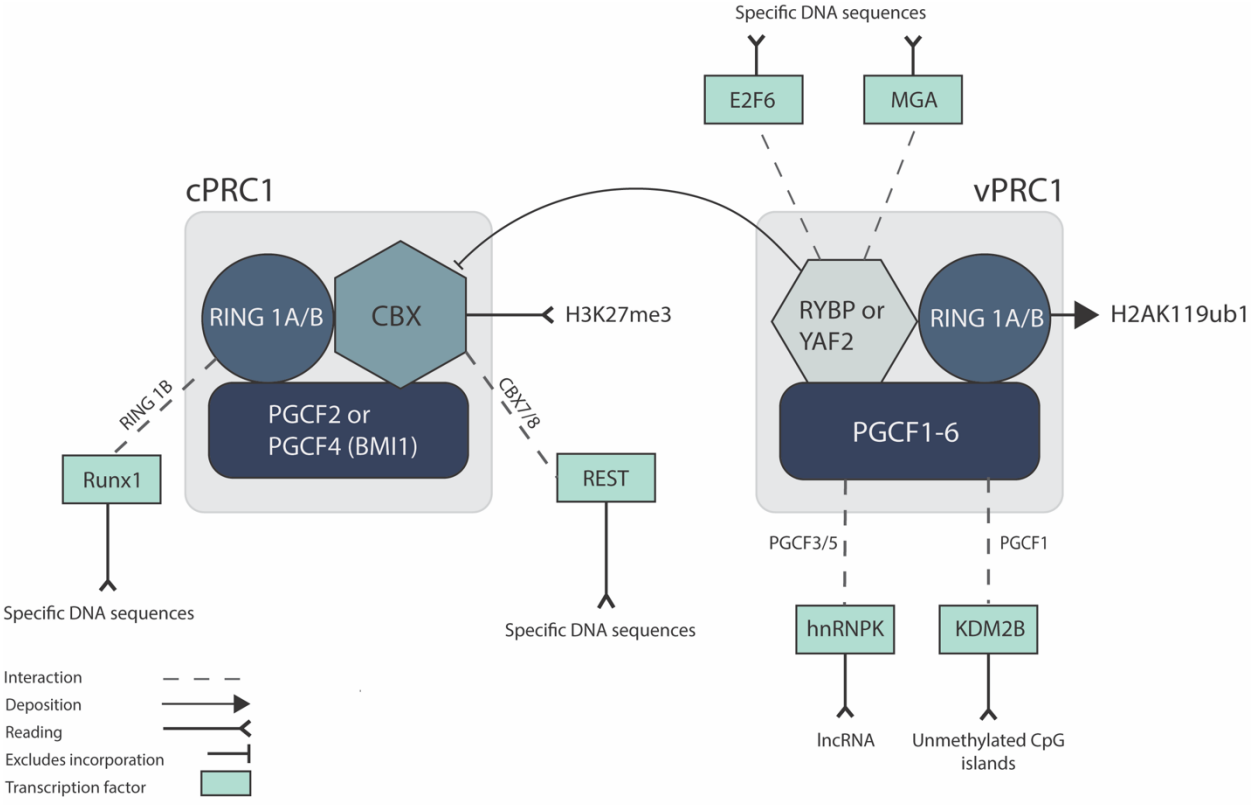

Figure 1.3 The Components of Canonical and Variant PRC1 Complexes: Canonical PRC1 (cPRC1) consists of either PGCF2 or PGCF4, along with RING1A/B and one of five chromobox (CBX) proteins. Although catalytically active, cPRC1 is thought not to contribute to the majority of H2AK119ub1. Chromobox proteins CBX2, 4, 6, 7 and 8 directly bind to H3K27me3, so cPRC1 recruitment to chromatin is dependent on PRC2 H3K27 methylation. Variant PRC1 (vPRC1) contains any of the six PGCF proteins, RING1A/B, and RYBP or YAF2. RYBP/YAF2 exclude CBX proteins from incorporating into the complex, and do not bind H3K27me3. vPRC1 recruitment is thus independent of PRC2 activity. RYBP stimulates RING1A/B activity, and vPRC1 writes most H2AK119ub1. Transcription factors RUNX1 and REST can interact with cPRC1 via RING1B and CBX7/8 respectively, recruiting the complex to specific target sequences of DNA. E2F6 and MGA can similarly recruit vPRC1 to specific DNA sequences by interaction with RYBP/YAF2, while hnRNPK can do so through interaction with PGCF3/5. KDM2B can recruit vPRC1 to unmethylated CpG islands. Figure was executed by Alison Francois.

The variability in composition of PRC1 complexes is reflective of their differential mechanisms of impacting gene expression and mechanisms of recruitment. Although all complexes contain the RING1/2 catalytic subunit, vPRC1 is predominantly responsible for mediating H2AK119ub1, likely because RYBP stimulates PRC1 E3

ubiquitin ligase activity (128, 157, 159, 162). There is evidence, at least in embryonic stem cells, that H2AK119ub1 is required for PRC2 recruitment and subsequent binding of both vPRC1 and cPRC1 (163, 164). These studies also revealed a direct role for H2AK119ub1 in repression of gene expression, and there is evidence for H2AK119ub1 inhibiting RNA polymerase elongation (165, 166), possibly through preventing the eviction of H2A/H2B dimers (167).

While vPRC1 is responsible for the majority of H2AK119ub1, cPRC1 appears to repress gene expression through chromatin compaction and long-range chromosomal interactions (168). For regions of chromatin that are bound by either vPRC1 or cPRC1 in ES cells, those bound by cPRC1 exhibit increased transcriptional repression compared to those bound by vPRC1 (169). cPRC1 compaction is driven by the CBX proteins like CBX2, 6, and 8, which contain a highly basic region that can drive chromatin compaction *in vitro* (130). Thus CBX2, 6, and 8-containing cPRC1 likely prevents gene expression by limiting access to transcriptional machinery. CBX7, which is the most abundant CBX in ES cells, lacks this basic domain and instead may function in transcriptional repression via mediating long-range chromosomal interactions (130, 169, 170). CBX2 also contains an intrinsically disordered region, which drives the formation of nuclear condensates known as Polycomb group bodies by phase separation (171). Therefore, differential expression of CBX paralogs in different cell types can lead to different degrees of compaction and gene silencing.

In mESCs, enzymatic activity of RING1A/1B is required for H2AK119ub1 and the majority of H3K27me3, indicating that at least in stem cells vPRC1-mediated Polycomb

repression is the predominant pathway (163, 164). Inhibition of this pathway also results in decreased association of cPRC1 at target genes usually bound by both vPRC1 and cPRC1 (163, 164). However, in these studies small subsets of genes were found to be associated with H3K27me3 and cPRC1 via PRC2.1-mediated H3K27me3 deposition. There is evidence for a pathway of vPRC1-PRC2.2-mediated fHC formation during early development of neural progenitor cells (NPCs), where the RING1A/B E3 ligase activity was found to be essential for repression of genes initially silenced during early neuronal development, but PRC1-mediated repression switched over to Ub-independence as stable silencing was maintained (172). These findings highlight the importance of considering cell type and differentiation state when exploring mechanisms of Polycomb repression.

Polycomb Silencing of Latent Herpesvirus Genomes:

The association of Polycomb proteins and histone modifications with latent viral genomes has been demonstrated in each family of human herpesviruses. The evidence linking the association of fHC with herpesvirus latency consists of mechanistic studies investigating the role of K27me histone readers, writers, and erasers in regulating viral gene expression during latency and reactivation.

Human Gamma Herpesviruses

For the Gamma herpesvirus Kaposi's sarcoma-associated herpesvirus (KSHV), the enrichment of H3K27me3 on silenced lytic promoters has been demonstrated in primary effusion lymphoma (PEL)-derived lines and latent SLK cells, and following *in*

vitro infection of endothelial cells and human PBMCs (173) (174-177) and closely mirrors that of the KSHV genome from Kaposi Sarcoma clinical isolates (178). PRC2 components EZH2 and SUZ12 are detectable on lytic promoters marked by H3K27me3 (175, 176), and inhibition or knockdown of EZH2 enhances viral gene expression in PEL-derived lines or following *de novo* infection of SLK cells (175, 176). H3K27me3 is lost upon reactivation and over-expression of H3K27 demethylase JMJD3 increases viral gene expression and incidence of reactivation from *in vitro* models of latency in B-cells and SLK cells (174, 175). Together, data from these studies indicate a functional role for H3K27me3 in maintaining KSHV lytic gene silencing during latency.

KSHV is also the best characterized of the herpesviruses in terms of the presence of PRC1 on the latent genome. Multiple studies have detected H2AK119ub1 on lytic promoters, with data indicating that it is deposited prior to K27 methylation in SLK cells (176). Core PRC1 component RING1B is also present at lytic promoters enriched for H2AK119ub1 in addition to vPRC1-associated proteins KDM2B and RYBP (176, 179, 180). Intriguingly, a recent study found that knockdown or inhibition of the PRC1 component PCGF4/Bmi1 in B cells resulted in loss of H2AK119ub1 from the *Rta* lytic gene promoter and induced increased levels of viral transcripts (181).

There is also evidence for Polycomb silencing in Epstein-Barr virus (EBV). H3K27me3 and EZH2 have been detected on the promoter of ZEBRA/BZLF1 (an early gene required for lytic induction) and on several lytic promoters in lymphoblastoid cell lines (LCL's), which contain latent EBV (182-184). EZH2 knockout, knockdown, or

inhibition alone is not sufficient to induce robust changes in ZEBRA expression in latently infected cells (182) (185) (186). However, PRC2 inhibition has been shown to enhance viral gene expression when in combination with other lytic induction triggers in latently infected cells (182, 185). Therefore, H3K27me3 appears important for maintaining silencing in response to additional triggers. The vPRC1 component KDM2B has also been detected at EBV promoters and exerts a repressive effect, although whether this is linked to vPRC1/H2AK119ub1 is unknown (187).

Human Beta Herpesviruses

For the prototypical human Beta herpesvirus, human cytomegalovirus (HCMV), there is experimental evidence that Polycomb silencing plays a role in the maintenance or establishment of HCMV latency. Inhibition of PRC2 prevented quiescence in both human monocytic leukemia THP-1 cell and embryonal carcinoma NT2D1 cell latency and reactivation models (188). In addition, PRC2 inhibition was sufficient to disrupt quiescence in NT2D1/THP1 models and knockdown of H3K27 demethylase JMJD3 reduced viral gene expression in a THP-1 reactivation model (188, 189). In a CD14+ experimental system of latency, overexpression of JMJD3/UTX resulted in increased lytic gene expression (190). Further, H3K27 demethylases JMJD3 and UTX are targeted to the HCMV major immediate-early promoter (MIEP) in both THP-1 cells and CD34+ cells as a potential way for the host cell to defend against latency (191). The MIEP is composed of the major immediate early promoter and enhancer regions and exerts control over immediate early gene expression, which is critical to initiating the viral cycle. In the presence of a viral protein UL138, recruitment of histone

demethylases is decreased, permitting increased association of H3K27me3 with the MIEP.

Human Alpha Herpesvirus HSV-1

Using mouse models of HSV-1 latency, multiple studies have found that the viral genome is enriched for H3K27me3 (121, 123, 124). The contribution of H3K27me3 to HSV-1 latency is also demonstrated by the observed requirement for JMJD3 and/or UTX activity in HSV-1 reactivation (99, 100). Consistent with H3K27me3 association with latent HSV-1, PRC2 component SUZ12 is associated with the HSV-1 genome as latency is established (192). Interestingly, H3K27me3 and PRC2 are not initially detected on the viral genome until approximately 10-15 days post-infection *in vivo*, a timepoint at which lytic genes have already been repressed (122). These kinetics suggest that PRC2-mediated H3K27me3 may not actively initiate lytic viral gene silencing but may instead maintain this repression. However, the functional role of PRC2 in the repression of lytic viral genes during latency establishment and maintenance has never been directly tested through inhibition or depletion of PRC2. H3K27me3's predecessor H3K27me2 may be deposited earlier and initiate gene silencing, but its enrichment has not been investigated on the HSV-1 genome. How PRC2 is recruited to the HSV-1 genome also remains unresolved, although there are theories involving a latent viral lncRNA (discussed below).

Recruitment of the PRC1 complex to the latent HSV-1 genome has been analyzed by chromatin immunoprecipitation (ChIP) for PCGF4/Bmi1, but no significant enrichment of this protein was detected on the lytic promoters examined (123, 192).

PCGF4 can be a subunit in either vPRC1 or cPRC1, although there are multiple PRC1 variants that lack PCGF4, as discussed above. If H2AK119ub or any core components of PRC1 (Ring1A/B) are recruited to the latent HSV-1 genome, or how such recruitment might occur at the molecular level, has never been reported. Therefore, the contribution of PRC1 to lytic viral gene repression during latency establishment, maintenance, and reactivation through functional studies has also never been reported.

The Contribution of (Viral) LncRNA's to Polycomb Silencing:

The only region of the HSV genome expressed to abundant levels during latency is the latency associated transcript (LAT) locus (193), although not all latent genomes express this locus (194-198). The LATs are a family of HSV-1 non-coding RNAs expressed from this locus, a primary 8.3kb transcript spliced is into 1.5kb and 2kb stable introns, and an exon that is further spliced into miRNAs (miR-H1 to miR-H8) (199, 200). The LAT promoter is enriched for H3K27me3 during latent infection, but a downstream region containing the long-term enhancer is depleted for this mark (121), likely due to CCCTC-binding factor (CTCF) sites on the HSV-1 genome that halt the propagation of repressive heterochromatin from nearby lytic genes onto the LAT (201-203). The LAT is also decorated with euchromatin-associated modifications during latency, including the di- and tri-methylation of lysine 4 on histone H3 (H3K4me3) and acetylated histone H3 on lysines 9 and 14 (121, 204, 205), suggesting its chromatin structure is "poised" rather than repressive.

The function of the LAT has remained enigmatic for decades. However, it is known that the LAT represses lytic viral gene expression weakly during acute infection and robustly during latent infection, suggesting it may actively aid in the establishment or the maintenance of latent infection (124, 206-210). Long noncoding RNAs (lncRNAs) can participate in gene silencing by transcriptional interference of anti-sense transcripts and recruitment of additional silencing proteins like histone deacetylases and demethylases (reviewed in (211)). Several miRNAs encoded by the LAT exist anti-sense to viral genes that promote lytic infection, including ICP0 (212) and ICP34.5 (213), suggesting the regulation of lytic infection in a complementary manner. However, the LAT has also been implicated in the modulation of viral heterochromatin on silenced lytic gene promoters in several studies. For example, the presence of the LAT is associated with enhanced constitutive heterochromatin mark H3K9me2 on viral promoters (120). Importantly, there is also a potential link between the LAT and Polycomb silencing, specifically PRC2 H3K27 tri-methylation, on the HSV-1 genome.

There are several ways that lncRNAs can interact with and modulate Polycomb silencing, although it should be acknowledged that additional factors like pre-existing histone post-translational modifications (PTMs), presence of transcription factors, composition of the Polycomb complexes, nature of the RNA, and active transcription can modify these relationships (214). First, the methyltransferase activity of PRC2 is inhibited by RNA binding and single-stranded RNA competes for PRC2 DNA binding (215) (Fig 1.4B). However, RNA itself and the RNA binding domain of EZH2 is also required for PRC2 binding to chromatin (216). A recent study addressed the conundrum

as to how lncRNAs play a role in promoting PRC2 recruitment and H3K27me3 formation when the complex is known to be inhibited by RNA binding. It was found that although binding to single-strand RNA (ssRNA) inhibited PRC2 activity, binding of double strand RNA (dsRNA) can relieve this repression (217). Hence, lncRNAs can promote Polycomb silencing by base paring with nascent RNA transcripts that have homologous sequences and thus overcome the repression of ssRNA imposed by binding to EZH2. (Fig 1.4C). The HCMV lncRNA 4.9 may regulate PRC2 function at a lytic promoter in such a manner. During a latent infection of CD14+ monocytes, lncRNA 4.9 interacts with PRC2 components EZH2 and SUZ12, and the RNA itself is enriched at the MIEP, which is also enriched for H3K27me3 (190).

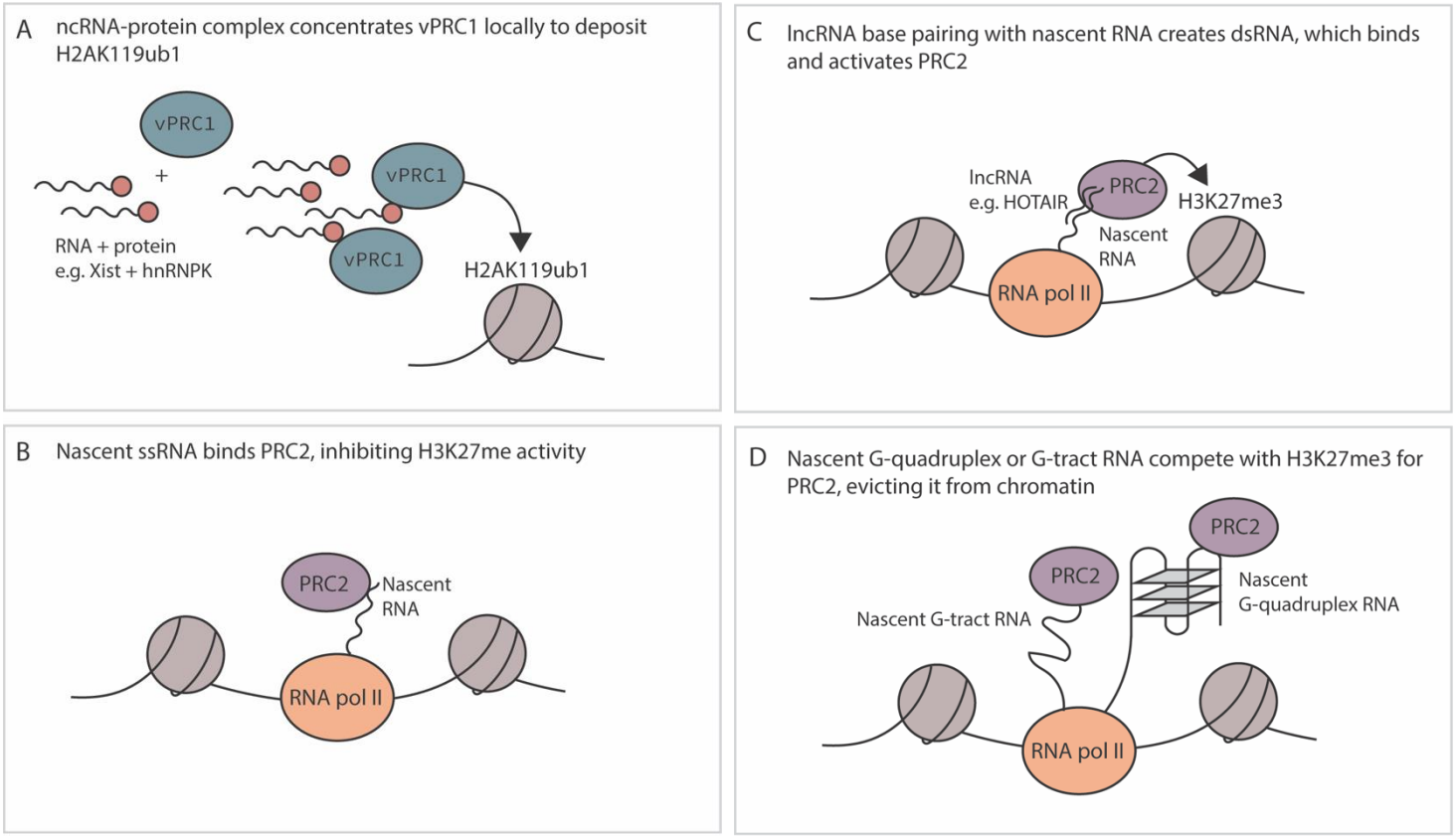

Figure 1.4 Roles for RNA in Modulating Polycomb Complex Binding and Facultative Heterochromatin Targeting: A: Non-coding RNA paired with an RNA-binding protein can concentrate variant PRC1 near chromatin and promote subsequent H2AK119ub1 deposition. This has been demonstrated for Xist and hnRNPK. B and C: Nascent RNA being transcribed by RNA polymerase II can inhibit PRC2 activity, but dsRNA formation by lncRNA base pairing to the nascent RNA can activate PRC2. HOTAIR is one such lncRNA. D: Nascent G-tract or G-quadruplex RNA have high binding affinity for PRC2, and can thus compete with H3K27me3 for PRC2 binding. PRC2 is evicted from the chromatin as a result of this competition. Figure was executed by Alison Francois.

LncRNA's may also play a role in evicting repressive chromatin. PRC2 component EZH2 has an affinity for a wide range of RNA species, with the highest binding affinity for RNA containing G tracts folded into G quadruplexes (also known as G4 structures) (215, 218). These RNA species can compete with H3K27me3 for PRC2 binding (Fig 1.4D). Therefore, herpesvirus lncRNA expression during reactivation could also modulate PRC2 recruitment away from DNA. KSHV PAN RNA is broadly detectable across the viral genome and promotes reactivation (219). PAN RNA also interacts with SUZ12 and EZH2 (219) and therefore may divert PRC2 away from chromatin and/or restrict PRC2 function, although this remains to be tested (220).

There is varying consensus on the role of the lncRNA LAT in modulating H3K27 methylation on the HSV-1 viral genome. One study found that in the absence of the LAT, H3K27me3 levels on the latent viral genome were decreased using two independent LAT-deletion viruses that were both compared to rescue viruses (122). A second study described the opposite, although this study did not use a rescue virus nor were experiments with the wild-type and LAT-null virus done in parallel (123). In addition, later sequencing of the virus used in this study demonstrated unexpected genomic changes, included regions substituted with HSV-2 sequence and an altered amino acid sequence within 13 different ORFs (221). The third study found that the LAT

repressed viral gene expression and did increase levels of H3K27me3 on the viral genome, but the increase was not significant (124). Therefore, whether a relationship between the LAT and PRC2 exists remains disputed, and a direct interaction between PRC2 and the LAT has not been demonstrated.

Potentially, the LAT could instead modulate Polycomb silencing through PRC1 akin to non-coding RNA X-inactive-specific transcript (Xist) (166). Xist is 17 kb RNA that is necessary for X chromosome inactivation, and it can also induce autosomal gene silencing as an exogenously inserted transgene. Distinct domains of the Xist RNA interact with different repressive proteins to orchestrate multiple events in epigenetic silencing of the X chromosome. A region of the Xist (the B repeat) binds heterogenous nuclear ribonucleoprotein K (hnRNPK) to indirectly recruit vPRC1 to catalyze H2AK119ub1 (159, 222). Xist does not interact directly with chromatin, and it is instead thought to increase the concentration of hnRNPK/vPRC1 in the vicinity of the region to be silenced. This is likely a common mechanism used by lncRNAs, at least in embryonic stem cells, where additional RNAs also involved in imprinting (*Airn*, *Kcnq1ot1 and Meg1)* interact with hnRNPK and Polycomb proteins (211).

HSV-1 Reactivation:

A Biphasic Nature

Periodically, HSV-1 re-initiates viral lytic gene expression following UV exposure, phycological stress, immune suppression, menstruation, secondary viral infection, or aging (8). Viral transcription can transition into the process of reactivation, which is

ultimately defined by the detection of new infectious virus production. Full reactivation mirrors the transcription of the HSV-1 genome during the initial lytic infection of neuronal or non-neuronal cells, where viral tegument protein VP16 drives the transcriptional cascade (IE genes → E genes → vDNA replication → L genes). Importantly, the removal of repressive histone modifications which coat the viral genome during latent infection (H3K9me2/3, H3K27me3) is ultimately required for reactivation, as the inhibition of H3K9 and H3K27 demethylases significantly reduce full reactivation *in vitro* and *ex vivo*, (99, 100, 109, 117).

However, there is accumulating evidence that HSV-1 reactivation occurs as a biphasic process and differs from transcription during initial *de novo* lytic infection. In this model, a synchronous transcriptional burst of all three classes of viral genes (IE, E, L), known as Phase I, precedes full reactivation or “Phase II”. In contrast to full reactivation, Phase I gene expression is independent of lytic transactivator VP16 (223), viral DNA replication (98, 117, 223), and heterochromatin removal, as the inhibition of H3K9 or H3K27 demethylases does not disrupt Phase I gene expression (98, 99, 109, 117). The validity of this biphasic model has been criticized as most experimental data that support this model have been acquired using *in vitro* models that use ACV to promote latency establishment. The concern is that biphasic reactivation is a remnant of antiviral use, and that Phase I gene expression is a sort of defunct reactivation event due to ACV-incorporated (and therefore presumably ”damaged”) viral genomes.

Phase I gene expression precedes full reactivation at a timepoint which varies depending on model system and reactivation stimulus. In *in vitro* models employing acyclovir during latency establishment and eliciting reactivation through PI3Kinase inhibition or neuronal hyper-excitability, peak Phase I gene expression occurs approximately 20 hours post stimulus (99, 109, 223). Kinetics appear to be hastened by using triggers in combination. In our novel *in vitro* model where latency takes a longer time to establish and where reactivation requires a triple combinatorial trigger, Phase I initiates approximately 12.5 hours post-stimulus (117). In an *ex vivo* model where ganglia are triggered to reactivate with the combination of PI3Kinase inhibition and axotomy, Phase I can proceed as early as 5 hours post-stimulus (98).

Viral genomes which progress through Phase I gene expression do not necessarily complete full reactivation. The transition from Phase I gene expression into full, Phase II reactivation can be perturbed by restrictive host cell proteins. Gadd45b, for example, appears to antagonize the HSV-1 late expression program to prevent full reactivation. Interestingly, Gadd45b mRNA is specifically increased in infected neurons in response to LY294002, suggesting that a viral factor may be mediating the gatekeeping into full reactivation or that host cells can respond to limit HSV reactivation (224).

HSV-1 Reactivation through Neuronal Stress Signaling:

In the context of a *de novo* lytic infection, VP16 is delivered to the host cell nuclei with the incoming virus' tegument. However, during a latent infection, transcription of the

VP16 gene is restricted and viral gene expression must initiate in the absence of VP16 protein. Therefore, reactivation from a latent infection is not initiated by VP16, but by alternative host or viral factors.

Initiation of reactivation during Phase I requires activated cellular c-Jun N-terminal kinase (JNK), which is specifically redirected to a physiologic neuronal stress signaling pathway through mixed lineage protein dual leucine kinase (DLK) and the JNK scaffold protein, JNK-interacting protein-3 (JIP3) (98, 99, 109, 112, 117). JNK activation results in the phosphorylation of serine (S10) neighboring repressive mark H3K9me3 on the viral genome during Phase I reactivation (99, 109). This “phospho/methyl switch” may enable viral transcription without the full removal of repressive marks on lytic promoters in Phase I reactivation, likely through the eviction of heterochromatin protein 1 (HP1). JNK may also result in the phosphorylation of serine (S28) neighboring repressive mark H3K27me3 on the viral genome, although this has not been directly demonstrated. Phosphorylation of the S28 residue occludes binding of PRC2 to H3K27me3 and permits gene expression (225), and this H3K27/S28 methyl/phospho switch has been observed on cellular promoters following cell stress (225, 226) and in neurons following stimulation (227).

The requirement of DLK/JNK for viral reactivation has been demonstrated using multiple systems and triggers converging upon diverse cellular pathways. For example, HSV-1 can co-opt an innate immune signaling pathway; IL-1β, which is released under conditions of fever and stress, induces neuronal hyper-excitation and subsequent

reactivation (109). HSV-1 reactivation is also elicited via disruption of neuronal DNA damage and repair pathways (112, 228). In response to a combinatorial stimulus of an NGF-deprivation mimic (LY294002), neuronal hyperexcitability (forskolin), and heat shock, we demonstrated that reactivation can be induced from a very silent form of latency established *in vitro* (117). DLK and/or JNK have been demonstrated as integral to reactivation when tested in these systems.

However, the full mechanistic role of DLK and JNK activation in mediating Phase I of HSV reactivation is not yet elucidated. Although histone phosphorylation likely permits a chromatin environment that is conducive to transcription, additional transcription or pioneer factors are also required to initiate lytic gene transcription during Phase I. In the neuronal stress signaling pathway, JNK up-regulates and activates its primary transcriptional factor target c-Jun. c-Jun is well known for mediating neuronal cell death and axon pruning following the loss of nerve-growth factor signaling, where it is both up-regulated and phosphorylated by DLK-mediated activation of JNK (99, 229, 230). As expected, c-Jun has also been shown to be up-regulated in response to neuronal stress stimuli in models of HSV-1 reactivation (99, 109). Interestingly, c-Jun-binding motifs are represented across lytic HSV-1 genes, and on the cellular genome c-Jun can act as a pioneer factor and maneuver through heterochromatin (231, 232). Therefore, it is likely that c-Jun mediates viral transcription from lytic gene promoters during Phase I gene expression, but this has not been directly tested. In fact, there has not been any neuronal host transcriptional/pioneer factors yet implicated in mediating Phase I gene expression, or full Phase II reactivation from the HSV-1 genome.

Heterogeneity of HSV-1 Latent Infection and Reactivation:

Importantly, latent infection and reactivation demonstrate substantial heterogeneity, reflected by the fact that only a proportion of a population of latently infected neurons will reactivate at any one time (109, 117, 233, 234). Within individual latently infected neurons, there is heterogeneous expression of lytic and latent transcripts and copy numbers of viral DNA (194, 195, 235). This heterogeneity is further maintained at a higher biological resolution, as individual viral genomes exhibit differential subnuclear positioning and association with host factors such as promyelocytic leukemia (PML) bodies and peri-centromeric regions (93). While factors such as the immune response or infectious viral dose may alter reactivation capacity, this heterogeneity is likely in part also owed to the intrinsic heterogeneity of the latent host cell, the neuron. Individual peripheral (sensory, sympathetic) neurons that compose mature ganglia differ in terms of mRNA expression profiles and protein synthesis of epigenetic remodeler complexes, stress hormone receptors, neurotrophic receptors, and ion channels (236-238), and these factors have all been demonstrated to mediate HSV-1 latency establishment and reactivation. Importantly, many of the experimental techniques used to investigate HSV-1 latent infection and reactivation are population-level, including but not limited to reverse transcriptase quantitative Polymerase Chain Reaction (RT-qPCR) and chromatin immunoprecipitation (ChIP). Our laboratory continues to employ these techniques but additionally places special emphasis on investigating these processes at the single-neuron and single-genome resolution.

Statement of Purpose:

In summary, HSV-1 can establish a latent infection within neurons, during which the viral genome is targeted by repressive chromatin. Periodically in response to stress, the HSV-1 genome may re-initiate lytic viral gene expression and progress into full reactivation, where repressive chromatin is removed from the viral genome and new infectious virus is made. Although HSV-1 reactivation causes ubiquitous and serious disease and facilitates the transmission of infectious virus to new hosts, there are currently no antivirals that target HSV-1 reactivation through its prevention.

With this dissertation, we aim to elucidate the molecular mechanisms behind how chromatin and neuronal stress signaling pathways (which can converge) silence the HSV-1 genome during a latent infection and are modified during reactivation, with the goal of manipulating this information into therapeutics that prevent HSV-1 reactivation and associated clinical consequences. In doing so, we also introduce new technology to study HSV-1 latency and reactivation at a single-cell and single-genome resolution and the intrinsic epigenetic signature of the specialized cell type of a neuron. The scientific questions addressed in this dissertation are summarized in Figure 1.5.

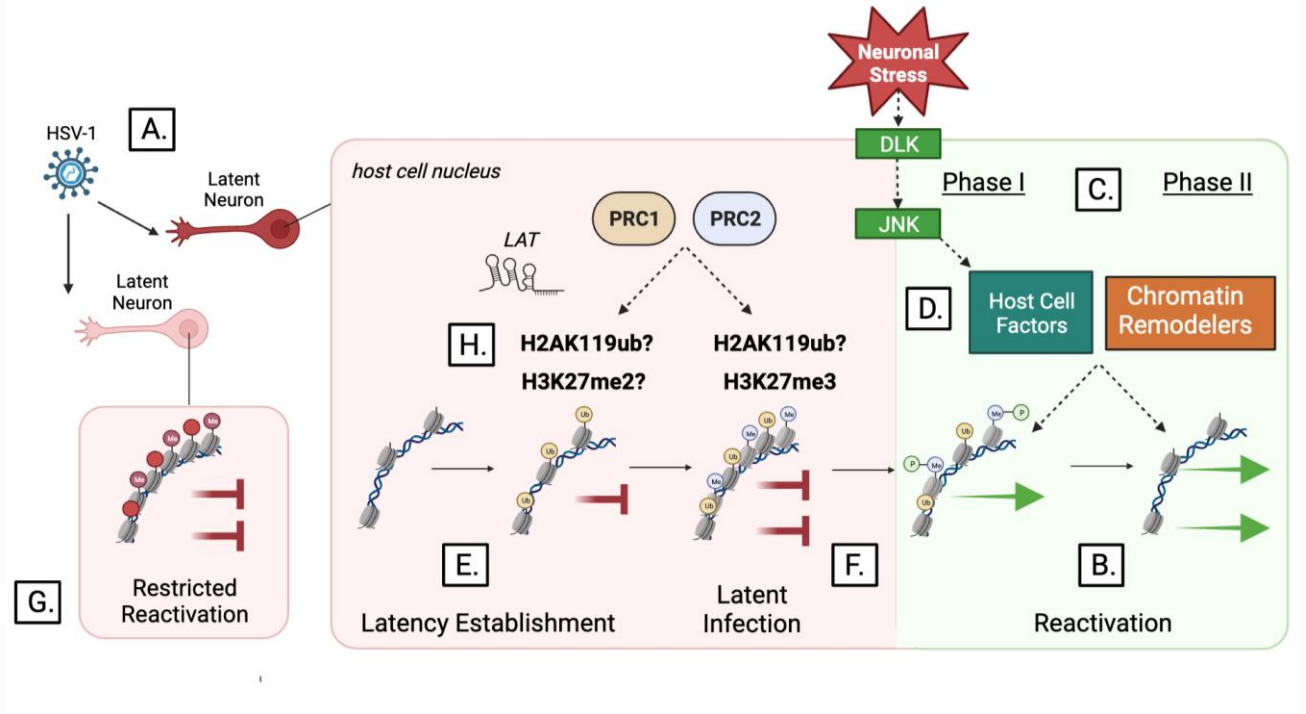

Figure 1.5 Scientific Questions Addressed in this Dissertation. HSV-1 can establish a latent infection within neurons, during which the viral genome is targeted by repressive chromatin. In response to stress, the viral genome may reactivate in a biphasic manner, during which chromatin is modified and eventually removed. We aim to create a primary model of HSV-1 latency and reactivation where A) the heterogeneity of these processes can be maintained and B) *de novo* reactivation can be differentiated from downstream cell-to-cell spread. C) As using such a model enables latency to be established without antivirals, we explore whether Phase I occurs in this system. D) We also inquire about which neuronal host cell signaling factors mediate Phase I and Phase II reactivation. We explore the functional role of PRC1 and PRC2-assocated modifications to HSV-1 latency establishment (E) and maintenance (F), and the viral genome's ability to reactivate (G). H) The mechanisms of potential Polycomb recruitment through LAT are also preliminarily explored.

Using a recombinant HSV-1 virus, we inquire whether we can construct a new primary neuron model of HSV-1 latency and reactivation in which the heterogeneity of these processes can be accurately recapitulated (Fig 1.5A) and initial transcription events during reactivation can be differentiated from downstream cell-to-cell spread (Fig 1.5B). As using such a model enables latency to be established without antivirals, we also ask whether Phase I exists independently of antiviral use (Fig 1.5C).

While histone phosphorylation may create a transcriptionally permissive environment on the HSV-1 genome during Phase I gene expression, the repertoire of neuronal stress signaling transcription and pioneer factors that drive viral gene transcription remains unknown. We investigate such factors led by the hypothesis that neuronal c-Jun pioneers through viral heterochromatin and acts as the most downstream transcriptional regulator of the JNK/DLK stress signaling pathway during Phase I (Fig 1.5D).

During a latent infection, HSV-1 lytic gene promoters associate with reversible Polycomb silencing. H3K27me3 and PRC2 are enriched on the latent HSV-1 genome *in vivo*, but the presence of H2AK119ub and the contribution of both PRC2 and PRC1 to viral gene repression during latency establishment (Fig 1.5E), maintenance (Fig 1.5F), and reactivation (Fig 1.5G) remains unknown. Using a combination of *in vivo* and *in vitro* techniques and our new recombinant virus, we explore the hypothesis that vPRC1 is recruited to the HSV-1 genome to deposit H2AK119ub on the viral genome and repress lytic viral genes in a manner that is amenable to later reactivation. The mechanism(s) of Polycomb recruitment to the HSV-1 genome, and whether these involve latent viral lncRNA LAT, are also unresolved. We therefore also begin to explore the hypothesis that vPRC1 is recruited to the HSV-1 genome by host factor hnRNPK in tandem with viral lncRNA LAT (Fig 1.5H).

~End of Chapter 1~

Chapter 2: DLK-Dependent Biphasic Reactivation of Herpes Simplex Virus Latency Established in the Absence of Antivirals

Parts of this chapter have been adapted from:

Dochnal, SA, Merchant, HY, Schinlever, AR, Babnis, A, Depledge, DP, Wilson, AC, & Cliffe, AR. DLK-Dependent Biphasic Reactivation of Herpes Simplex Virus Latency Established in the Absence of Antivirals. *Journal of virology*, 96(12). doi:10.1128/jvi00508-22 (2022)

Abstract

Understanding the molecular mechanisms of herpes simplex virus type 1 (HSV-1) latent infection and reactivation in neurons requires the use of *in vitro* model systems. Establishing a quiescent infection in cultured neurons is problematic as any infectious virus released can superinfect the cultures. Previous studies have used the viral DNA replication inhibitor acyclovir to prevent superinfection and promote latency establishment. Here, we describe a new model system using HSV-1 Stayput-GFP, a reporter virus that is defective for cell-to-cell spread. This enables the study of latency establishment and reactivation at the single-neuron level, and importantly establishes latent infections without the need for acyclovir. The establishment of a latent state requires a longer time frame than previous models using DNA replication inhibitors. This results in a decreased ability of the virus to reactivate using established inducers, and as such, a combination of reactivation triggers is required. Using this system, we demonstrate that biphasic reactivation occurs even when latency is established in the absence of acyclovir. Importantly, Phase I lytic gene expression still occurs in a histone demethylase and viral DNA replication independent manner, and requires DLK activity. These data demonstrate that the two waves of viral gene expression following HSV-1 reactivation are independent of secondary infection and not unique to systems that require acyclovir to promote latency establishment.

Introduction

Herpes simplex virus 1 (HSV-1) is a globally prevalent pathogen with the capacity to infect both sensory and autonomic neurons (14-17). Following neuronal infection, HSV-1 can enter a lytic replication cycle, establish a lifelong latent infection, or potentially undergo a limited amount of lytic gene expression even prior to latency establishment (10, 194, 208, 239-244). While latency is largely asymptomatic, periodic reactivation of the virus can result in cutaneous lesions, keratitis, and encephalitis. Epidemiological studies have also linked HSV infection with an increased risk of developing late onset Alzheimer's disease (48, 245-252).

The regulated expression of viral lytic transcripts has been well characterized following lytic infection (223, 253, 254). The HSV-1 genome enters the host cell epigenetically naked (75-77) but becomes chromatinized by histones bearing transcriptionally permissive histone modifications (81-85, 255-259). Viral gene expression is initiated from the genome in response to viral trans-activator and tegument protein VP16, which forms a complex with cellular factors involved in transcriptional activation, including general transcription factors, ATP-dependent chromatin remodelers, and histone modifying enzymes to promote expression of immediate-early (IE) genes (84, 87, 260-263). Synthesis of the IE proteins is required for early (E) mRNA transcription. Products of the early viral genes enable viral DNA replication. Viral genome synthesis is a pre-requisite for true-late (TL) mRNA transcription, likely due to a shift in genome accessibility and increased binding of host transcriptional machinery (264). In contrast to productive infection, during HSV-1

latency, viral lytic mRNAs are largely transcriptionally repressed and promoters assemble into silent heterochromatin marked by the tri-methylation of histone H3 lysine 27 (H3K27me3) and di/tri-methylation of histone H3 on lysine 9 (H3K9me2/3) (119-123, 193). The initiation of viral gene expression during reactivation is induced from a heterochromatin-associated viral genome and occurs in the absence of viral activators like VP16. Latent HSV-1 therefore relies on host factors to act on the epigenetically silent viral genome and induce lytic gene expression.

The mechanisms that regulate entry into lytic gene expression to permit reactivation remain elusive. Using primary neuronal models of HSV-1 latent infection, reactivation has been found to progress in a two-step or bi-phasic manner. Phase I is characterized as a synchronous wave of lytic viral transcripts, occurring approximately 20 hours post-stimulus (99, 109, 223, 224, 265). There is evidence that this initial induction of lytic gene expression is not dependent on the lytic trans-activator VP16, or viral protein synthesis (223, 266). Instead, cellular factors, including the stress kinases dual leucine zipper kinase (DLK) and c-Jun N terminal kinase (JNK), are required for Phase I entry (99, 109). Importantly, viral gene expression occurs despite the persistence of heterochromatin on viral promoters. Instead, JNK-dependent histone phosphorylation of histone H3S10 results in a methyl/phospho switch, which can permit gene expression even while the repressive H3K9me3 histone modification is maintained (99). The second wave of viral lytic gene expression, Phase II, occurs approximately 48 hours post-stimulus. Phase II reactivation is characterized by the full transcriptional viral cascade, including viral DNA replication, and ultimately infectious virus production

(223). In contrast to Phase I, viral protein synthesis, heterochromatin removal, VP16-mediated transactivation, and viral DNA replication are required for Phase II (99, 109, 223).

In vitro systems of HSV-1 latency are required to study the mechanisms of latency establishment and reactivation that cannot be easily studied *in vivo* (8, 114, 267, 268). *In vitro* models more readily enable functional studies, and immune system components can be included to understand how the host immune response impacts latency and reactivation (93, 108). However, there are complications involved in establishing latency *in vitro*. As also observed in animal models, only a sub-population of infected neurons enter a latent state whereas other neurons become lytically infected (118, 194, 269, 270). This leads to a superinfection of the cultures and an inability to establish a latent infection. Therefore, many existing *in vitro* models have used viral DNA replication inhibitors, predominantly acyclovir (ACV), to establish latency *in vitro* (99, 103, 105, 106, 115, 116, 234). ACV is proposed to inhibit viral DNA replication by incorporating into actively replicating viral genomes in lytic cells, although there is also evidence from ACV-resistant strains that ACV can also inhibit the viral DNA polymerase (62, 271, 272). There are some caveats associated with ACV use as the process of DNA replication and subsequent late gene expression cannot be studied in lytic neurons during latency establishment. Moreover, the fate of any genomes that incorporate ACV is unknown. Therefore, new model systems are required in which latency establishment can be tracked without the need for viral DNA replication inhibitors. Such a system can also be used to determine whether the use of ACV in the cultures alters mechanisms of

lytic gene expression during reactivation. Here we describe the use of a novel HSV-1 reporter virus Stayput-GFP, which provides a powerful new methodology to investigate the establishment and reactivation from latent infection at the single neuron level without the need for DNA replication inhibitors.

Results

Construction of a gH-null US11-GFP HSV-1.

To construct a recombinant HSV-1 that is deficient in cell-to-cell spread and can also be used to visualize cells containing detectable viral late protein, Us11 tagged with GFP (273) was inserted into an existing glycoprotein H (gH)-null virus, SCgHZ (274) (Fig. 2.1A). gH is essential for HSV-1 cell entry as it mediates fusion between the virus envelope and host cell membrane (275, 276). The GFP-tagged true-late protein is a useful indicator of both lytic infection and reactivation, and Us11-GFP wild-type virus has been used as such in several HSV-1 latency systems (103, 107, 109, 112, 114, 224). The tagged virus has previously been reported to express the full complement of HSV-1 genes, as wild-type Patton strain (273).

We first verified that the resulting virus (named Stayput-GFP) was deficient in cell-to-cell spread in non-neuronal and neuronal cells but otherwise undergoes gene expression and replication as a wild-type virus. The genome sequence and transcriptome of Stayput-GFP was validated by nanopore gDNA and direct RNA sequencing, respectively (Fig. 2.1B-C). As determined through plaque assay, the ability to produce infectious virus was perturbed in the gH-deletion strain (Fig. 2.1D) but was rescued using previously constructed gH-complementing cell line, Vero-F6 (Fig. 2.1E). Importantly, replication in this cell line was indistinguishable from the parent SCgHZ and Us11-GFP Patton strain, which we chose for comparison as this virus has previously been used for latent infection studies in primary neurons.

To demonstrate cell-to-cell spread deficiency in neurons, we quantified GFP-positive neurons over time. Infection of murine sympathetic neurons at an MOI of 0.5 PFU/cell resulted in detectable GFP-positive neurons, which remained constant after 24 hours post-infection (Fig. 2.1F), while the surrounding GFP-negative neurons remained GFP-negative (Fig. 2.1G). This contrasts with the wild-type US11-GFP condition where the number of lytic-infected neurons increased substantially over time. Therefore, Stayput-GFP infection was equivalent to Us11-GFP upon initial infection but failed to spread within the neuronal culture.

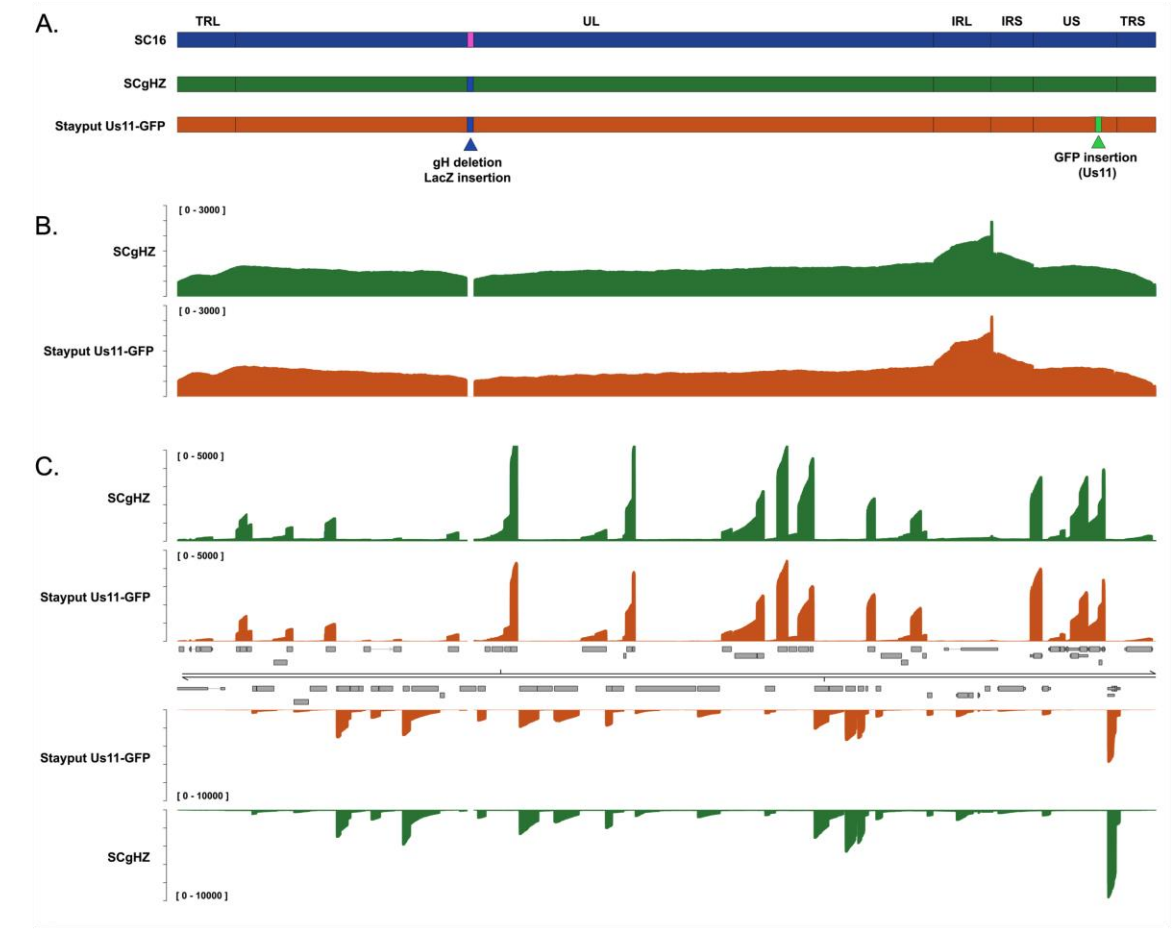
A.
TRL
UL
IRL
IRS
US
TRS
SC16
SCgHZ
Stayput Us11-GFP
gH deletion
LacZ insertion
GFP insertion
(Us11)
B.
[0 - 3000]
SCgHZ
[0 - 3000]
Stayput Us11-GFP
C.
[0 - 5000]
SCgHZ
[0 - 5000]
Stayput Us11-GFP
Stayput Us11-GFP
[0 - 10000]
SCgHZ
[0 - 10000]

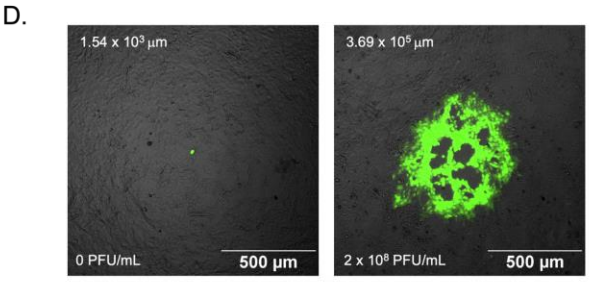
D.
1.54 x 10³ µm
0 PFU/mL
500 µm
3.69 x 10⁵ µm
2 x 10⁸ PFU/mL
500 µm

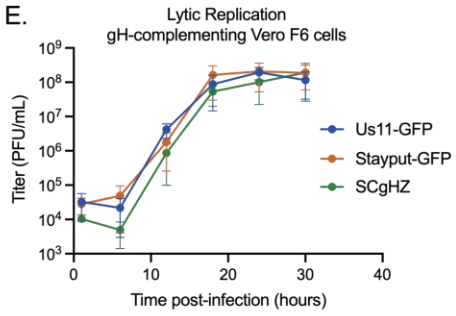
E.
Lytic Replication
gH-complementing Vero F6 cells
Titer (PFU/mL)
Time post-infection (hours)
Us11-GFP
Stayput-GFP
SCgHZ

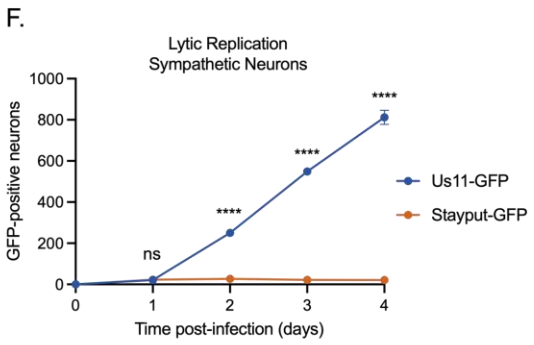
F.
Lytic Replication
Sympathetic Neurons
GFP-positive neurons
Time post-infection (days)
ns
****
****
****
Us11-GFP
Stayput-GFP

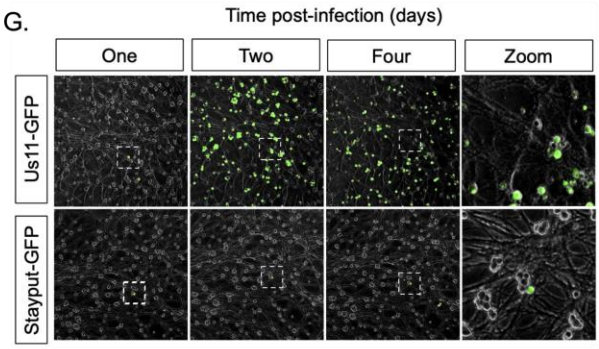
G.
Time post-infection (days)
One
Two
Four
Zoom
Us11-GFP
Stayput-GFP

Figure 2.1 Stayput-GFP replicates as wild-type but is unable to spread. (A) Schematic overview of HSV-1 strain SC16, the gH-deletion mutant SCgHZ, and Stayput-GFP. The gH deletion / LacZ insertion and Us11-GFP insertion sites are shown by blue and green triangles, respectively. (B-C) Coverage plots derived from (B) nanopore gDNA sequencing and (C) nanopore direct RNA sequencing of SCgHZ and Stayput-GFP. Sequence read data were aligned against the SC16 reference genome and demonstrate a drop in coverage at the gH locus. (D) Plaque forming assay of Stayput-GFP on Vero (left) or gH-complementing Vero-F6 (right) cells 48 hours post-infection at a 10^{-7} dilution. GFP-positive area in example image reported top left of each image. Titer of viral stock reported bottom left of each image. (E) Vero-F6 cells were infected with Stayput-GFP, SCgHZ, or Us11-GFP at an MOI of 5. Infectious virus was collected over time and titrated on Vero-F6 cells (n=3 biological replicates). (F-G) Neonatal sympathetic neurons were infected at an MOI of 0.5 PFU/cell with Stayput-GFP or Us11-GFP in the absence of DNA replication inhibitors. Us11-GFP-positive neurons were counted over time (n=3 biological replicates). Shapiro-Wilk normality test. Unpaired student's t test between Us11-GFP and Stayput-GFP. ****p<0.0001. The means and SEMs are shown. Stayput-GFP was constructed by Austin R. Schinlever and Aleksandra Babnis. Experiments from Panels A-C were performed by Husain Y. Merchant and Daniel P. Depledge.

Reactivation of Stayput-GFP in a primary neuronal model.

To confirm that Stayput-GFP undergoes reactivation in a manner comparable to the backbone SCgHZ, we infected mouse primary sympathetic neurons in the presence of viral DNA replication inhibitor ACV (99, 103, 105, 106, 234). ACV prevents the production of infectious virus, and thus superinfection of the cultures. Following infection, ACV was removed, and reactivation was triggered adding a PI3-kinase inhibitor LY294002 (Fig. 2.2A), which mimics loss of a branch of the NGF-signaling pathway in neurons (277) and has previously been found to induce reactivation (99, 103, 107, 108). Following the addition of the reactivation stimulus, viral gene expression increased uniformly between Stayput-GFP, SCgHZ, and wild-type Us11-GFP at 20 hours post-stimulus (Fig. 2.2C). Viral gene expression continued to increase from 20 to 48 hours for all three viruses, and GFP-positive neurons were visible for both GFP-

tagged viruses by 48 hours (Fig. 2.2B, 2.2D). This indicates that even in the absence of cell-to-cell spread, reactivation progressed over a 48-hour period, initiating with viral mRNA production and later detection of viral late protein.

By 72 hours-post stimulus, GFP and viral gene transcription were significantly up-regulated in wild-type Us11-GFP in comparison to Stayput-GFP or SCgHZ, suggesting that at this time-point, the readout of reactivation for wild-type Us11-GFP is confounded by cell-to-cell spread (Fig. 2.2B, 2.2E). We are therefore unable to differentiate between genuine reactivation and downstream cell-to-cell spread using a wild-type virus. Previous attempts to reduce cell-to-cell spread include using pooled human gamma globulin or the viral DNA packaging inhibitor WAY-150138 (103, 278-280). However, using Stayput-GFP offers a built-in mechanism to prevent cell-to-cell spread during reactivation and permit quantification of the progression to reactivation at the single neuron level.

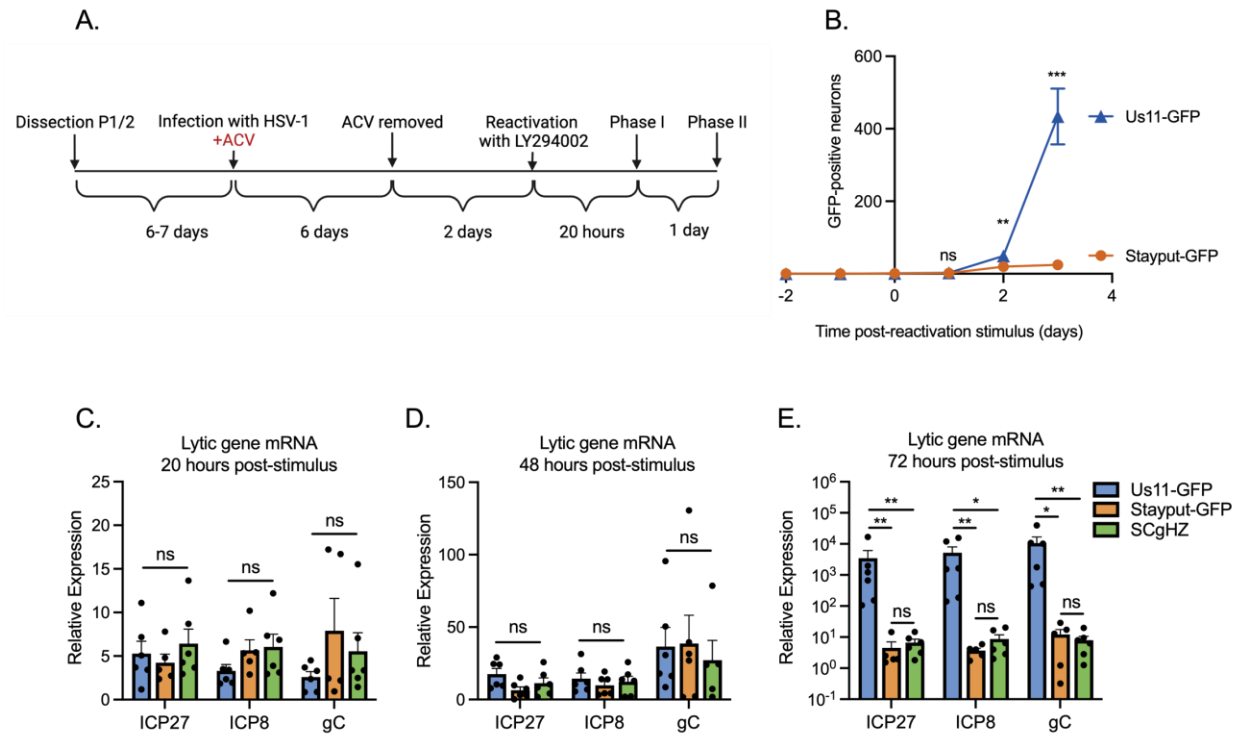

Figure 2.2 Stayput-GFP in a latency and reactivation model using ACV to promote latency establishment. (A) The latency and reactivation model scheme. Neonatal sympathetic neurons were infected with Stayput-GFP, parent virus SCgHZ, or wild-type Us11-GFP at an MOI of 7.5 PFU/cell in the presence of ACV (50 μM). Then, 6 days later, ACV was removed, and 2 days later, cultures were reactivated with LY294002 (20 μM). (B) The numbers of GFP-positive neurons in a single well (containing approximately 5,000 neurons) for Stayput-GFP and wild-type Us11-GFP were counted over time. (C to E) Viral gene expression also was quantified by RT-qPCR for immediate early (*ICP27*), early (*ICP8*), and late (*gC*) genes at 20 h (C), 48 h (D), and 72 h (E) poststimulus. Relative expression to unreactivated samples and cellular control (mGAPDH). $n = 6$ biological replicates from 3 litters. Normality was determined by Kolmogorov-Smirnov test in panels B to E. Mann-Whitney (B) or Kruskal-Wallis with comparison of means (C to E); *, $P < 0.05$; **, $P < 0.01$; ***, $P < 0.001$. The means and SEMs are represented. Individual biological replicates are indicated in panels C to E.

Stayput-GFP can be used to create a quiescence model of neuronal infection in the absence of viral DNA replication inhibitors.

When wild-type virus is used for neuronal infection, superinfection of the cultures occurs (Fig. 2.1F), and a latent infection cannot be established. By infecting with Stayput-GFP, we posited that we could create a model of latency establishment without the use of DNA replication inhibitors. Following the infection of neonatal sympathetic neurons at an MOI of 7.5 PFU/cell, the number of GFP-positive neurons emerged by 1-day post-infection, increased until 3 days post-infection, and then decreased until reaching zero by 30 days post-infection (Fig. 2.3A). The peak number of GFP-positive neurons was approximately 1,000. Given that 5,000 neurons were plated per well, this equates to approximately 20% of the population of neurons that progress to become Us11-GFP positive. The length of time required for Us11-GFP to be lost from the cultures was surprising and may result from the previously characterized restricted cell death in neurons (281), or a gradual shut-off in protein synthesis in a sub-population of neurons that survive even Late gene expression. Single-cell tracking demonstrates that at least a proportion of neurons that become GFP-positive also end up staining positive for cell death marker SYTOX™ Orange (Fig. 2.3B-C). This data suggests that most neurons that undergo a lytic infection end up undergoing cell death. However, accurately tracking all neurons over time to determine whether all GFP positive neurons do die is problematic because individual neurons shift over time. Therefore, we cannot definitively conclude that all GFP positive neurons undergo cell death.

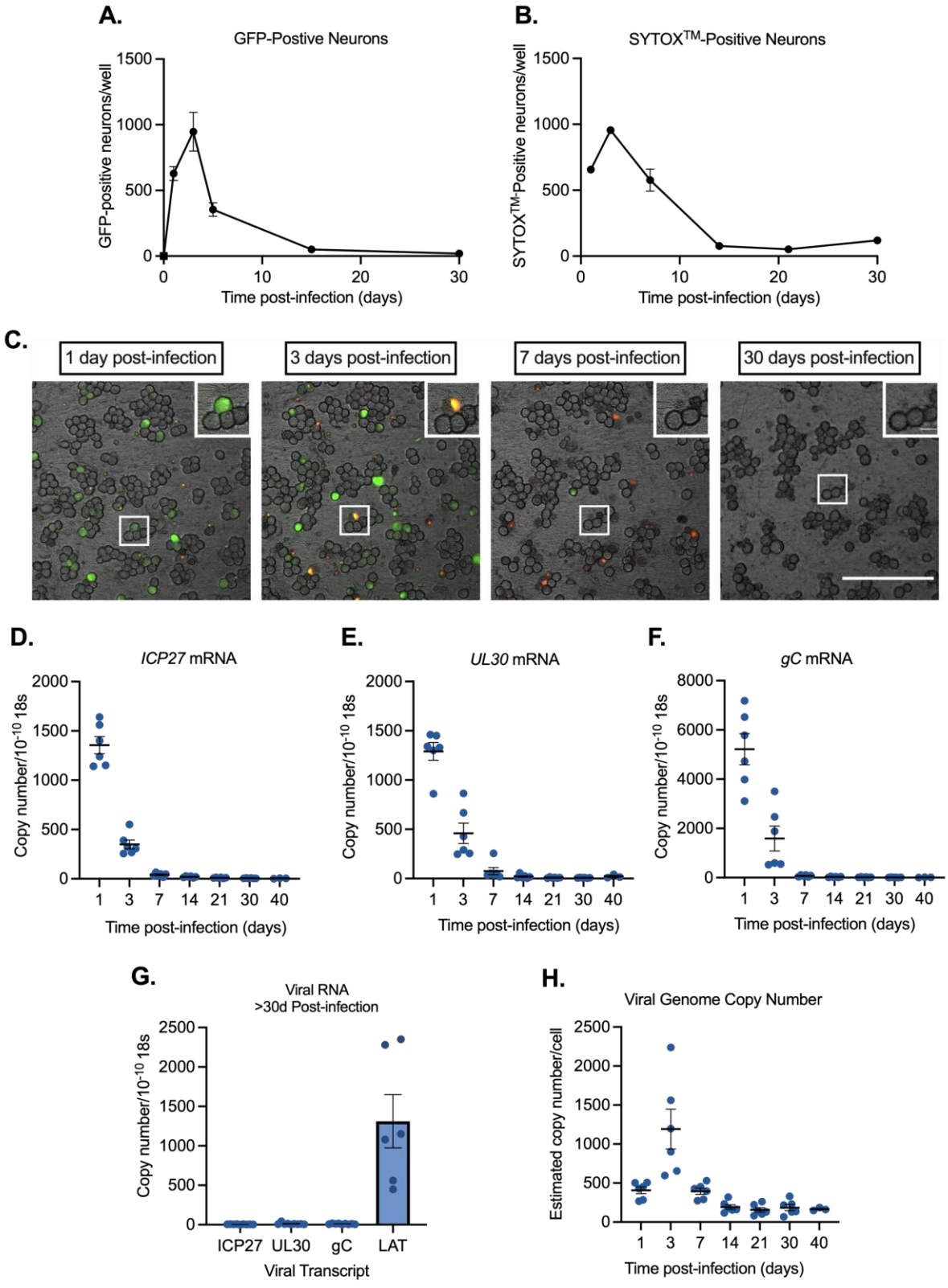
A.
GFP-Postive Neurons
GFP-positive neurons/well
1500
1000
500
0
0
10
20
30
Time post-infection (days)
B.
SYTOX™-Positive Neurons
SYTOX™-Positive neurons/well
1500
1000
500
0
0
10
20
30
Time post-infection (days)
C.
1 day post-infection
3 days post-infection
7 days post-infection
30 days post-infection
D.
ICP27 mRNA
Copy number/10-10 18s
2000
1500
1000
500
0
1
3
7
14
21
30
40
Time post-infection (days)
E.
UL30 mRNA
Copy number/10-10 18s
2000
1500
1000
500
0
1
3
7
14
21
30
40
Time post-infection (days)
F.
gC mRNA
Copy number/10-10 18s
8000
6000
4000
2000
0
1
3
7
14
21
30
40
Time post-infection (days)
G.
Viral RNA
>30d Post-infection
Copy number/10-10 18s
2500
2000
1500
1000
500
0
ICP27
UL30
gC
LAT
Viral Transcript
H.
Viral Genome Copy Number
Estimated copy number/cell
2500
2000
1500
1000
500
0
1
3
7
14
21
30
40
Time post-infection (days)

Figure 2.3 Stayput-GFP can be used to create a quiescence model in the absence of viral DNA replication inhibitors in neonatal sympathetic neurons. Neonatal sympathetic neurons were infected with Stayput-GFP at an MOI of 7.5 PFU/cell, and the numbers of Us11-GFP-positive neurons were quantified. (A) $n = 9$ biological replicates from 3 litters. (B) SYTOX Orange-positive neurons were also quantified over time ($n = 3$). (C) Following infection, the same field of view was imaged to track GFP and SYTOX Orange (250 μm scale bar for field of view [FOV], 25 μm scale bar for zoom) over time. (D to G) Lytic (D to F) and latent (G) viral transcripts ($n = 6$) were quantified up to 40 days postinfection. (H) Viral DNA load ($n = 6$) was also quantified up to 40 days postinfection. Individual biological replicates along with the means and SEMs are shown.

All classes of lytic viral gene expression emerged by 1-day post-infection and then decreased over the span of 30-days post-infection (Fig. 2.3D-F). In contrast to the lytic transcripts, LAT expression was maintained over the infection scheme of 30-40 days and was approximately 400-fold higher than lytic transcripts from 30 days onwards (Fig. 2.3G). This indicated that LAT-positive neurons persisted over this period, likely reflecting entry into quiescence. In agreement with this hypothesis, at 40 days post-infection there are approximately 200 viral DNA copies per cell, demonstrating that viral genomes persist (Fig. 2.3H). Together, these data show that infection of sympathetic neurons with a cell-to-cell defective virus results in a remaining population of neurons containing viral genomes and the LAT transcript. Notably, this mimics events following *in vivo* infection of mice.

The ability of HSV-1 to undergo reactivation decreases with length of time infected.

The presence of viral genomes and LAT transcripts suggested that HSV-1 had established a quiescent infection 30 days post-infection. Therefore, we hypothesized that some genomes enter latency, which is defined by an ability to reactivate in

response to a stimulus. We thus attempted to reactivate cultures with LY294002 (20 μM). However, we were unable to detect an increase in GFP-positive neurons after the addition of the trigger (Fig. 2.4A). We were also unable to detect a change in immediate early, early, or late transcripts (data not shown). This was unexpected as LY294002 has repeatedly been shown to elicit robust reactivation *in vitro* and was able to induce Stayput-GFP in a model using ACV to promote latency establishment (Fig. 2.2). Therefore, we sought to determine whether the inability to induce reactivation was due to the lack of ACV or the more prolonged time between initial infection and the addition of the reactivation stimulus. We infected neonatal cultures in the presence of ACV and reactivated over increasing lengths of time. ACV was removed from all cultures 6 days post-infection. We found that the number of GFP-positive neurons following addition of LY294002 decreased as the length of time infected increased (Fig. 2.4B). This was not likely due to a loss of viral genomes, as viral genome copy number and LAT expression remained constant over this period (Fig. 2.3G-H) and therefore instead reflected a more repressed viral genome unable to undergo reactivation upon PI3-kinase inhibition.

Neurons are known to undergo intrinsic maturation, even in culture (282, 283). Therefore, the increased age of the neuron could have also impacted the ability of HSV-1 to undergo reactivation. Hence, we investigated how reactivation changed with increased neuronal maturation (Fig. 2.4C). We infected cultured neurons with Stayput-GFP at an MOI of 7.5 at the postnatal (P) ages of P8, P16, and P24 and then reactivated 8 days later. These postnatal ages of infection were chosen to reactivate at

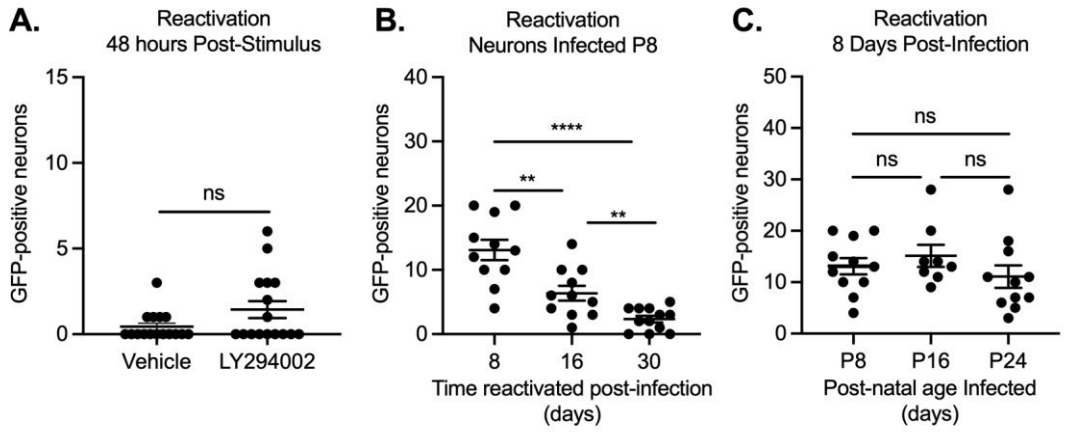

Figure 2.4 Reactivation decreases with length of time infected. Sympathetic neurons were infected with Stayput-GFP at an MOI of 7.5 PFU/cell and were treated with LY294002 when GFP-positive neurons were no longer detected (approximately 30 days postinfection). GFP-positive neurons were quantified over time; (A) peak GFP (48 h poststimulus) is represented. Neonatal SCGs were infected at age postnatal day 8 (P8) with Stayput-GFP in the presence of ACV. (B) ACV was removed 6 days postinfection, and reactivation was triggered at the indicated times postinfection. (C) Neonatal SCGs were infected as described above after different lengths of time *in vitro*, representing indicated postnatal ages, and reactivated 8 days postinfection with LY294002. $n = 12$ biological replicates from 3 litters. Normality was determined by the Kolmogorov-Smirnov test. Unpaired Student's *t* test (B) or the Mann-Whitney test (A and C) was used based on normality of data. **, $P < 0.01$; ***, $P < 0.001$; ****, $P < 0.0001$. Individual biological replicates along with the means and SEMs are shown.

the same ages of reactivation in Fig 2.4B. Importantly, we did not detect a decrease in reactivation output as the age of the neuron increased. Together, these data indicate that the decreased ability of Stayput-GFP to reactivate in a model that did not require ACV to establish quiescence was due to the longer time frame of infection and not associated with a lack of ACV in the cultures or increased age of the neuron.

Viral gene expression can be induced following long-term quiescent infection when multiple triggers are combined.

We next sought to determine whether other known stimuli of HSV-1 reactivation could induce Us11-GFP expression, indicative of entry into reactivation. We attempted a number of triggers including forskolin (110, 111, 284, 285) and heat-shock/hyperthermia (96, 113, 286-291), which are both known inducers of HSV-1 reactivation. Alone these stimuli did not induce Us11-GFP expression or viral lytic mRNA induction (data not shown). However, when heat-shock (43°C for 3h), in addition to forskolin (30 μM) and LY294002 (both pulsed for 20 hours) were combined, Us11-GFP positive neurons were detected at 48 hours post-stimulus, indicating progression to reactivation (Fig. 2.5A). Superinfection was also used as this can induce rapid and robust reactivation, likely resulting in delivery of viral tegument proteins. In comparison to superinfection, the combined heat-shock/forskolin/LY294002 trigger resulted in reduced entry into reactivation/Us11-GFP expression, indicating that only a sub-population of neurons undergo reactivation with this combined trigger, which is consistent with previous studies investigating the mechanism of HSV-1 reactivation both *in vivo* and *in vitro* (223, 233, 234, 292). Importantly, GFP-positive neurons at 48 hours post-stimulus co-stained with viral immediate early protein ICP4, early protein ICP8, as well as late capsid protein ICP5 (Fig. 2.5B). ICP8 staining appeared to form replication compartments, suggesting viral DNA replication occurs at this time. ICP5 capsid staining was also detectable in GFP-positive axons (Fig. 2.5C).

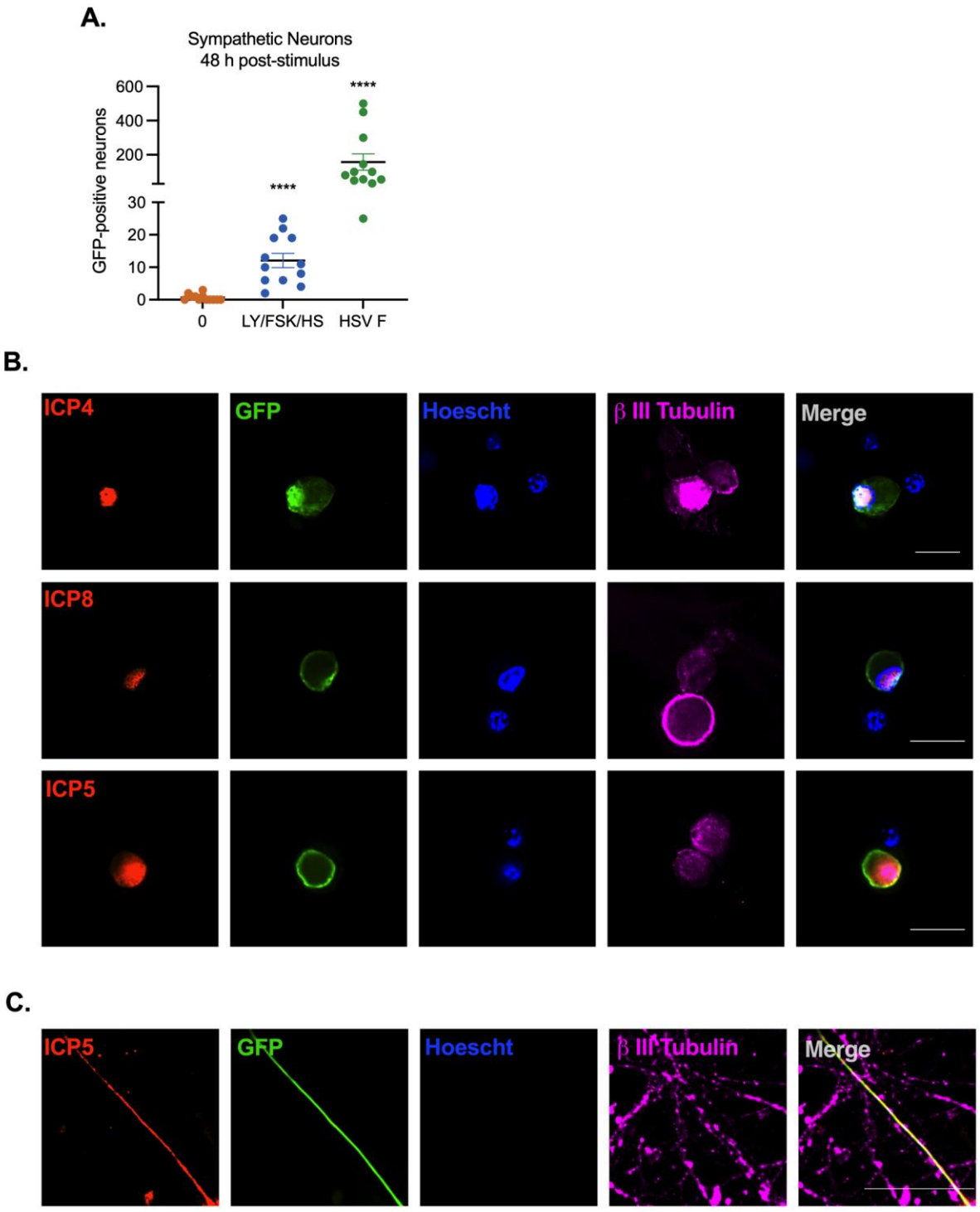
A.
Sympathetic Neurons
48 h post-stimulus
GFP-positive neurons
600
400
200
30
20
10
0
****
****
0
LY/FSK/HS
HSV F
B.
ICP4
GFP
Hoescht
β III Tubulin
Merge
ICP8
ICP5
C.
ICP5
GFP
Hoescht
β III Tubulin
Merge

Figure 2.5 Viral protein synthesis can be induced from neurons quiescently infected with Stayput-GFP using a combination of stimuli. Neonatal sympathetic neurons or adult sensory neurons were infected at an MOI of 7.5 PFU/cell with Stayput-GFP in the absence of viral DNA replication inhibitors. Following the loss of GFP, signaling quiescence of the culture, wells were reactivated with a variety of triggers, including combinations of LY294002 (20 μM), forskolin (60 μM), and heat shock (43°C for 3 h), as well as a superinfection with untagged F strain at an MOI of 10 PFU/cell. (A) GFP was quantified over time, and the peak GFP, at 48 h poststimulus, is depicted. *n* = 12 biological replicates. (B to C) Neurons were fixed at 48 h poststimulus and stained with viral immediate early (*ICP4*), early (*ICP8*) (B), or late (*ICP5*) (C) protein (red), GFP (green), Hoescht (blue), and β II tubulin (magenta). 25-μm scale bar.

We went on to investigate whether viral mRNA expression was induced prior to the detection of Us11-GFP positive neurons. Using the triple stimulus, we detected an increase in viral lytic transcripts as early as 10 hours post-stimulus, which continued to increase, peaking at 48 hours post-stimulus (Fig. 2.6). Detection of immediate-early (Fig. 2.6A) and early transcripts (Fig. 2.6B) was slightly more robust than late transcripts (Fig. 2.6C-F). Because of the less robust increase in late gene expression, multiple late genes were analyzed, including the leaky late transcript VP16 and true-late transcripts encoding *gC*, *UL10*, and *UL36*. All late transcripts analyzed were not significantly increased beyond the latent samples until 20 hours post-stimulus (Fig. 2.6C-F).

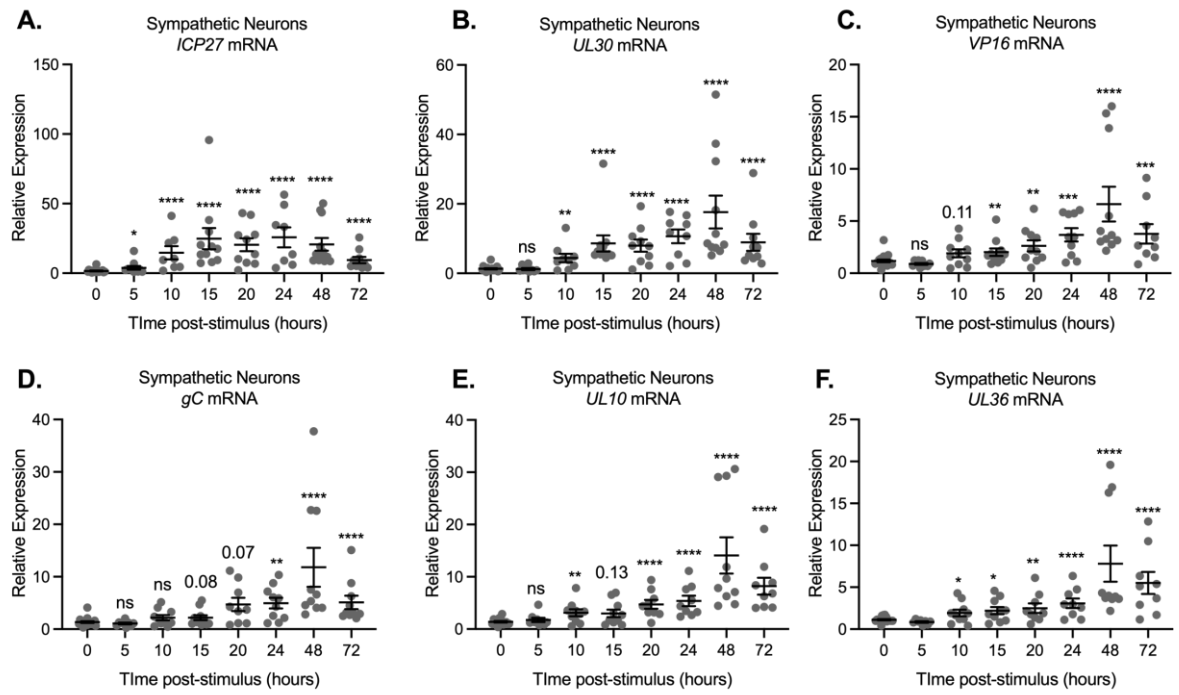

Figure 2.6 Viral gene expression can be restarted following latency establishment. Neonatal sympathetic neurons or adult sensory neurons were infected at an MOI of 7.5 PFU/cell with Stayput-GFP in the absence of viral DNA replication inhibitors. Following the loss of GFP, signaling quiescence of the culture, wells were reactivated with a variety of triggers, including combinations of LY294002 (20 μM), forskolin (60 μM), and heat shock (43°C for 3 h). (A to F) Immediate early (A), early (B), and late (C to F) viral transcripts were investigated over time following the stimulus. Reactivated samples were compared to latent samples described as 0 h poststimulus. $n = 9$ biological replicates from 3 litters. Mann-Whitney against 0 h (A to D). Normality was determined by the Kolmogorov-Smirnov test; *, $P < 0.05$; **,$P < 0.01$; ***, $P < 0.001$; ****, $P < 0.0001$. Individual biological replicates along with the means and SEMs are shown.

We were also interested to determine whether a similar quiescent infection could be established in adult sensory neurons and whether the kinetics of viral lytic gene expression were similar between sensory and sympathetic cultures. Following infection with Stayput-GFP in primary trigeminal ganglia (TG) neurons, GFP also increased by 1-day post-infection and then was lost over time (Fig. 2.7A). Assuming 5,000 neurons per well, Us11-GFP-positive neurons account for approximately 12% of the culture. GFP

was repeatedly lost within 15 days, a shorter period than that which is observed in neonatal sympathetic neurons. We also confirmed that the triple combinatorial stimulus elicits robust GFP re-emergence in adult TGs (Fig. 2.7B). Similar to what we observed in the sympathetic neurons, Us11-GFP positive neurons were detected by 48 hours post-stimulus. Intriguingly, superinfection only induced GFP expression to equivalent levels as the triple stimuli, which may be reflective of the repressive nature of sub-population of mature sensory neurons to lytic replication and reactivation (118, 269). The kinetics of viral lytic gene expression in sensory neurons following the reactivation stimulus mirrored those in sympathetic neurons, with an IE and E gene expression robustly induced by 15 hours post stimuli (Fig. 2.7C-D) and late gene expression by 20 hours (Fig 2.7E-F). Together, these data indicate that *in vitro* models of latency and reactivation can be established in sympathetic and sensory neurons in the absence of ACV and reactivation can be induced using a combination of triggers. In both models, a wave of lytic mRNA expression was detected at 15-20 hours post-stimulus, which was approximately 24 hours prior to the detection of Us11-GFP positive neurons.

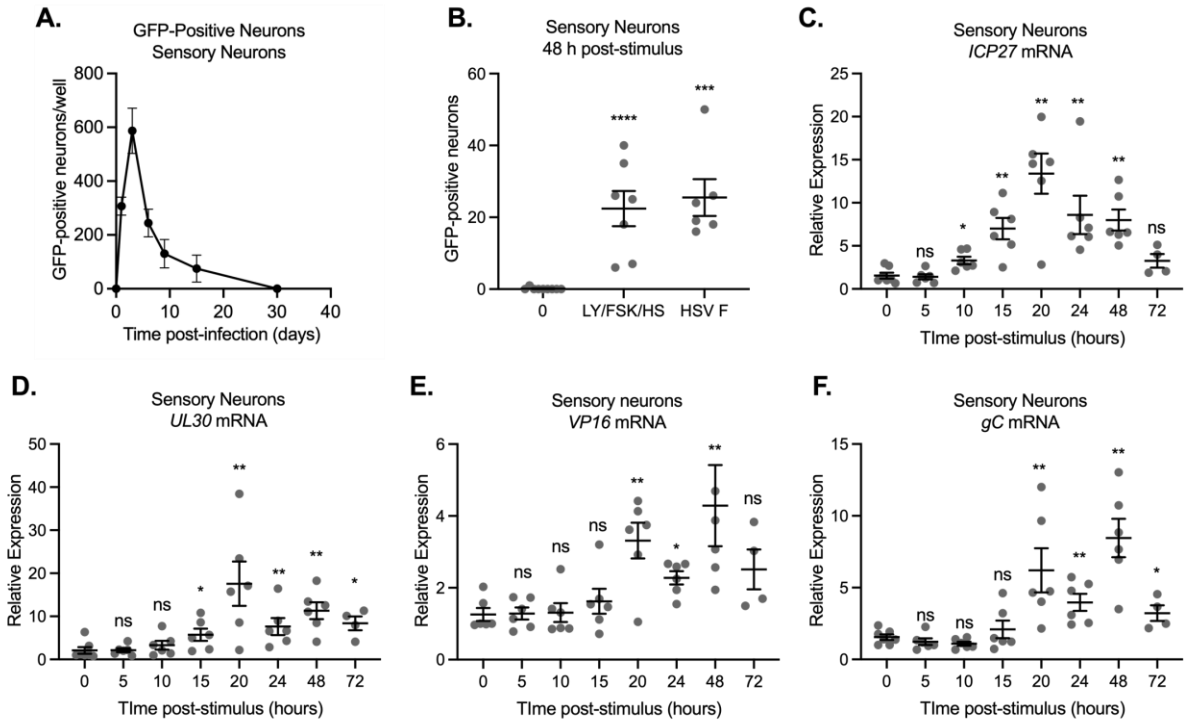

Figure 2.7 Reactivation from quiescently infected adult sensory trigeminal ganglia neurons. Neurons isolated from the trigeminal ganglia (TG) of female mice were infected with Stayput-GFP at an MOI of 7.5 PFU/cell. (A) The resolution of lytic infection was monitored over time by imaging and counting GFP-positive neurons. $n = 12$ biological replicates from 3 dissections. The mean and SEM are shown. Following the loss of GFP, signaling quiescence of the culture, wells were reactivated with a combination of LY294002 (20 μM), forskolin (60 μM), and heat shock (43°C for 3 h), as well as a superinfection with untagged F strain at an MOI of 10 PFU/cell. (B) GFP was quantified over time, and the peak GFP, at 48 h poststimulus, is depicted. $n = 9$ biological replicates. (C to F) Immediate early (C), early (D), and late (E and F) viral transcripts were investigated over time following the stimulus. $n = 6$ replicates. Mann-Whitney test against 0 h; *, $P < 0.05$; **, $P < 0.01$; ***, $P < 0.001$; ****, $P < 0.0001$. Individual biological replicates along with the means and SEMs are shown.

Neurons infected with Stayput-GFP undergo a DLK-dependent Phase I of reactivation.

Phase I reactivation has largely been investigated using *in vitro* models in which ACV has been used to promote latency establishment. In addition, Phase I has been found to occur with the single triggers of forskolin or LY294002 (99, 109, 223). The requirement of multiple triggers for reactivation suggested that multiple cell-signaling pathways converged to have a synergistic effect and induce reactivation in this more repressive model. Therefore, we were interested to determine whether the characteristics of Phase I reactivation occurred in the model of quiescent infection established in the absence of ACV and using the more robust trigger to induce reactivation. Potential Phase I viral transcription was investigated at 12.5 hours post-stimulus by RT-qPCR and Phase II was investigated when Us11-GFP positive neurons could be detected (48 hours post-stimulus). A characteristic of Phase I expression is the requirement of the stress kinase dual leucine zipper kinase (DLK) (99, 109). Therefore, using the DLK-specific inhibitor GNE3511 4 μM (293), we investigated the effect of DLK on reactivation in our system. We found up-regulation of immediate early/early transcripts 12.5 hours post-stimulus was eliminated with the addition of the DLK inhibitor (Fig. 2.8A-C). Further, full reactivation, demonstrated by peak GFP expression at 48 hours, was also reduced to baseline levels upon the addition of the DLK inhibitor (Fig. 2.8D). Therefore, using our new model of HSV-1 latency our data demonstrate that the initiation of viral lytic gene expression is dependent on DLK activity.

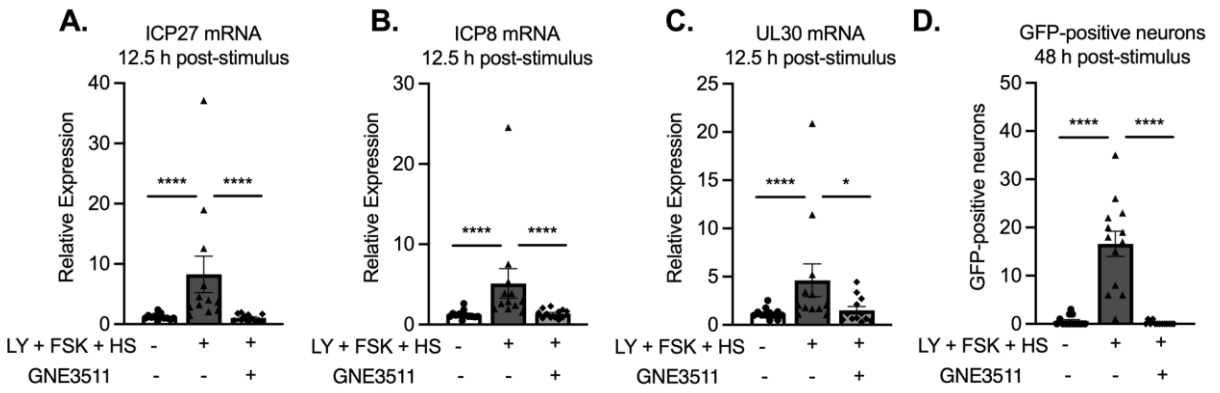

Figure 2.8 Reactivation is dependent on DLK. Cultures were infected with Stayput-GFP at an MOI of 7.5 PFU/cell in the absence of ACV. Following loss of GFP, cultures were reactivated with a combination of LY294002, forskolin, and heat shock in the presence of DLK inhibitor GNE-3511 (4 μM). (A to D) Immediate early (*ICP27*) and early (*ICP8/UL30*) viral genes (A to C) were investigated at 12.5 h poststimulus, and GFP was counted over time (D). Peak GFP, consistently around 48 h poststimulus, is presented. $n = 9$ biological replicates from 3 litters. Normality was determined by the Kolmogorov-Smirnov test. Mann-Whitney test; *, $P < 0.05$; **, $P < 0.01$; ***, $P < 0.001$; ****, $P < 0.0001$. The mean and SEM are shown.

In addition to the dependence on DLK activity, a further characteristic of Phase I gene expression is the induction of viral mRNA transcripts independently of the activity of histone de-methylase enzymes required for full reactivation. Therefore, we also triggered reactivation in the presence of de-methylase inhibitors. GSK-J4 is known to specifically inhibit the H3K27 histone demethylases UTX and JMJD3 (294) and has previously been found to inhibit HSV-1 reactivation but not Phase I gene expression (99, 109). OG-L002 is an LSD1 specific inhibitor. LSD1 has previously been shown to be involved in removal of H3K9me2 from HSV-1 genomes and its activity is required for full reactivation but not Phase I gene expression (99, 109, 261). , The initial expression of lytic transcripts at 12.5 hours post-stimulation was not inhibited by either OG-L002 or GSK-J4 (Fig. 2.9A-B). Full reactivation was reduced in the presence of OG-L002 or GSK-J4 as demonstrated by GFP-positive neurons at 48 hours (Fig. 2.9C). For OG-

L002, the reduction in the numbers of GFP-positive neurons was not significant, indicating that removal of H3K9me2 may not be as important as removal of H3K27me3 in this model system. Importantly, the initiation of gene expression in a manner that is independent of histone demethylase activity occurs when reactivation is induced by a triple stimulus and in a primary neuronal model in which latency was established without ACV.

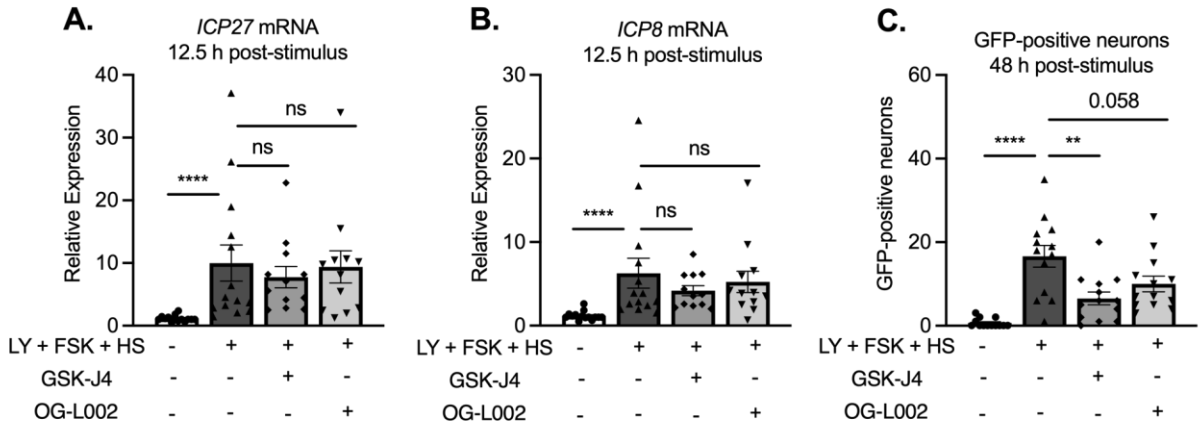

Figure 2.9 The early phase of lytic gene expression following a reactivation stimulus is independent of demethylase activity. Cultures were infected with Stayput-GFP at an MOI of 7.5 PFU/cell. Following loss of GFP, cultures were reactivated with a combination of LY294002, forskolin, and heat shock in the presence of H3K27 demethylase inhibitor GSK-J4 (2 μM) or H3K9 demethylase inhibitor OG-L002 (20 μM). Immediate early (*ICP27*) and early (*ICP8/UL30*) viral genes (A to C) were investigated at 12.5 h poststimulus, and GFP was counted over time. Peak GFP is presented. $n = 3$ biological replicates from 3 litters. Normality was determined by the Kolmogorov-Smirnov test. Mann-Whitney; *, $P < 0.05$; **, $P < 0.01$; ***, $P < 0.001$; ****, $P < 0.0001$. The mean and SEM are shown.

During Phase I, there is no detectable replication of viral genomes even though true late gene expression occurs (99, 109). In addition, using ACV models to establish latency, late gene expression has previously been found to occur to equivalent levels when viral DNA replication is inhibited during reactivation. Although we did observe late

gene expression during the initial period of lytic gene induction (12.5-20 hours), the increase was less robust than IE and E genes and appeared slightly delayed, not reaching significance for all analyzed late transcripts until 24 hours post-stimulus. Therefore, we investigated whether this late gene induction was dependent on viral DNA replication by reactivating in the presence of ACV. The addition of ACV did not inhibit the induction of lytic transcripts at 22 hours post-stimulus. Importantly, we included multiple true Late genes in this analysis, and all were induced to equivalent levels in the presence and absence of ACV (Fig. 2.10A-C). Therefore, the initial expression of late genes following a reactivation stimulus is independent of viral DNA replication. However, the addition of ACV did inhibit entry in full reactivation, demonstrated by Us11-GFP positive neurons at 48 hours post-stimulus, indicating that ACV was capable of blocking robust late gene expression at this late time-point (Fig. 2.10D). In summary, using a model system in which a quiescent infection is established without the need for ACV, all the previous characteristics of Phase I gene expression (dependence on DLK and independence of histone demethylase activity and viral DNA replication) were still observed.

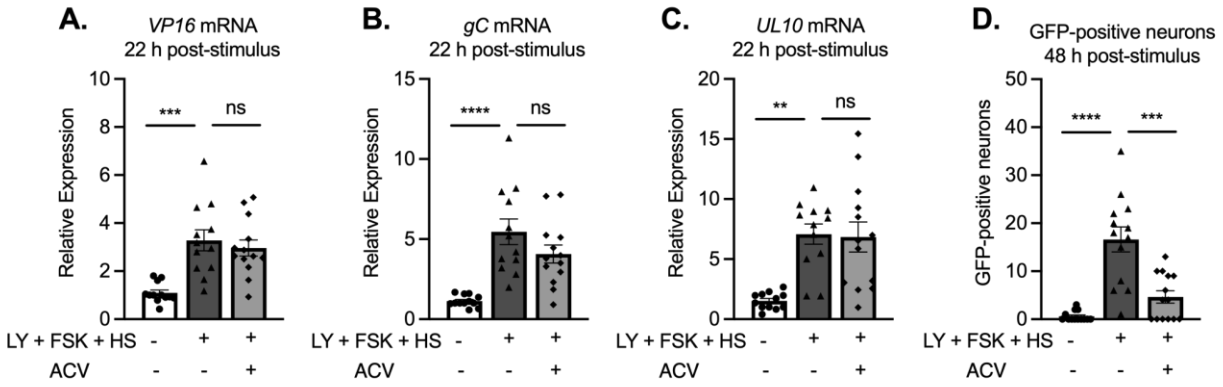

Figure 2.10 Differential dependence on viral DNA replication between phase I and II reactivation. Cultures were infected with Stayput-GFP at an MOI of 7.5 PFU/cell in the absence of ACV. Following loss of GFP, cultures were reactivated with a combination of LY294002, forskolin, and heat shock in the presence of ACV (50 μM). (A to D) Late (*VP16*, *gC*, *UL10)* genes (A to C) were investigated at 22 h poststimuli. GFP was counted over time, and peak GFP is presented (D). $n = 12$ biological replicates. Normality was determined by the Kolmogorov-Smirnov test. Mann-Whitney; *, $P < 0.05$; **, $P < 0.01$; ***, $P < 0.001$; ****, $P < 0.0001$. The mean and SEM are shown.

Discussion

We envision multiple uses for the Stayput-GFP virus model developed here for investigating HSV-1 neuronal infection *in vitro*. The Stayput-GFP virus is advantageous in models that otherwise use DNA replication inhibitors to promote latency establishment because it allows for the separation of initial viral gene expression/protein synthesis events and readouts from events that result from cell-to-cell spread. In addition, even in systems where ACV is used, there can be low levels of lytic replication or spontaneous reactivation after removal of ACV from cultures. The use of Stayput-GFP helps limit the confounding effects of spontaneous reactivation events by inhibiting subsequent cell-to-cell spread, while at the same time identifying neurons that escape quiescence. Further, the GFP tag serves as an imaging indicator in real time of when *de novo* lytic infection is resolved and latency is considered established. We are also able to track viral DNA replication and downstream late viral transcription and protein synthesis during the latency establishment process *in vitro*. The fate of lytic neurons, whether they undergo cell death or turn off gene expression programs and enter the latency pool, can also be investigated by tracking GFP and cell death at a single-cell level.

There are also some limitations to our system. Although there is some discrepancy in what defines reactivation (295), it is ultimately defined by the production of infectious virus. Due to the nature of the gH-deletion virus, *de novo* virus is by design non-infectious and we are unable to demonstrate reactivation in its strictest definition.

That said, we can readily demonstrate the re-emergence of all classes of viral gene transcripts, synthesis of viral capsid protein and replication compartment formation.

An intriguing finding in our study is that reactivation output decreases as length of infection increases. A potential explanation is that the viral genome becomes increasingly chromatinized over time, leading to a more repressive phenotype. In support of this hypothesis, the association of the facultative heterochromatin mark H3K27me3 with the HSV-1 genome increases dramatically between 10- and 15-days post-infection *in vivo* (122). The kinetics of H3K27me3 deposition remain to be investigated *in vitro*, but if they mirror *in vivo* observations, this could suggest that active chromatinization and reinforcement of silencing continues even after initial shut-down of viral gene expression. In the cellular context, H3K27me3 is linked with the recruitment of canonical Polycomb repressor complex 1 (cPRC1), which may reinforce silencing through long-range chromosomal interactions or 3D compaction (119, 296, 297). It is therefore possible that even following H3K27me3 formation on the genome, there are additional layers of protein recruitment that build up over time. In addition, it is also possible that the accumulation of viral non-coding RNAs expressed in latency could impact cellular pathways resulting in decreased signaling to the viral genome for reactivation. The use of the Stayput-GFP model system will permit these different avenues to be explored.

Our model system recapitulates the hallmarks of reactivation Phase I, which has previously been explored in *in vitro* systems using a DNA replication inhibitor. These

data are interesting considering the discrepancies in conclusions drawn about reactivation between *in vitro* and *in vivo* modeling. There is evidence *ex vivo* for a Phase I as all classes of viral gene are expressed in a disordered, non-cascade fashion when a combination of explant and nerve-growth factor deprivation are used (101). However, in other models of reactivation *ex vivo*, there is evidence that Phase-I-like gene expression may not occur, especially from studies investigating the requirement for histone demethylase inhibitors. These latter experiments used explant (axotomy) to induce reactivation and found that the earliest induction of lytic gene expression is dependent on H3K9 demethylase activity (260, 261). In a recent study from our lab, we have found that Phase I reactivation can occur *ex vivo* when axotomy is combined with PI3-kinase inhibition, although with more rapid kinetics than those observed here (98). These discrepancies between may result from the different trigger used to induce reactivation or currently unknown effects of latency established *in vivo*. Importantly, here we have demonstrated that any potential differences between *in vivo* and *in vitro* observations on the mechanisms of reactivation do not result from the use of ACV to establish a quiescent infection. It is worth noting that despite decreases in GFP-positive neurons following reactivation in the presence of either H3K9 or H3K27 demethylase inhibitor, some neurons still become GFP-positive especially in the OG-L002 (H3K9 demethylase inhibitor) treated neurons. Although viral genomes have previously been shown to be enriched for both H3K9me2/3 and H3K27me3 in latency (99, 120, 121, 123) the relationship between the different modifications and whether they exist on the same or different genomes is not known. In addition, whether reactivation occurs from genomes differentially enriched for H3K9me2/3 or H3K27me3 when different triggers of

reactivation are used has not been investigated. One possible explanation is that the triple stimuli used here may be a more effective reactivation trigger for H3K27me3 enriched genomes. Further work using the Stayput-GFP model system will help determine whether there is heterogeneity in the heterochromatin on viral genomes and the role of removal of specific types of heterochromatin for reactivation in response to different stimuli.

Phase I, in addition to occurring synchronously and independently of histone demethylases, also occurs in the absence of viral protein synthesis. In an *in vitro* model employing ACV during latency establishment and stimulus LY294002 during reactivation, it is demonstrated that initial viral transcription occurs before the appearance of viral late protein synthesis and, specifically, independently of viral transactivator VP16 (223, 224). Therefore, cellular host factors must be responsible for instigating the initial reactivation process. Evidence from an *in vitro* model system has demonstrated these events are in fact navigated by cellular proteins JNK and DLK (99). Interestingly, host cell proteins may also be implicated in restricting the full reactivation process, including Gadd45b which appears to antagonize the HSV-1 late expression program to prevent full reactivation (224). Interestingly, Gadd45b mRNA is increased in response to LY294002 only in infected neurons, suggesting perhaps that a viral factor may be mediating the gatekeeping from Phase I to Phase II reactivation.

In our system, Phase I gene expression was dependent on the neuronal regulator of JNK activity, DLK, highlighting the central role of DLK in HSV-1 reactivation.

DLK is a cell protein implicated in neuronal stress signaling upstream of cellular protein JNK (298). It has previously been found to be essential for HSV-1 reactivation following PI3-kinase inhibition (99), as well as neuronal hyper-excitability through forskolin (109). However, it has not, until now, been shown to be central to reactivation mediated by heat shock. Although heat shock has been used as a trigger for HSV-1 reactivation (96, 113, 286-291), the downstream molecular events following this stimulus are not well elucidated. Multiple studies have demonstrated that heat shock during reactivation leads to the up-regulation of heat shock proteins, although none of them knowingly relate to DLK. Following hyperthermia-induced reactivation *in vivo*, heat shock protein HSP60 and HSP40 have been demonstrated to be up-regulated (291). Components of the heat shock response pathway have also been demonstrated to be up-regulated by LY294002 treatment in an *in vitro* system (224), including HSP70. In fact, in this same system, treatment with cultures of heat shock factor 1 (HSF-1) activator compound causes robust reactivation. Outside of the virological context, heat shock protein chaperone HSP90 has been shown to bind and maintain DLK stability *in vivo* and it is specifically required for DLK function following axon injury signaling (299). It is a possibility that heat shock in our system is enhancing the function of DLK. Therefore, multiple signals may converge on DLK, which is then able to activate JNK and histone phosphorylation and to promote lytic gene expression from the heterochromatin-associated viral genome for reactivation to occur. Indeed, synergy has been demonstrated to enhance DLK activity in neurons (300). This central role for DLK is especially important as it is largely a neuron-specific protein that regulates the response

to multiple forms of stress (301) and is therefore a potential target for novel therapeutics that would prevent HSV-1 gene expression and ultimately reactivation.

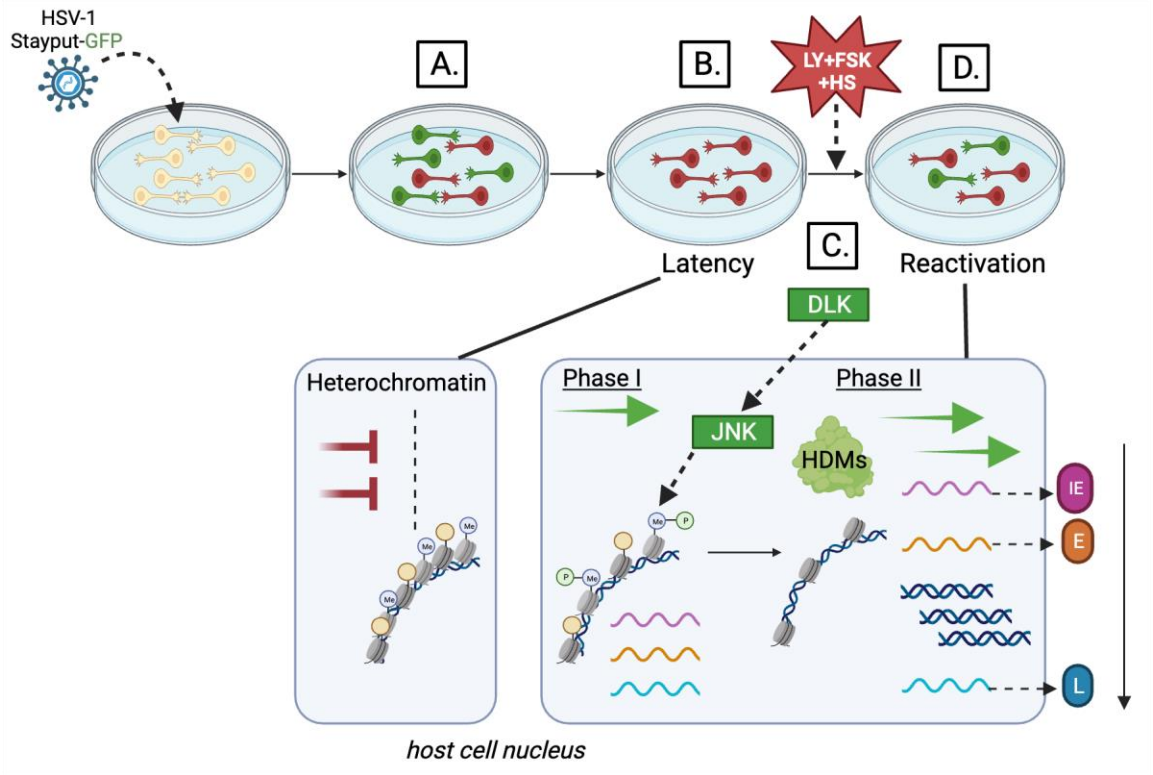

Figure 2.11 Summary. (A) Following infection with HSV-1 Stayput-GFP in the absence of antivirals, a population of neurons become lytically infected (green) or latently infected (red). Lytically infected neurons enter the latent population or die and are washed away from the cultures-and these events can be tracked at a single neuron resolution. (B) Over 30 days post-infection, lytic infection is resolved and latency is established. (C) Following treatment with a triple combination trigger, latent viral genomes undergo reactivation in a biphasic manner. Phase I is a DLK-dependent, synchronous burst of viral gene expression that does not require histone H3K9 or H3K27 demethylase (HDM) activity. IE mRNA and protein are shown in magenta, E mRNA and protein in orange, and L mRNA and protein in blue. (D) Individual neurons in which full reactivation occurs can be identified and quantified through the expression of GFP fluorescence.

~End of Chapter 2~

Chapter 3: c-Jun Signaling During Initial HSV-1 Infection Modulates Latency to Enhance Later Reactivation in addition to Directly Promoting the Progression to Full Reactivation

Parts of this chapter have been adapted from:

Dochnal, SA, Whitford AL, Francois AK, Krakowiak PA, Cuddy SR, & Cliffe, AR. c-Jun Signaling During Initial HSV-1 Infection Modulates Latency to Enhance Later Reactivation in addition to Directly Promoting the Progression to Full Reactivation *In review*. (2023)

Abstract

Herpes simplex virus-1 (HSV-1) establishes a latent infection in peripheral neurons and can periodically reactivate to permit transmission and clinical manifestations. Viral transactivators required for lytic infection are largely absent during latent infection and therefore HSV-1 relies on the co-option of neuronal host signaling pathways to initiate its gene expression. Activation of the neuronal c-Jun N-terminal kinase (JNK) cell stress pathway is central to initiating biphasic reactivation in response to multiple stimuli. However, how host factors work with JNK to stimulate the initial wave of gene expression (known as Phase I) or the progression to full, Phase II reactivation remains unclear. Here, we found that c-Jun, the primary target downstream of neuronal JNK cell stress signaling, functions during reactivation but not during the JNK-mediated initiation of Phase I gene expression. Instead, c-Jun was required for the transition from Phase I to full HSV-1 reactivation and was detected in viral replication compartments of reactivating neurons. Interestingly, we also identified a role for both c-Jun and enhanced neuronal stress during initial neuronal infection in promoting a more reactivation-competent form of HSV-1 latency. Therefore, c-Jun functions at multiple stages during HSV latent infection of neurons to promote reactivation. Importantly, by demonstrating that initial infection conditions can contribute to later reactivation abilities, this study highlights the potential for latently infected neurons to maintain a molecular scar of previous exposure to neuronal stressors.

Introduction

Long-term viral infection can be regulated at multiple steps by the activation of host-cell signaling pathways. The Herpesviruses establish lifelong latent infections within specific host cells and periodically reactivate to permit transmission. During latent infection, the double-stranded DNA herpesvirus genomes reside in an epigenetically silent state, coated with host histone proteins within host nuclei (173, 193, 302-305). The transcription of viral lytic mRNAs is largely repressed and therefore viral proteins that mediate lytic gene transactivation during productive infection are largely absent. To reactivate, repressed herpesviruses rely on host signaling pathways that appear to play important physiological roles in their respective latent cell type. For example, the Gammaherpesvirus Epstein-Barr virus (EBV) establishes latency in memory B cells, and reactivation can be initiated following B cell receptor ligation and activation (306). Likewise, the Betaherpesvirus human cytomegalovirus (HCMV) establishes a latent infection in hematopoietic progenitor cells and reactivation can be initiated through cytokine signaling, including TNFα, which mediates differentiation (307-310). Following activation of these signaling pathways, host transcriptional factors activated downstream of signaling pathways can bind viral genomes to initiate lytic expression (311). Understanding the contribution of host cell proteins to the initiation of reactivation can help uncover the mechanisms of viral expression and ultimately identify targets for therapeutics that can prevent the occurrence of reactivation.

The Alphaherpesvirus, Herpes Simplex Virus-1 (HSV-1), establishes a latent infection in post-mitotic neurons, during which lytic promoters are assembled into

heterochromatin, as defined by the enrichment of trimethylated histone H3 lysine 27 (H3K27me3) and di- and tri-methylated lysine 9 (H3K9me2/3) (119, 121, 123, 124, 201). Periodically, following common physiological stressors like fever, UV exposure, and psychological stress, full reactivation, as characterized by new infectious virus production, can occur. At the neuronal level, the activation of certain signaling pathways have been found to induce reactivation (reviewed in (8)). These include the loss of neurotrophic factor support (99, 103, 105, 107, 108, 117, 312, 313), enhanced neuronal hyperexcitability (109, 117), and perturbation of the DNA damage response and axonal damage (233, 314). However, unlike the studies of EBV and HCMV, the host transcription factors that act downstream of a reactivation stimulus are largely unknown.

Transcriptionally, full reactivation of HSV-1 mirrors *de novo* acute replication, which takes place in neuronal and non-neuronal cells; viral immediate early (IE) gene transcription precedes and is essential to early (E) gene expression, which is required for viral DNA (vDNA) replication, and subsequent late (L) gene transcription. Efficient IE gene expression and therefore the entire downstream lytic transcriptional cascade during acute infection or full reactivation, requires viral trans-activator VP16. VP16 complexes with cellular factors involved in transcriptional activation, including general transcription factors, ATP-dependent chromatin remodelers, RNA polymerase, and histone-modifying enzymes that may remove repressive H3K9me2/3 and add euchromatin-associated modifications (84, 87, 260-262, 315). In the context of acute infection, VP16 is delivered to the host cell nuclei with the incoming virus' tegument. However, during a latent infection, transcription of the gene encoding VP16 (*UL48*) is

restricted and therefore viral gene expression must initiate in the absence of VP16 protein by alternative host or viral factors.

There is accumulating evidence that reactivation is a biphasic process. Phase I gene expression precedes “full reactivation” (also referred to as “Phase II”) as a transcriptional burst of all classes of lytic viral genes, with late gene expression being uncoupled from viral DNA replication. This Phase I gene expression phenomenon has been observed in both *in vitro* and *ex vivo* models of HSV reactivation (98, 99, 109, 117, 223, 265). The use of *in vitro* model systems has enabled the molecular mechanisms of Phase I and Phase II reactivation to be further teased apart. In these models, Phase I reactivation does not require VP16 nor activation of the host histone demethylase enzymes that remove H3K27me3 and H3K9me2 (99, 109, 117, 223, 265). However, Phase I reactivation, and as well as the progression to full Phase II, requires the activation of cellular c-Jun N-terminal kinase (JNK), which is specifically redirected to a physiologic neuronal stress signaling through mixed lineage kinase protein dual leucine kinase (DLK) and the JNK scaffold protein, JNK-interacting protein-3 (JIP3). The contribution of this neuronal stress signaling pathway was first demonstrated during reactivation using small molecule inhibitor LY294002, which inhibits the activation of the PI3-kinase and AKT-pathways that occur downstream of NGF-signaling (99). Since this discovery, the requirement of DLK/JNK for viral reactivation has been demonstrated using multiple systems and triggers converging upon diverse cellular pathways. HSV-1 can co-opt an innate immune signaling pathway mediated by IL-1, which induces neuronal hyperexcitation and subsequent reactivation (109). HSV-1 reactivation is also

elicited via disruption of neuronal DNA damage or repair pathways, for example through the addition of DNA damaging agents or the inhibition of the ATM-dependent repair pathway by AKT inhibition (112, 228). In response to a combinatorial stimulus of an NGF-deprivation mimic (LY294002), neuronal hyperexcitability (forskolin), and heat shock, reactivation can be induced from a very silent form of latency established *in vitro* (117). DLK is integral to reactivation using all these stimuli and, JNK has also demonstrated to be required when tested in these systems.

JNK activation during Phase I of HSV-1 reactivation results in the phosphorylation of serine (S10) neighboring repressive mark H3K9me3, and possibly H3K27me3, on the viral genome during Phase I (99). This phospho/methyl switch is known to result in the eviction of repressive reader proteins and therefore likely permits a chromatin environment that is conducive to transcription (316-318). However, additional host proteins, including transcription and pioneer factors, that directly promote viral gene expression would also be required for Phase I reactivation. Moreover, JNK lacks DNA binding capabilities, which suggests that an additional DNA-binding protein mediates JNK recruitment to viral chromatin.

DLK-mediated activation of JNK both up-regulates and phosphorylates its primary transcriptional factor target c-Jun, which can mediate neuronal cell death and axon pruning following the loss of nerve-growth factor signaling (298, 319-321). We previously observed c-Jun activation in neuronal models used for HSV-1 latency following PI3-kianse inhibition (99) and forskolin treatment (109). Unlike traditional

transcription factors, c-Jun can maneuver or pioneer through heterochromatin to modulate genome accessibility in a broad range of host cells, including neurons (231, 232). c-Jun is a basic leucine zipper domain (bZIP) protein that therefore must dimerize to bind DNA, and c-Jun binds most potently to Fos proteins as the “AP-1” complex to AP-1/TRE elements on the cellular genome (322-324). In the case of human gamma herpesvirus EBV, viral factor BZLF1, which shares substantial homology with AP-1, pioneers through heterochromatin on the latent genome and acts as a switch between latency and lytic replication, recruiting remodeling complexes that can remove H3K27me3 (325). Interestingly, c-Jun and c-Fos up-regulation in neurons has been recorded upon HSV-1 infection and reactivation *in vivo* (326, 327), and c-Fos is the primary readout for neuronal hyper-excitability, which has been demonstrated to initiate reactivation *in vitro* (109). However, c-Jun can also homodimerize or heterodimerize with other transcriptional activator proteins including ATF family members, other Jun family proteins, and PU.1. We therefore set out to investigate whether AP-1, and specifically c-Jun, are critical to HSV-1 reactivation, with the hypothesis that c-Jun up-regulation and phosphorylation by JNK acts to induce Phase I gene expression. Interestingly, we found that c-Jun protein was required for reactivation during Phase II, but does not function directly during Phase I. In carrying out this study we also found that activation of c-Jun via neuronal stress during *de novo* infection resulted in enhanced reactivation. Therefore, we show that cell stress, and potentially other signals that could activate c-Jun during initial neuronal infection, can have a long-term impact on either the neuron or viral chromatin to regulate the propensity of HSV-1 to reactivate.

Results

AP-1 is not required for HSV-1 reactivation *ex vivo* or *in vitro*.

On the cellular genome, c-Jun is best characterized as heterodimerizing with the transcriptional factor c-Fos in the AP-1 complex, which subsequently undergoes a conformational change to bind DNA. c-Jun and c-Fos are respectively implicated in the NGF-deprivation and neuronal hyperexcitability pathways, both of which are co-opted by HSV-1 to reactivate. Therefore, we proposed that c-Jun mediates HSV-1 reactivation through the AP-1 complex. We began in an *ex vivo* model, where latently infected ganglia were reactivated with PI3-kinase inhibition using LY294002 in the presence or absence of AP-1 inhibitor T-5224. We considered T-5224 to be a good candidate to examine in the context of HSV reactivation in a mouse model as it is a well-characterized, selective inhibitor of AP-1 DNA-binding (328). T-5224 was synthesized based upon a three-dimensional (3D) pharmacophore model and *in silico* modeling derived from the X-ray crystal structure of the basic region-leucine zipper (bZIP) domains of c-Fos and c-Jun bound to a DNA fragment containing the AP-1 consensus site. T5224 is therefore specifically synthesized to target the DNA-binding pocket domain formed by the unique combination of c-Jun and c-Fos. Moreover, T-5224 is also capable of inhibiting HMCV re-entry into robust lytic replication in $CD34^{+}$ hematopoietic progenitor cells (329). PI3-kinase signaling is lost following the deprivation of NGF (277) and this is commonly used to trigger reactivation *in vitro* (93, 99, 103, 107, 108) and in combination with axotomy *ex vivo* (98). In addition, PI3-kinase inhibition in sympathetic neuronal-like PC12 cells has previously been shown to result in increased levels of Fos and c-Jun (330). We have previously identified a Phase I wave of gene expression *ex vivo* proceeds quickly, as early as 5 hours post-stimulus (98). We therefore decided to

investigate a later time-point when full reactivation in the *ex vivo* model can be detected (20 hours post-stimulus) to initially determine whether T-5224 can inhibit any stage of reactivation.

Unexpectedly, the addition of T-5224 did not decrease LY294002-mediated reactivation *ex vivo* (Fig 3.1A-C) as indicated by IE (ICP27), E (ICP8) and L (gC) gene expression, indicating that the c-Fos-AP1 transcription factor was not required for lytic gene expression *ex vivo* in response to PI3-kinase inhibition with axotomy. However, one caveat to these *ex vivo* conditions is that it is difficult to ensure full penetrance of the drug, although we have previously shown that DLK-inhibitors, JNK-inhibitors, and acyclovir can inhibit explant induced reactivation (98).

As a complementary approach and to test reactivation in intact neurons, we also examined the ability of T-5224 to inhibit reactivation in an *in vitro* model of HSV latent infection. Latent infection was established in primary sympathetic neurons isolated from the superior cervical ganglia (SCG) of newborn mice as described previously (93, 99, 109, 117). Neurons were infected with a gH-null virus containing Us11-GFP (Stayput-GFP), which permits the quantification of individual reactivating neurons during full, Phase II reactivation. The addition of T-5224 did not prevent reactivation as quantified by the numbers of GFP-positive following LY294002-mediated reactivation and instead showed a slight increase in reactivation (although this increase was slightly below the level of significance; $p = 0.0671$ Mann-Whitney test, Fig 3.1D). The addition of T-5224 slightly enhanced LY294002-mediated Phase I gene expression as determined by the

levels of representative viral lytic viral transcripts ICP27 and ICP8 at 18 hours post-stimulus (Fig 3.1E-F); for ICP27 but not ICP8 this enhancement was statistically significant. Therefore, inhibition of the AP-1 complex via T-5224 did not prevent, and even slightly enhanced, PI3-kinase induced reactivation.

HSV-1 reactivation via PI3-kinase inhibition shares features with neuronal apoptosis in immature neurons following NGF deprivation. Loss of NGF-signaling results in loss of PI3-kinase inhibition and DLK/JNK activation, and cell death depends on DLK, JNK, and c-Jun, which promote the induction of pro-apoptotic BH3-only proteins. Therefore, we investigated whether T-5224 could prevent apoptosis mediated by loss of NGF-signaling. Interestingly, T-5224 did not prevent NGF-deprivation induced cell death in cultured sympathetic neurons (Fig 3.1G), suggesting NGF-deprivation signaling in this neuronal subtype may not be mediated through c-Jun and c-Fos, but by c-Jun and an alternative binding partner. This is a conceivable possibility as a similar phenotype has been previously demonstrated; in rat cerebellar granule neurons, c-Jun mediates apoptosis through dimerization with ATF2 rather than c-Fos (331).

Complementary to the *ex vivo* experiments, we also investigated whether AP-1 inhibition disrupted reactivation elicited by the commonly used alternative trigger forskolin. We recently demonstrated that forskolin drives HSV-1 reactivation through neuronal excitation rather than the interruption of the nerve growth deprivation pathway by LY294002, although both triggers are dependent on neuronal stress signaling kinase DLK (109). The readouts of GFP-positive neurons representative of Phase II (Fig 3.1H)

and viral gene transcription during Phase I (Fig 3.1I-J) were not depleted with T-5224 in combination with forskolin, but instead enhanced. Therefore, c-Jun as a part of the AP-1 complex is not required for HSV-1 reactivation. This data rather suggests that the specific combination of c-Jun and c-Fos could be repressive to HSV-1 biphasic reactivation.

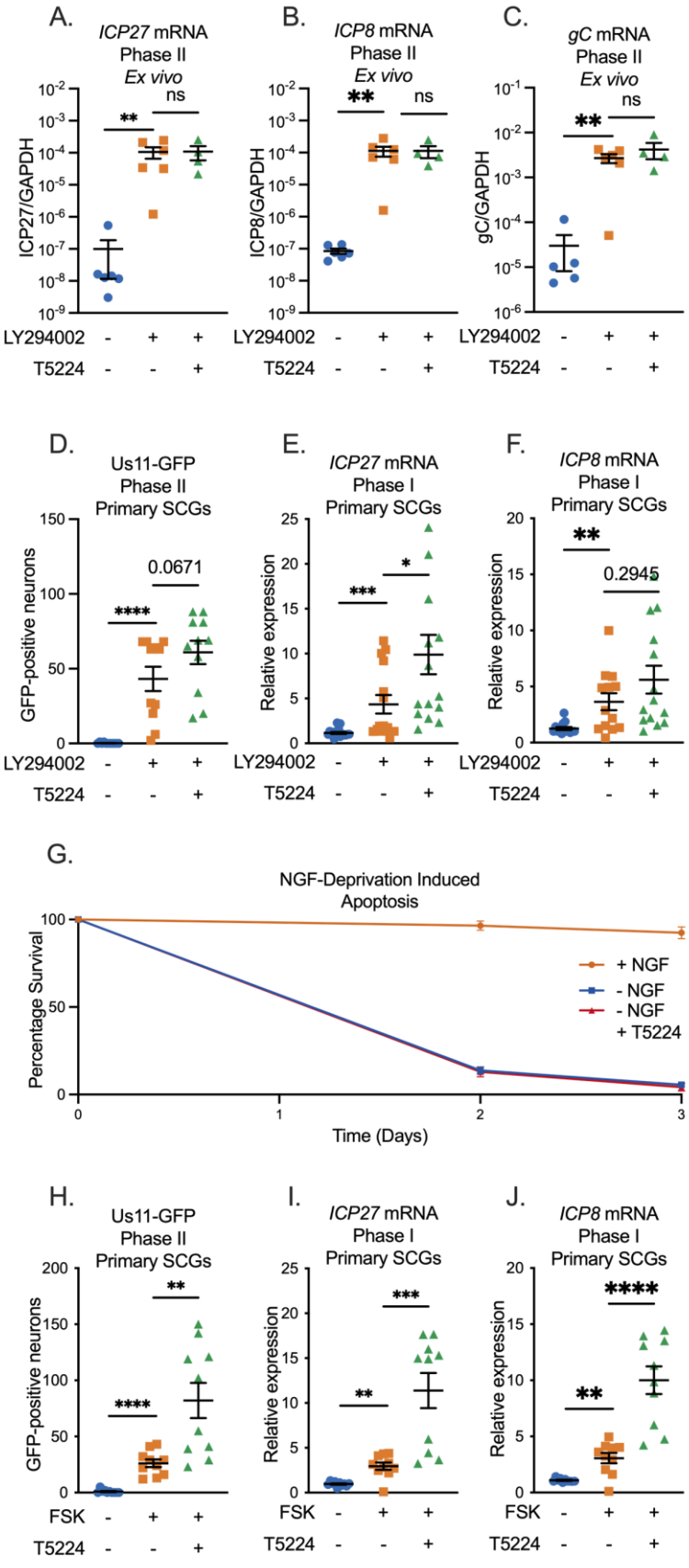
A.
ICP27 mRNA
Phase II
Ex vivo
ICP27/GAPDH
**
ns
B.
ICP8 mRNA
Phase II
Ex vivo
ICP8/GAPDH
**
ns
C.
gC mRNA
Phase II
Ex vivo
gC/GAPDH
**
ns
LY294002 - + +
T5224 - - +
D.
Us11-GFP
Phase II
Primary SCGs
GFP-positive neurons
****
0.0671
E.
ICP27 mRNA
Phase I
Primary SCGs
Relative expression
***
*
F.
ICP8 mRNA
Phase I
Primary SCGs
Relative expression
**
0.2945
G.
NGF-Deprivation Induced
Apoptosis
Percentage Survival
+ NGF
- NGF
- NGF
+ T5224
Time (Days)
H.
Us11-GFP
Phase II
Primary SCGs
GFP-positive neurons
****
**
FSK - + +
T5224 - - +
I.
ICP27 mRNA
Phase I
Primary SCGs
Relative expression
**
***
J.
ICP8 mRNA
Phase I
Primary SCGs
Relative expression
**
****

Figure 3.1 AP-1 is not required for HSV-1 reactivation *ex vivo* or *in vitro*. (A-C) Mice were infected with WT HSV-1 by corneal scarification, and trigeminal ganglia (TG) were dissected 28 days following infection. Ganglia were reactivated for 20 hours in neuronal media alone, or with the addition of LY294002 (40 μM) or LY294002 and AP-1 inhibitor T-5224 (20 μM). Viral mRNA quantification is shown for the immediate early ICP27 (A), early ICP8 (B), and late gC (C) transcripts normalized to cellular the control mRNA, GAPDH. At least 4 biological replicates; Mann-Whitney test. (D-F) Latently infected primary sympathetic SCG neurons were reactivated with LY294002 (20 μM), in the presence or absence of the AP-1 inhibitor T-5224 (20 μM). The number of GFP-positive neurons at 48 hours post-stimulus is shown (D). 11 biological replicates from 4 separate dissections; Mann-Whitney test. Viral gene expression at 18 hours post-stimulus relative to latent samples quantified by RT-qPCR for ICP27 (E) or ICP8 (F) normalized to the cellular control mGAPDH.15 biological replicates from 4 independent dissections; Mann-Whitney test. (G) Neurons were treated with media containing NGF or NGF-deprived with or without T-5224 20 μM. Cell death per field of view was quantified over time based on numbers of surviving neurons. 2 biological replicates. (H-J) Latently infected neurons were reactivated with forskolin (60 μM) in the presence or absence of T-5224 and the number of GFP-positive neurons at 48 hours post-stimulus (H) and relative expression of lytic transcripts ICP27 (I) and ICP8 (J) at 18 hours post-stimulus are presented. 10 biological replicates from 3 independent dissections; Mann-Whitney test. Normality determined by Kolmogorov-Smirnov test. Individual biological replicates along with the means and SEMs are represented. *, $P < 0.05$; **, $P < 0.01$. ns, not significant. One replicate from experiments in Panels D & H was performed by Sean R. Cuddy.

c-Jun depletion prior to latency establishment perturbs both Phase I gene expression and full reactivation.

To Investigate the contribution of c-Jun to HSV-1 latency and reactivation, we used an *in vitro* primary neuronal model because this permits the easy manipulation of c-Jun at different times during the latency/reactivation cycle. In addition, robust reactivation can be achieved in intact neurons using this system. Latent infection was established in sympathetic neurons isolated from the superior cervical ganglia (SCG) of newborn mice as described previously (93, 99, 109, 117). Neurons were infected with a gH-null virus containing Us11-GFP (Stayput-GFP), which permits the quantification of

individual reactivating neurons neuronal model (117). Depletion of c-Jun protein was validated in SCG neurons using three independent shRNA lentiviruses (Fig 3.2A). c-Jun was depleted from primary neurons using the two most effective lentiviruses (sh-cJun2 and sh-cJun3) and subsequently infected with HSV-1 Stayput-GFP at an MOI of 7.5 PFU/cell in the presence of acyclovir (ACV; 50μM) for six days. Two days post removal of the acyclovir, the infected neurons were reactivated with the PI3-kinase inhibitor, LY294002 (20 μM), and the number of Us11-GFP-positive neurons was quantified at 48 hours post-treatment, which is indicative of Phase II reactivation, in addition to Phase I lytic gene expression analysis at 18 hours post-treatment. Despite similar viral DNA loads during latency (Fig 3.2B), both full reactivation (Fig 3.2C, F) and Phase I gene expression (Fig 3.2D-E, G-H) were significantly reduced in c-Jun depleted cultures. Therefore, the presence of c-Jun protein during HSV latent infection was required for the initial exit from latency and Phase I gene expression.

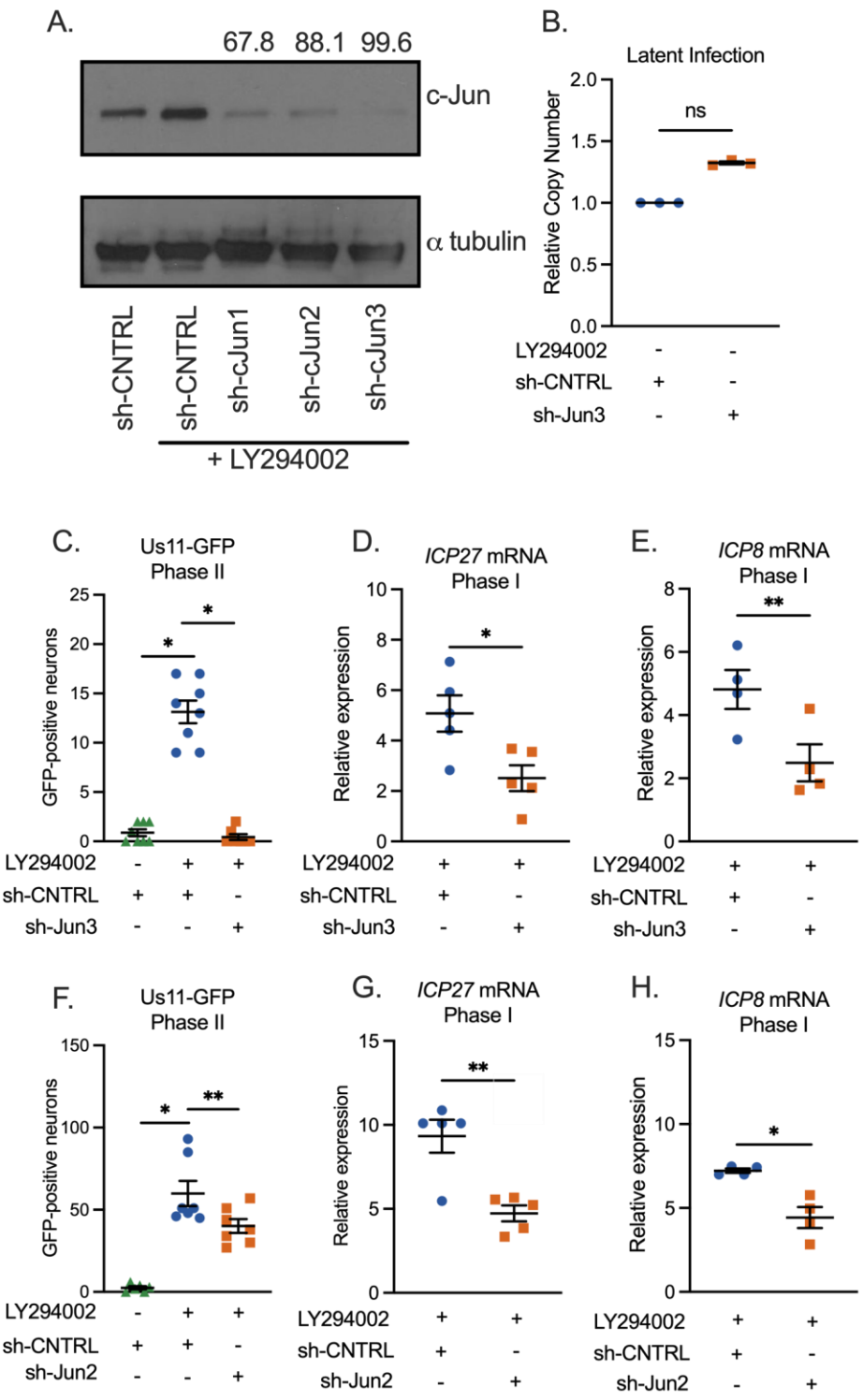
A.
67.8 88.1 99.6
c-Jun
α tubulin
sh-CNTRL
sh-CNTRL
sh-cJun1
sh-cJun2
sh-cJun3
+ LY294002
B.
Latent Infection
Relative Copy Number
ns
LY294002
sh-CNTRL
sh-Jun3
C.
Us11-GFP
Phase II
GFP-positive neurons
LY294002
sh-CNTRL
sh-Jun3
D.
ICP27 mRNA
Phase I
Relative expression
LY294002
sh-CNTRL
sh-Jun3
E.
ICP8 mRNA
Phase I
Relative expression
LY294002
sh-CNTRL
sh-Jun3
F.
Us11-GFP
Phase II
GFP-positive neurons
LY294002
sh-CNTRL
sh-Jun2
G.
ICP27 mRNA
Phase I
Relative expression
LY294002
sh-CNTRL
sh-Jun2
H.
ICP8 mRNA
Phase I
Relative expression
LY294002
sh-CNTRL
sh-Jun2

Figure 3.2 c-Jun depletion prior to latency establishment limits both Phase I gene expression and full reactivation. A) Neurons were transduced with a non-targeting shRNA control lentivirus or one of three independent lentiviruses expressing shRNAs that target Jun (sh-cJun1, sh-cJun2, sh-cJun3). 5 days post transduction, LY294002 was added to neurons for 18 hours and western blotting for c-Jun or a-tubulin was performed. The percentage knockdown of c-Jun normalized to a-tubulin is shown. B-H) Following c-Jun depletion with sh-cJun3 (B-E) or sh-cJun2 (F-H), primary neurons were infected with Stayput-GFP at an MOI of 7.5 PFU/cell in the presence of acyclovir (ACV; 50 μM) for six days and then reactivated two days after the removal of acyclovir with LY294002 (20 μM). B) Quantification of relative latent viral DNA load at 8 days post-infection. Biological replicates from 3 separate dissections C & F) Quantification of the number of GFP-positive neurons at 48 hours post-stimulus. Individual biological replicates from at least 3 individual dissections. D-E, G-H) Relative viral gene expression at 18 hours post-stimulus compared to latent samples quantified by RT-qPCR for ICP27 (D,G), ICP8 (E,H) normalized to cellular control mGAPDH. Statistical comparisons were made using normal or non-normal (Wilcoxon, B, C, F) Paired t-Test. Biological replicates from at least 3 individual dissections. Individual biological replicates along with the means and SEMs are represented. * $P < 0.05$; ** $P < 0.01$. 2 replicates of the experiment in Panel D-E were performed by Abigail Whitford.

c-Jun depletion following latency establishment does not prevent entry into Phase I.

The data shown in Figure 1 support our hypothesis that c-Jun mediates Phase I gene expression and ultimately full reactivation downstream of the DLK/JNK signaling cascade. However, these experiments come with the caveat that c-Jun was depleted prior to HSV-1 infection and therefore we cannot rule out an indirect role of c-Jun in latency establishment that ultimately perturbs reactivation. To test the role of c-Jun solely in Phase I reactivation, the time point where both DLK and JNK act to promote exit from latency, and therefore reactivation, we depleted c-Jun following HSV-1 infection and latency establishment and analyzed Phase I gene expression. In contrast to what we observed following depletion of c-Jun prior to infection, Phase I gene expression was not perturbed following c-Jun depletion after latency establishment (Fig

3.3A-C). Importantly, we verified knockdown at the RNA level for each replicate (Fig 3.3D). This phenotype was not limited to a single shRNA clone as Phase I gene expression remained unchanged with the additional two independent c-Jun lentiviruses (Fig 3.3E-G) that were previously validated (Fig. 3.2A). In addition, this phenotype was not limited to one trigger as c-Jun was also not required for Phase I gene expression triggered by forskolin (Fig 3.3H-K). In contrast, c-Jun depleted cultures displayed unexpectedly enhanced Phase I gene expression following treatment with forskolin. Therefore, our data indicate that c-Jun does not play a direct role alongside DLK and JNK in supporting Phase I gene expression during reactivation. In addition, these data contrasted what was observed for the impact of c-Jun depletion pre-infection on entry into Phase I gene expression.

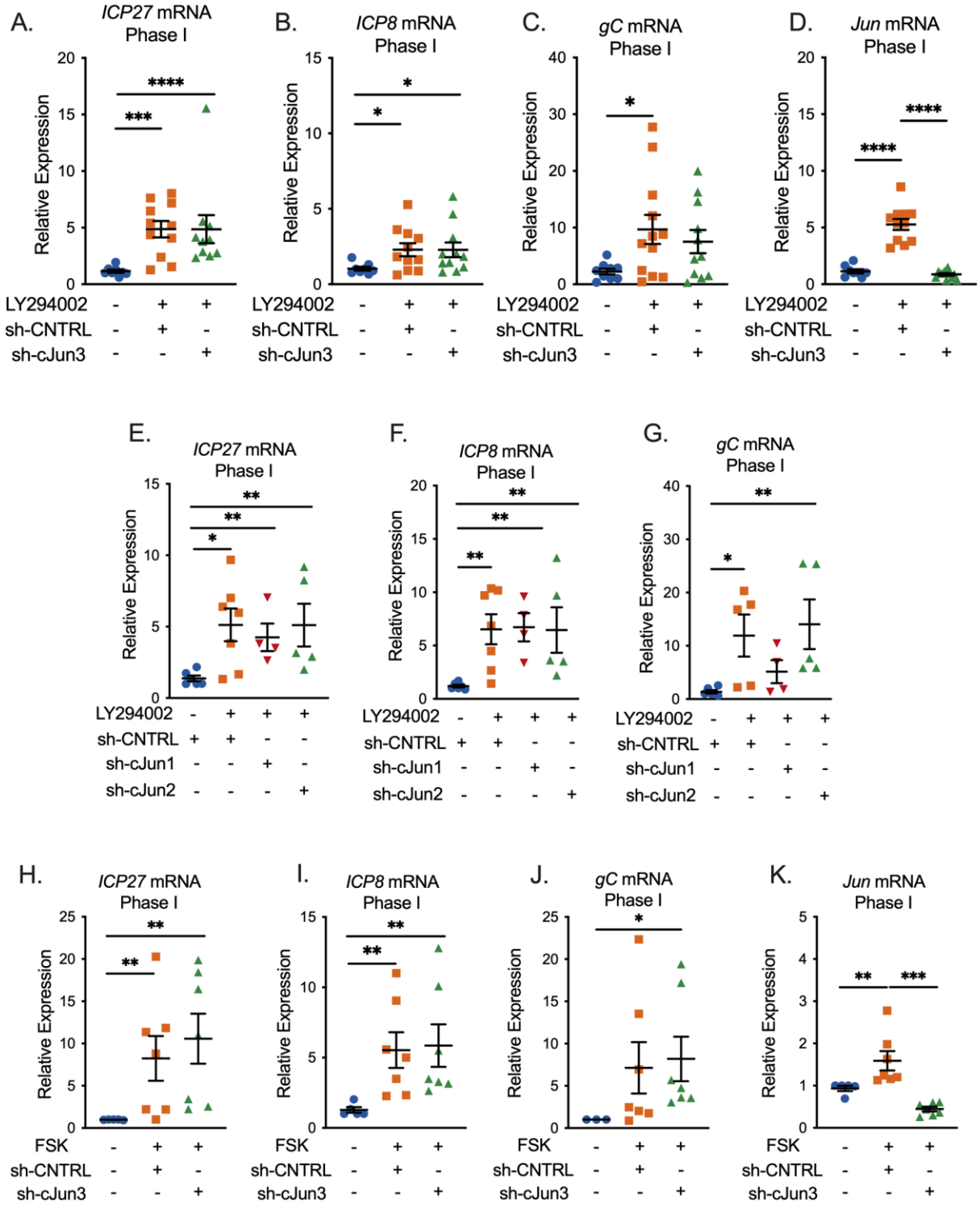
A.
ICP27 mRNA
Phase I
Relative Expression
LY294002
sh-CNTRL
sh-cJun3
B.
ICP8 mRNA
Phase I
C.
gC mRNA
Phase I
D.
Jun mRNA
Phase I
E.
ICP27 mRNA
Phase I
sh-cJun1
sh-cJun2
F.
ICP8 mRNA
Phase I
G.
gC mRNA
Phase I
H.
ICP27 mRNA
Phase I
FSK
I.
ICP8 mRNA
Phase I
J.
gC mRNA
Phase I
K.
Jun mRNA
Phase I

Figure 3.3 c-Jun is not necessary for Phase I gene expression. (A-K) Latently infected neurons were transduced with a non-targeting shRNA lentivirus or sh-cJun3, sh-cJun2, or sh-cJun1 at 6 days post-infection and reactivated 5 days later. In (A-G) neurons were reactivated with LY294002 and in (H-K) with forskolin. RT-qPCR was carried out at 18 hours post-reactivation for; ICP27 (A, E, & H), ICP8 (B, F, & I), gC (C, G, & J) and cellular Jun (D&K) at 18 hours post-stimulus is represented. N=6 biological replicates from at least 3 independent dissections. Statistical comparisons were made using non-normal (Mann-Whitney) t-Test. Individual biological replicates along with the means and SEMs are represented. * $P < 0.05$; ** $P < 0.01$.

c-Jun is Required for the Expression of Late Genes during Full (Phase II) Reactivation.

Although we did not detect a role for c-Jun in entry into Phase I gene expression, we went on to examine whether it played any role during HSV-1 reactivation. We therefore again depleted c-Jun prior to reactivation and quantified entry into full, Phase II reactivation. We now did detect a role for c-Jun during Phase II/full reactivation, as the numbers of Us11-GFP positive neurons were significantly decreased following c-Jun depletion (Fig 3.4A). This was verified using a second c-Jun shRNA lentiviral clone (Fig 3.4G). This indicated that c-Jun was required for Us11 expression. Because Us11 is a true late gene, we additionally quantified immediate early (Fig 3.4B), early (Fig 3.4C), and late viral transcripts (Fig 3.4D-E) during Phase II. Importantly, c-Jun was specifically required for expression of the late genes tested and not the immediate early gene ICP27 nor the early gene ICP8. The impact of c-Jun depletion on late gene expression was validated using a second c-Jun shRNA clone (Fig 3.4H &I). We also quantified the impact of c-Jun depletion on the progression to full reactivation induced by forskolin. Consistent with the data for PI3-kinase induced reactivation, the numbers of Us11-GFP positive neurons were decreased in the c-Jun depleted neurons, and this was verified using two independent shRNA clones (Fig 3.4F & J). Therefore, these data indicate that

c-Jun is directly required for full, Phase II HSV reactivation and acts specifically on late viral transcripts.

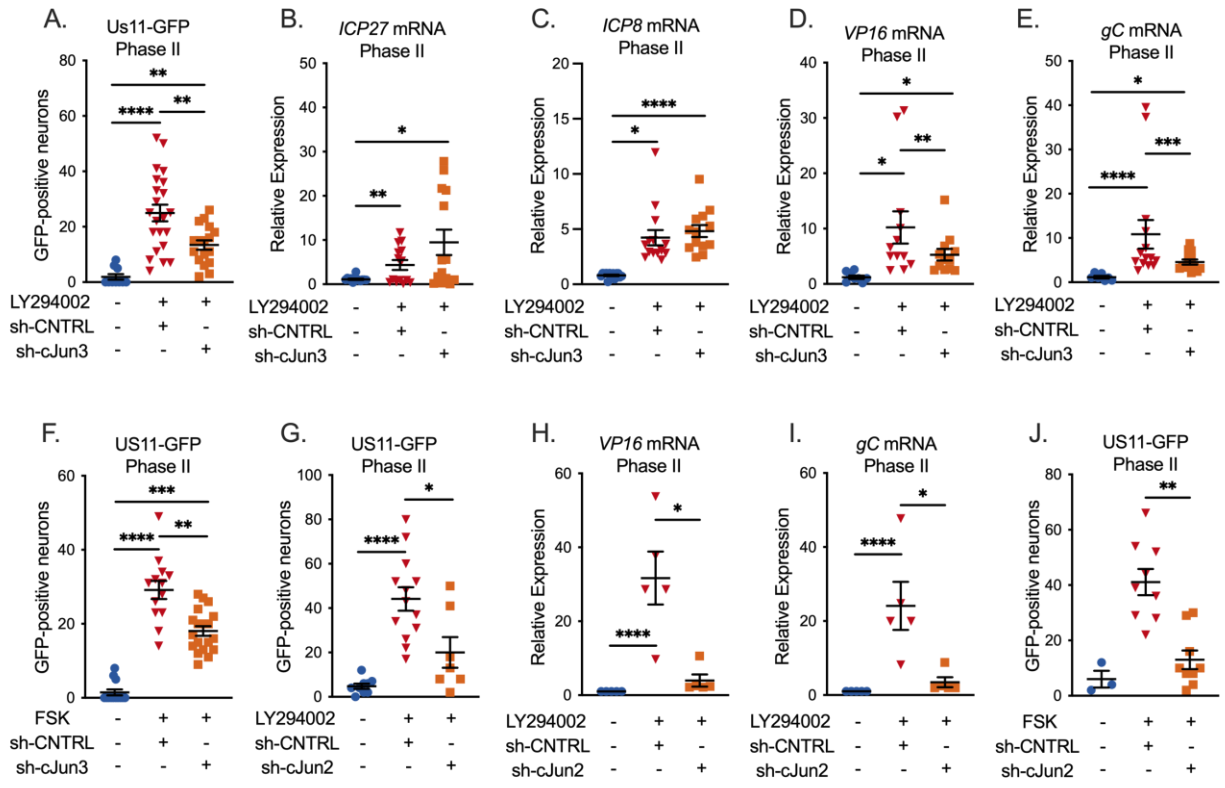

Figure 3.4 c-Jun is necessary for full HSV-1 reactivation. (A-F) Neurons were infected with HSV-1 and transduced at 6 days post-infection with a non-targeting shRNA lentivirus or sh-cJun3 (A-F) or sh-cJun2 (G-J) and reactivated 5 days later. Acyclovir was added for the first six days post-infection. (A,G) Quantification of Us11-GFP-positive neurons following reactivation with LY294002. (B-E, H-I) RT-qPCR for viral mRNA transcripts ICP27 (B), ICP8 (C), VP16 (D,H) gC (E,I), at 48 hours post-reactivation with LY294002. (F,J) Quantification of Us11-GFP-positive neurons following reactivation with forskolin. Individual replicates from at least 4 separate dissections are shown. Statistics determined by normal or non-normal (Wilcoxon-test, A, F-J) paired T-test. Individual biological replicates along with the means and SEMs are represented. * $P < 0.05$; ** $P < 0.01$. ns, not significant.

c-Jun is required for full lytic replication in neurons.

Phase II reactivation has previously been demonstrated to transcriptionally mirror HSV-1 *de novo* lytic infection in non-neuronal and neuronal cells, which contrasts with Phase I. Therefore, we investigated the contribution of c-Jun to *de novo* lytic infection in sympathetic neurons. Following c-Jun depletion and infection with HSV-1 Stayput-GFP, we quantified the numbers of Us11-GFP-positive neurons at 48 hours post-infection. This timepoint was chosen as it is when we previously detected the maximum number of GFP-positive neurons following *de novo* infection with Stayput-GFP (117). Consistent with our observation that c-Jun is required for full HSV-1 reactivation, the number of GFP-positive neurons indicative of *de novo* lytic infection events in this model system was robustly reduced following infection in c-Jun-depleted cultures (Fig 3.5A). In addition, viral DNA replication (Fig 3.5B) and transcription of all three classes of lytic genes, IE ICP27, E ICP8, L VP16, and TL gC and gM were robustly decreased in c-Jun depleted cells (Fig 3.5C), demonstrating that c-Jun is required for *de novo* lytic infection in neurons. These data suggest that c-Jun is a critical mediator of HSV-1 reactivation and lytic infection in neurons. However, these data also indicate that the mechanism of action may differ in reactivation versus *de novo* infection as c-Jun was required for expression of all three classes of viral genes during *de novo* infection but not during reactivation.

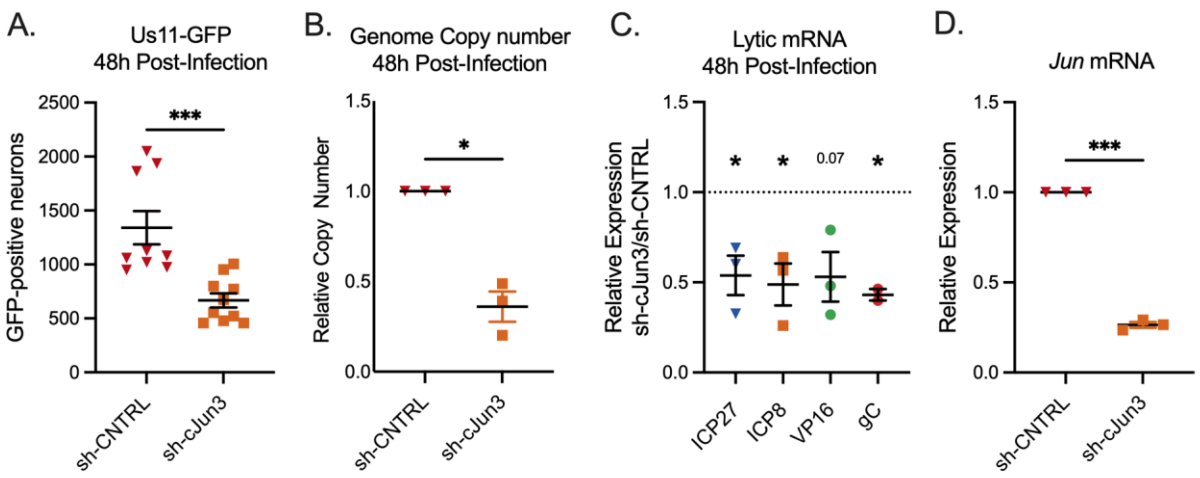

Figure 3.5: c-Jun is necessary for maximum *de novo* lytic infection in neurons. (A-H) Neurons were transduced with a non-targeting shRNA lentivirus or sh-cJun3 and infected with HSV-1 Stayput-GFP in the absence of viral DNA replication inhibitors 5 days post-transduction at an MOI of 5 PFU/cell for 48 hours. (A) Quantification of the numbers of GFP-positive neurons. Replicates from 3 separate dissections are shown; Unpaired t-test. (B) qPCR for viral DNA copy number. (C) RT-qPCR for viral mRNAs ICP27, ICP8, VP16, and gC. (D) RT-qPCR for Jun. Replicates from 3 separate dissections are shown; Paired t-test. Individual biological replicates along with the means and SEMs are represented. * $P < 0.05$; ** $P < 0.01$. One replicate from experiments in Panels A-C was performed by Patryk Krakowiak.

c-Jun is present in HSV-1 replication compartments during full reactivation.

As a DNA-binding protein, we proposed that c-Jun could modify viral gene expression during reactivation either directly on the viral genome or indirectly by altering a host cell factor. We therefore employed a single-cell imaging approach where the co-localization of c-Jun with individual reactivating neurons could be analyzed. As anticipated, c-Jun was not co-localized with latent viral genomes prior to the addition of the reactivation stimulus LY294002 (data not shown). To quantify c-Jun co-localization with viral genomes during Phase II reactivation, neurons were pulsed with 5-Ethynyl-2'-deoxycytidine (EdC; 10 μM) for 1 hour prior to carrying out Click-Chemistry to visualize

viral genomes, along with immunofluorescence for c-Jun. We observed a robust up-regulation of c-Jun only in reactivating neurons (Fig 3.6A). Importantly, c-Jun robustly co-localized with replicating viral genomes during Phase II of reactivation (Fig 3.6A). This co-localization was quantified using a Pearson's coefficient between c-Jun and EdC-Pulse (Fig 3.6B). Therefore, c-Jun is both up-regulated specifically in reactivating neurons and is recruited into viral replication compartments.

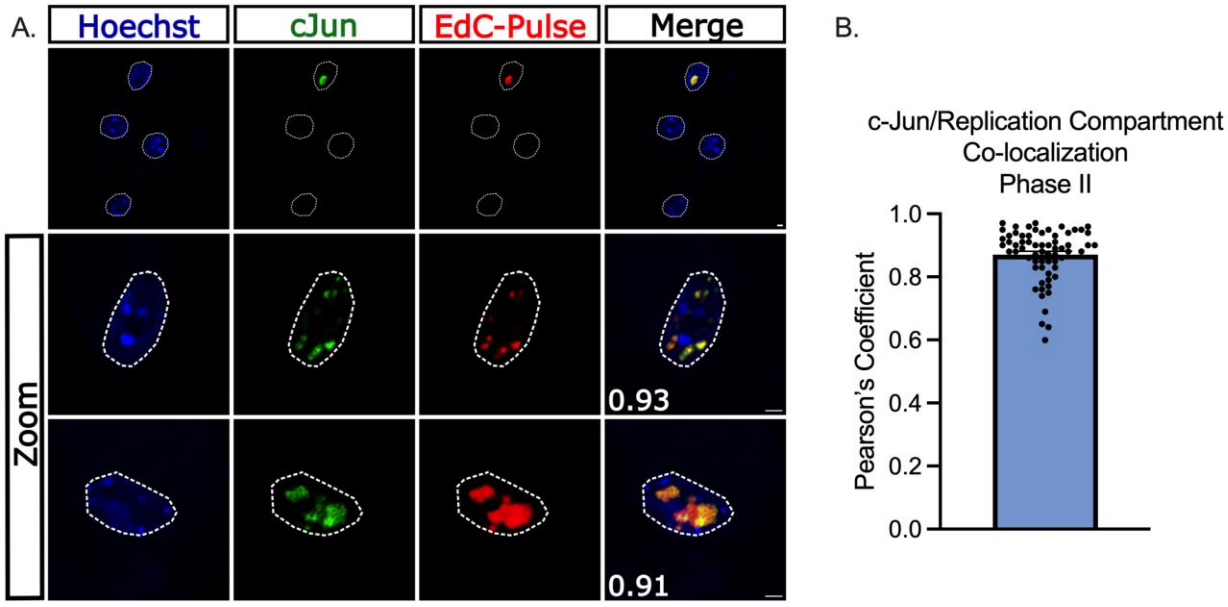

Figure 3.6 c-Jun colocalizes with replicating viral DNA during HSV-1 reactivation. (A-B) Latently infected neurons were reactivated with LY294002 and pulsed with 10 μM EdC for 1 hour to label viral DNA replication compartments. Nuclear stain Hoechst is shown in blue, and immunofluorescence was performed to visualize c-Jun in green. EdC-Pulse was visualized using click chemistry (shown in red). (A) Representative images of reactivating neurons. Scale bar = 10 μm. Pearson's coefficient between c-Jun and EdC-Pulse featured in bottom left corner of merge. (B) Compiled Pearson's coefficients. 35 individual neurons; 2 biological replicates. Experiments from Panels A-B were performed by Abigail Whitford.

Activation of neuronal stress signaling during latency establishment enhances future reactivation.

So far, our data point to a role for c-Jun specifically in stimulating late gene expression during Phase II reactivation. However, an additional observation was the differential phenotypes when c-Jun was depleted before infection versus before reactivation. This differential impact suggested that c-Jun signaling during initial infection promoted a form of viral latency that was more amenable to reactivation. As c-Jun is activated in response to neuronal stress signaling, we investigated how the active manipulation cell stress pathways and therefore enhanced c-Jun activation during initial infection impacted the later ability of the virus to reactivate. Inoculum with or without HSV-1 Stayput-Us11-GFP was added to neonatal sympathetic neurons in the presence or absence of nerve growth factor (NGF) for 3.5 hours. Immediately following the removal of this inoculum, the neurons were fixed and assayed for the presence of nuclear-localized and phosphorylated c-Jun (ser63), as an indication of c-Jun activation. The percentage of neurons under each condition demonstrating nuclear localized phosphorylated c-Jun was quantified from multiple fields of view, along with the mean intensity of the nuclear staining of each neuron. Using this approach, we were able to verify that NGF deprivation during the inoculation period is sufficient to elicit c-Jun activation, as anticipated (Fig. 3.7A-B). Interestingly, the neurons in the cultures infected with HSV-1 had enhanced c-Jun phosphorylation in both NGF-positive and -negative conditions as measured by the percentage of p-c-Jun-positive (Fig 3.7C). Therefore, HSV-1 *de novo* infection can also promote neuronal stress signaling indicated by c-Jun phosphorylation, which was also consistent with c-Jun activation during Phase II reactivation.

Following our validation that c-Jun phosphorylation could be enhanced during initial infection by omitting NGF from the inoculum, we investigated the impact on HSV-1 reactivation. In agreement with the pre-latency establishment c-Jun depletion experiments (Fig 3.2), the perturbation of the NGF signaling pathway during initial infection did not alter latent viral DNA load (Fig 3.7D). However, in cultures where NGF had been deprived during the inoculation period and where c-Jun activation was enhanced, we observed enhanced reactivation stimulated with LY294002 based on the quantification of Us11-GFP-positive neurons at 48 hours post-treatment (Fig 3.7E). Importantly, Phase I gene expression, as analyzed through ICP27 and ICP8 expression 18 hours post-stimulus, was also enhanced in the cultures infected under NGF-deprivation conditions (Fig 3.7F-G). Therefore, these data indicate that enhanced neuronal stress mediated by reduced NGF-signaling and enhanced c-Jun phosphorylation, results in an enhanced ability of HSV-1 to ultimately undergo reactivation without impacting the latent viral load.

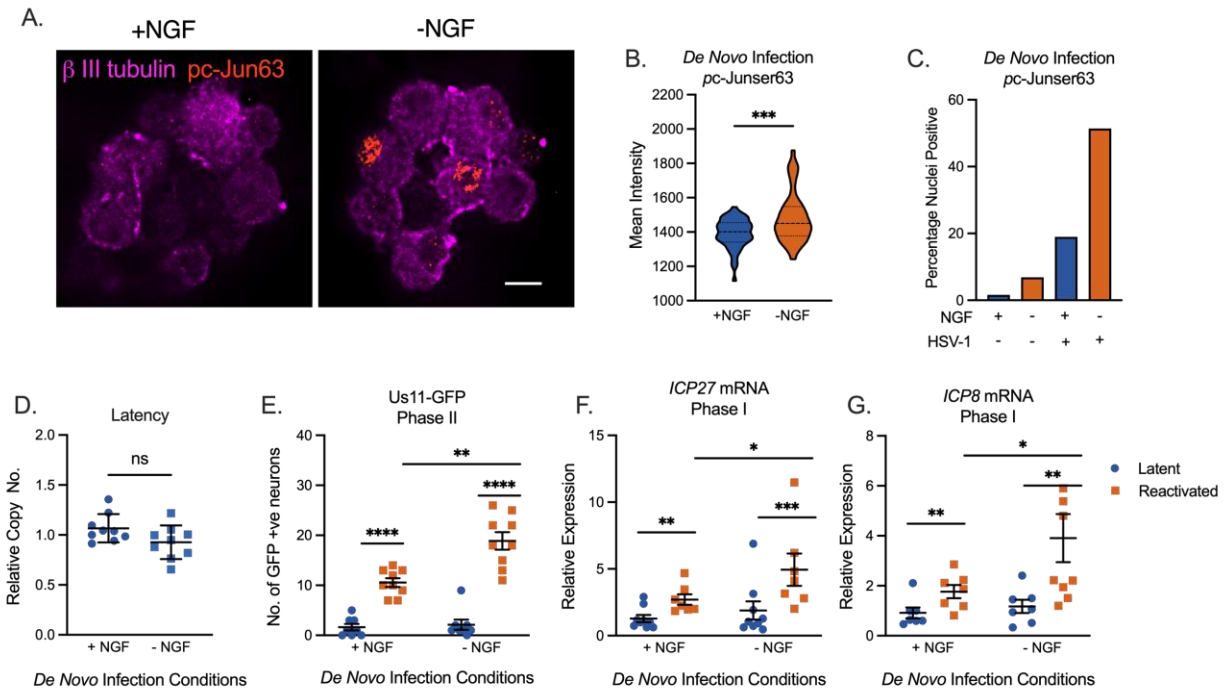

Figure 3.7: Stress Signaling Events during De Novo HSV-1 Infection (A-C) Neonatal sympathetic cultures were infected with Stayput-GFP in inoculation media with or without nerve growth factor (NGF) for 3.5 hours and subsequently fixed and stained for neuronal marker B III tubulin (magenta) or phosphorylated c-Jun (orange). Representative image of nuclear phosphorylated c-Jun is demonstrated Scale bar = 10 µm. (B) Mean signal intensity for phosphorylated c-Jun in the nucleus following infection. N=100 from 1 biological replicate. (C) Quantification of proportion of neurons with pc-Jun-positive nuclei pooled from several fields of view. (D-G) Neuronal cultures were latently infected. NGF was either included or omitted during the 3.5 hours inoculation period. Cultures were later reactivated with LY294002 20 µM. (D) Latent viral DNA load. Replicates from 3 dissections shown. The peak number of GFP-positive neurons 48 hours post-stimulus (E) and relative expression of ICP27 (F) or ICP8 (G) transcripts 18 hours post-stimulus were quantified to analyze full reactivation and Phase I gene expression, respectively. Replicates from 3 dissections shown. Statistical comparisons were made using normal or non-normal (Mann-Whitney, E) t-Test. Individual biological replicates along with the means and SEMs are represented. * $P < 0.05$; ** $P < 0.01$.

Discussion

c-Jun is both a transcription and pioneer factor that is known to regulate host gene expression in neurons following cell stress. The up-regulation and phosphorylation of c-Jun following DLK-mediated activation of JNK is a key step in both neuronal apoptosis and axon pruning following the interruption of nerve growth factor signaling (281, 298, 332). The up-regulation of c-Jun-dependent genes is consistent with the kinetics of HSV-1 Phase I gene expression (333), hence our initial hypothesis that c-Jun plays a direct role in HSV-1 Phase I gene expression. However, our data indicate that c-Jun functions to promote reactivation but not during the JNK-dependent Phase I wave of lytic gene expression. In carrying out this study, we also observed that cell stress conditions during *de novo* infection have a long-term impact on either neurons themselves or the viral genome resulting in an enhanced ability of the virus to reactivate. This has important implications for how neurons have a memory of previous cellular stresses and for interpretations of HSV reactivation studies.

Although not required for Phase I gene expression, we did identify a role for c-Jun in promoting late gene expression during full, Phase II reactivation. Notably, this finding was also distinct from the role of c-Jun in promoting the expression of all three classes of viral genes during *de novo* infection. The exact mechanism of action and explanation for this difference between *de novo* infection and reactivation are unclear. One possible difference is the nature of the viral chromatin during reactivation versus *de novo* infection. The starting point for reactivation is a genome with a regularly spaced nucleosomal structure (334) and associated with heterochromatin (120, 121), whereas

the viral genome during *de novo* infection is highly accessible and lacks a regular nucleosomal structure (81, 84, 193, 257, 259, 335). Although the nature of the nucleosomal structure and overall accessibility of the viral genome during Phase II is currently unknown, it is possible that prior to viral DNA replication potential c-Jun binding sites are inaccessible. Additional proteins may also be activated in response to reactivation triggers that act during Phase I and on IE and E genes during Phase II as discussed below.

Because we were unable to detect a role for c-Jun during Phase I gene expression and IE/E gene expression during Phase II, this suggests additional undetermined host factors instead play a role. Additional candidates known to be activated or induced in response to reactivation triggers include other bZIP proteins such as Fos, JunD, ATF3 and Ddit3 (CHOP), along with other transcription factors; NF-Y, Gadd45α, Gadd45γ, and FOXO (333). As AP-1 inhibition enhances viral gene expression (Fig 3.1), c-Fos may play a repressive role in Phase I gene expression. Indeed, our preliminary data support this hypothesis (Fig 3.8), although whether c-Fos binds directly to the viral genome remains to be tested. In a previous study, depletion of Gadd45α had no impact on HSV-1 reactivation (224). An intriguing candidate for promoting Phase I gene expression is NF-Y complex because it has been implicated in the recruitment of JNK to chromatin during neuronal differentiation (336), and NF-Y has been identified as potentially stimulating transcription of the IE gene ICP0 in response to heat-stress (288), making NF-Y a viable candidate for driving initial reactivation events. Additional pioneer factors that may have a role in stimulating viral gene expression

during reactivation are the Krüppel-like transcription factors (KLF) proteins, particularly KLF15 and KLF4 (337). KLF family members are up-regulated in corticosteroid-mediated reactivation of the related Bovine Herpesvirus-1 and may transactive viral immediate-early promoters (338-340). KLF4 is a well-known pioneer factor that activates previously silenced genes, a role that has been well characterized during cellular reprogramming (341, 342). The potential role of these proteins in regulating the transcription of HSV-1 genes from silenced heterochromatin during the different stages of HSV-1 reactivation therefore warrants further investigation.

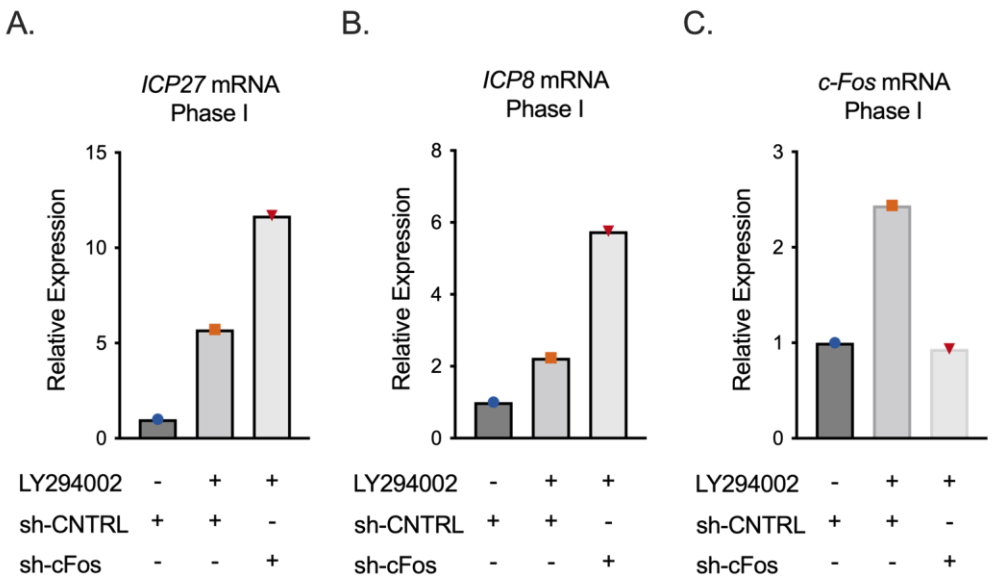

Figure 3.8 c-Fos may enhance Phase I gene expression. (A-C) Latently infected neurons were transduced with a non-targeting shRNA lentivirus or lentivirus-expressing an shRNA targeting c-Fos at 6 days post-infection and reactivated 5 days later with LY294002. RT-qPCR was carried out at 18 hours post-reactivation for viral immediate early transcript ICP27 (A), viral early transcript ICP8 (B), and cellular control c-Fos (C). 1 biological replicate.

c-Jun functions through either homo- or heterodimerization. Whether c-Jun binds to an additional bZIP protein to promote late gene expression is unknown. c-Jun can

dimerize with Fos, Jun, CREB, or ATF family members. Recently, we found that JNK/DLK-dependent reactivation mediated by forskolin required CREB, as the addition of CREB inhibitor 666-15 restricted full reactivation as quantified by the number of GFP-positive neurons (109), although these data come with the caveat that a role for CREB has not been validated using genetic approaches. As observed here for c-Jun, CREB activity was not required for Phase I gene expression. Further, mapping the exact binding sites on the viral genome will help identify underlying sequence motifs bound by c-Jun, which can vary depending on the interacting protein (343). We did attempt to perform Cleavage Under Target & Release Under Nuclease (CUT&RUN) for c-Jun during Phase II reactivation. However, we found that the background signal for viral genomes from the non-specific control antibody was much higher on Phase II reactivating neurons than during latent infection (data not shown, computational analysis was performed with Alison Francois). For reasons that are not clear, ongoing viral DNA replication may result in substantial background in the CUT&RUN reaction, and therefore resolving c-Jun interacting sites on replicating viral genomes is currently problematic.

We also report a role for c-Jun for maximal *de novo* lytic infection in neurons as indicated by decreased of all classes of viral lytic genes, viral DNA replication, and late viral protein synthesis. Consistent with previous reports investigating lytic replication in non-neuronal cells, we found that HSV-1 infection and reactivation induced c-Jun activation (344, 345). However, a direct role for c-Jun during lytic replication has not previously been reported. Interestingly, a previous study from our lab found that JNK

inhibition during *de novo* infection in neurons did not impact immediate early viral gene expression, although viral replication and the expression of other later classes of viral genes were not explored in this study (99). There, it remains possible that during *de novo* infection, c-Jun may be activated through an alternative pathway.

Environmental stressors have long been reported to correlate with HSV-1 reactivation and clinical disease. Fewer studies have explored the impact on HSV-1 and clinical outcomes when stress occurs during initial inoculation. Evidence from mouse models suggest that psychological stress during inoculation with HSV-1 enhances acute infection, as measured by infectious titer and pathology (346, 347). Complementary evidence from primary autonomic neurons similarly demonstrates elevated acute viral DNA replication and infectious virus production following HSV-1 infection in combination with stress hormone epinephrine (104). However, the impacts of stress during initial infection on later reactivation until now have not yet been investigated. Our findings suggest that additional stress that enhances c-Jun signaling during initial infection could exacerbate future reactivation. This has important implications for understanding the contributions to clinical HSV disease and why certain individuals may be more prone to reactivation than others. In addition, this observation has important experimental implications because it means that any manipulations performed on the virus or host during latency establishment could have an indirect effect on reactivation, and ideally the contribution of viral and host factors should be studied solely during reactivation to draw meaningful conclusions on their direct effects.

How the viral genome or neuron itself retains a memory of the initial infection conditions remains unclear. We previously found that viral genomes could retain a memory of interferon signaling during initial infection to result in restricted reactivation, which was mediated by association with repressive Promyelocytic Leukemia Nuclear Bodies (PML-NBs) (93). We now extend this study and show that cell stress has a converse effect and can prime future reactivation events. Given c-Jun's ability to bind DNA and navigate chromatinized environments, it is tempting to speculate that stress signaling through c-Jun modifies the epigenetic nature of viral and/or host genomes to potentially induce a form of silencing that is more primed for transcriptional activation. Outside of the context of viral infection, early life stress has been implicated in leaving such a "chromatin scar" in the central nervous system, with changes in epigenetic signatures particularly for H3K27 and H3K79 methylation (348, 349) and a dysregulated priming of genes. Further studies on the mechanism of HSV latent infection and changes in the host and viral epigenetics will be important to understand how both the virus, and potentially neurons themselves, have a memory of previous cell stress or immune events and the impact on future responses.

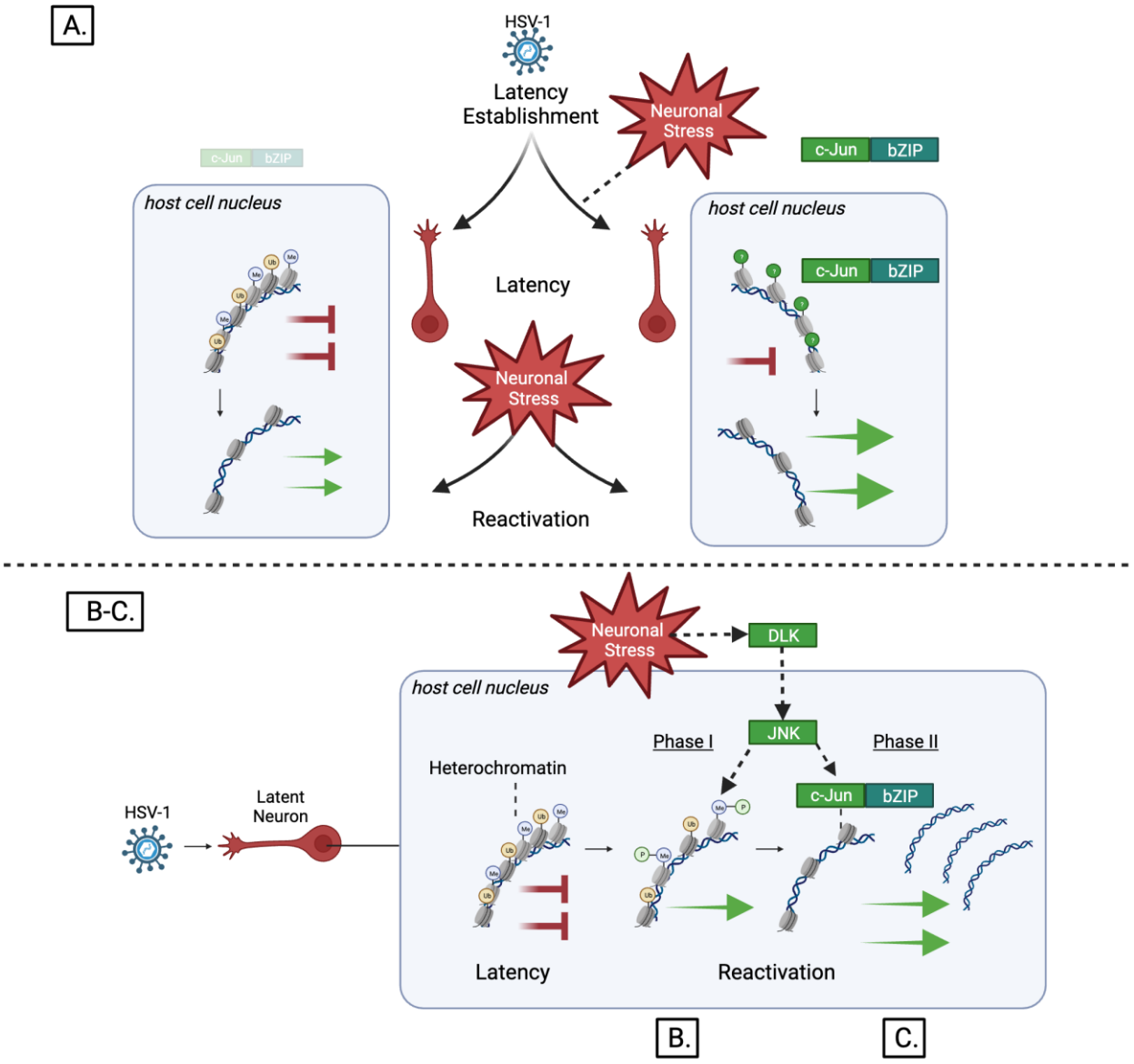

Figure 3.9 Working Model. (A) Neuronal stress signaling and c-Jun activation during initial infection promotes the establishment of more reactivation-competent viral genomes. (B-C) Direct Role of c-Jun in Reactivation. (B) c-Jun does not enhance Phase I gene expression. (C) However, c-Jun acts on the viral genome to promote full, Phase II reactivation.

Chapter 4: Histone H2A Ubiquitination Mediates the Establishment of Reactivation-Competent HSV-1 Latent Infection

Parts of this chapter have been adapted from:

Dochnal, SA, Francois, AK, & Cliffe, AR. Histone H2A ubiquitination mediates the establishment of reactivation competent HSV-1 latent infection. *In prep.* (2023)

Abstract

During a latent infection of peripheral neurons, HSV-1 genes associate with reversible Polycomb silencing. H3K27me3 and PRC2 are enriched on the latent HSV-1 genome *in vivo*, but the presence of H2AK119ub and the contribution of both PRC2 and PRC1 to viral gene repression during latency establishment, maintenance, and reactivation remains unknown. The mechanism(s) of Polycomb recruitment to the HSV-1 genome are also unresolved. Here, we identify populations of latent viral genomes that associate with H2AK119ub, PRC1 component Ring1B, or H3K27me3. Our data further indicate a predominate role for PRC1-mediated H2AK119ub in viral gene silencing during HSV-1 latency establishment. On the cellular genome, hnRNPK can recruit PRC1 in tandem with lncRNAs. We confirm the viral latent lncRNA, the LAT, and hnRNPK interact in neurons and demonstrate that hnRNPK represses viral gene expression during latency establishment. We also find that PRC1 activity during latency establishment promotes the formation of more reactivation-competent latent viral genomes. Our data supports a model of latency establishment wherein viral lncRNA LAT recruits PRC1 to deposit H2AK119ub on the viral genome, promoting viral gene repression in a manner that is amenable to reactivation through pro-transcriptional reader ZRF1. Our findings also support the notion of heterogeneity in HSV-1 latency and reactivation, enhance the resolution at which these processes can be studied, and contribute to the general biological understanding of the epigenetic signature of the specialized cell type of a neuron.

Introduction

Human Herpesviruses are characterized by their ability to establish a lifelong latent infection in select host cells. Latency has been associated with malignancy in some human herpesviruses (350-352), and clinical significance arises for all when the virus periodically reactivates through the lifetime of the host. Latent viral genomes of all families of human herpesviruses associate with repressive heterochromatin, which is then modified upon reactivation (119). Therefore, studying the epigenetic regulation of herpesviruses has been a subject of interest, with the goal of manipulating this information to create therapies in the form of 1) “shock and kill”, where the viral epigenome is manipulated to reactivate to be cleared by the immune response or 2) “lock and block”, where the viral epigenome is manipulated into a permanent state of silencing.

Alpha herpesvirus Herpes Simplex Virus-1 (HSV-1) establishes a latent infection within post-mitotic peripheral neurons, and reactivation can cause recurrent pain, blindness, and encephalitis. There is also accumulating evidence linking HSV-1 infection and neurodegenerative disease such as late-onset dementia and Alzheimer’s disease (AD) (248). The latent HSV-1 viral genome associates with heterochromatin, including Polycomb silencing (121-124, 201). Polycomb silencing is characterized by the tri-methylation of lysine 27 on histone H3 (H3K27me3) a histone modification written by Polycomb repressor complex 2 (PRC2). Over a decade ago, multiple laboratories demonstrated both H3K27me3 and PRC2 core component Suz12 to be enriched on the latent HSV-1 genome *in vivo* (121, 123, 124, 353). Since, studies in several model

systems have demonstrated that H3K27 demethylation, and therefore heterochromatin removal, is required for full HSV-1 reactivation (98-100, 109, 117). However, PRC2 and H3K27me3 are not significantly enriched on lytic viral gene promoters until approximately 14 days post-infection, when viral genes have already been silenced for quite some time (122). These data suggest that PRC2 may support the maintenance of a latent infection rather than its active promotion through driving initial viral gene repression events. However, the functional role of PRC2 in HSV-1 latency establishment and reactivation using PRC2 inhibition or depletion has never been reported. Moreover, whether the HSV-1 genome is enriched in H3K27me2 has not been investigated. H3K27me2 is also deposited by PRC2 prior to H3K27me3 and can initiate cellular gene repression independently of H3K27me3 (137, 354).

On the cellular genome, H3K27me3 may be accompanied by Polycomb repressor complex 1 (PRC1), which can deposit the mono-ubiquitination of H2AK119 (H2AK119ub). PRC1 can be broadly divided into one of two forms: canonical (cPRC1) and non-canonical/variant (vPRC1) (129, 130). These forms vary in their composition and therefore their mechanisms of recruitment and silencing. All forms of PRC1 are comprised of the enzymatic Ring1A/Ring1B core and at least one PCGF protein. cPRC1 contains either PCGF2 or PCGF4, and one of five chromobox domain (CBX) proteins (119, 154). As CBX proteins bind H3K27me3, cPRC1 recruitment can therefore be PRC2-dependent (119, 156, 157). On the other hand, vPRC1 lacks CBX proteins and is therefore recruited to DNA independently of PRC2. vPRC1 instead associates

with proteins RYBP and YAF2, which drive vPRC1 to deposit H2AK119ub more efficiently than cPRC1 (128, 157, 159, 162).

The presence of PCGF4 (also known as BMI1), which can be associated with cPRC1, was investigated on the latent HSV-1 genome but was not found to be significantly enriched on lytic gene promoters through chromatin immunoprecipitation (ChIP) (123). Whether core components of PRC1 (Ring1A/B) and the H2AK119ub mark are enriched on the latent HSV-1 viral genome, and whether these have any functional impact on HSV-1 latency establishment, latency maintenance, or reactivation remains unknown. In fact, whether PRC1 targeting and gene silencing are active processes in a differentiated peripheral neuron remains widely unexplored, even in a context independent of infection. The study of Polycomb composition, and mechanisms of recruitment and silencing has thus far been largely limited to cells of a more embryonic nature (reviewed in (119)) and where there is a pre-existing epigenetic template that complicates these studies. When a herpesvirus genome enters a host cell nucleus, it does so as epigenetically naïve, meaning it does not contain a pre-existing chromatin template (75-80). Therefore, HSV-1 also serves as a tool to study the basic mechanisms of Polycomb recruitment and silencing in a neuron.

Here, we demonstrate that H2AK119ub is enriched on lytic viral genes during latent infection established both *in vivo* and *in vitro,* and we confirm the genome-wide enrichment of H3K27me3 with the latent HSV-1 genome *in vitro*. We find that H2AK119ub, PRC1 core component Ring1B, and H3K27me3 each associate with a

proportion of latent viral genomes, and that H2AK119ub and Ring1B associate with a proportion of repressed HSV-1 viral genomes during active latency establishment and viral gene silencing. Consistently, the perturbation of PRC1 but not PRC2 enhances viral gene expression, and nuclei of lytic infected neurons are devoid of PRC1 core component Ring1B.

Host cell protein hnRNPK can bind and recruit vPRC1 (and therefore H2AK119ub) to the cellular genome in tandem with lncRNAs. The latency-associated transcript (LAT) is a lncRNA only expressed in a proportion of latently infected neurons. The 8.3 kb primary transcript is spliced into two stable introns and various microRNAs (199, 200). While the function of the LAT has remained enigmatic for decades, there is evidence that the LAT modulates the nature of H3K27me3 enrichment of the HSV-1 genome from several groups (122-124). Our collaborator Igor Jurak found that the LAT interacts with cellular protein hnRNPK in an unbiased, but artificial system (unpublished). Therefore, we speculate that the LAT recruits vPRC1 to the viral genome, a hypothesis that is supported by data in this chapter. We first confirm the interaction of the LAT and hnRNPK in neurons. We also find that hnRNPK depletion enhances viral gene expression, suggesting that hnRNPK, like vPRC1-mediated H2AK119ub, represses the HSV-1 viral genome during active stages of latency establishment.

Interestingly, PRC1 inhibition during latency establishment dramatically reduces the ability of latent viral genomes to reactivate. We also find that a pro-transcriptional reader of H2AK119ub, ZRF1, relocates to the nuclei of neurons that have reactivated from

latency. These data altogether support a model in which vPRC1 mediates lytic viral gene silencing in a manner that is amenable to reactivation events, allowing the virus to both evade the immune system and routinely transmit to new hosts.

Results

HSV-1 is enriched in PRC1-mediated H2AK119ub during latent infection established *in vivo*.

The PRC2 component Suz12 and H3K27me3 have previously been demonstrated on the latent HSV-1 genome using an *in vivo* mouse model (122, 123, 193). However, whether the Polycomb silencing mark H2AK119ub associates with the viral genome has not previously been investigated. Following *in vivo* infection and latency establishment 30 days post-infection, latently infected trigeminal ganglia were harvested and subject to chromatin immunoprecipitation (ChIP) for H2AK119ub, as well as negative control IgG and positive control H2A as previously described (99, 122). We observed a significant enrichment of H2AK119ub on repressed lytic viral gene promoters, including immediate early gene ICP27 and early gene ICP8, during latent infection (Fig 4.1A). H3K27me3 has also previously been shown to be enriched on these lytic viral gene promoters in a mouse model (121, 123, 124).

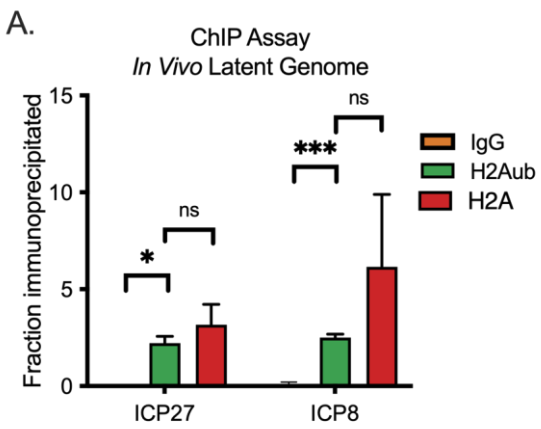

Figure 4.1 Association of histone H2AK119ub with wild-type (WT) herpes simplex virus 1 (HSV-1) genome during latent infection established *in vivo*. (A) Mice were infected with WT HSV-1, and latent trigeminal ganglia (TG) were collected 30 days post-infection. Chromatin immunoprecipitation (ChIP) was performed using an IgG control (orange), H2AK119ub (green), or H2A (red) antibody to analyze binding to promoters of immediate early viral gene ICP27 and early viral gene ICP8. Enrichment over Input determined. 3 biological replicates; Welch's t-test. Normality determined by Shapiro-Wilk test. Means and SEMs are represented. *, $P < 0.05$; **, $P < 0.01$. ns, not significant. Experiments in Panel A were performed by Alison Francois and Anna Cliffe.

H2AK119ub and H3K27me3 associate with a population of latent HSV-1 genomes *in vitro*.

We also investigated the enrichment of H2AK119ub and H3K27me3 on the viral genome during a latent infection established in primary neuron cultures. These experiments are informative as this reductionist approach informs whether Polycomb silencing is targeted to the HSV-1 genome independently of the immune system, and whether the neuronal host cell and/or the genomic sequence of HSV-1 are sufficient for Polycomb recruitment to the epigenetically naïve HSV-1 genome. Moreover, we sought to confirm the presence of Polycomb silencing on the HSV-1 genome *in vitro*, as this would validate the use of this system to explore the impact Polycomb on HSV-1 latency and reactivation. The use of an *in vitro* system in this scenario is highly advantageous,

as within it we can readily inhibit or deplete Polycomb repressor complex components. Using our *in vitro* system, we can also apply a single-cell approach to investigate potential heterogenous Polycomb recruitment to individual viral genomes.

Primary neonatal sympathetic neurons were infected with HSV-1 Stayput-GFP (previously characterized in (117)) at an MOI of 10 in the presence of viral DNA replication inhibitor acyclovir (ACV) to promote latency establishment. Neurons were collected 30 days post-infection, a time point at which latency has been fully established *in vitro* (117) and mirrors what is documented *in vivo* (121-123). CUT&RUN was subsequently performed using control IgG, along with antibodies against H2AK119ub and H3K27me3. The CUT&RUN enriched DNA was then subject to next generation paired-end sequencing and analysis through a computational published on IO protocols (Zheng Y et al (2020) Protocol.io). The recent advent of CUT&RUN enabled us to assess the chromatin landscape of the viral genome in primary neurons as it requires very few cells (a limiting factor in our cultures) and informs on the regions of binding at a high, single-nucleotide resolution (355). An additional advantage to using our primary neuron system of HSV-1 latency is that a robust pool of latently infected neurons can be achieved (99, 107, 117, 267). Therefore, the use of probes to enrich HSV-1 genome reads was unnecessary during CUT&RUN library preparation.

As observed *in vivo*, both H2AK119ub and H3K27me3 were broadly and robustly enriched over IgG controls across the latent HSV-1 genome (Fig 4.2A). Notably, both H2AK119ub and H3K27me3 decorated repressed lytic genes, including ICP27 and

ICP0 (Fig 4.2B). Interestingly, there were several regions on the transcriptionally active latency-associated transcript (LAT) of the viral genome notably devoid of H2AK119ub or H3K27me3 signal. CCCTC binding factor (CTCF)-bound insulator sites scattered along the LAT have long been proposed to halt the propagation of repressive heterochromatin from the surrounding viral genome (202, 353, 356). In support of this theory, we find that the regions devoid of H2AK119ub and H3K27me3 signal on the LAT align to the single-base pair resolution of where these CTCF sites are located (Fig 4.2B).

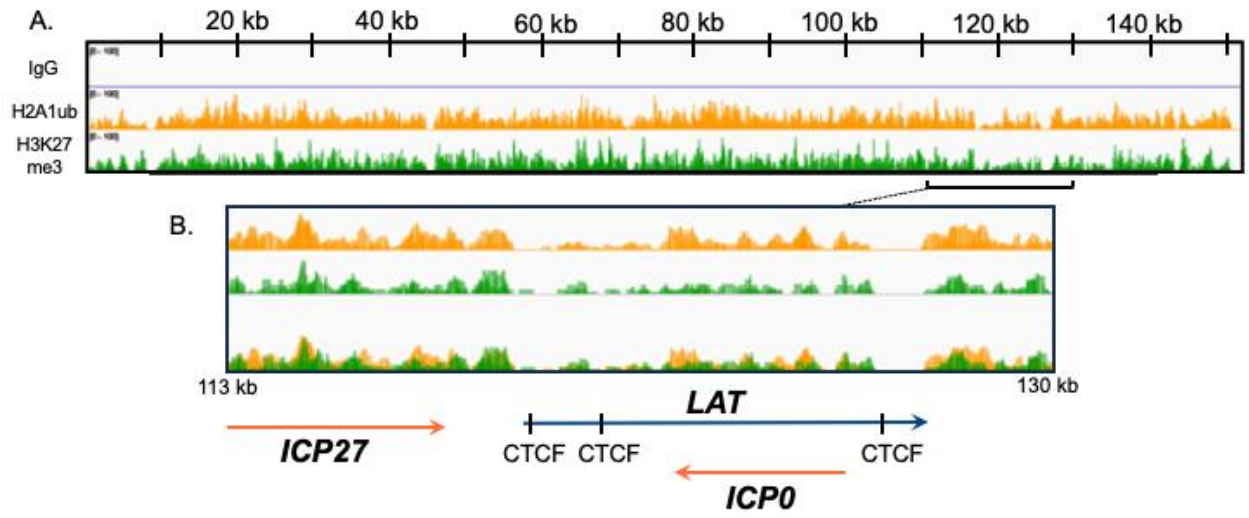

Figure 4.2 H2AK119ub and H3K27me3 association with the HSV-1 genome during latent infection established *in vitro*. (A-B) Primary neurons were infected with HSV-1 Stayput-GFP in the presence of viral DNA replication inhibitor acyclovir (ACV). 30 days post-infection, neurons were collected, permeabilized, and CUT&RUN was performed for IgG control (blue), H2AK119ub (orange), or H3K27me3 (green). (A) CUT&RUN -signals of merged experimental replicates along the 152 kB HSV-1 genome. (B) Zoom view of merged replicates of H2AK119ub (orange) and H3K27me3 (green) from kilobase 113 to kilobase 130 of the viral genome including the latency-associated transcript, LAT, as well as lytic transcripts ICP27 and ICP0. CTCF sites on the LAT are demarcated. Equivalent scale between conditions, 0-100. Computational analysis performed with Alison Francois.

These data are the first to demonstrate genome-wide PRC1-mediated H2AK119ub recruitment to the repressed HSV-1 genome during latent infection. However, only a proportion of neurons containing latent viral genomes will reactivate at any one time (93, 109, 117, 223, 224, 292). While bulk-sequencing provides a comprehensive genome-wide view of the viral chromatin landscape, it cannot account for possible heterogeneous silencing mechanisms between individual viral genomes or within cultured neurons. Therefore, we next employed an additional *in vitro* approach to investigate PRC1 and PRC2 association with the latent viral genome at the single-cell and individual viral genome level.

Primary neurons were infected with an EdC-labelled HSV-1 virus at an MOI of 5 and fixed at 30 days post-infection. Using a combination of click chemistry and immunofluorescence, we analyzed the 3-dimensional co-localization of the latent HSV-1 genome with PRC1 and PRC2-mediated histone modifications. When the HSV-1 genome (visualized in red) co-localizes with the histone modification or PRC1/2 component investigated (visualized in green) in a Z-stack, a punctum of yellow signals a co-localization event. In agreement with the CUT&RUN and ChIP-qPCR data, we observed the viral genome colocalizing with clusters of H3K27me3 (Fig 4.3A). and H2AK119ub (Fig 4.3C) using this methodology. Ring1B, a core component of PRC1, stains as punctate and therefore the appearance of co-localization with the also punctate HSV-1 viral genome is striking (Fig 4.3D).

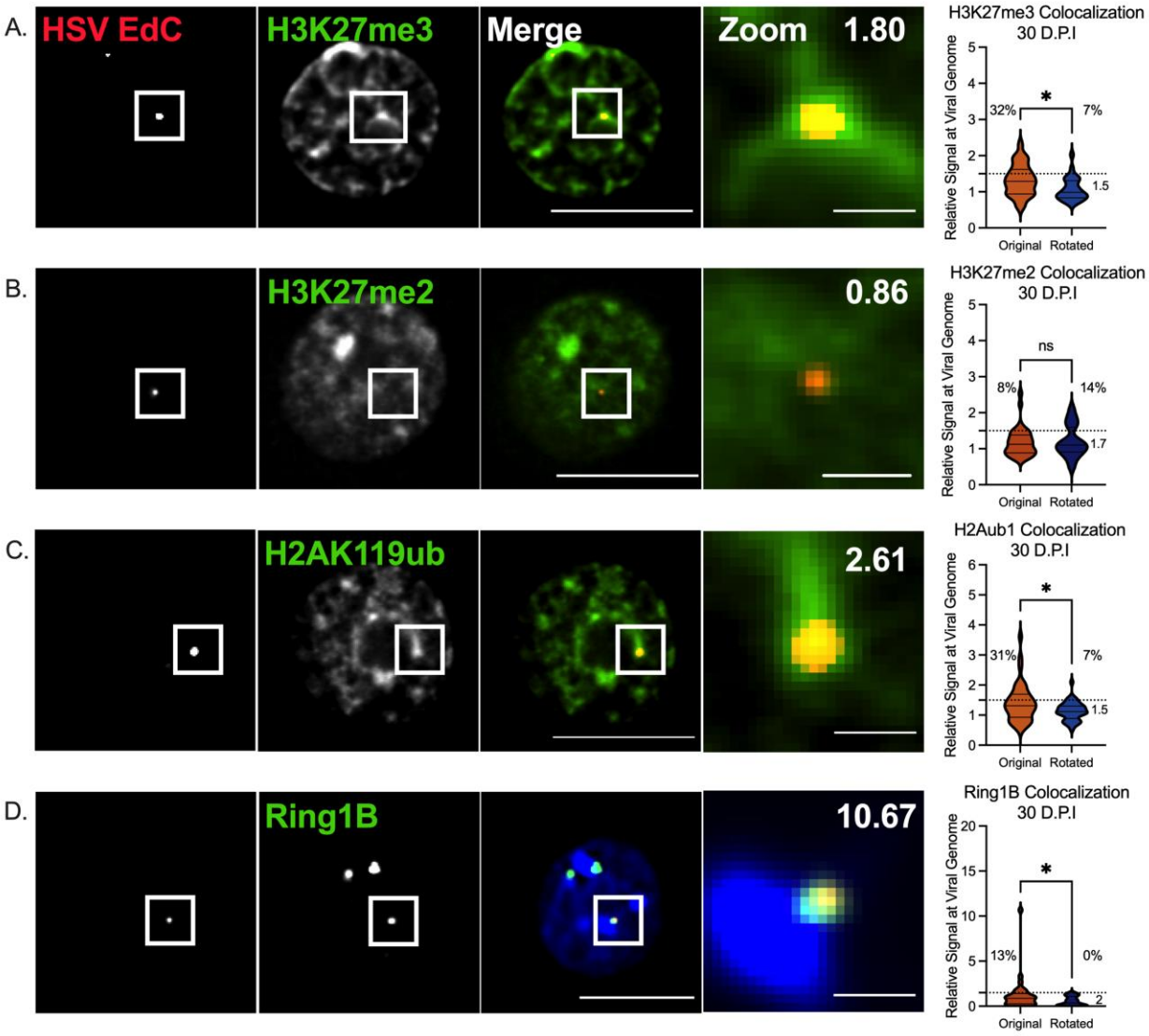
A.
HSV EdC
H3K27me3
Merge
Zoom 1.80
H3K27me3 Colocalization
30 D.P.I
Relative Signal at Viral Genome
32%
7%
1.5
Original
Rotated
B.
H3K27me2
0.86
H3K27me2 Colocalization
30 D.P.I
ns
8%
14%
1.7
C.
H2AK119ub
2.61
H2Aub1 Colocalization
30 D.P.I
31%
7%
1.5
D.
Ring1B
10.67
Ring1B Colocalization
30 D.P.I
13%
0%
2

Figure 4.3 Single viral genome analysis demonstrates a population of latent HSV-1 genomes associated with H3K27me3, H2AK119ub, and Ring1. (A-D) Primary sympathetic neurons were infected with EdC-labeled HSV-1 in the presence of acyclovir/ACV (10 μM during inoculation period and 50 μM following removal of inoculum). 30 days post-infection, latently infected neurons were fixed and stained for histone modifications H3K27me3 (A), H3K27me2 (B), or H2AK119ub (C), or PRC1 core component Ring1B (D), and the HSV-1 genome was visualized through click chemistry. Nuclear Hoechst stain shown in blue where nucleus is not prominently outlined by histone modification. Enrichment values of chromatin mark/reader/writer with each individual HSV-1 genome analyzed were calculated in a high-throughput and unbiased manner using computational program NucSpotA. Representative images of HSV-1 genome (red) and the chromatin modification or reader/writer (green); 10 μm scale, 1 μm scale for zoom. Enrichment value for representative image demonstrated in top right corner of zoom panel. Statistical significance of co-localization was determined through paired comparison of enrichment values from original images and control images where the viral genome was rotated 90 degrees to achieve random placement. Threshold enrichment values for co-localization for each stain, and the proportion of neurons which are greater than or equal to this threshold, are respectively demarcated by a dashed line and percentage. Minimum 50 images from 2 biological replicates; Wilcoxon test. Normality determined by Kolmogorov-Smirnov test. *, $P < 0.05$; **, $P < 0.01$. ns, not significant.

However, histone modification stains are broadly nuclear, suggesting incidences of overlap in green and red signal can be random coincidence versus genuine co-localization. Therefore, to measure co-localization in a high-throughput and unbiased fashion, we used our recently developed program NucSpotA (Francois et al, manuscript in preparation). NucSpotA measures the enrichment of the modification (based on the intensity of the immunofluorescence signal) at the viral genome, in comparison to the entire nucleus. By also measuring the enrichment values of the same stain on a set of control images where the viral genome is rotated 90 degrees, we could determine whether co-localization with the HSV-1 genome in original images is higher than that obtained for random placement of the viral genome. We further assigned a threshold for the enrichment values by eye and calculate the proportion of viral genomes that meet

this threshold to estimate what proportion of latent viral genomes are co-localized with these Polycomb modifications and components during latent infection.

In agreement with our population-level findings, the HSV-1 genome significantly co-localized with H3K27 tri-methylation at 30 days post-infection (Fig 4.3A). Specifically, we found that H3K27me3 co-localized with a subset of latent viral genomes, approximately one-third. We also investigated the colocalization of the trimethylation's predecessor mark, H3K27me2, which is understudied despite its ability to be deposited by PRC2 and being capable of initiating silencing on the cellular genome (137, 354). Intriguingly, H3K27me2 is the more abundant modification on the host genome, although its direct role in gene silencing compared to trimethylation is not understood (137). A recent study did identify a novel histone reader specifically for H3K27me2 as the tudor domain-containing protein PHD finger protein 20 (PHD20) (354). Binding of PHD20 to H3K27me2 results in recruitment of the repressive Mi-2/nucleosome remodeling and deacetylase complex, at least in cancer cells, providing a direct mechanistic link between H3K27me2 and transcriptional repression. However, H3K27me2 was not significantly enriched at this time point (Fig 4.3B). Importantly, the latent HSV-1 genome also significantly co-localizes with H2AK119ub in approximately one-third of the infected neurons (Fig 4.3C) and colocalizes with core PRC1 component Ring1B at in a smaller proportion of latent viral genomes analyzed (10%) (Fig 4.3D). We have yet to measure Ring1A co-localization with the HSV-1 genome. Therefore, using multiple methods, our data demonstrate enrichment for H2AK119ub and H3K27me3 but not H3K27me2 on at least a sub-population of viral genomes.

PRC1 associates with the viral genome during active stages of viral gene silencing.

As previously determined by performing ChIP on ganglia in a mouse model, PRC2 (specifically Suz12) and associated H3K27me3 are not enriched on the viral genome until lytic viral genes have already been silenced (122). These observed kinetics suggest that PRC2 plays a role in the maintenance of viral gene repression, rather than its initiation. Given the known function of vPRC1-medited H2AK119ub in driving gene silencing before H3K27me3 deposition (163-167), at least in embryonic stem cells, we posited that H2AK119ub may be deposited prior to H3K27me3. In addition, the dimethyl form of H3K27me2 can occur rapidly and precede H3K27me3 and can silence cellular genes independently of H3K27me3 (354) (136, 138).

Therefore, we investigated the kinetics of H3K27me2, H3K27me3, and H2AK119ub following the infection of primary neurons. Several time points were preliminarily surveyed, but here we present the acute time point of 3 days post-infection; a time point at which we have previously observed a steep reduction in lytic viral gene expression during latency establishment (117). In agreement with previous *in vivo* findings, H3K27me3 was not found to be significantly co-localized with latent viral genomes at this 3-day post-infection time point (Fig 4.4A). In addition, we did not observe co-localization of H3K27me2 with the viral genome (Fig 4.4B). In contrast, we found that the viral genome was significantly enriched above rotational controls for both H2AK119ub and Ring1B at this time point, respectively in 30% and 10% of latent viral genomes analyzed (Fig 4.4C-D). Notably, these proportions are equivalent to those calculated for each respective analysis at the 30-day time point (Fig. 4.3), suggesting

that viral genomes acquire H2AK119ub or Ring1B quickly post-infection and maintain them as latency is established over time. The obvious caveat to these findings is that, while we have employed a rigorous, high-throughput system to analyze co-localization, co-localization does not translate to direct binding. Therefore, these PRC1/2 recruitment kinetics must also be validated using techniques such as ChIP-sequencing *in vivo* and CUT&RUN-sequencing *in vitro* in future studies.

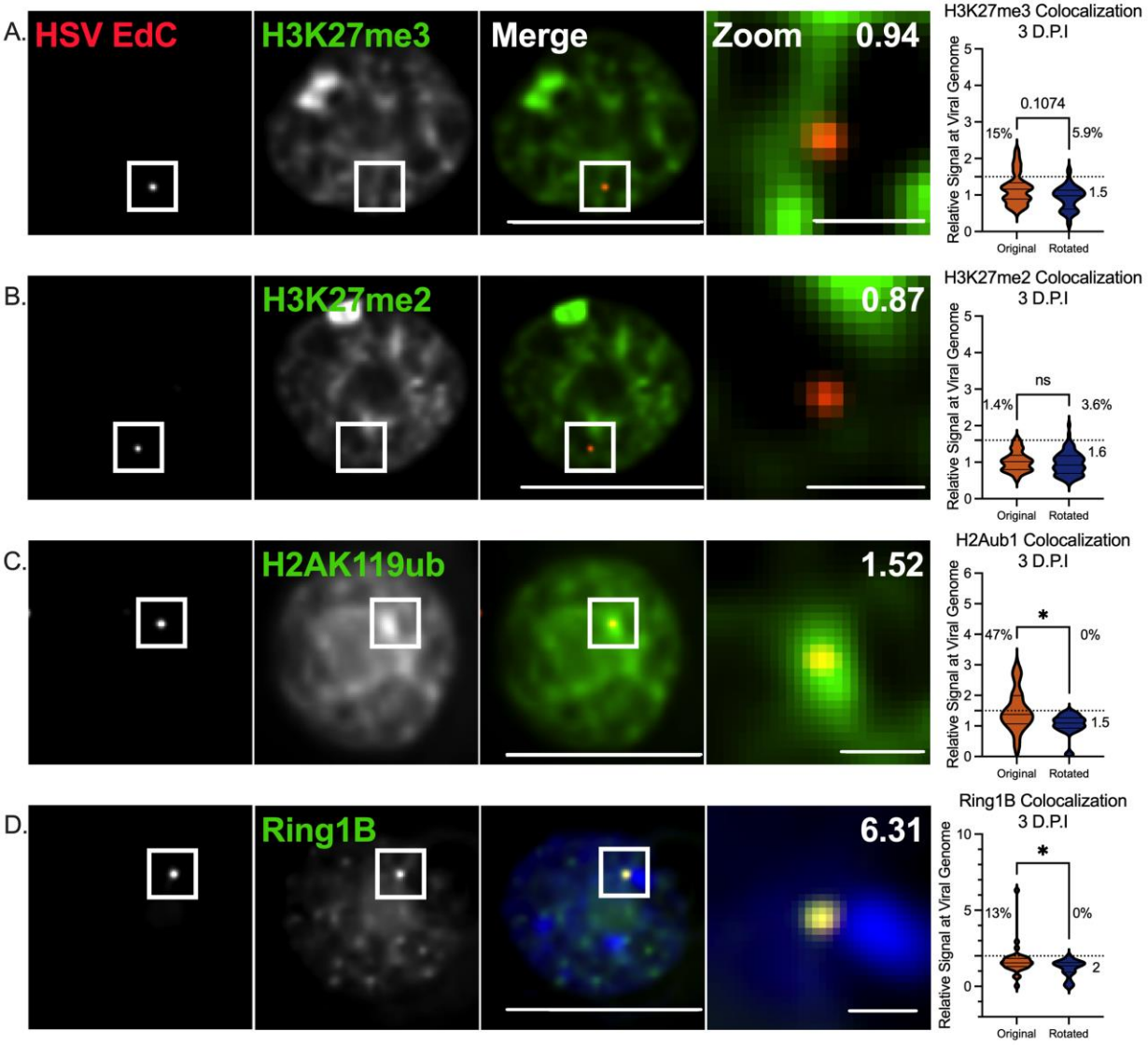

Figure 4.4 Single viral genome analysis demonstrates a population of HSV-1 genomes associated with H2AK119ub and Ring1 during times of active viral gene silencing. Primary sympathetic neurons were infected with EdC-labeled HSV-1 in the presence of ACV. 3 days post-infection, infected neurons were fixed and stained for histone modifications H3K27me3, H3K27me2, or H2AK119ub, or PRC1 core component Ring1B, and the HSV-1 genome was visualized through click chemistry. Nuclear Hoechst stain featured in blue where nucleus is not prominently outlined by histone modification. Enrichment values of chromatin mark/modifier with each individual HSV-1 genome analyzed were calculated in a high-throughput and unbiased manner using computational program NucSpotA. (A) Representative images of HSV-1 genome (red) and the chromatin modification or reader/writer (green); 10 μm scale, 1 μm scale for zoom. Co-localization value for representative image demonstrated in top right corner of zoom panel. (B-E) Statistical significance of co-localization was determined through paired comparison of enrichment values from original images and control images where the viral genome was rotated 90 degrees to achieve random placement. Threshold enrichment values for co-localization for each stain, and the proportion of neurons which are greater than or equal to this threshold, are respectively demarcated by a dashed line and percentage. Minimum 50 biological replicates; Wilcoxon test. Normality determined by Kolmogorov-Smirnov test. *, $P < 0.05$; **, $P < 0.01$. ns, not significant.

During active latency establishment, we can differentiate between transcriptionally active and repressed viral genomes by staining for lytic viral Infected Cell Protein 4 (ICP4; fuchsia). Interestingly, only in ICP4-negative nuclei did we see co-localization between HSV-1 and Ring1B (Fig 4.5A-B). These data suggest that PRC1 not only associates with HSV-1 genomes during initial silencing, but that these associated genomes are repressed, presumably from their association with PRC1.

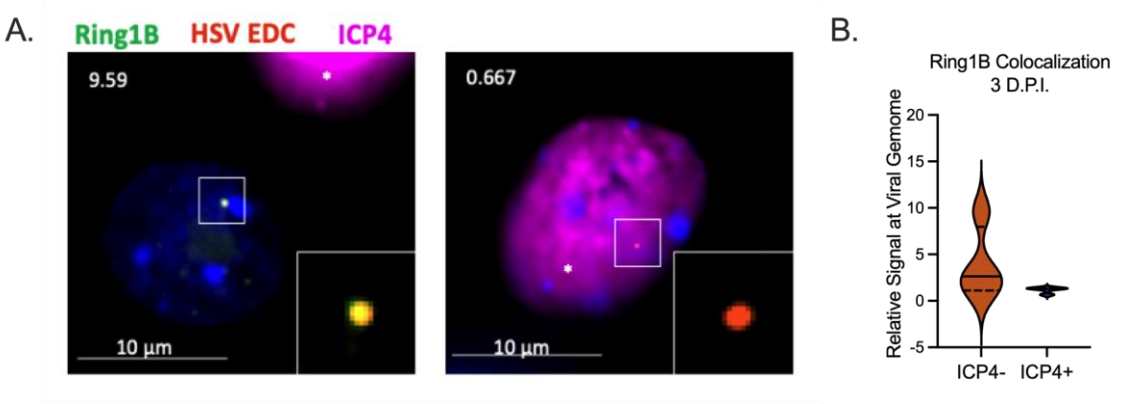

Figure 4.5 Ring1B co-localizes with repressed HSV-1 genomes during times of active viral gene silencing. (A-B) Primary sympathetic neurons were infected with EdC-labeled HSV-1 in the presence of ACV. 3 days post-infection, infected neurons were fixed and stained for PRC1 core component Ring1B (green) and viral protein ICP4 (fuschia), and the HSV-1 genome (red) was visualized through click chemistry. Nuclear Hoescht stain shown in blue. Enrichment values of Ring1B with each individual HSV-1 genome analyzed were calculated for transcriptionally repressed (ICP4-) and transcriptionally active (ICP4+) viral genomes in a high-throughput and unbiased manner using computational program NucSpotA. (A) Merged representative images of Ring1B with repressed (ICP4-, lefthand image) versus transcriptionally active (ICP4+, righthand image) viral genomes; 10 μm scale, 1 μm scale for zoom. Enrichment value for representative images demonstrated in top left corner, zoom of merged HSV-1 genome and Ring1B staining in bottom right corner of respective images. (B) Images were binned into ICP4+ and ICP4- nuclei, and Ring1B enrichment values at the HSV-1 genome were calculated using NucSpotA and compared between conditions. 10 cells from 1 biological replicate; Mann-Whitney test. Normality determined by Kolmogorov-Smirnov test. *, $P < 0.05$; **, $P < 0.01$. ns, not significant.

PRC1 represses viral gene expression in neurons during the early stages of infection.

PRC1 association with repressed HSV-1 genomes, and the kinetics of this association, suggests PRC1 and H2AK119ub actively silence these genomes. However, our data on binding, co-localization, and viral gene repression are thus far correlative. We therefore took a functional approach to investigate the contribution of

vPRC1 and PRC2 to the repression of viral lytic gene expression. Neonatal sympathetic neurons were infected with HSV-1 Stayput-GFP in the presence of PRC1 inhibitor PTC-209 (357), and viral gene expression was analyzed for all three classes of viral genes over time. Here, we present data from 3 days post-infection, the time point at which we have previously demonstrated H2AK119ub and Ring1B colocalization (Fig 4.4C-D). We observed a subtle but statistically significant increase in all classes at viral transcripts upon PRC1 inhibition with PTC-209 (Fig 4.6A-C). This phenotypic increase was also trending when this experiment was carried out in cultured sensory neurons from adult murine trigeminal ganglia, although additional repeats are required (Fig 4.6D-F), and a greater fold change in viral gene expression was observed upon inhibition in the sensory versus sympathetic cultures. The role of PRC1 in viral gene silencing could be more impactful in the sensory neuronal cultures, which differ from the sympathetic cultures in terms of both age and neuronal subtype which may imply changes in epigenetic mechanisms of silencing. We have previously observed differences in reactivation capacity between these two types of cultures, suggesting relevance of silencing mechanisms may also differ (93, 117).

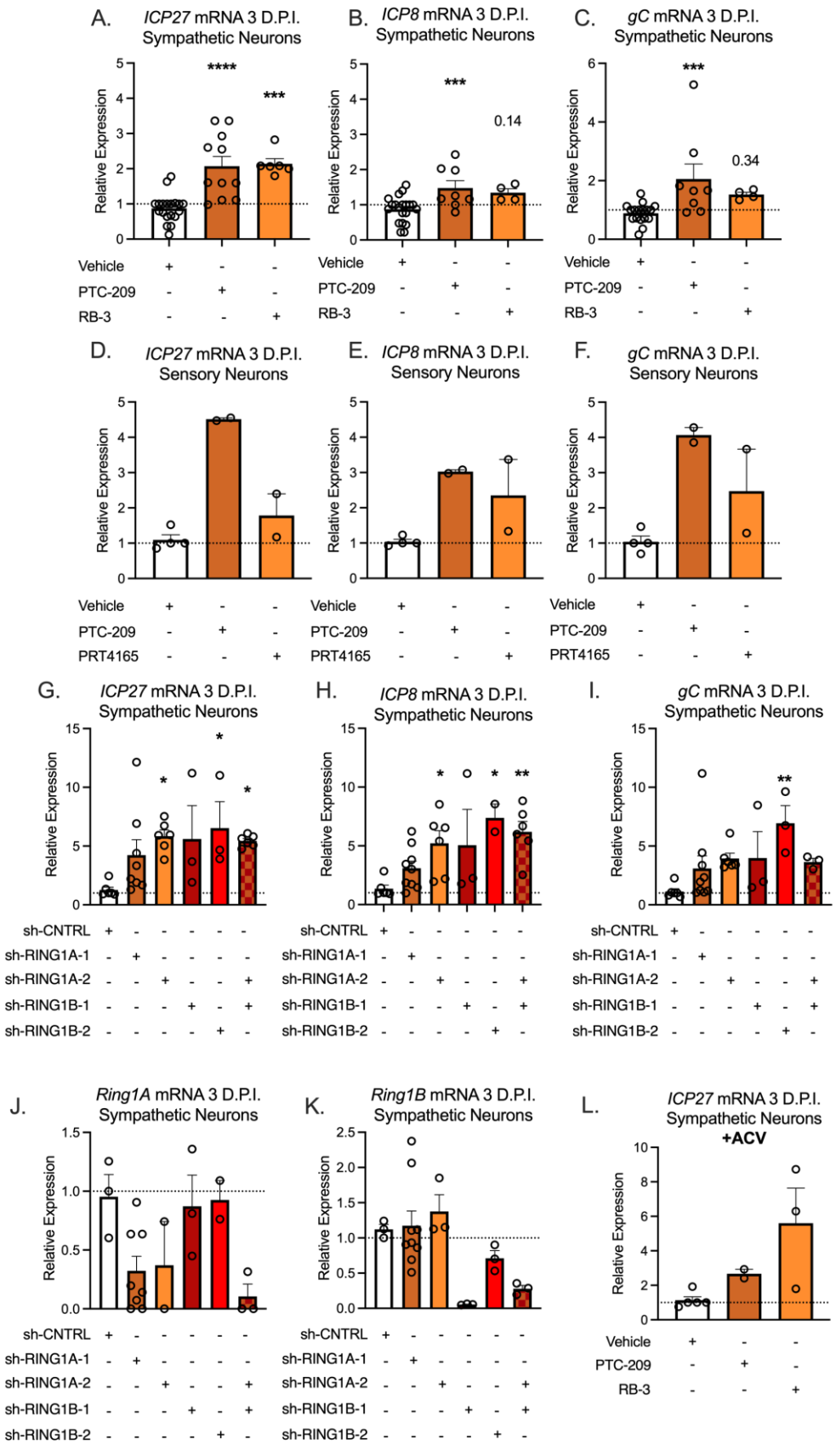
A.
ICP27 mRNA 3 D.P.I.
Sympathetic Neurons
B.
ICP8 mRNA 3 D.P.I.
Sympathetic Neurons
C.
gC mRNA 3 D.P.I.
Sympathetic Neurons
Relative Expression
****
***
0.14
0.34
Vehicle
PTC-209
RB-3
D.
ICP27 mRNA 3 D.P.I.
Sensory Neurons
E.
ICP8 mRNA 3 D.P.I.
Sensory Neurons
F.
gC mRNA 3 D.P.I.
Sensory Neurons
PRT4165
G.
ICP27 mRNA 3 D.P.I.
Sympathetic Neurons
H.
ICP8 mRNA 3 D.P.I.
Sympathetic Neurons
I.
gC mRNA 3 D.P.I.
Sympathetic Neurons
sh-CNTRL
sh-RING1A-1
sh-RING1A-2
sh-RING1B-1
sh-RING1B-2
J.
Ring1A mRNA 3 D.P.I.
Sympathetic Neurons
K.
Ring1B mRNA 3 D.P.I.
Sympathetic Neurons
L.
ICP27 mRNA 3 D.P.I.
Sympathetic Neurons
+ACV

Figure 4.6 Inhibition or depletion of PRC1 enhances HSV-1 lytic gene expression represses HSV-1 during times of active viral gene silencing. (A-F) Neonatal sympathetic neurons (A-C) or adult sensory neurons (D-F) were treated with PRC1 inhibitors 2 μM PTC-209, 25 μM RB-3, or 40 μM PRT4165 pre-infection for 1 hour, during inoculation with HSV-1 Stayput-GFP in the absence of ACV and following the removal of inoculum for 3 days post-infection. Expression of lytic viral immediate early gene ICP27 (A,D), early gene ICP8 (B,E), or late gene gC (C,F) were analyzed normalized to cellular control 18s. Expression relative to vehicle conditions depicted. Sympathetic neurons; 3 biological replicates with Mann-Whitney against Vehicle control. Sensory neurons; 1 biological replicate. (G-K) Neonatal sympathetic neurons were transduced with a non-targeting shRNA control lentivirus or one of two independent lentiviruses expressing shRNAs that target Ring1A (sh-Ring1A1, sh-Ring1A2) or Ring1B (sh-Ring1B1, sh-Ring1B2), or both Ring1A and Ring1B (sh-Ring1A1 and sh-Ring1B2). 5 days post transduction, neurons were infected with HSV-1 Stayput-GFP in the absence of ACV. Expression of immediate early ICP27 (G), early ICP8 (H), and late gC (I) viral genes and cellular Ring1A (J) and Ring1B (K) 3 days post-infection were analyzed and normalized to cellular control 18s. Expression relative to shRNA control demonstrated. 2 biological replicates; Mann-Whitney against sh-CNTRL. (L) Neonatal sympathetic neurons were treated with PRC1 inhibitor 2 μM PTC-209 or 25 μM RB-3 pre-infection for 1 hour, during inoculation with HSV-1 Stayput-GFP in the presence of ACV and following the removal of inoculum for 3 days post-infection. ACV was kept in the media for 3 days post-infection. Expression of lytic viral immediate early gene ICP27 was analyzed normalized to cellular control 18s. Expression relative to vehicle conditions demonstrated. 1 biological replicate. Normality determined by Kolmogorov-Smirnov test. *, $P < 0.05$; **, $P < 0.01$. ns, not significant.

Although PTC-209 has been demonstrated to reduce H2AK119ub on cellular DNA in neurons, the exact mechanism of PTC-209 is unclear. PTC-209 could also involve the degradation of BMI-1 at the transcriptional or translational level, which may confer some off-target effects in our cultures. BMI1 traditionally associates with one form of PRC1 (cPRC1) that does not efficiently carry out H2AK119ub (128, 157, 159, 162). Moreover, BMI-1 depletion in neuroblastoma cells has been demonstrated to induce DNA damage and apoptosis seemingly independently of its Polycomb PRC1/2 interacting partners (358). We therefore recently had PRC1 inhibitor RB-3 synthesized, which directly binds to Ring1A/B and blocks its association with chromatin and ability to deposit H2AK119ub (359). Our preliminary studies demonstrate that treatment with RB-3 in neonatal sympathetic neurons during infection enhances lytic viral gene expression at 3 days post-infection (Fig 4.6A-C). This increase is statistically significant for immediate early gene ICP27, and trending for early gene ICP8, and late gene gC.

We also produced lentiviruses expressing shRNAs targeting the core components of PRC1, Ring1A and Ring1B. Neonatal sympathetic neurons were transduced 5 days prior to infection with HSV-1 Stayput-GFP, and viral gene expression was analyzed at 3 days post-infection. Ring1 knockdown was verified during each individual replicate at the level of RNA (Fig 4.6J-K). The co-depletion of both Ring1A and Ring1B was carried out because previous studies have shown redundancy between the two proteins in vPRC1 activity (360). For each class of viral lytic genes, viral gene expression was enhanced with the single knockdown of Ring1A or Ring1B and dual Ring1A/B knockdown (Fig 4.6G-I). These changes in gene expression were notably greater than

those observed with PRC1 inhibitor treatment, as Ring1 depletion reached up to an approximately 15-fold increase in viral gene expression. These functional data in combination with our kinetic data suggest that PRC1 and H2AK119ub are deposited onto the HSV-1 genome early during latency establishment to silence viral lytic genes.

While both PRC1 inhibitors enhanced viral gene expression, the fold changes were lower than anticipated, exhibiting 2-fold changes on average. We reasoned that this subtle phenotype may be attributed to increased neuronal death due to enhanced lytic infection upon PRC1 inhibition. Neuronal death from pervasive lytic infection at three days post-infection would clear lytic transcripts from cultures and under-estimate the effect of these inhibitors. Therefore, we inhibited PRC1 in neonatal sympathetic neurons with RB-3 in the presence of antiviral acyclovir (ACV) (Fig 4.6L). ACV inhibits viral DNA replication, and we have also found that it limits lytic gene expression, and may therefore result in less neuronal cell death even with enhanced lytic gene expression resulting from vPRC1 inhibition (117). Upon analysis of viral gene expression 3 days post-infection in the presence of ACV, we observed a dramatically enhanced and statistically significant increase in immediate early viral transcript ICP27 under RB-3 treatment conditions, averaging a 6-fold enhancement of viral gene expression in +ACV conditions versus the < 2-fold enhancement without the use of ACV. We therefore also anticipate a more robust increase with Ring1 depletion with the addition of antiviral ACV. We have not directly demonstrated enhanced neuronal death upon PRC1 inhibition, but these data suggest that this may have at least partially obscured a PRC1 inhibitor phenotype.

PRC2 does not repress viral gene expression in neurons during the early stages of infection.

We performed similar experiments using PRC2 inhibition or depletion in neonatal sympathetic neurons and adult sensory neurons. We hypothesized that PRC2 would not disrupt viral gene expression at early time points post-infection due to its later deposition kinetics. Neonatal sympathetic neurons (Fig 4.7A-C) or adult sensory neurons (Fig 4.7D-F) were infected with HSV-1 Stayput in the presence of PRC2 inhibitors and viral gene transcription of all classes of lytic genes were analyzed relative to vehicle control. PRC2 inhibitor treated samples did not display enhanced lytic gene expression in either neuronal subtype. Later time-points post-infection were also surveyed and did not demonstrate increases in viral gene expression (data not shown). We also depleted the core component of PRC2, Suz12, using one of three independent shRNA-targeting lentiviruses and subsequently infected cultures. It has previously been demonstrated that Suz12 is required for PRC2 activity and that its elimination prevents its function (134, 361). Upon Suz12 depletion, as validated at the level of RNA during each individual replicate in Fig 4.7J, the expression of all three classes of viral genes analyzed did not demonstrate an enhancement at 3 days post-infection (Fig 4.7G-I).

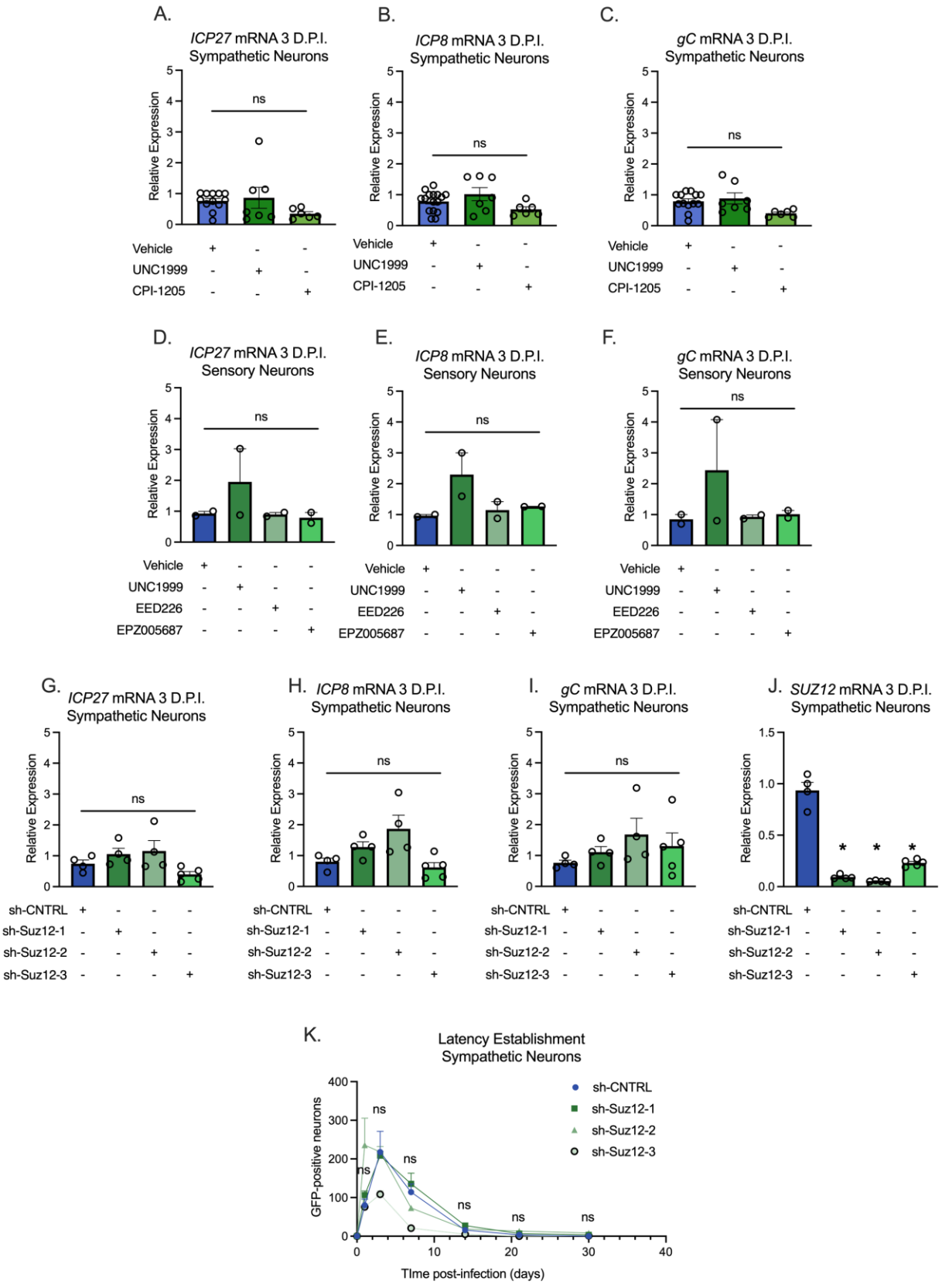
A.
ICP27 mRNA 3 D.P.I.
Sympathetic Neurons
Relative Expression
ns
Vehicle + - -
UNC1999 - + -
CPI-1205 - - +
B.
ICP8 mRNA 3 D.P.I.
Sympathetic Neurons
Relative Expression
ns
Vehicle + - -
UNC1999 - + -
CPI-1205 - - +
C.
gC mRNA 3 D.P.I.
Sympathetic Neurons
Relative Expression
ns
Vehicle + - -
UNC1999 - + -
CPI-1205 - - +
D.
ICP27 mRNA 3 D.P.I.
Sensory Neurons
Relative Expression
ns
Vehicle + - - -
UNC1999 - + - -
EED226 - - + -
EPZ005687 - - - +
E.
ICP8 mRNA 3 D.P.I.
Sensory Neurons
Relative Expression
ns
Vehicle + - - -
UNC1999 - + - -
EED226 - - + -
EPZ005687 - - - +
F.
gC mRNA 3 D.P.I.
Sensory Neurons
Relative Expression
ns
Vehicle + - - -
UNC1999 - + - -
EED226 - - + -
EPZ005687 - - - +
G.
ICP27 mRNA 3 D.P.I.
Sympathetic Neurons
Relative Expression
ns
sh-CNTRL + - - -
sh-Suz12-1 - + - -
sh-Suz12-2 - - + -
sh-Suz12-3 - - - +
H.
ICP8 mRNA 3 D.P.I.
Sympathetic Neurons
Relative Expression
ns
sh-CNTRL + - - -
sh-Suz12-1 - + - -
sh-Suz12-2 - - + -
sh-Suz12-3 - - - +
I.
gC mRNA 3 D.P.I.
Sympathetic Neurons
Relative Expression
ns
sh-CNTRL + - - -
sh-Suz12-1 - + - -
sh-Suz12-2 - - + -
sh-Suz12-3 - - - +
J.
SUZ12 mRNA 3 D.P.I.
Sympathetic Neurons
Relative Expression
*
*
*
sh-CNTRL + - - -
sh-Suz12-1 - + - -
sh-Suz12-2 - - + -
sh-Suz12-3 - - - +
K.
Latency Establishment
Sympathetic Neurons
GFP-positive neurons
sh-CNTRL
sh-Suz12-1
sh-Suz12-2
sh-Suz12-3
ns
TIme post-infection (days)

Figure 4.7 Inhibition or depletion of PRC2 does not enhance HSV-1 lytic gene expression during times of active viral gene silencing. (A-F) Neonatal sympathetic neurons (A-C) or adult sensory neurons (D-F) were treated with PRC2 inhibitors (green; 1 μM UNC-1999, 10 μM CPI-1205, 25 μM EED226, or 0.5 μM EPZ005687) pre-infection for 1 hour, during inoculation with HSV-1 Stayput-GFP, and following the removal of inoculum for 3 days post-infection. Expression of lytic viral immediate early (A,D), early (B,E), or late genes (C,F) were analyzed normalized to cellular control 18s. Expression relative to vehicle conditions shown. Sympathetic neurons; 4 biological replicates with Mann-Whitney against Vehicle control. Sensory neurons; 1 biological replicate with Mann-Whitney against Vehicle control. Normality determined by Kolmogorov-Smirnov test. (G-K) Neonatal sympathetic neurons were transduced with a non-targeting shRNA control lentivirus or one of three independent lentiviruses expressing shRNAs that target Suz12 (sh-Suz12-1, sh-Suz12-2, shSuz12-3). 5 days post transduction, neurons were infected with HSV-1 Stayput-GFP. Expression of immediate early ICP27 (G), early ICP8 (H), and late gC (I) viral genes and cellular Suz12 gene (J) 3 days post-infection were analyzed and normalized to cellular control 18s. Expression relative to shRNA control demonstrated. (K) The number of GFP-positive neurons, indicative of lytic infection events, was quantified over time as latency was established.
1 biological replicate; Mann-Whitney against sh-CNTRL. Normality determined by Shapiro-Wilk test. *, $P < 0.05$; **, $P < 0.01$. ns, not significant.

As an additional readout of lytic infection, the number GFP-positive neurons indicative of individual lytic infection events was tracked over time following HSV-1 Stayput-GFP infection of Suz12-depleted cultures. In agreement with our viral gene expression data, there was no increase in the numbers of GFP-positive neurons following Suz12 depletion at any of the time points analyzed post-infection, including time points after the establishment of latency (Fig 4.7K). Therefore, our data suggest that, in contrast to PRC1, PRC2 does not promote HSV-1 lytic gene silencing during the establishment of a latent infection.

We also directly investigated whether continuous PRC1 and PRC2 activity was required for the maintenance of HSV-1 latent infection. Following the establishment of latency, cultures were treated with PRC1 or PRC2 inhibitors and the number of GFP-

positive neurons was quantified over time. Us11-GFP in this experiment serves as an indicator of single neurons which escape from quiescence. Inhibition of either PRC1 or PRC2 did not result in an increase of GFP-positive neurons compared to the control group. The positive control, LY294002, was also included which resulted in a robust increase in GFP-positive neurons (Fig 4.8). LY294002 is a PI3-kinase inhibitor and well-characterized HSV-1 reactivation stimulus in multiple *in vitro* and *ex vivo* models (8, 98, 99, 107, 224, 267). These experiments may require repetition with PRC1/2 depletion versus inhibition or using a longer incubation period to track spontaneous reactivation events. However, our current data suggest that once PRC1-mediated silencing initiates viral gene repression at early times post-infection, the enzymatic activities of Ring1 or EZH1/2 are not continuously required for the maintenance of repression.

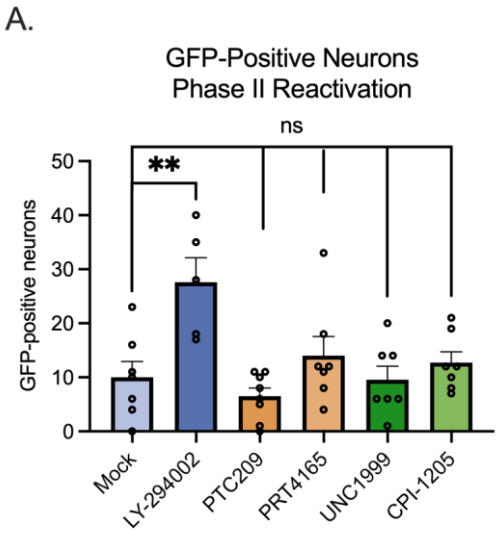

Figure 4.8 Inhibition of PRC1 or PRC2 is not sufficient to elicit reactivation from latently infected neurons. (A) Primary sympathetic neurons latently infected with HSV-1 Stayput-GFP in the presence of ACV. 6 days following infection, ACV was removed from cultures, and spontaneous reactivation, as indicated by GFP-positive neurons, was monitored for two additional days. 8 days post-infection, latently infected cultures were treated with vehicle control (light blue), positive control stimulus LY-294002 (dark blue; 20 μM), PRC1 inhibitors (orange; PTC-209 2 μM, PRT4165 40 μM), or PRC2 inhibitors (green; UNC1999 1 μM, CPI-1205 10 μM). GFP-positive neurons indicative of full reactivation events were monitored over time. The peak number of GFP-positive neurons at 48 hours post-stimulus was quantified. 5 biological replicates Ordinary One-Way ANOVA; Normality determined by Kolmogorov-Smirnov test. *, $P < 0.05$; **, $P < 0.01$. ns, not significant.

Ring1 is excluded from the nucleus upon lytic infection of neurons.

Upon HSV-1 infection in the primary neuronal Stayput-GFP model system culture, only a subset of neurons in culture establish latency, whereas other neurons become lytic infected (117). This is consistent with what has been previously observed following infection *in vivo* (13, 194). However, Ring1B is detectable in the nucleus in each neuronal cell in uninfected cultures, as determined by immunofluorescence (Fig 4.9A). In effort to determine how lytically infected neurons might deal with repressive, nuclear PRC1, we imaged Ring1B localization following HSV-1 infection in a model without ACV (Fig 4.9B). As anticipated, two population of neurons were observed at 3 days post-infection, ICP4/Us11-GFP-positive neurons, which are lytically infected, and ICP4/Us11-GFP-negative neurons, which are either quiescently infected or uninfected. Importantly, we observed differential Ring1B staining patterns between these two populations of neurons. In ICP4/Us11-GFP-negative neurons, Ring1B staining was broadly nuclear and exhibited occasional puncta, as previously observed (Fig 4.4).

However, Ring1B staining was notably absent from the nucleus of ICP4/Us11-GFP-positive neurons. Nuclear localization of core PRC1 component Ring1 therefore appears incompatible with transcriptionally active lytic viral infection. Given the nuclear localization of Ring1B in all neurons prior to infection, these data suggest that either the virus or host likely initiates the re-localization or degradation of repressive Ring1 to promote viral transcriptional activation and lytic infection. This data also suggests that the enhancement of viral gene expression observed in the presence of PRC1 inhibition or depletion is an underestimation of PRC1's ability to silence HSV-1 genomes, as there is likely an additional mechanism at play to overcome PRC1-mediated silencing in the cultures.

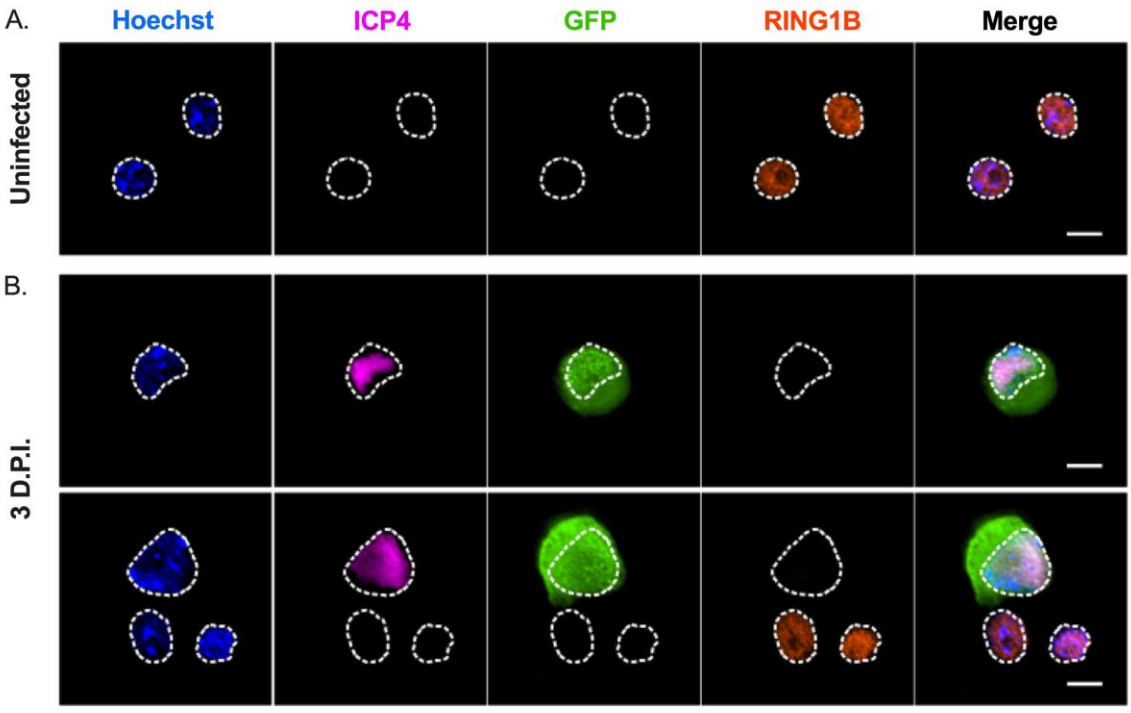

Figure 4.9 PRC1 localization following *de novo* lytic HSV-1 infection in neurons. (A-B) Primary sympathetic neurons were mock infected (A) or infected with HSV-1 Stayput-GFP (B) in the absence of antivirals. Neurons were fixed 3 days post-infection and stained for nuclear stain Hoechst (blue), viral proteins ICP4 (fuchsia) and Us11 fused to GFP (green), and core PRC1 component Ring1B (orange). Lytic infected nuclei encircled in white. Scale bar 10 μM.

Potential LAT/hnRNPK-mediated PRC1 recruitment to the HSV-1 genome

We next turned our attention to the mechanisms of vPRC1 recruitment to the HSV-1 genome. One potential mechanism of recruitment and/or activation of PRC1 and PRC2 to mediate deposition of histone post-translational modifications is via binding to long noncoding RNAs (lncRNAs). Notably, during the establishment and maintenance of HSV-1 latent infection, the virus expresses a lncRNA "LAT" at least in a proportion of neurons. The exact molecular functions of the LAT are unknown, and while it is not essential for the establishment of a latent infection, it may modulate lytic gene expression and promote increased association with H3K27me3 (121, 124).

During our investigation on the impact of PRC1 to HSV-1 latency and reactivation, our collaborator Igor Jurak shared data with us that the LAT interacts with cellular heterogenous nuclear ribonucleoprotein K (hnRNPK) in HEK 293T cells (unpublished). This interaction was discovered following immunoprecipitation with a LAT probe followed by mass-spectrometry and was recapitulated using three independent methods of binding analysis. There is thus the prospect that hnRNPK and the LAT may in tandem recruit PRC1 to HSV-1 genomes during latency establishment. We have yet

to test this hypothesis directly but have acquired several pieces of supporting experimental data discussed below.

One caveat to LAT-hnRNPK interaction finding is that the experiments were performed in HEK 293T's, cells that would not otherwise physiologically express the LAT or be capable of sustaining a latent infection with HSV-1. We therefore aimed to investigate whether this interaction occurred in a more physiologically relevant neuronal model. To investigate LAT/hnRNPK binding, we used Lund Human Mesencephalic (LUHMES) neuronal cells, which have previously been demonstrated to support HSV-1 quiescent infection and express the LAT (116), and are easily scalable to generate large amounts of material. Three days following infection with HSV-1 Stayput-GFP, we performed RNA-immunoprecipitation (RNA-IP) for hnRNPK. Importantly, the binding of the LAT to hnRNPK was substantially and statistically enhanced over control cellular RNAs (Fig 4.10A). Therefore, hnRNPK does bind the LAT during early times post-infection in neurons, when H2AK119ub targeting to viral genomes is also occurring.

There are caveats with the use of LUHMES in this experiment. LUHMES are derived from neuronal cells of the mesencephalon and therefore the central nervous system (362, 363), not the peripheral nervous system where HSV-1 establishes a latent infection. Moreover, LUHMES are differentiated from embryonic cells, but HSV-1 does not infect fetal neurons and is acquired during young adulthood for most. Also, the epigenetic signature of embryonic neurons has been demonstrated to differ from that of mature neurons (364). Lastly, our laboratory and others have also been unable to

achieve reactivation in these cultures (Fig 4.11). Ideally, primary PNS neurons would be used for the RNA-IP. However, we could not accumulate the substantial cellular material that was required to perform an RNA-Immunoprecipitation from our cultures. However, we have verified that hnRNPK in our primary neurons is robustly transcribed (RNA-seq, data not shown) and translated (western blotting, Fig 4.10B). Further, hnRNPK appears to co-localize with the HSV-1 genome in these neurons during early time-points post-infection (Fig 4.10C).

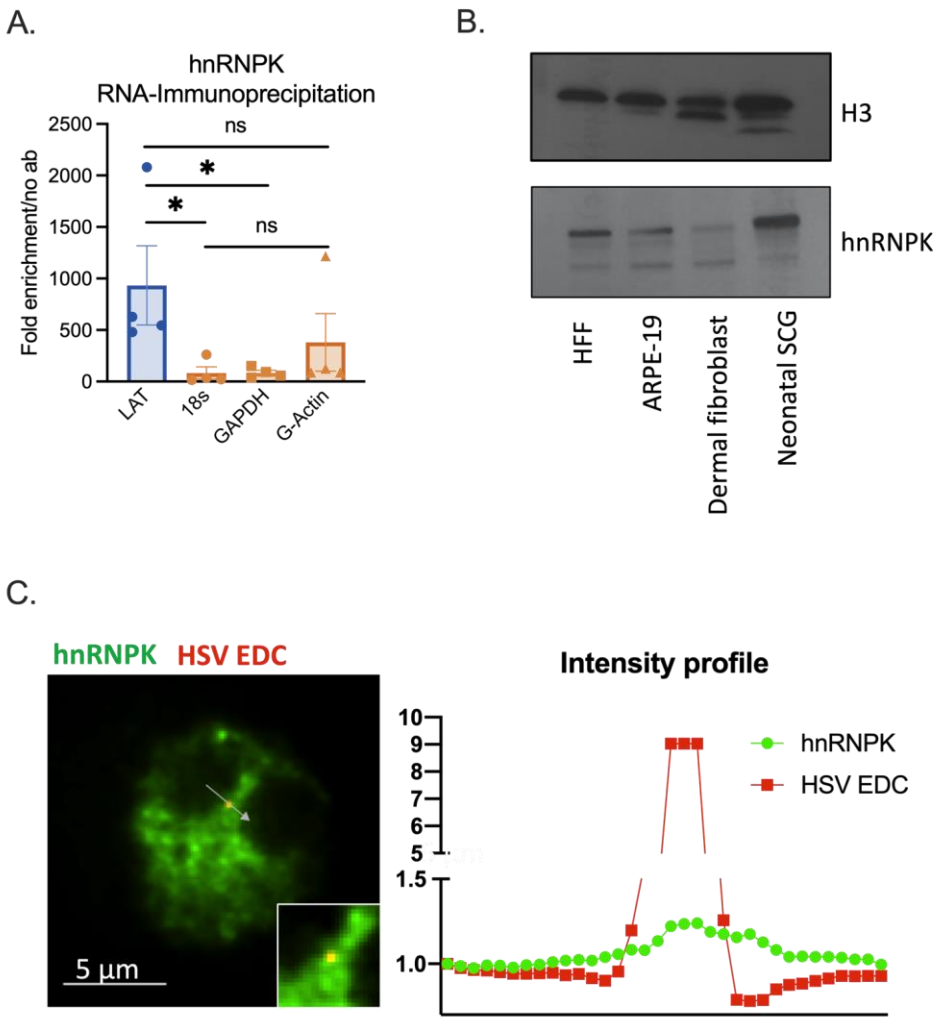

Figure 4.10 hnRNPK in neurons. (A) LUHMES were infected with HSV-1 Stayput-GFP and collected 3 days post-infection. RNA-immunoprecipitation was performed using negative control IgG antibody or hnRNPK antibody, and the copy numbers of viral latent transcript LAT (blue) and cellular controls (orange) were determined by RT-qPCR through standard curves. Fold enrichment represents hnRNPK IP copy number divided by IgG control IP copy number for each transcript. 2 biological replicates; Mann-Whitney. Normality determined by Kolmogorov-Smirnov test. *, $P < 0.05$; **, $P < 0.01$. ns, not significant. (B) Western blotting for hnRNPK and histone H3 was performed using equal amounts (15 μg) of protein lysed and isolated cell types including human foreskin fibroblasts (HFF), ARPE-19s, murine dermal fibroblasts, and murine neonatal sympathetic neurons (neonatal SCG). (C) Primary neurons were infected with EdC-labeled HSV-1 in the presence of ACV). 3 days post-infection, infected neurons were fixed and stained for hnRNPK (green), and the HSV-1 genome (red) was visualized through click chemistry. (Left) Merged representative image demonstrated co-localization of hnRNPK with HSV-1 viral genome. Scale bar 5 μm. 10x zoom in bottom left corner of image. (Right) Intensity profile and overlap of hnRNPK and HSV-1 genome through arrow demarcated in lefthand image.

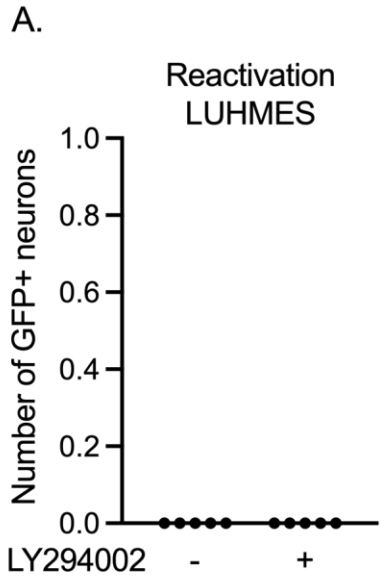

Figure 4.11 Reactivation cannot be achieved in LUHMES with LY294002. (A) Neurons were infected with HSV-1 Stayput-GFP in the absence of antiviral ACV. Following the loss of GFP in cultures, latently infected LUHMES were triggered to reactivate with LY294002. (A) Following the addition of LY294002, the number of Us11-GFP-positive neurons, indicative of reactivating neurons, was monitored and quantified up to 5 days post-stimulus. 5 biological replicates; Paired t-test. Normality determined by Shapiro-Wilk test. *, $P < 0.05$; **, $P < 0.01$. ns, not significant.

We also investigated if hnRNPK had any functional impact on viral gene silencing during latency establishment. Two independent shRNA-mediated lentiviruses targeting hnRNPK were created and validated in neurons (Fig 4.12A). Following transduction with

the lentivirus expressing the shRNA that gave the greatest reduction in hnRNPK protein levels, sympathetic neurons were infected with HSV-1 Stayput-GFP, and viral mRNA expression, viral DNA replication, and cell death were monitored over the course of latency establishment. At 3 days post-infection, cultures depleted of hnRNPK demonstrated enhanced expression of viral lytic genes ICP27, ICP8, and gC (Fig 4.12B). In contrast, the LAT remained unchanged with hnRNPK depletion. The LAT serves as a control as it remains transcribed pervasively during latency, unlike viral lytic genes. Moreover, hnRNPK has been demonstrated to degrade RNA and therefore analyzing LAT expression also served to investigate whether hnRNPK was degrading the RNA with which it associates. In line with the lytic viral mRNA data, we also observed enhanced viral DNA replication over the course of latency establishment and increased cell death at later timepoints, likely due to enhanced lytic infection (Fig 4.12C-D). Together, these data suggest that hnRNPK is repressive to HSV-1 lytic infection.

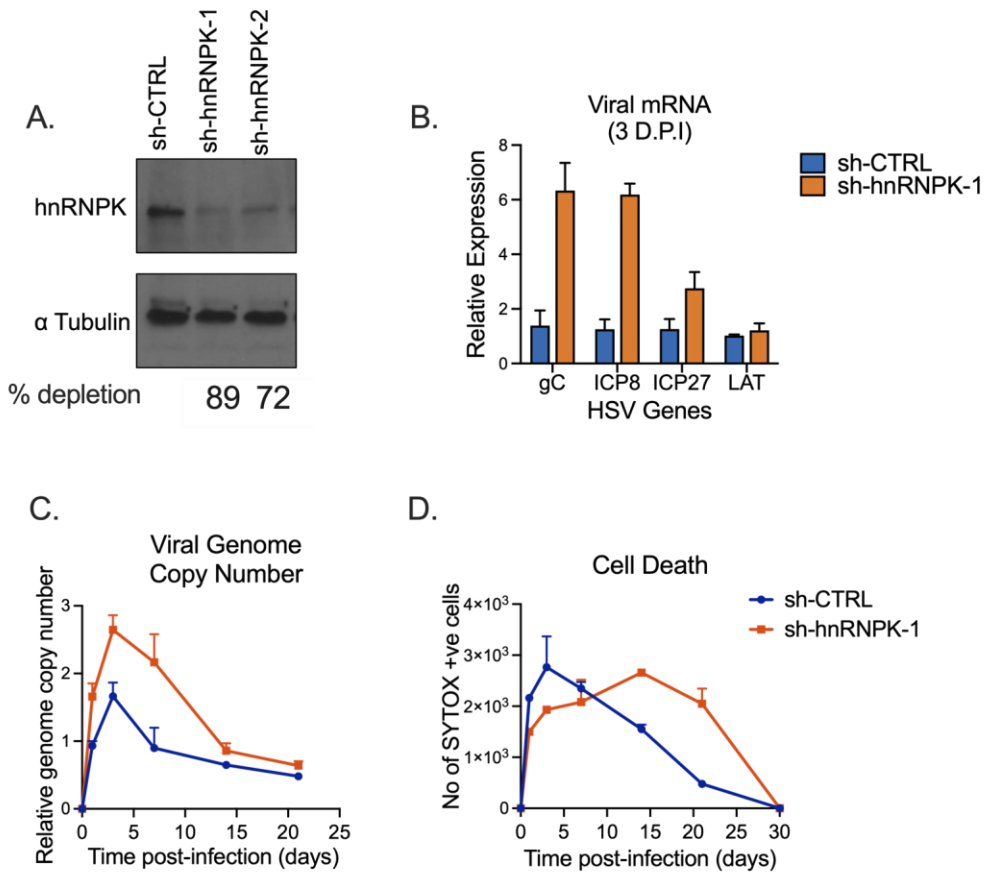

Figure 4.12 hnRNPK depletion enhances viral gene expression during latency establishment in neurons. (A-D) Neonatal sympathetic neurons were transduced with a non-targeting shRNA control lentivirus or one of two independent lentiviruses expressing shRNAs that target hnRNPK (sh-hnRNPK-1, sh-hnRNPK-2). (A) Western blot validation of knockdown in neurons 5 days post-transduction. (B-D) 5 days post-transduction with sh-hnRNPK-1, neurons were infected with HSV-1 Stayput-GFP in the absence of antivirals. (B) Expression of lytic viral immediate early gene ICP27, early gene ICP8, and late gene gC, as well as latent viral gene LAT, relative to sh-CTRL and cellular control 18s three days post-infection. (C-D) Viral DNA replication and cell death relative to sh-CTRL over the course of latency establishment.

PRC1 inhibition reduces future reactivation *in vitro*.

Only a proportion of HSV-1 genomes associated with H2AK119ub, Ring1B, and H3K27me3 during established latency (Fig 4.3, Fig 4.4). It was therefore likely that other repressed latent viral genomes associate with alternative forms of repressive chromatin. The constitutive chromatin histone post-translational modifications H3K9me2 and H3K9me3, which are considered to be more permanent than Polycomb silencing, are enriched on latent HSV-1 genomes (120, 193), although whether constitutive chromatin binds the same viral genomes undergoing Polycomb silencing is unknown. We and others have also demonstrated that only a proportion of individual latent genomes initiate reactivation in response to different stimuli (8, 93, 109, 117, 224, 292). Therefore, it is likely that individual latent HSV-1 genomes associate with various forms of chromatin that may be more or less primed for reactivation.

We therefore investigated the ability of viral genomes that undergo Polycomb silencing to reactivate. We did this by inhibiting PRC1 or PRC2 during latency establishment in the presence of viral DNA replication inhibitor acyclovir (ACV). The use of ACV here permits the equal establishment of latent infection despite PRC1/2 inhibitor treatment because viral DNA copy number remains stable (Fig 4.13A). Also, ACV reduces lytic gene expression and therefore somehow promotes quiescence (Fig 4.14A). Following latency establishment in the presence of PRC1/2 inhibitors, cultures were stimulated with LY294002, and the number of GFP-positive neurons at 48 hours post-stimulus was quantified as a readout of neurons that have undergone the full HSV-1 reactivation.

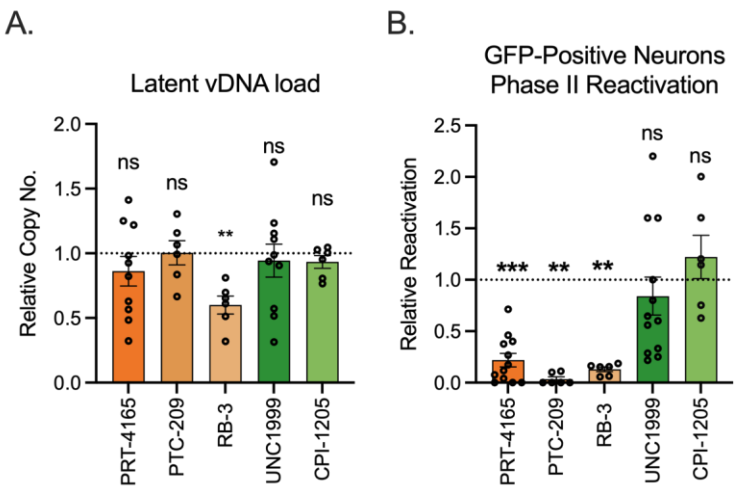

Figure 4.13 Inhibition of PRC1 but not PRC2 during latency establishment disrupts future reactivation. (A-B) Primary sympathetic neurons were treated with a vehicle control, or with PRC1 (orange; PRT4165 40 μM, PTC-209 2 μM, RB-3 25 μM), or PRC2 inhibitors (green; UNC1999 1 μM, CPI-1205 10 μM) pre-infection for 1 hour, during inoculation with HSV-1 Stayput-GFP in the presence of ACV and following the removal of inoculum. 6 days following infection, ACV and respective inhibitors were removed from cultures, and spontaneous reactivation, as indicated by GFP-positive neurons, was monitored for two additional days. Latently infected cultures were reactivated with LY294002 and GFP-positive neurons indicative of full reactivation events were monitored over time. (A) Latent viral DNA copy number normalized to vehicle controls. (B) The peak number of GFP-positive neurons at 48 hours post-stimulus presented as a fraction of vehicle control reactivation output. 3 biological replicates; Mann-Whitney against Vehicle control. Normality determined by Kolmogorov-Smirnov test. *, $P < 0.05$; **, $P < 0.01$. ns, not significant.

Interestingly, when PRC1 activity was inhibited during the establishment of latency, and therefore presumably the deposition of the H2AK119ub mark onto HSV-1 genomes was prevented, future reactivation was decreased (Fig 4.13B). This phenotype was recapitulated using three independent PRC1 inhibitors. This reduction in reactivation occurred despite equivalent latent viral DNA copy numbers (Fig 4.13A), and therefore the reduced capacity to reactivate under PRC1 inhibition was not due to fewer viral genomes that established a latent infection. Notably, this reactivation defect was not observed when PRC2 was inhibited during this timeframe using two independent

inhibitors. These data demonstrate that Polycomb silencing, specifically H2AK119ub deposition, during the early phase of latency establishment promotes latter reactivation, possibly via the formation of more reactivation-competent latent HSV-1 genomes.

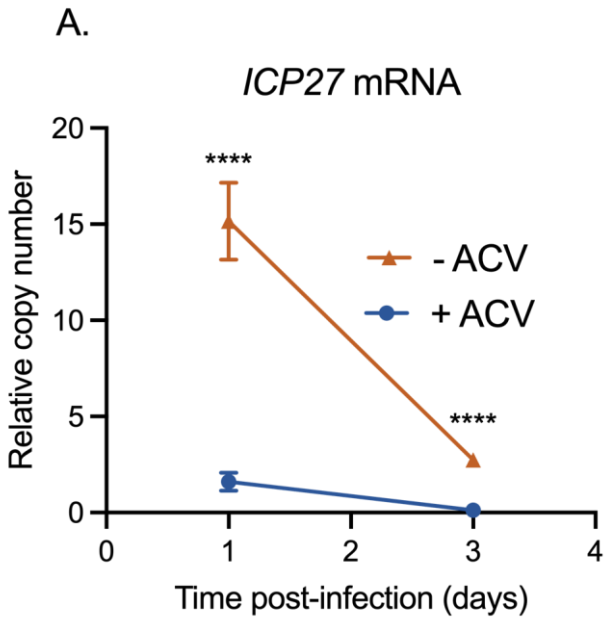

Figure 4.14 ACV represses HSV-1 lytic gene expression during latency establishment (A) Primary sympathetic neurons were infected with HSV-1 Stayput-GFP in the absence (orange) or presence (blue) of ACV. Immediate early lytic viral gene copy number was quantified at early time-points post-infection and normalized to cellular control 18s.3 biological replicates; Unpaired t-test. Normality determined by Kolmogorov-Smirnov test. *, $P < 0.05$; **, $P < 0.01$. ns, not significant.

H2AK119ub reader ZRF1 localizes to the nucleus during reactivation of neurons.

Given the repressive nature of H2AK119ub, this modification must be modified or removed from the HSV-1 genome during reactivation. Outside of the context of viral infection, one publication has implicated a novel protein Zuotin-related factor 1 (ZRF1) in the reading of the H2AK119ub mark to enable gene expression on cellular genomes

(365). As a preliminary approach, we investigated the localization of ZRF1 in latently infected neurons and neurons that were reactivated with LY294002 48 hours post-stimulus.

Neurons in which full reactivation occurred were identified through the expression of viral proteins ICP8 (fuchsia) and Us11 (fused to GFP, green). ICP8 and Us11-GFP were not detected in unreactivated cultures, as anticipated. In this culture, comprised of latently infected and uninfected neurons, there was a faint, homogenous ZRF1 staining through the cytoplasm and nucleus (Fig 4.15A). Following the addition of stimulus LY294002, a striking nuclear localization of ZRF1 was exhibited solely in ICP8 or Us11-GFP-positive neurons (Fig 4.15B). This is not direct evidence for ZRF1-mediated reactivation, which would require functional depletion studies, but these data do demonstrate that nuclear ZRF1 localization and reactivation are linked processes.

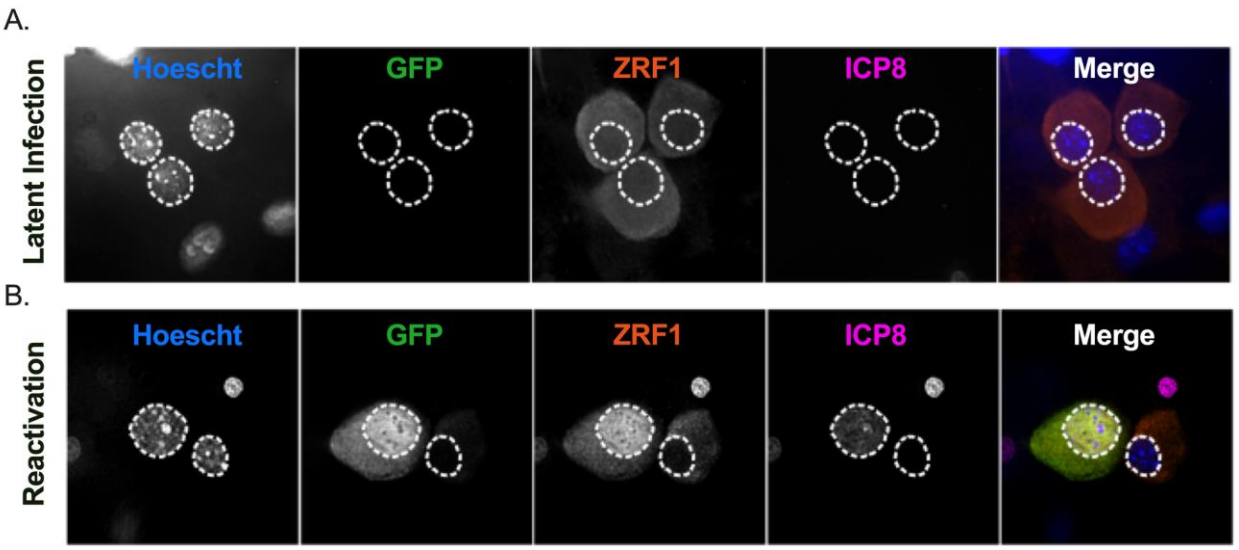

Figure 4.15 ZRF1 localizes to neuronal nuclei during HSV-1 reactivation. (A-B) Primary sympathetic neurons were infected with HSV-1 Stayput-GFP in the presence of ACV. 6 days following infection, ACV was removed from cultures. 8 days post-infection, latently infected cultures were triggered with LY-294002. Latently infected (A) and reactivated neurons 48 hours post-stimulus (B) were fixed and stained for Hoescht (blue), viral proteins ICP8 (fuchsia) and Us11 fused to GFP (green), and ZRF1 (orange). Reactivated nuclei encircled in white.

Interestingly, the addition of reactivation stimuli to uninfected neurons is not sufficient to trigger ZRF1 localization to the nucleus (Fig 4.16). LY294002 addition to uninfected neurons did not result in ZRF1 nuclear localization, and this was assessed during a variety of time points (Fig 4.16B). We tested a panel of additional triggers that we have found previously to induce reactivation, including the neuronal hyperexcitability trigger forskolin (Fig 4.16C), a triple combinatorial trigger of LY294002, forskolin, and heat shock (Fig 4.16D), the BET domain inhibitor JQ1 (Fig 4.16E), and the STING agonist DMXAA (Fig 4.16F, unpublished). However, mean intensity analysis of ZRF1 signal using NIS elements did not reveal any significant differences between mock and

stimulus-treated neurons. Therefore, ZRF1 localization to the nucleus is coincident with reactivating HSV-1.

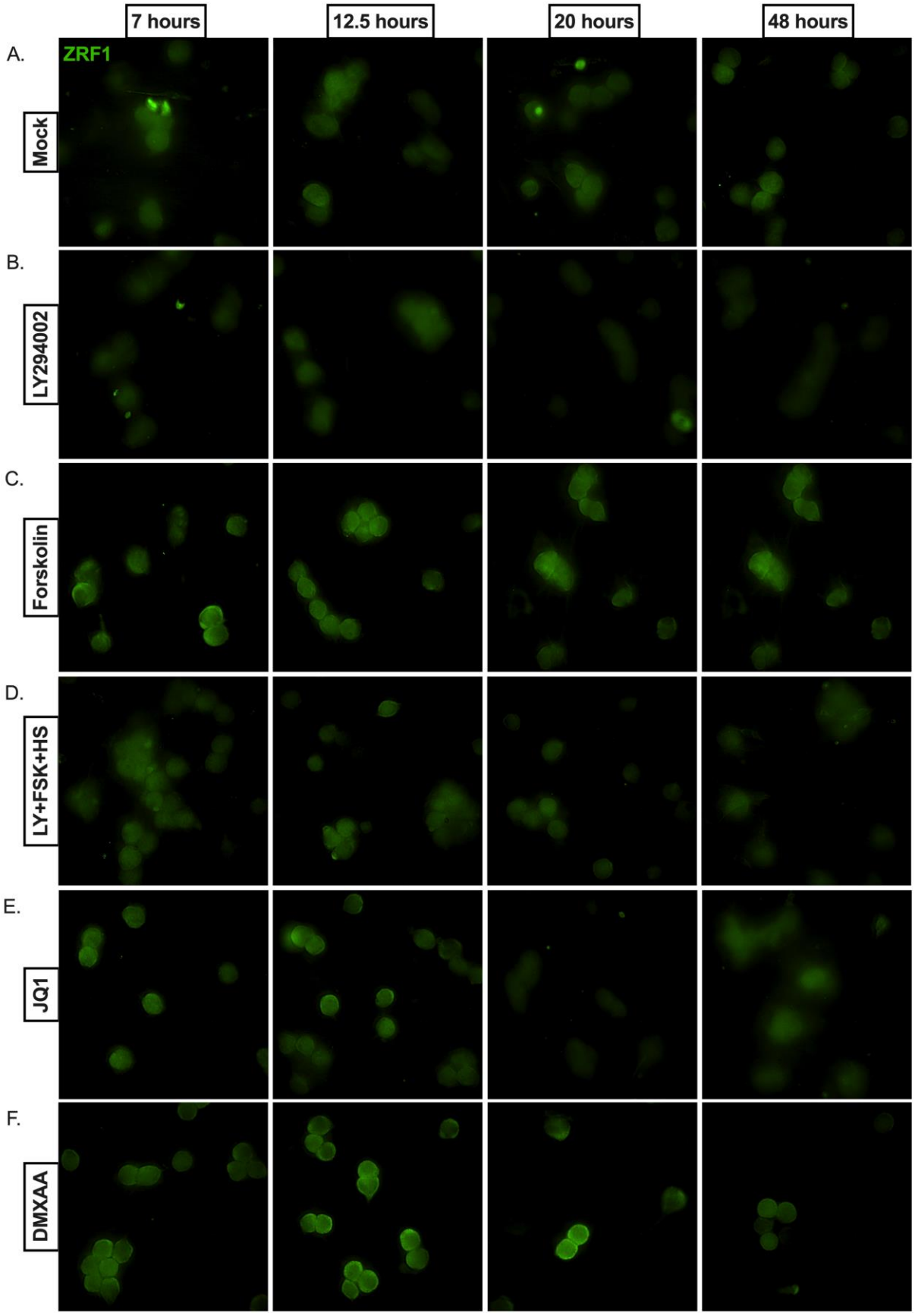
7 hours
12.5 hours
20 hours
48 hours
A.
ZRF1
Mock
B.
LY294002
C.
Forskolin
D.
LY+FSK+HS
E.
JQ1
F.
DMXAA

Figure 4.16 ZRF1 neuronal localization requires HSV-1 infection. (A-F) Uninfected primary sympathetic neurons were treated with reactivation stimuli, including Mock (A), 20 μM LY294002 (B), 60 μM forskolin (C), 20-hour pulse of LY294002 and forskolin, alongside a 3-hour heat shock incubation at 43C (D), 20-hour pulse of 1 μM JQ1 (E), 20-hour pulse of 50 μg/mL DMXAA (F) and stained for ZRF1 (green) at 7-, 12.5-, 20-, and 48-hours post-stimulus.

PRC1 inhibition reduces viral gene expression in lytically infected non-neuronal cells.

As these studies on the roles of PRC1 and PRC2 during HSV-1 latency establishment and reactivation in a neuron were unfolding, we also investigated if PRC1 had any impact on viral gene expression during the lytic infection of non-neuronal cells. As non-neuronal cells do not establish a latent infection, a role for repressive PRC1 was not expected; we hypothesized these cells may escape viral gene silencing due to low endogenous protein levels of PRC1/2 components or perhaps PRC1/2 degradation. However, a fellow lab member observed that Ring1B and H2AK119ub both co-localized with transcriptionally active HSV-1 genomes in lytically infected non-neuronal cells (Alison Francois, data not shown), suggesting PRC1 may be relevant in this system. We therefore tested the impact of PRC1 on lytic viral gene expression. Interestingly, upon HSV-1 infection in the presence of PRC1 inhibition, the transcription of lytic viral genes from each gene class was significantly reduced (Fig 4.17), suggesting PRC1 promotes this process in non-neuronal cells. We have since observed that ZRF1 co-localizes with lytic viral genomes upon infection of this system (data not shown). Therefore, we speculate that a similar mechanism of lytic viral gene expression occurs in the *de novo* lytic infection of non-neuronal cells and the reactivation of neuronal cells, where ZRF1 is co-opted to (re)-initiate viral gene expression using the otherwise repressive H2AK119ub modification on the HSV-1 genome.

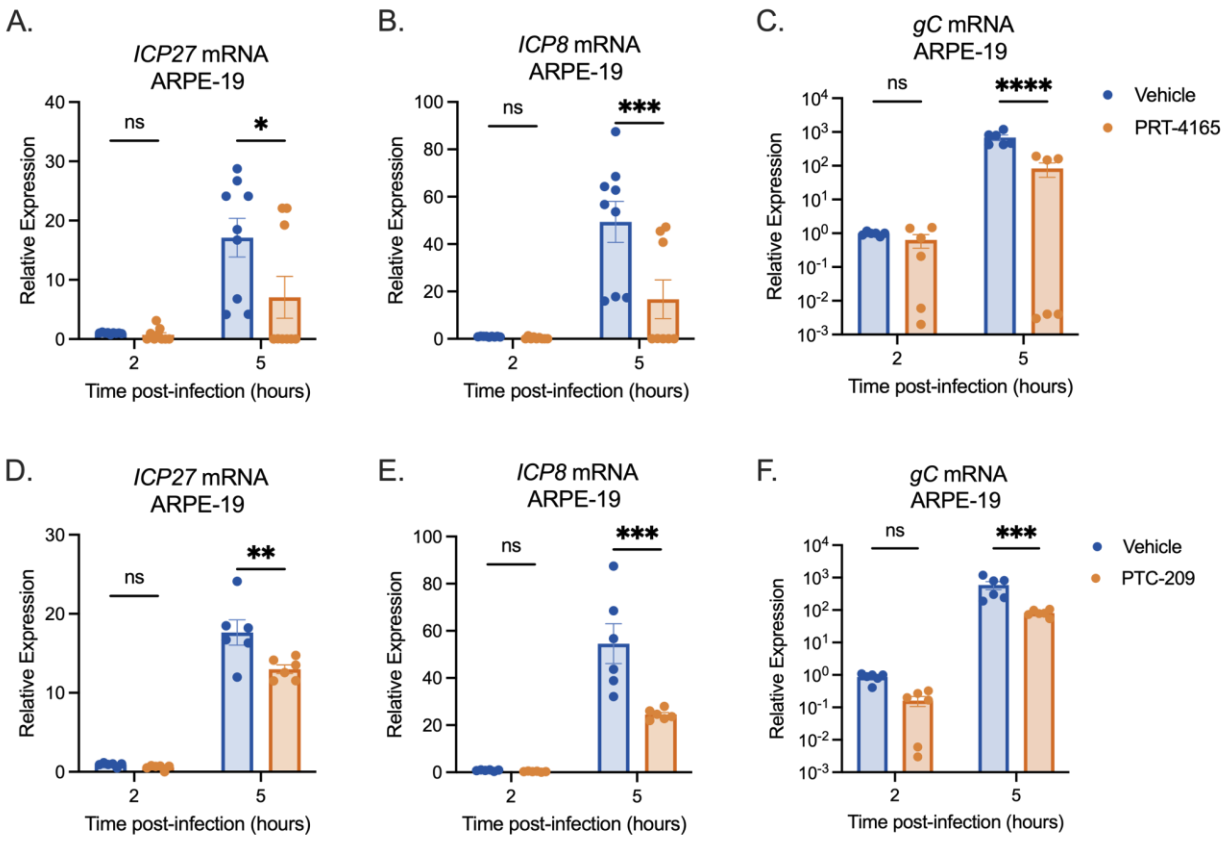

Figure 4.17 PRC1 inhibition during de novo HSV-1 infection of non-neuronal cells dampens viral gene expression. (A-F) ARPE-19s were treated with vehicle control DMSO, PRC1 inhibitors 40 μM PRT4165 (A-C) or 2 μM PTC-209 (D-F) pre-infection for 1 hour, during inoculation with HSV-1 Syn17+, and following the removal of inoculum. RNA was collected for each condition at 2- or 5- hours post-infection, and the expression of lytic viral immediate early gene ICP27 (A,D), early gene ICP8 (B,E), or late gene (C,F) was analyzed and normalized to cellular control 18s. Expression relative to vehicle conditions at 2 hours post-infection shown. 2 biological replicates; 2way ANOVA. Normality determined by Kolmogorov-Smirnov test. *, $P < 0.05$; **, $P < 0.01$. ns, not significant.

Discussion

Here we demonstrate that PRC1-mediated H2AK119ub is enriched on the HSV-1 genome during latency established *in vivo* and *in vitro*. Interestingly, the enrichment of PRC1 component BMI1 was previously explored on the latent HSV-1 genome in a mouse model, but not found to be significant (122, 123). However, it has become clear over time from studies on the cellular genome that Polycomb repressor complexes can be found in a multitude of forms (129, 130, 154). BMI1 traditionally associates with one form of PRC1 (cPRC1) that does not efficiently carry out H2AK119ub (128, 157, 159, 162). Therefore, the enrichment of H2AK119ub but not BMI1 on the HSV-1 genome is not confounding. What is unexpected is that H2AK119ub is actively targeted to the HSV-1 genome in the specialized cell type of a post-mitotic peripheral neuron. Studies on the cellular genome have thus far suggested that vPRC1-mediated H2AK119ub deposition and silencing is abundant in embryonic cells, like neuronal progenitor cells/NPCs, but decreases in relevance to cellular genome silencing and maintenance as cells differentiate (172). Our work now demonstrates that in response to environmental stimuli, such as a viral infection, H2AK119ub deposition is very much still a relevant process in post-mitotic neurons. We also confirm the kinetics of H3K27me3 enrichment previously observed *in vivo*, where the HSV-1 genome becomes enriched in H3K27me3 at later time points post-infection after lytic genes have been repressed (122, 123).

It remains unclear if H2AK119ub and H3K27me3 bind the same latent viral genomes, and whether PRC2's recruitment depends on PRC1. On the cellular genome,

it is increasingly appreciated that PRC2 can be recruited in a manner that is dependent on prior H2AK119ub deposition or independently of H2AK119ub (139, 144, 147). By directly comparing the CUT&RUN-sequencing reads (Fig 4.2) of H2AK119ub and H3K27me3 we can potentially infer co-enrichment at the same regions of the viral genome. There are regions on the viral genome where H2AK119ub and H3K27me3 demonstrate overlap as well as regions where these modifications exist independently suggesting both independent and interdependent PRC1/PRC2 recruitment mechanisms to the HSV-1 genome may be at play. However, these regions require a more formal, ordered, and comprehensive future analysis. Consistent with the CUT&RUN-sequencing data, the shared proportion between H2AK119ub and H3K27me3 (one-third) raises the possibility that these modifications bind to the same individual viral genomes. However, we cannot currently rule out the possibility that these modifications are on different individual viral genomes, a finding which would be obscured by this population-level analysis The binding of both H2AK119ub and H3K27me3 to the same regions of the HSV-1 genome could only be confirmed by performing re-ChIP, which is a method to perform sequential ChIP assays for different modifications, or high-resolution single-cell analyses with dual immunofluorescence. Importantly, the role of H2AK119ub in promoting H3K27me3 has predominately been studied in embryonic stem cells and during the early stages of differentiation (144-147, 152). The protein that promotes PRC2 recruitment to H2AK119ub to mediate H3K27me3 addition (JARID2) is altered in differentiated cells in that a truncated version predominates that lacks both the H3AK119ub reader domain and PRC2 binding domain (152, 366). We were also only able to detect this truncated version of JARID2 in our primary neuronal cultures (data

not shown). Therefore, is remains unresolved whether H2AK119ub1 can directly promote H3K27me3 in neurons and on the HSV genome, and the contribution of JARID2.

These are also the first functional studies that directly probe the contributions of PRC1/2 to HSV-1 lytic viral gene silencing during latency establishment. Importantly, we find that H2AK119ub represses lytic genes during the early stages of latency establishment. Consistent with its kinetics, PRC2 does not actively repress viral gene expression, at least not during the time points tested here. These data altogether suggest a model where PRC1 is targeted to the viral genome to initiate viral gene repression and H3K27me3 is subsequently recruited to reinforce and maintain viral gene repression. PRC2-mediated H3K27me3 is still relevant to viral repression despite not initiating viral gene silencing as H3K27 de-methylation is required for full reactivation, for at least a proportion of latent HSV-1 genomes *in vitro* and *ex vivo* (98-100, 109, 117). The mechanism of PRC2-mediated silencing however remains unknown. cPRC1 has been traditionally viewed as the “reader” of the H3K27me3 that initiates silencing. Alternatively, BAHCC1 has recently been proposed as a reader of H3K27me3 and associates with transcriptional corepressors, including SAP30BP and HDAC, to induce silencing (367). Our RNA-sequencing data acquired from uninfected neonatal sympathetic neurons include low BAHCC1 reads, but this may change in response to infection, and these data cannot inform on how abundant BAHCC1 is at the protein level.

While our data suggests PRC1 represses HSV-1 lytic genes during latency establishment, its mechanism of silencing remains unknown. The H2AK119ub modification itself may repress viral gene expression by inhibiting RNA polymerase elongation or possibly preventing the eviction of H2A/H2B dimers (165-167). The mechanisms of silencing via cPRC1 appear to be more repressive (169). Silencing via cPRC1 is mediated by chromobox (CBX) proteins through chromatin compaction, phase body formation, and long-range chromosomal interactions (130, 169-171). The differential co-localization of HSV-1 genomes with H2AK119ub and Ring1B may speak to two independent PRC1 mechanisms of silencing. One advantage to our single-genome resolution system is that we were able to discern that approximately 30% of latent genomes analyzed co-localized with H2AK119ub and only approximately 10% co-localized with core PRC1 component Ring1B. One possibility is that Ring1 associates with the viral genome transiently and the incidences of perfect Ring1B colocalization are the exact moments as the PRC1 complex deposits H2AK119ub onto viral genomes. It is unknown, even in the cellular context independent of infection, if Ring1 stably associates with DNA following the deposition of its respective modification. An alternative explanation is that Ring1B does not exhibit colocalization as a writer of H2AK119ub in the vPRC1 complex, but instead as a component of the cPRC1 complex. Co-localization events with the H2AK119ub mark could be indicative of vPRC1 recruitment, H2AK119ub deposition, and silencing while Ring1B co-localization may instead be indicative of a less pervasive, more repressive cPRC1-mediated silencing on a subset of genomes. cPRC1 has been demonstrated to be recruited independently of vPRC1/H3K27me3 through sequence motifs (161, 368). It is possible that Ring1A, the

co-localization of which has not yet been investigated, may predominantly be responsible for the deposition of H2AK119ub via vPRC1, whereas Ring1B may mediate viral gene repression through the cPRC1 complex. Previous literature suggests Ring1A and Ring1B serve redundant functions in pluripotent stem cells (360), but the role of each Ring1 isoform has not been investigated in a neuron. Notably, we observe increased viral gene expression following the individual depletion of Ring1A or Ring1B (Fig 4.6), further suggesting that Ring1A/B do not serve redundant silencing functions in this system. Given the high degree of heterogeneity of Polycomb silencing, it is possible that herpesviruses actively manipulate the nature of fHC on the viral genome to a form most advantageous for viral persistence and/or reactivation.

Despite its nuclear presence in 100% of uninfected neurons, the detection of Ring1B is lost in the nuclei of HSV-1 infected neurons that are undergoing lytic infection evidenced by the presence of viral protein. Interestingly, using a proteomic dataset from our collaborator, we have observed that protein abundance of Ring1 (RNF168) is decreased in human keratinocytes upon lytic infection with HSV-1 (369), but there is the potential for a neuronal-specific response. We can only speculate that a viral or host protein may exclude or degrade Ring1B and PRC1-mediated silencing in lytically infected neurons. There are multiple host proteins that repress HSV-1 infection, as well as viral proteins that in turn can target such host proteins (recently reviewed in (370)). For example, PML bodies appear to encapsulate and repress the HSV-1 genome upon lytic infection in non-neuronal cells, but viral protein ICP0 degrades these repressive bodies in return, allowing viral transcription to proceed (371-376). Host factor USP7 was

demonstrated to stabilize forms of vPRC1 at the post-transcriptional level and transcriptionally repress AUTS2, which otherwise inhibits H2AK119ub capabilities of the vPRC1 complex (377). Interestingly, in non-neuronal cells, ICP0 recruits USP7 from the nucleus to the cytoplasm (378, 379).

In agreement with our collaborator Igor Jurak, our data indicate that hnRNPK and the LAT interact in neurons as determined by RNA-IP for hnRNPK and subsequent qPCR. The ideal next step is to resolve in primary neurons if the HSV-1 genome simultaneously co-localizes with hnRNPK protein and the LAT RNA through a combination of click chemistry, immunofluorescence, RNA FISH, and NucSpotA. The co-localization of hnRNPK and the H2AK119ub mark or Ring1B with the HSV-1 genome would also be compelling supporting evidence. Another approach would then be to analyze H2AK119ub co-localization with the viral genome using NucSpotA and CUT&RUN for H2AK119ub following hnRNPK depletion. Additional preliminary evidence also indirectly supports the hypothesis of hnRNPK/LAT mediated recruitment of PRC1 and H2AK119ub to the HSV-1 genome. We found that hnRNPK depletion enhanced lytic infection, as quantified by lytic viral mRNA and viral DNA replication during early stages of latency establishment. Peak changes in viral gene expression occurred concurrently with the time point we observed Ring1B and H2AK119ub co-localization with HSV-1 genomes. This hnRNPK depletion phenotype would be the expected outcome if hnRNPK were responsible for recruiting repressive PRC1/H2AK119ub to the HSV-1 genome.

Our finding that only a population of HSV-1 genomes associate with Polycomb silencing is intriguing, but not unexpected. There is abundant evidence that the ability of each latent viral genome to reactivate is not equal (93, 109, 117, 224, 292). Synergizing these findings, we speculate that the ability of the HSV-1 genome to reactivate may depend on the form of chromatin it acquires. In the absence of PRC1, HSV-1 is still able to establish a latent infection, and in fact, establishes the same relative amount of latent DNA genomes in the presence of antiviral ACV. We speculate that following vPRC1 inhibition, HSV-1 genomes acquire an alternative form of chromatin that is more difficult to remove or modify during reactivation. Specifically, we hypothesize that Polycomb silencing is eventually compensated by constitutive chromatin, or an alternative form of Polycomb silencing containing only H3K27me3. Modifications that constitute such constitutive chromatin include the di- and tri-methylation of histone H3 lysine 9, H3K9me2/3, which have previously been identified on the latent HSV-1 genome. Whether constitutive chromatin only binds to a subset of latent genomes, and whether constitutive chromatin and Polycomb bind to the same individual HSV-1 genomes has not yet been investigated.

PRC1-mediated silencing may be more amenable to reactivation, but the question of how repressive H2AK119ub is modified or removed following a reactivation stimulus is still unresolved. Accumulating evidence increasingly suggests that HSV-1 reactivation is a biphasic process. Initial viral gene expression events during Phase I are independent of the removal of repressive heterochromatin, which is instead modified to enable viral gene expression. Repressive H3K9me2, for example, undergoes a

phospho-methyl switch, where histone phosphorylation on a neighboring serine allows viral gene expression to occur despite the persistence of repressive H3K9me (99). During Phase II, repressive heterochromatin is fully removed.

We hypothesize that H2AK119ub is read by ZRF1 during Phase I and therefore modified to enable viral gene expression. We analyzed ZRF1 localization during full, Phase II reactivation as this is the endpoint of reactivation and we sought to determine if ZRF1 was relevant at any time point during reactivation as a preliminary effort. One model is that during Phase II reactivation, H2AK119ub is fully removed from the viral genome by de-ubiquitinase (DUB) BRCA1-associated protein 1, BAP1. Interestingly, BAP1 has previously been demonstrated to associate with host cell factor 1 (HCF-1), which may also be required for the progression to the full, Phase II reactivation by interacting with viral protein VP16 (380-383). Future studies should investigate ZRF1's impact on Phase I gene expression and full HSV-1 reactivation using shRNA-mediated lentiviruses targeting ZRF1, which we have created and validated at least at the level of RNA (Fig 4.18).

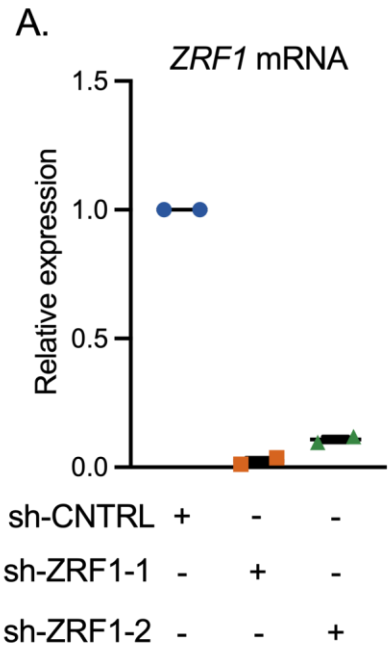

Figure 4.18 ZRF1 depletion via shRNA-mediated lentivirus. (A) Neonatal sympathetic neurons were transduced with a non-targeting shRNA control lentivirus or one of two independent lentiviruses expressing shRNAs that target ZRF1 (sh-ZRF1-1, sh-ZRF1-2). 5 days post-transduction, RNA was collected and ZRF1 mRNA expression was analyzed via RT-qPCR. 1 biological replicate.

With these data synergized, we propose a model where HSV-1 may use its lncRNA LAT and host cell factor hnRNPK to modulate the nature of the viral chromatin and ultimately enable later reactivation through ZRF1 (Fig 4.19).

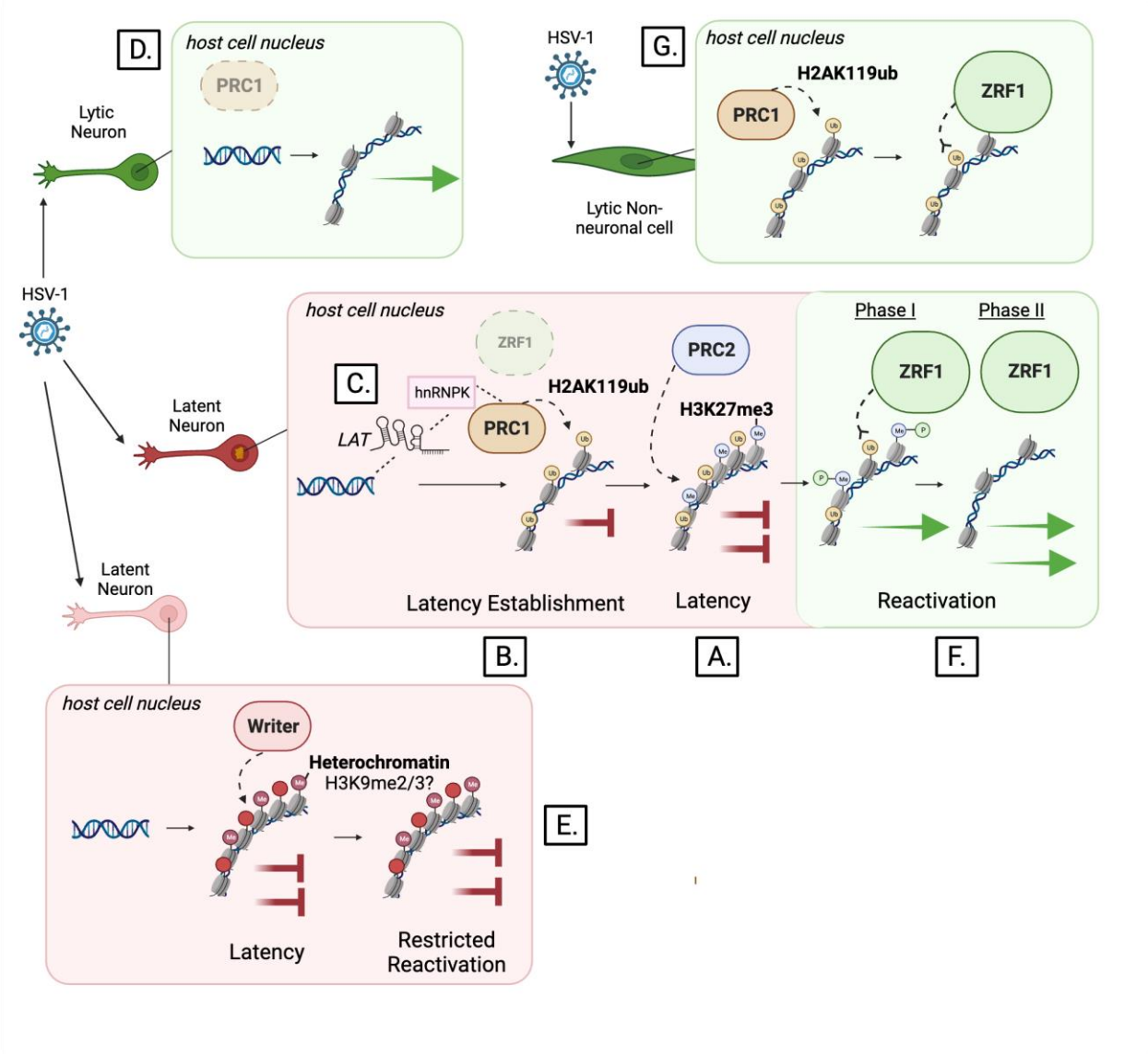

Figure 4.19 Working Model. (A) The latent HSV-1 genome is enriched in both H2AK119ub and H3K27me3, although whether these mark the same individual viral genomes is unknown. (B) PRC1-mediated H2AK119ub is deposited onto the HSV-1 genome during active stages of viral gene silencing and represses lytic viral genes. (C) Viral lncRNA, the latency-associated transcript/LAT, binds host hnRNPK to potentially recruit PRC1 to the HSV-1 genome. (D) The nuclear presence of repressive Ring1B is not compatible with lytic infection in neurons. (E) Alternative heterochromatin forms may be less amenable to reactivation than PRC1-mediated H2AK119ub and silencing. (F) Pro-transcriptional ZRF1 localizes to the nuclei of reactivating neurons and therefore may mediate lytic gene transcription through the reading of H2AK119ub. (G) Non-neuronal cells may co-opt both H2AK119ub and pro-ZRF1 to enable lytic viral gene expression during *de novo* infection.

~End of Chapter 4~

Chapter 5: Lessons, Future Directions, and Impact

Parts of this chapter have been adapted from:

Dochnal, SA, Francois, AK, & Cliffe, AR. De Novo Polycomb Recruitment: Lessons from Latent Herpesviruses. *Viruses*, 27;13(8):1470 doi: 10.3390/v13081470. (2021)

Over the course of this dissertation, we developed a novel recombinant HSV-1 virus and primary model system that were then used to explore the impact of facultative heterochromatin and neuronal stress signaling on HSV-1 latency establishment and reactivation. My direct conclusions and immediate implications and future directions are detailed in their respective chapter discussions. In the following pages, I will first synergize these findings and discuss their overall impact on HSV-1 biology. I will then detail larger unresolved questions and future directions.

Lessons & Implications

Modeling HSV-1 latent infection and reactivation.

This dissertation began with the creation and characterization of a new recombinant HSV-1 virus, Stayput-GFP (Chapter 2). The use of this virus is advantageous to studying HSV-1 latency and reactivation in models that do or do not also employ antivirals to promote latency. First, due to its cell-to-cell spread deficiency, Stayput-GFP protects against superinfection and the elimination of latency resulting from spontaneous reactivation events. Importantly, Stayput-GFP also enables the study of reactivation at the single-neuron level. Given the heterogeneity of HSV-1 latency and reactivation, this is a hugely advantageous addition to the field. An accurate representation of the proportion of latently infected neurons that respond to certain reactivation stimuli can be achieved. Moreover, the mechanisms behind reactivation triggered by various stimuli can be accurately investigated as initial viral transcription events can be discerned from downstream viral transcription and replication that results from cell-to-cell spread. An additional advantage to this model is the ability to track the

survival of individual neurons during reactivation, as well as conduct experiments using multiple rounds of reactivation-this could not be achieved previously due to superinfection issues. Using Stayput-GFP, latency can also be established *in vitro* without the requirement for viral DNA replication inhibitors, allowing for the study of viral DNA replication and downstream late viral transcription and protein synthesis during latency establishment. The Us11-GFP tag also enables the live single-neuron tracking and investigation of the fate of lytic infection events as latency is established in this model. Notably, Stayput-GFP is adapted to study both sympathetic neurons and sensory neurons. Both neuronal types are relevant to HSV-1 biology but feature intrinsic differences in their biology (104, 234). The ability to study latency and reactivation in both systems enables their mechanistic differences in these processes to be compared.

Air matters: Normoxic incubation, neuronal stress, HSV-1 latency, and reactivation.

During the development of this model, we began culturing primary neurons in oxygen conditions (5% oxygen, hereafter “normoxia”), which mirror the physiological conditions of the human nervous system (384) and have been demonstrated to support neuronal differentiation, survival, and resistance to inflammatory injury in cultured neural stem cells (385-388). Our neurons were previously cultured under atmospheric conditions (20% oxygen), which is routine across laboratories studying HSV-1 or general neuroscience. However, cultures incubated at atmospheric conditions exhibited poor health at any time point past 8 days post-infection in the absence of ACV although 1) Us11-GFP signal persisted and 2) latency is established over the course of 30 days

in vivo. I therefore evaluated neuronal viability in atmospheric versus normoxia incubation conditions using a portable chamber and custom gaseous mix. The axons of neurons were far more degenerated in atmospheric cultures versus normoxia cultures (Fig 5.1A-B). These neurons were plated in microfluidic chambers to enable the easy visualization of the axonal components as they are separated from cell bodies in this system. There were also other additional indicators of improved neuronal health and viability in normoxia conditions, such as less pcJunSer63 staining (an indicator of neuronal stress) and increased soma size (Fig 5.1C-D). Importantly, using normoxia conditions, primary neurons were able to be cultured up to 70 days without infection with limited impact on viability, and neurons infected with HSV-1 Stayput-GFP could be cultured past 30 days post-infection, the timepoint at which US11-GFP disappeared and latency was established. In fact, more viral genomes persisted during latency established under normoxia conditions in a model devoid of ACV, likely an indirect result of neuronal viability (Fig 5.1E). These normoxia data were supplemental to the creation of our primary neuron model and therefore not incorporated (except for the Materials and Methods section) into Chapter 2 and its corresponding publication. However, this information deserves emphasis. HSV-1 is well-known to reactivate in response to neuronal stress *in vitro* and *in vivo* and has specifically been demonstrated to respond to axon damage (233, 314), reminiscent of the axonal degeneration we observe under atmospheric conditions in Fig 5.1A-B. We also show in this dissertation that neuronal stress signaling during latency establishment changes the nature of future reactivation events and that neuronal activated c-Jun (which is enhanced under conditions of neuronal stress and in atmospheric cultures) promotes HSV-1 full

reactivation (Chapter 3). Therefore, the study of latency and reactivation are likely to have significant effects on experimental outcomes. In fact, we have observed that full reactivation in atmospheric conditions is more robust than that achieved in normoxia (Fig 5.2).

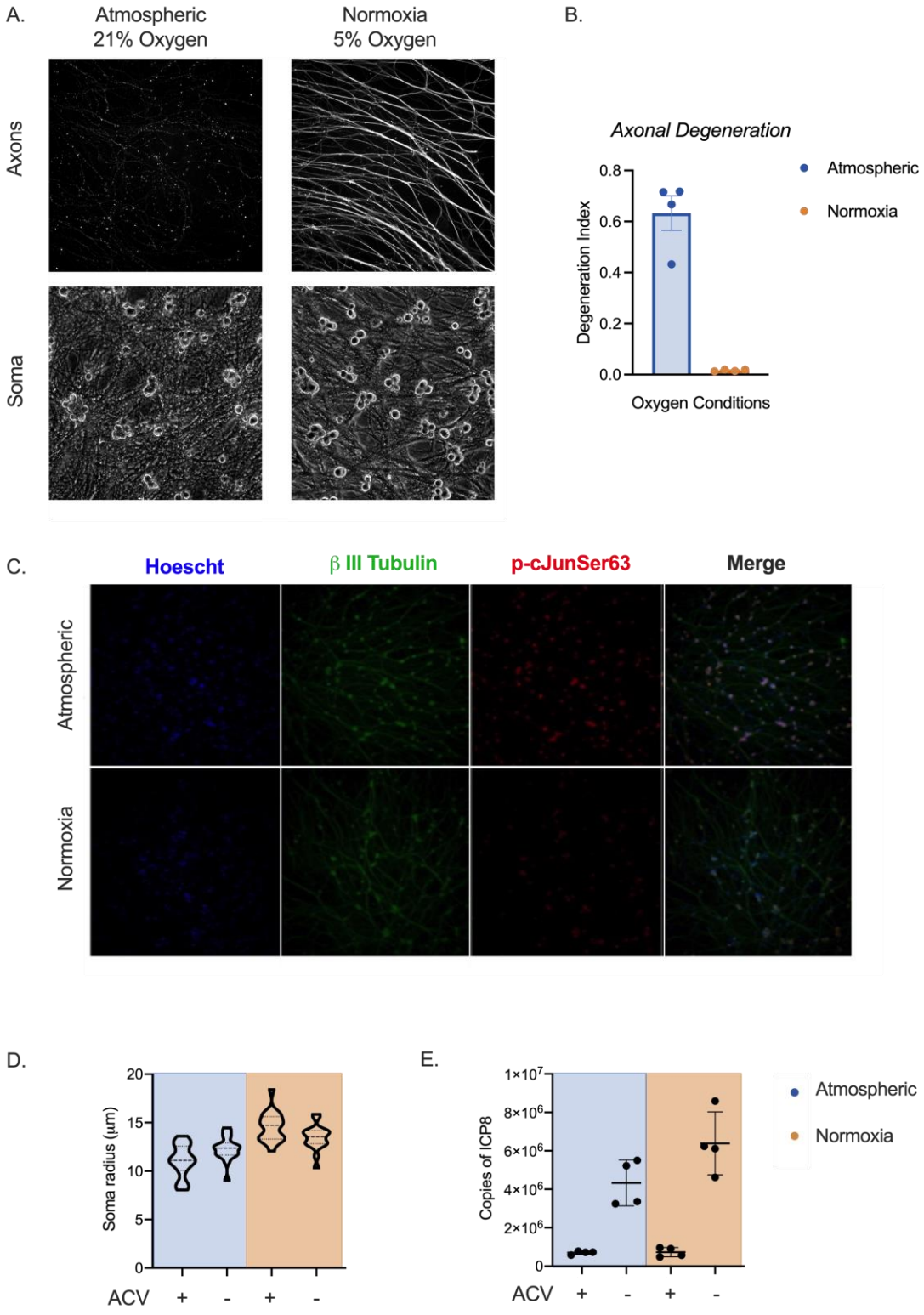
A.
Atmospheric
21% Oxygen
Normoxia
5% Oxygen
Axons
Soma
B.
Axonal Degeneration
Degeneration Index
0.8
0.6
0.4
0.2
0.0
Oxygen Conditions
Atmospheric
Normoxia
C.
Hoescht
β III Tubulin
p-cJunSer63
Merge
Atmospheric
Normoxia
D.
Soma radius (μm)
20
15
10
5
0
ACV + - + -
E.
Copies of ICP8
1×10^7
8×10^6
6×10^6
4×10^6
2×10^6
0
ACV + - + -
Atmospheric
Normoxia

Figure 5.1 Normoxia conditions improve neuronal health. (A-B) Neonatal sympathetic neurons were cultured in microfluidic chambers for 10 days in atmospheric versus normoxia conditions and a degeneration index was calculated via ImageJ (4 FOVs each condition). (A) Representative images of axons (top) and soma (bottom) under each condition. (B) Degeneration index calculated for axons of each condition. (C) Sympathetic neurons were cultured in wells for 10 days atmospheric versus normoxia conditions and immunofluorescence was performed for Hoescht (blue), neuronal marker B III tubulin (green), and neuronal stress marker, c-Jun phosphorylated at serine 63 (red). (D-E) Neurons cultured in atmospheric versus normoxic conditions were infected with HSV-1 Stayput-GFP in the presence (or absence) of antiviral ACV to promote latency establishment and cultured for several days post-infection. (D) Soma size during latency was calculated with NIS-Elements Image Analysis. (E) Viral DNA load during latency is shown. Minimum 50 images from 1 biological replicate.

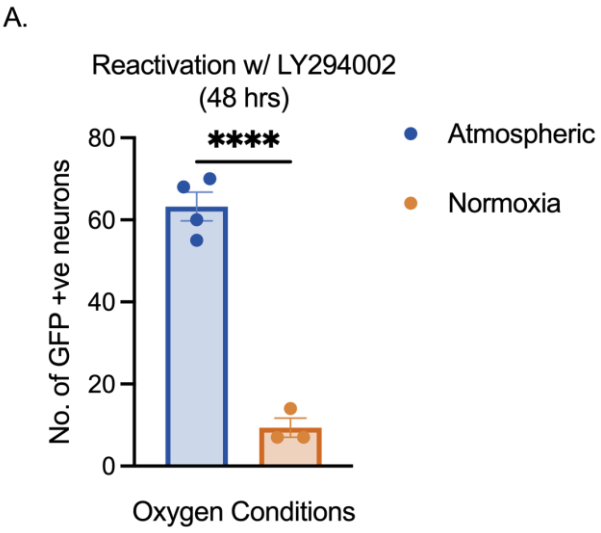

Figure 5.2 HSV-1 reactivation in neurons is decreased under normoxic conditions. (A) Neurons cultured in atmospheric (20% oxygen) or normoxia (5%) conditions were latently infected with HSV-1 Stayput-GFP in the presence of antiviral ACV. Two days following ACV removal, cultures were reactivated with LY294002. The number of Us11-GFP positive neurons, indicative of reactivation events, is shown here. 2 biological replicates; unpaired t-test. Individual biological replicates along with the means and SEMs are represented. *, $P < 0.05$; **, $P < 0.01$. ns, not significant.

Promise for human models.

As relayed in the introductory chapter, murine neurons constitute a highly advantageous and relevant system in which to study HSV-1 latency and reactivation, as well as basic neuron biology. However, I foresee that the combination of the following advances will enable the use of more systems of human origin to comparatively

investigate HSV-1 latency and reactivation: 1) normoxia culture conditions, which enable the culture of sensitive cells 2) Stayput-GFP HSV-1, which enables the live-tracking of latency establishment and protects against superinfection events, and 3) the triple combination trigger, which elicits reactivation from very silent forms of latency. A fellow lab member has already co-opted all three of these conditions to achieve reactivation in HD10.6 cells, an immortalized human dorsal root ganglion (sensory) cell line (unpublished). Human models are not to be used as a replacement for murine models, but an adjuvant to their study. For example, latency is established more rapidly in human LUHMES (Fig 5.3) versus sympathetic or sensory primary neurons (Chapter 2). LUHMES are much less amenable to reactivation as well (Chapter 4). Rather than viewing these data as inconsistencies, we can use human and murine models to elucidate if and why these differences exist past species, like neuronal origin or age.

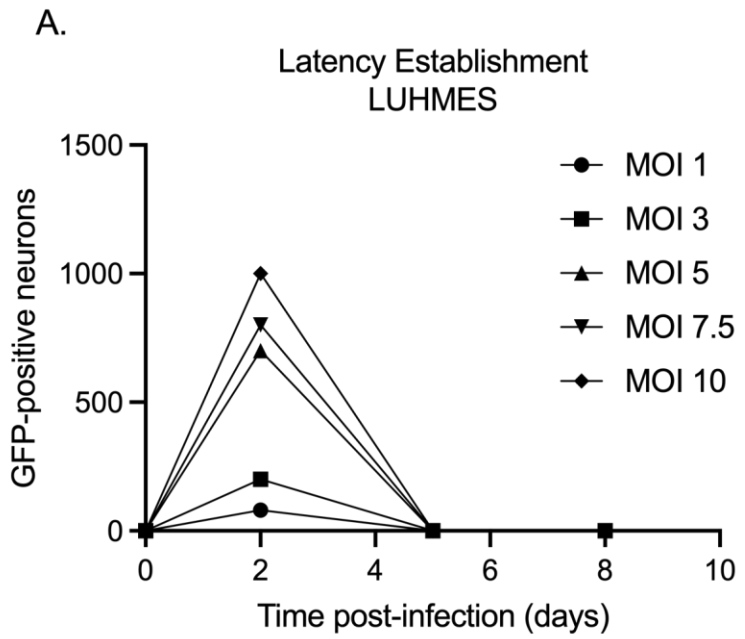

Figure 5.3 Latency Establishment with HSV-1 Stayput-GFP in LUHMES. (A) Neurons were infected with HSV-1 Stayput-GFP at several MOIs in the absence of antiviral ACV. The number of US11-GFP-positive neurons, indicative of lytic infection events, was quantified over the course of latency establishment. 1 biological replicate.

Unconditional knockouts/deletions confound the study of HSV-1 latency and reactivation.

When studying HSV-1 reactivation, greater care should be taken when depleting viral or host factors to discern whether these targets directly modify reactivation or indirectly modify reactivation by changing latency establishment. Our exploration of the role of transcriptional factor c-Jun emphasizes this point (Chapter 3). c-Jun depletion prior to HSV-1 infection reduced Phase I gene expression, which supported our original hypothesis that c-Jun directly modifies Phase I reactivation. Only after the depletion of c-Jun following latency establishment were we able to discern that c-Jun does not

directly impact Phase I gene expression but modifies the “type” of latency established. This finding complicates the interpretation of studies that have used mutant HSV-1 to study reactivation *in vitro* and *in vivo*, such as HSV-1 with mutations in viral protein VP16-encoding gene *UL48* (223, 266, 292), as the absence of this protein during latency establishment could change the nature of heterochromatin or cell signaling and therefore perturb reactivation. Our data therefore further support the use of *in vitro* HSV-1 latency and reactivation systems where depletions in both viral or host mRNA or protein can easily be performed before or after the establishment of latency. Systems in which conditional depletions can be carried out *in vitro* or *in vivo* are ideal and should be employed when available and optimized (389, 390).

Science is never simple: Themes of heterogeneity in HSV-1 latency and reactivation and intrinsic to neurons.

Themes of heterogeneity in HSV-1 latency and reactivation are consistent throughout this dissertation. HSV-1 latency is increasingly regarded as a heterogenous process, as there is variability observed within latent ganglia in terms of viral DNA copy number, lytic gene transcription, latent gene transcription, the subnuclear positioning of latent viral genomes, and the association of latent viral genomes with host proteins (8, 93, 194, 195, 235, 269). HSV-1 reactivation is increasingly regarded as a nonuniform process as only a population of latently infected neurons reactivate in response to a particular stimulus (93, 109, 117, 292, 391). This heterogeneity tremendously complicates the study of HSV-1 biology and requires the use of higher-resolution versus population-level experimental techniques. However, it also accurately recapitulates *in*

vivo physiology (292) and is crucial to understanding any unintended effects of therapies that disrupt these processes.

Themes of heterogeneity first emerge in Chapter 2, during the creation of our new model system. First, heterogeneity is observed between individual neurons in response to infection. Upon infection with HSV-1 Stayput-GFP, a population of neurons produce a lytic infection and die. Following clearance of this lytic population, we know a separate latent population remains in culture as 1) there is detectable viral DNA 2) the viral lncRNA the LAT is pervasively transcribed and 3) we were able to elicit reactivation from these cultures using our combinatorial stimulus. We note that there are also differences between neuronal subtypes in terms of how quickly lytic infection is resolved, as measured through Us11-GFP in models using HSV-1 Stayput-GFP in the absence of ACV. Adult sensory neurons demonstrated less Us11-GFP-positive neurons and lost Us11-GFP signal quicker than sympathetic neurons. As the same number of neurons were plated and infected with equal amounts of virus for each neuronal subtype, these experiments support the previous finding that adult sensory neurons are more repressive for HSV-1 infection (104, 392). Differences between lytic and latently infected neurons also arise in Chapter 4 when exploring the relationship between Polycomb and HSV-1 latency. We demonstrate the differential staining of Ring1B in lytic infected versus latently infected neurons. Whether this differential is a result of something inherent in each individual neuron (can a host component make Ring1B susceptible to re-localization?) or if this is a downstream result of lytic infection is unclear.

Moreover, there is heterogeneity observed within the population that achieves latency. This is in part attributed to mechanisms of silencing by chromatin. Support for such a model comes from our work in Chapter 4. First, we demonstrate that only a proportion of latent viral genomes associate with PRC1 and PRC2-mediated modifications, and whether these populations are further separate is unknown. Moreover, Ring1B, the core component of PRC1, associates with only a subset of the H2AK119ub-associated viral genomes. The differences in Polycomb silencing in adult sensory and neonatal sympathetic neurons still require further exploration. However, we observe that PRC1 inhibition may enhance lytic gene expression in sensory neurons to greater levels than in sympathetic neurons. This may indicate that PRC1 silencing is more abundant in this neuronal subtype or this age of a neuron. My preliminary western blot analyses performed on neurons from several different neuron types, models, and sexes, do not conclude any obvious major differences in terms of PRC1/2 protein abundance (data not shown). However, relative expression of the LAT in adult sensory neurons versus neonatal sympathetic neurons is greater at the 3-day post-infection (data not shown), suggesting a greater abundance of LAT may account for more robust PRC1-mediating silencing in adult sensory neurons.

These differences between latently infected neurons likely translate into differences observed in reactivation. As previously observed in other models of latency and reactivation, only a proportion of latently infected neurons that responded to our triple combinatorial stimulus in sympathetic neurons and sensory neurons (Chapter 2). Moreover, full reactivation is inhibited but not completely depleted upon the addition of

H3K27 or H3K9 demethylases (Chapter 2). This could mean that these inhibitors did not completely prevent demethylase activity. However, it could also indicate that a population of viral genomes reactivate despite demethylase inhibition. The implication is that a subset of latent viral genomes may be silenced through H3K27 methylation or H3K9 methylation, and therefore the removal of these repressive marks is only pertinent to a proportion of neurons reactivating from latency. Importantly, the inhibition of H2AK119ub deposition during latency establishment reduces reactivation (Chapter 4), suggesting that different forms of chromatin may be more or less amenable to reactivation. Not only is there heterogeneity between latent genomes, but this heterogeneity can be manipulated into a certain outcome for HSV-1 reactivation, a concept relevant for therapies. The promotion of one form of chromatin that is incapable of reversal over another more amenable to this process could reap clinical benefits. This concept of manipulating heterogeneity can also be used to explain and predict variations in clinical outcome. Our work on c-Jun demonstrates that neuronal stress signaling enhances future reactivation by promoting the formation of more reactivation-component viral genomes (Chapter 3). Independently of whether this phenomenon is mediated through chromatin on the viral genomes or cell signaling events within latently infected neurons, neuronal stress during the acquisition of an HSV-1 infection may serve as an indicator of future reactivation potency and clinical distress.

Good (and bad) things take time: a model of gradual HSV-1 chromatinization over the course of latency establishment.

The work in this dissertation also supports a model of HSV-1 latency as something that develops and changes over time rather than an immediate process. While H2AK119ub is rapidly recruited to the viral genome, H3K27 methylation is only

acquired during later stages of silencing (Chapter 4). In Chapter 2, we find that the ability of HSV-1 to reactivate decreases with increasing lengths of time infected. We predicted this was likely due to gradual chromatinization of the HSV-1 viral genome over time, and our later findings in fact support this notion. Moreover, Polycomb has also been demonstrated to propagate on the cellular genome, where the deposition of one repressive modification also recruits additional readers and writers to deposit more of this same modification, supporting a positive feedback loop of chromatinization and increasingly silencing the target gene. While this is speculation, I draw attention to the slight differences in the staining patterns observed for H2AK119ub and Ring1B for 3 days and 30 days post-infection (Chapter 4). Particularly in the case of Ring1B, there appear to be 1) less puncta per neuronal nuclei and 2) the puncta that do persist appear brighter by eye. In the case of H2AK119ub, the clusters of H2AK119ub around the HSV-1 genome also appear more intense in signal and almost circular at 30 days post-infection. This slight change in staining pattern for both H2AK119ub and Ring1B could of course be attributed to the age of the neuron, which increases with length of time infected, but one might speculate that overtime PRC1 recruits more PRC1 and H2AK119ub to the HSV-1 viral genome which enhance silencing.

This extended model of latency has two major implications for HSV-1. First, it impacts the modeling of HSV-1. Laboratories that study HSV-1 latency, particularly in relation to the epigenetics, should wait for longer periods of time post-infection for latency to be considered established. It also speaks to the physiological relevance of combination triggers required to elicit HSV-1 reactivation in such models. Second, this

model also has clinical implications. The requirement of combinatorial stimuli to elicit reactivation may imply that it takes a combination of stressors in a patient to elicit the reactivation response. This extended model also implies that PRC1 but not PRC2 is at the core of viral gene repression and that the virus is easier to reactivate at early times post-infection, considerations for therapies using either “shock and kill” or “lock and block” strategies.

HSV-1 as a Model for Polycomb Silencing

Despite its intricacy, the study of Polycomb targeting and silencing to the mammalian genome is still in its infancy largely due to limitations in modeling. Most Polycomb studies have been carried out in mESCs and IPSC’s, and *de novo* targeting to regions of the cellular genome is challenging as the full removal of the pre-existing epigenetic template is hard to achieve (136, 138). As herpesvirus genomes enter the host cell nucleus as epigenetically naïve, latent infection theoretically provides an excellent opportunity to study *de novo* Polycomb silencing in several specialized cell types. However, even the most comprehensive studies of Polycomb silencing on gamma herpesvirus (KSHV, EBV) genomes come with modeling caveats. The major cell type harboring latent gamma herpesvirus infection *in vivo* are B cells, which are largely refractory to *de novo* KSHV/EBV infection *in vitro*. Therefore, KSHV/EBV epigenetic studies rely on cell lines derived from naturally infected KSHV-induced lymphoproliferation (primary effusion lymphoma, PEL), or EBV-transformed lymphoblastoid cell lines (LCL’s). As constitutively-infected cells are not ideal to investigate the early events in latency establishment, attempts at studying Polycomb

recruitment and silencing to the viral genome during *de novo* infection have been made for KSHV using endothelial-like cell lines. However, the most commonly used cell line (SLK) was recently identified to as a mutated renal carcinoma cell line, of which the physiological relevance to KSHV or Polycomb silencing is debated (174, 176, 393). Therefore, the methods of studying *de novo* Polycomb recruitment and silencing in HSV-1 as introduced in this dissertation are unique as they allow us to study Polycomb silencing 1) in the specialized and relevant cell type of a neuron 2) using an epigenetically naïve template 3) in a system that can be manipulated and modified for the removal or over-expression of PRC1/2 in functional studies, and also 4) at the single-cell or single-genome resolution versus population-level techniques. For example, because of the central role JARID2 in vPRC1/PRC2.2-mediated PcG-silencing, the observation of H2AK119ub1 on the HSV-1 genome, and the potential change in function following differentiation, examining the role of JARID2 in HSV-1 latency will uncover how PRC2.2 contributes to gene silencing outside of the context of embryonic stem cells.

Biphasic reactivation: obscure idea to valid model of viral transcription

The theory of biphasic HSV-1 reactivation was first introduced in 2012 and has been met with some skepticism since. One concern was that the evidence for Phase I gene expression was largely derived from *in vitro* models that employ antivirals like acyclovir to promote latency establishment. Phase I gene expression was argued to be a sort of defunct burst of gene expression by to viral genomes which had incorporated or been damaged by ACV. In this dissertation, I constructed a new *in vitro* model system of HSV-1 latency and reactivation in primary neurons that does not require the

use of antivirals to promote latency establishment. Using this non-ACV model, I validate the Phase I phenomena and overall biphasic mechanism of reactivation (117). During the period of my dissertation, there have also been additional publications in alternative models that further support the concept of a HSV reactivation progressing through two waves. In an *in vitro* model that uses neuronal hyperexcitability trigger forskolin to elicit reactivation (109), “Phase I” was observed at approximately 20 hours post-stimulus. In an *ex vivo* model where LY294002 is used in combination with explant to elicit reactivation (98), Phase I occurs at approximately 5 hours post-stimulus. Therefore, Phase I gene expression can be detected in both *in vitro* and *ex vivo* models of HSV latency, in the presence or absence of acyclovir, and in response to different reactivation triggers.

The implication of the existence of Phase I gene expression is that there are mechanistic differences between HSV-1 transcription during *de novo* lytic infection and reactivation, as previously noted (63, 99). This consideration is central for future modeling and for differentiating the impact of therapies prophylactically or following reactivation events. During *de novo* lytic infection, viral transcription occurs in cascade fashion wherein IE gene transcription and translation precedes E gene transcription and translation, which is necessary for viral DNA replication, which is subsequently required for L gene transcription. During Phase I gene expression, gene expression is uncoupled from viral DNA replication and the transcription of early and late genes can occur independently of viral protein synthesis. Moreover, Phase I occurs independently of viral transactivator protein VP16, which enters the host cell from the virion’s tegument upon

de novo infection and sets off the transcriptional cascade. In this dissertation, we introduce additional evidence which supports the notion that HSV-1 *de novo* lytic infection and reactivation are distinct processes in a neuron. We find that c-Jun promotes lytic gene expression in both scenarios, but with subtle differences in impact (Chapter 3). During *de novo* infection, c-Jun promotes the viral transcription of all classes of viral lytic genes, including immediate early genes and early genes. In contrast, c-Jun does not initiate the transcription of any of the classes of genes during Phase I gene expression. During full, Phase II reactivation, c-Jun does enhance lytic gene expression, but only that of late genes, the expression of which follows viral DNA replication.

Unresolved Questions & Future Directions

The interplay between Polycomb silencing and constitutive heterochromatin on the HSV-1 genome.

Additional repressive chromatin modifications, H3K9me2 and H3K9me3, have also been observed on the latent HSV-1 genome. Whether these modifications and Polycomb silencing are coupled, mark the same viral genomes, or cooperatively work to silence the viral genome is unknown. There is accumulating evidence on the co-existence of H3K9 methylation and PRC2-mediated H3K27 methylation. Euchromatic histone-lysine N-methyltransferase 2 (EHMT2/G9a) heterodimerizes with euchromatic histone-lysine N-methyltransferase 1 (EHMT1/GFLP) to establish H3K9 methylation, however EHMT2 has also been demonstrated to catalyze H3K27 mono- and di-methylation in biochemical assays (394). Further, EHMT2 interacts with PALI1, allowing the assembly and activity of a EHMT2-PAL1-PRC2 super-complex (395). There is also potential interplay between PRC1-mediated silencing and H3K9 methylation, although

previous work in mouse embryonic stem cells suggested these two processes excluded one another (396-399). In human and murine somatic cells, BMI1 is required for H3K9 methylation formation and silencing, and BMI-1 co-immunoprecipitated with HP1 and other H3K9me3 readers/writers (400). These studies also specifically demonstrated in murine neurons that BMI-1 and H3K9me3 enrichment co-localizes in pericentric heterochromatin (401). Also, H3K9me3 peptides were demonstrated to bind CBX proteins through surface plasmon resonance (SPR). Therefore, it is likely that at least one form of PRC1 (with this evidence pointing to canonical PRC1), can associate and co-regulate constitutive heterochromatin in a neuron in the context of HSV-1 infection. Interestingly, the binding of CBX proteins to the H3K9me3 peptide was significantly reduced upon the phosphorylation of the adjacent serine 10 (401). This "phospho/methyl switch" has been demonstrated to occur on the HSV-1 genome during the very initial transcriptional stages of reactivation but it has never been linked with Polycomb silencing (99). A simple but telling experiment would be to determine if constitutive heterochromatin and Polycomb silencing bind onto the same individual viral genomes by dual immunofluorescence staining of H3K9me3 and H3K27me3, H2AK119ub, or Ring1 and subsequent co-localization quantification using NucSpotA. Re-ChIP analyses can also be performed for these heterochromatin modifications in a mouse model.

How is Polycomb recruited to HSV-1 genomes?

Our preliminary data align with the hypothesis that hnRNPK and the LAT recruit PRC1 to viral genomes during latency establishment in neurons. Viral LAT expression may therefore actively promote a type of gene silencing that is capable of reactivating.

In fact, the LAT has been demonstrated to enhance reactivation in several models, further supporting this theory (390, 402). Back in 2009, the hypothesis that the LAT recruits PRC2 and therefore H3K27-methylation to the HSV-1 genome was conceived. Three studies were published that addressed this possibility without consensus. Our proposal that LAT recruits PRC1 is interesting as it could potentially shed light on these findings. If the LAT recruits PRC1, and PRC2 recruitment/activity is even partially dependent on the H2AK119ub, then there would be at least subtle changes in H3K27me3 upon LAT-deletion in a population-level study. The LAT could impact the nature of Polycomb silencing on the latent genome, but not be fully required for PRC2 targeting. In support of this, SUZ12 appears to be recruited to similar levels to the lytic viral promoters tested even in the absence of the LAT during the establishment of latency (192).

Now that we have optimized CUT&RUN-sequencing to work in primary neurons (Chapter 4), I hope to next directly explore H2AK119ub binding across the viral genome in the presence and absence of hnRNPK using my validated shRNA-mediated lentiviruses. We (Matt Loftus, unpublished) have also now generated Stayput-GFP LAT-deletion mutants to determine the role the LAT might play in PRC1 recruitment and compare the phenotypes of these viruses to the hnRNPK depletion phenotype. In addition to CUT&RUN-sequencing for H2AK119ub, we will also analyze lytic viral gene expression and viral DNA replication over latency establishment using these LAT-deletion mutants. The LAT has been demonstrated to repress lytic gene transcription during acute infection, but only *in vivo* thus far (209). We therefore can independently

investigate the requirement of hnRNPK and the LAT on PRC1 recruitment and have demonstrated LAT/hnRNPK binding. Additionally demonstrating the simultaneous co-localization of LAT, hnRNPK, and the HSV-1 genome through a combination of single molecule fluorescence *in situ* hybridization (smFISH), click chemistry, and immunofluorescence would provide compelling evidence that hnRNPK and the LAT act in concert with one-another.

There are of course alternative mechanisms independent of the LAT and hnRNPK that may mediate Polycomb recruitment to the HSV-1 genome. In fact, one must exist as PRC1 is recruited to the HSV-1 genome in non-neuronal cells (data not shown, Alison Francois) where the LAT is not actively transcribed. An attractive possibility is host protein KDM2B, which recruits vPRC1 to cellular genomes by binding unmethylated GC-rich sequences (128, 160). This is a viable possibility as HSV-1, like the other human herpesviruses, is extremely GC-rich (403). In fact it is theorized (although not directly demonstrated) that KSHV uses its intrinsic GC-richness and KDM2B to recruit Polycomb (180) (404). Our RNA-sequencing data demonstrates KDM2B expression in our uninfected sympathetic cultures (data not shown), and I have performed immunofluorescence experiments for KDM2B these cultures. Interestingly, KDM2B stains as cytoplasmic puncta (data not shown). However, this is not grounds to exclude the potential of KDM2B to recruit PRC1 as we 1) have not validated the specificity of this antibody and 2) KDM2B could localize to the neuronal nucleus upon HSV-1 infection, a possibility we have not explored. Interestingly, my

immunofluorescence experiments in uninfected dermal fibroblasts demonstrate KDM2B staining that is both perinuclear and punctate nuclear (data not shown).

Alternatively, PRC1 could be recruited to the HSV-1 genome using host transcription factor RUNX1, which recruits Ring1B and subsequent H2AK119ub deposition in primary thymocytes (368). RUNX1 binding sites are pervasive in the HSV-1 genome, and the overexpression of RUNX1 has been shown to repress HSV lytic gene expression in neuroblastoma cells (405). RUNX1 is also pervasively transcribed in sensory neurons and sympathetic neurons, where HSV-1 readily establishes latency. Future experiments could deplete KDM2B or RUNX1 and analyze PRC1-recruitment to the viral genome through CUT&RUN. More preliminary analyses can be performed by analyzing colocalization of H2AK119ub in the presence or absence of KDM2B or RUNX1.

The mechanism of recruitment for PRC2 and H3K27 methylation to the viral genome is also unresolved. One hypothesis is that PRC1/H2AK119ub recruits PRC2 to the genome. Our CUT&RUN-sequencing data demonstrate peaks where H2AK119ub and H3K27me3 exist both dependently and independently of each other on viral genomes (Chapter 4). Therefore, mutual recruitment is possible although we cannot discern from this population-based technique whether H2AK119ub and H3K27me3 decorate the same individual viral genomes. Further, PRC1-mediated recruitment of PRC2 has previously been demonstrated to occur on cellular genomes through recognition of H2AK119ub1 by PRC2.2 in ESCs is via JARID2. However, JARID2 is

found in one of two isoforms, and the longer isoform is the one capable of H2AK119ub1 and PRC2 binding. In many lineage committed cells, including primary lymphocytes and keratinocytes, the predominant isoform of JARID2 is ΔN-JARID2 (152). In line with this finding, I was unable to detect the long isoform of JARID2 via western blot in our primary neurons, although it was detectable in other non-neuronal cell types (data not shown). This is not confirmation that the proper JARID2 isoform used for recruitment is not translated and utilized in primary neurons, there may be issues with its detection. However, this blot suggests an alternative mechanism of PRC2 recruitment 1) using PRC1 but independent of JARID2, or 2) independent of PRC1 altogether. KSHV expresses mi-RNAs that downregulate JARID2 despite the viral genome becoming enriched in both H2AK119ub and H3K27me3, thus supporting the existence of an alternative mechanism of recruitment in differentiated cells (406, 407).

An alternative hypothesis involves nucleosomal density. PRC2 activity may also be enhanced by a dense, polysomal structure with an optimal DNA linker length of 40 bp (408). CryoEM of AEBP2-containing PRC2 demonstrates positioning of the EZH2 SET domain in close proximity to the neighboring unmodified histone (147). Therefore, a dense nucleosomal structure (at least one containing H3K27me3) likely facilitates spread of K27 methylation from an initiating site, although how nucleosomal density may co-ordinate *de novo* lysine methylation is currently unknown. In the case of HSV-1 and KSHV, H3 nucleosome occupancy accumulates prior to H3K27me3 (176, 192). For HCMV, H3 deposition occurs rapidly on the HCMV genome during latent infection, suggesting it may be deposited prior to H3K27me3 (409).

Further, PRC2 interacts with the highest affinity to G-quadruplexes, which are demonstrated on the immediate early promoters/regulatory regions of HSV-1, HSV-2, VZV, HMCV, EBV, and KSHV (410-412). A second transcriptional repressor, RE1-silencing transcription factor (REST, also known as neuron-restrictive silencing factor (NRSF)) can interact with PRC1 and PRC2 and maintains PRC1/2 binding to neuronal genes in the human teratocarcinoma NT2-D1 cells and mESCs (413). However, REST can also limit PRC2 binding around CpG-rich regions in murine embryonic cells (413). The HSV-1 genome carries numerous predicted REST binding sites and may repress the ability of HSV-1 to transcribe lytic viral genes and reactivate (414) (415). Any of the models of PRC1 and PRC2 recruitment remain to be tested.

hnRNPK and the LAT: one step closer to solving the enigma?

One of the most enticing findings presented in this dissertation is that the LAT and hnRNPK interact in neurons. The LAT was identified decades ago (416), but its function still remains mysterious. In this dissertation, I propose that hnRNPK and the LAT in tandem target PRC1 to HSV-1 genomes in neurons. However, the original finding of Igor Jurak that the hnRNPK and LAT interact has major implications even if the function of this interaction is outside of the realm of Polycomb silencing. On the cellular genome, hnRNPK can work with RNAs (as well as proteins) to both enhance or repress gene expression (417). In the case of gene expression, hnRNPK often prevents the binding of miRNAs to mRNAs and subsequent degradation. There are also several mechanisms of repression that hnRNPK can carry out with lncRNAs. First, lncRNA association with hnRNPK can lead to the formation of repressive bodies known as

paraspeckles. However, given the broad, homogenous nuclear staining of hnRNPK in HSV-infected neurons (Chapter 4), I find this alternative unlikely. hnRNPK has also been implicated in repression using lncRNAs through heterochromatin recruitment. As described earlier, the lncRNA Xist can recruit PRC1 and H2AK119ub during X chromosome inactivation (222). However, there are additional examples of lncRNA-mediated recruitment in tandem with hnRNPK. LncRNA LBCS has been demonstrated to recruit PRC2 component EZH2 to DNA, and lncRNAp21 has been shown to recruit H3K9 methyltransferases to DNA (418). The LAT has been shown to promote H3K9 methylation on the viral genome, and therefore a model where hnRNPK and the LAT recruit H3K9 methylases or a complex containing a combination of chromatin remodelers is feasible. There are in fact differing reports on if and how the LAT modulates reactivation (124, 208, 402). If the LAT promotes different forms of heterochromatin that are more or less amenable to reactivation in different models, this could explain the discrepancies between these studies. There is also the potential that hnRNPK and the LAT recruit complexes to the host cell genome rather than the viral genome. There are broader studies that can be performed to identify the function and importance of the LAT/hnRNPK interaction, such as PAR-CLIP-sequencing to discern where the precise region on the LAT where hnRNPK binds (and to make mutations in this region) or a more global RNA-IP-sequencing which will illuminate whether the LAT modulates the binding of hnRNPK to host RNAs.

~End of Chapter 5~

Chapter 6: Materials and Methods

Reagents

Compounds used in the study are described in Table 1. Compound concentrations were used based on previously published IC50s and assessed for neuronal toxicity using the cell body and axon health and degeneration index as previously published (109). All compounds had an average score less than or equal to 1.

Table 1. Compounds used and concentrations

Compound	Supplier	Identifier	Concentration
NGF 2.5S	Alomone Labs	N-100	50 ng/mL
GDNF	Peprotrech	450-44	50 ng/mL
Aphidicolin (APH)	AG Scientific	A-1026	3.3 µg/ml
L-glutamic acid	Millipore Sigma	G5638	3.7 µg/ml
Acycloguanosine	Millipore Sigma	A4669	10 µM, 50 µM
Primocin	Invivogen	ant-pm-1	100 µg/ml
PRIME-XV IS21 Neuronal Supplement	Irvine Scientific	91142	1:50
Neurobasal Medium™, minus phenol red	Gibco	12348017	
BrainPhys	STEMCELL Technologies	05791	
Molecular Probes SYTOX Orange Nucleic Acid Stain	Thermo Fisher Scientific	S11368	1:5000

G418/Geneticin	Gibco	10131-035	250 µg/ml
GNE-3511	Millipore Sigma	5.33168.0001	4 µM
GSK-J4	Sigma Aldrich	SML0701	2 µM
OG-L002	Selleck Chemicals	S7237	20 µM
LY294002	Tocris	1130	20-40 µM
Forskolin	Tocris	1099	60 µM
T-5224	Cayman Chemical Company	22904	20 µM
DMXAA	Invivogen	tlrl-isdc	5 µg/mL
JQ1	Cayman Chemical Company	11187	1 µM
AFDye 555 Azide Plus	Click Chemistry Tools	1479-1	10 µM
EdC	Sigma-Aldrich	T511307	10 µM
PTC-209	Tocris	5191	2 µM
RB-3			25 µM
PRT4165	Sigma-Aldrich	SML1013-5MG	40 µM
UNC1999	Cayman Chemical Company	14621	1 µM
CPI-1205	Selleck Chemicals	S8353	10 µM
EED226	Cayman Chemical Company	22031	25 µM

EPZ005687	Cayman Chemical Company	13966	0.5 μM

Construction of Stayput-GFP

Stayput-GFP was created by inserting an eUs11-GFP tag into the previously created gH-deficient HSV-1 SCgHZ virus (strain SC16) through co-transfection of SCgHZ viral DNA and pSXZY-eGFP-Us11 plasmid (273) in Vero F6 cells, Transfections were carried on in 6 well plates using 2 μg of viral DNA and 2 μg of pSXZY-eGFP-Us11 and 8ul of jetPRIME® (Polyplus). GFP-positive plaques were subjected to 4 rounds of plaque purification.

Preparation of HSV-1 virus stocks

Stayput-GFP, as well as SCgHZ, is propagated and titrated on previously constructed gH-complementing F6 cells, which contain copies of the gH gene under the control of an HSV-1 gD promoter, as described in (274). Vero F6 cells were maintained in Dulbecco's Modified Eagle's Medium (Gibco) supplemented with 10% FetaPlex (Gemini BioProducts) and 250 μg/mL of G418/Geneticin (Gibco).

HSV-1 stocks of eGFP-Us11 Patton, Syn17+, and KOS (for *in vivo* experiments) were grown and titrated on Vero cells obtained from the American Type Culture Collection (Manassas, VA). Cells were maintained in Dulbecco's Modified Eagle's Medium (Gibco) supplemented with 10% FetalPlex (Gemini Bio-Products) and 2 mM L-Glutamine.

eGFP-Us11 Patton (HSV-1 Patton strain with eGFP reporter protein fused to true late protein Us11 (273) was kindly provided by Dr. Ian Mohr at New York University.

Single-step growth curve

1×10^5 Vero F6 cells were seeded per well in a 24-well plate. 24 hours later, when the cells had reached approximately 90% confluency, cells were infected with Stayput-GFP, SCgHZ, or wild-type Patton Us11-GFP at an MOI of 5 PFU/cell for 1 hour at 37°C with gentle rocking (60 rpm). Inoculum was then removed and replaced with 400 μL of media. At the specified time-points, 400 μL of 9% sterile milk was added to the well and the plates were frozen in the -80C. Following three freeze thaw cycles, titrations were carried out on Vero F6 cells.

Viral genomic DNA sequencing

Genomic DNA was isolated from stocks of SCgHZ and Stayput-GFP using the Qiagen DNeasy Blood and Tissue kit. 250 ng of gDNA was used as input for the SQK-LSK109 genomic DNA by ligation protocol (Oxford Nanopore Technologies Ltd.) and resulting libraries were loaded onto individual R9.4.1 flongles for 20 hours of sequencing. Resulting raw fast5 datasets were basecalled using Guppy v4.2.2 (-f FLO-MIN106 -k SQK-RNA002) with only reads passing filter used for subsequent analyses. *De novo* assembly was performed as follows. First, HSV-1 reads were extracted from the total pool by aligning against the HSV-1 strain SC16 reference genome (MN159383.1) using MiniMap2. HSV-1 reads shorter than 1,000 nt were subsequently filtered out prior to performing de novo assembly with Canu (419). Canu yielded a single circular contig for

both SCgHZ and Stayput-GFP which was manually linearized at the canonical HSV-1 start site. Four rounds of genome polishing was performed using racon (420) before a final round of SNP calling was achieved using medaka (https://github.com/nanoporetech/medaka). Results are available in European Nucleotide Archive under the accession PRJEB51869.

Direct RNA sequencing

For both SCgHZ and Stayput-GFP, NHDFs (passage 13) were infected at an MOI of 10. At 6 hours post infection, the supernatant was removed and cells washed once with PBS prior to lysing with 8 ml Trizol. Total RNA was extracted according to Trizol manufacturer's instructions and eluted in nuclease-free water. Nanopore direct RNA-Seq libraries were prepared for each sample using between ~500 ng of poly(A) RNA that was previously isolated from 30 µg of total RNA using the Dynabeads™ mRNA Purification Kit (Invitrogen, 61006). The poly(A) RNA was spiked with 0.5 µL of a synthetic Enolase 2 (ENO2) calibration RNA (Oxford Nanopore Technologies Ltd.) and direct RNA-Seq libraries prepared according to the standard SQK-RNA002 protocol (Oxford Nanopore Technologies Ltd.). Raw fast5 datasets were then basecalled using Guppy v4.2.2 (-f FLO-MIN106 -k SQK-RNA002) with only reads passing filter used for subsequent analyses. Sequence reads were aligned against the Stayput-GFP genome using MiniMap2 (Li, 2018) (-ax splice -k14 -uf --secondary=no), with subsequent parsing through SAMtools and BEDtools (421, 422). Here sequence reads were filtered to retain only primary alignments (Alignment flag 0 (top strand) or 16 (bottom strand)). Figures

associated with this study were generated using the R packages Gviz (423) and GenomicRanges (424).

Primary neuronal cultures

Sympathetic neurons from the superior cervical ganglia (SCG) of post-natal day 0–2 (P0-P2) CD1 Mice (Charles River Laboratories) were dissected as previously described (99). Sensory neurons from the trigeminal ganglia (TG) or adult (P21-24) CD1 Mice (Charles River Laboratories) were dissected as previously described (425). Rodent handling and husbandry were carried out under animal protocols approved by the Animal Care and Use Committee of the University of Virginia (UVA). Ganglia were briefly kept in Leibovitz's L-15 media with 2.05 mM L-Glutamine before dissociation in Collagenase Type IV (1 mg/mL) followed by Trypsin (2.5 mg/mL) for 20 min each at 37℃. Dissociated ganglia were triturated, and approximately 5-10,000 neurons per well were plated onto rat tail collagen in a 24-well plate. Sympathetic neurons were maintained in CM1 (Neurobasal Medium supplemented with PRIME-XV IS21 Neuronal Supplement (Irvine Scientific), 50 ng/mL Mouse NGF 2.5S, 2 mM L-Glutamine, and Primocin). Aphidicolin (3.3 µg/mL) was added to the CM1 for the first 5 days post-dissection to select against proliferating cells. Sensory neurons were maintained in the same media supplemented with GDNF (50 ng/ml; Peprotech 450-44), and more Aphidicolin (6.6 µg/mL) was used for the first 5 days as more non-neuronal cells tend to be dissected with this neuron type.

Lytic HSV-1 Infection

Non-neuronal ARPE-19s (DMEM 10% FP) or dermal fibroblasts (DMEM 10% FBS) were infected with HSV-1 Syn17+ at MOI 3 PFU/cell (following quantification of cells per well) in Dulbecco's Phosphate Buffered Saline (DPBS) + $CaCl_2$ + $MgCl_2$ supplemented with 1% fetal bovine serum and 4.5 g/L glucose for 1 h at 37°C. Post infection, inoculum was replaced with feeding media.

P6-8 SCG neurons were infected with Stayput Us11-GFP at MOI 7.5 PFU/cell, assuming 10,000 cells per well in Dulbecco's Phosphate Buffered Saline (DPBS) + $CaCl_2$ + $MgCl_2$ supplemented with 1% fetal bovine serum and 4.5 g/L glucose for 3.5 h at 37°C. Post infection, inoculum was replaced with feeding media (as described above). Acyclovir (ACV) was not utilized in these infections. Lytic infection was quantified by counting number of GFP-positive neurons or performing reverse transcription–quantitative PCR (RT–qPCR) of HSV-1 lytic mRNAs isolated from the cells in culture.

Establishment and reactivation of latent HSV-1 infection in primary neurons

Neonatal SCGs were infected at postnatal days 6-8 with either Us11-GFP, SCgHZ, or Stayput-GFP at an MOI of 7.5 PFU/cell assuming 10,000 cells/well in DPBS +CaCl2 +MgCl2 supplemented with 1% Fetal Bovine Serum, 4.5 g/L glucose, and either with or without 10 μM Acyclovir (ACV) for 3 hr at 37℃. Post infection, inoculum was replaced with feeding media with or without 50 μM ACV. Reactivation was carried out in BrainPhys (Stem Cell Technologies) supplemented with 2 mM L-Glutamine, 10% Fetal

Bovine Serum, Mouse NGF 2.5S (50 ng/mL) and Primocin. Reactivation was quantified by counting number of GFP-positive neurons or performing Reverse Transcription Quantitative PCR (RT-qPCR) for HSV-1 lytic transcripts.

Mouse Infections

Five-week-old male and female CD-1 mice (Charles River Laboratories) were anesthetized by intraperitoneal injection of ketamine hydrochloride (80 mg/kg of body weight) and xylazine hydrochloride (10 mg/kg) and inoculated with 1 × 106 PFU/eye of virus (in a 5 μL volume) onto scarified corneas, as described previously (122). Mice were housed in accordance with institutional and National Institutes of Health guidelines on the care and use of animals in research, and all procedures were approved by the Institutional Animal Care and Use Committee of the University of Virginia. Criteria used for clinical scoring based on the formation of lesions and neurological and eye symptoms are shown in Table 2 and were based on a previously established scoring scale (426). Mice were randomly assigned to groups, and all experiments included biological replicates from independent litters.

Table 2. Clinical scoring scale for HSV-infected mice.

Score	Description of score by type		
	Lesion	**Eye**	**Neurological**
0	None	No symptoms	No symptoms
1	Small area of broken skin (<0.5cm)	Pus around edges	Hunched, normal movement

2	Area of broken skin 0.5-1cm	Pus and squint	Hunched, slow movement
3	Bleeding, scabbing, or pustules	Closed	Hunched, labored breathing and/or hind-leg paralysis
4	Broken skin >1cm with multiple pustules or scabbing	Scab formation	Hunched, ruffled fur, little/no movement
5	Severe scabbing or bleeding with pustules	Severe scabbing	Moribund or dead

RNA-IP

Three days following infection with Stayput-GFP at an MOI of 10, LUHMEs were fixed in 0.1% formaldehyde 10 minutes at RT, followed by quenching with 0.125 M glycine for 5 minutes at RT. RNA-IP was carried out using Magna RIP RNA-Binding Protein Immunoprecipitation (Millipore, 17-701), per attached protocol with several adjustments made based on Hendrickson *et al*, 2016 (427): Samples were sonicated following fixation through incubation in lysis buffer for 10 minutes of ice, followed by sonication on 10% amplitude for 0.7 seconds on and 1.3 seconds off at 30 seconds for 90 seconds total. Pause between 30 second intervals and place sample on ice. Following immunoprecipitation and during RNA purification, the following incubation was performed: 55˚C for 30 minutes for proteinase K and an additional 65˚C for 1 hour to reverse crosslinking. Following RNA purification, residual DNA was eliminated through

TURBO DNA-free Kit TURBO DNase Treatment and Removal Reagents (ambion, AM1907).

Western Blotting

Neurons were lysed in RIPA Buffer with cOmplete, Mini, EDTA-Free Protease Inhibitor Cocktail (Roche) and PhosSTOP Phosphatase Inhibitor Cocktail (Roche) on ice for 2 hours with regular vortexing to aid lysis. Insoluble proteins were removed via centrifugation, and lysate protein concentration was determined using the Pierce Bicinchoninic Acid Protein Assay Kit (Invitrogen) using a standard curve created with BSA standards of known concentration. Equal quantities of protein (15–50 µg) were resolved on 4–20% gradient SDS-Polyacrylamide gels (Bio-Rad) and then transferred onto Polyvinylidene difluoride membranes (Millipore Sigma). Membranes were blocked in PVDF Blocking Reagent for Can Get Signal (Toyobo) for 1 hr. Primary antibodies were diluted in Can Get Signal Immunoreaction Enhancer Solution 1 (Toyobo) and membranes were incubated overnight at 4˚C. HRP-labeled secondary antibodies were diluted in Can Get Signal Immunoreaction Enhancer Solution 2 (Toyobo) and membranes were incubated for 1 hr at room temperature. Antibody usage is recorded in Table 4. Blots were developed using Western Lightning Plus-ECL Enhanced Chemiluminescence Substrate (PerkinElmer) and ProSignal ECL Blotting Film (Prometheus Protein Biology Products) according to manufacturer's instructions. Blots were stripped for reblotting using NewBlot PVDF Stripping Buffer (Licor). Band density was quantified in ImageJ.

Preparation of lentiviral vectors

Lentiviruses expressing shRNA against C-JUN (Jun-1 = TRCN0000360511, cJun-2 = TRCN0000055205, Jun-3 = TRCN0000042696), c-FOS (Fos1= TRCN0000231167), hnRNPK (hnRNPK-1 = TRCN0000295993 hnRNK-2 = TRCN0000295994), Ring1A (Ring1A-1 = TRCN0000040561 Ring1A-2 = TRCN0000040562), Ring1B (Ring1B-1 = TRCN0000226018, Ring1B-2= TRCN0000226019), SUZ12 (Suz12-1 = TRCN0000234040, Suz12-2 = TRCN0000218848, Suz12-3 =TRCN0000123893) or a control lentivirus shRNA (empty pLKO.1 or pLKO.5 vector) were prepared by co-transfection with psPAX2 and pCMV-VSV-G (428) using the 293LTV packaging cell line (Cell Biolabs). Supernatant was harvested at 40- and 64-h post-transfection and filtered using a 45 μM PES filter. Sympathetic neurons were transduced overnight in neuronal media containing 8 μg/ml protamine sulfate and 50 μM ACV.

CUT&RUN Sequencing

A minimum of approximately 120,000 neurons were plated for each CUT&RUN reaction. Neurons were collected following 10-minute incubation with trypsin at 37℃ without fixation. Neurons were permeabilized with 0.01% digitonin (concentration optimized for neurons) and CUT&RUN was performed using reagents included in the CUT&RUN Kit (EpiCypher) according to attached protocol. Periodic quality checks as recommended and detailed by protocol Appendix were performed and passed for neurons. CUT&RUN libraries were prepared using CUT&RUN Library Prep Kit (EpiCypher) and subject to pair-ended partial-lane sequencing and de-multiplexing using NovaSeq (Novogene). Data analysis was performed using command line and R

code, and workflow, adapted from tutorial on IO protocols (Zheng Y et al (2020) Protocol.io). The Rivanna high-performance computing environment (UVA Research Computing) was used for command line data processing. The HSV-1 SC16 genome sequence (NCBI NC_KX946970.1) was used in combination with the mm39 mouse genome assembly (RefSeq NC_000071.7) to make a joint Bowtie2 index genome. Sequence alignment was performed with bowtie2 with the following settings*: --end-to-end --very-sensitive --no-mixed --no-discordant --phred33 -I 10 -X 700.* Separate alignments was performed to spike-in *E. Coli* DNA (MG1655, Genbank U00096.3), from which sequencing depth was calculated and reads normalized accordingly before filtering into separate human and viral bedgaph files. Data quality control and visualization were performed using R. Two experimental replicates were performed.

EdC Pulse

To visualize replicating viral DNA, reactivating cultures were pulsed with 10 μM EdC in reactivation media for 1 hour prior to fixation and processing through click chemistry.

Click Chemistry

For EdC-labeled HSV virus infections, an MOI of 7.5 was used. EdC labelled virus was prepared using a previously described method (429). Click chemistry was carried out a described previously (430) with some modifications. Neurons were washed with CSK buffer (10 mM HEPES, 100 mM NaCl, 300 mM Sucrose, 3 mM MgCl2, 5 mM EGTA) and simultaneously fixed and permeabilized for 10 minutes in 1.8% methonal-free formaldehyde (0.5% Triton X-100, 1% phenylmethylsulfonyl fluoride (PMSF)) in CSK

buffer, then washed twice with PBS before continuing to the click chemistry reaction and immunostaining. Samples were blocked with 3% BSA for 30 minutes, followed by click chemistry using EdC-labelled HSV DNA and the Click-iT EdU Alexa Flour 555 Imaging Kit (ThermoFisher Scientific, C10638) according to the manufacturer's instructions. For immunostaining, samples were incubated overnight with primary antibodies in 3% BSA. Following primary antibody treatment, neurons were incubated for one hour in Alexa Fluor® 488-, 555-, and 647-conjugated secondary antibodies for multi-color imaging (Invitrogen). Nuclei were stained with Hoechst 33258 (Life Technologies). Images were acquired at 60x using an sCMOS charge-coupled device camera (pco.edge) mounted on a Nikon Eclipse Ti Inverted Epifluorescent microscope using NIS-Elements software (Nikon). Images were analyzed and intensity quantified using ImageJ.

Immunofluorescence

Neurons were fixed for 15 min in 4% Formaldehyde and blocked in 5% Bovine Serum Albumin and 0.3% Triton X-100 and incubated overnight in primary antibody. Following primary antibody treatment, neurons were incubated for 1 hr in Alexa Fluor 488-, 555-, and 647-conjugated secondary antibodies for multi-color imaging (Invitrogen). Nuclei were stained with Hoechst 33258 (Life Technologies). Images were acquired using an sCMOS charge-coupled device camera (pco.edge) mounted on a Nikon Eclipse Ti Inverted Epifluorescent microscope using NIS-Elements software (Nikon). Images were analyzed using ImageJ.

Table 3. Antibodies			
Designation	**Source or reference**	**Identifiers**	**Additional Information**
Anti-cJun (Mouse monoclonal)	BD Biosciences	Cat #610326	WB (1:1,000)
Anti-a-tubulin (Mouse monoclonal)	Millipore sigma	Cat #T9026	WB (1:2500)
Anti-Rabbit IgG Antibody (H+L), Peroxidase (Goat polyclonal)	Vector Labs	Cat #PI-1000	WB (1:10,000)
Anti-mouse IgG Antibody (H+L), Peroxidase (Horse polyclonal	Vector Labs	Cat #PI-2000	WB (1:10,000)
Phospho-c-Jun (Ser63) II	Cell Signaling Technology	Cat #9261	IF (1: 400)
Beta III Tubulin	EMD Millipore	Cat #9354	IF (1:500)
IgG	EMD Millipore	12-370	CUT&RUN ChIP-qPCR
c-Jun	EpiCypher	13-2019	CUT&RUN 0.5 µg per reaction
c-Jun			IF
H2A	Cell Signaling Technology	12349S	ChIP-qPCR
H2AK119ub	Cell Signaling Technology	8240S	ChIP-qPCR (1:100) CUT&RUN IF (1:1600)
H3K27me3	Cell Signaling Technology		CUT&RUN IF
H3K27me2	Cell Signaling Technology		IF
Ring1B	Cell Signaling Technology	5694S	IF, WB
ICP4	Abcam	ab6514	IF (1:850)
ICP5	Abcam	ab6508	IF
ICP8	Abcam	ab20194	IF
GFP	Abcam	ab13970	IF
ZRF1	Novus Biologicals	NBP1-82627	IF

hnRNPK	Proteintech	11426-1-AP	RNA-IP
hnRNPK	Cell Signaling Technology	4675S	IF 1:100 WB 1:800
H3	Cell Signaling Technology		WB
Alpha-tubulin	Cell Signaling Technology		WB

Analysis of mRNA expression and viral genome copy number

To assess expression of HSV-1 lytic mRNA, total RNA was extracted from approximately 5,000 neurons using the Quick-RNA Miniprep Kit (Zymo Research) with an on-column DNase I digestion. mRNA was converted to cDNA using the Maxima cDNA synthesis kit (Thermo Fisher) using random hexamers for first-strand synthesis and equal amounts of RNA (20–30 ng/ reaction). To assess viral DNA load, total DNA was extracted from approximately 5,000 neurons using the Quick-DNA Miniprep Plus Kit (Zymo Research). qPCR was carried out using PowerUp™ SYBR Green Master Mix (Thermoscientific). Relative mRNA/DNA copy numbers were determined using the Comparative CT (ΔΔCT) method normalized to mRNA levels in latently infected samples. Viral RNAs were normalized to mouse reference gene 18s ribosomal RNA. All samples were run in duplicate on an Applied Biosystems QuantStudio 6 Flex Real-Time PCR System and the mean fold change compared to the reference gene calculated. Exact copy numbers were determined by comparison to standard curves of known DNA copy number of viral genomes or plasmid containing 18S rRNA (p18S.1 tag was a gift from Vincent Mauro; Addgene plasmid # 51729 ; http://n2t.net/addgene:51729 ; RRID:Addgene_51729, (431).

Table 4. Sequences of Primers Used	
Primer	**Sequence 5’ to 3’**
mGAPDH 1SF	CAT GGC CTT CCG TGT GTT CCT A
mGAPDH 1SR	GCG GCA CGT CAG ATC CA
hGAPDH F	CAC CGC CGC ATC CTC CTC TTC
hGAPDH R	TGT GTG CCG CCC GAC AGC
ICP27 F	GCA TCC TTC GTG TTT GTC ATT CTG
ICP27 R	GCA TCT TCT CTC CGA CCC CG
ICP8 1SF	GGA GGT GCA CCG CAT ACC
ICP8 1SR	GGC TAA AAT CCG GCA TGA AC
gC F	GAG TTT GTC TGG TTC GAG GAC
gC R	ACG GTA GAG ACT GTG GTG AA
VP16 F	GGA CCG GAC GGA CCT TAT
VP16 R	GGT TGC TTA AAT GCG TGG TG
LAT F	TGT GTG GTG CCC GTG TCT T
LAT R	CCA GCC AAT CCG TGT CGG
UL30 F	CGC GCT TGG CGG GTA TTA ACA T
UL30 R	TGG GTG TCC GGC AGA ATA AAG

Statistical Analysis

All statistical analyses were performed using Prism V10. The normality test and statistical test used for each figure are denoted in the figure legends. Individual

biological replicates are plotted, each corresponding to a single well of cells/neurons. All neuronal experiments were repeated from pooled neurons from at least 3 litters.

References

1. Dupin N, Fisher C, Kellam P, Ariad S, Tulliez M, Franck N, van Marck E, Salmon D, Gorin I, Escande JP, Weiss RA, Alitalo K, Boshoff C. 1999. Distribution of human herpesvirus-8 latently infected cells in Kaposi's sarcoma, multicentric Castleman's disease, and primary effusion lymphoma. Proc Natl Acad Sci U S A 96:4546-51.
2. Bechtel JT, Liang Y, Hvidding J, Ganem D. 2003. Host range of Kaposi's sarcoma-associated herpesvirus in cultured cells. J Virol 77:6474-81.
3. Boshoff C, Schulz TF, Kennedy MM, Graham AK, Fisher C, Thomas A, McGee JO, Weiss RA, O'Leary JJ. 1995. Kaposi's sarcoma-associated herpesvirus infects endothelial and spindle cells. Nat Med 1:1274-8.
4. Thorley-Lawson DA, Hawkins JB, Tracy SI, Shapiro M. 2013. The pathogenesis of Epstein-Barr virus persistent infection. Curr Opin Virol 3:227-32.
5. Sindre H, Tjoonnfjord GE, Rollag H, Ranneberg-Nilsen T, Veiby OP, Beck S, Degre M, Hestdal K. 1996. Human cytomegalovirus suppression of and latency in early hematopoietic progenitor cells. Blood 88:4526-33.
6. Hahn G, Jores R, Mocarski ES. 1998. Cytomegalovirus remains latent in a common precursor of dendritic and myeloid cells. Proc Natl Acad Sci U S A 95:3937-42.
7. Elder E, Sinclair J. 2019. HCMV latency: what regulates the regulators? Med Microbiol Immunol 208:431-438.
8. Suzich JB, Cliffe AR. 2018. Strength in diversity: Understanding the pathways to herpes simplex virus reactivation. Virology 522:81-91.
9. James C, Harfouche M, Welton NJ, Turner KM, Abu-Raddad LJ, Gottlieb SL, Looker KJ. 2020. Herpes simplex virus: global infection prevalence and incidence estimates, 2016. Bull World Health Organ 98:315-329.
10. Proenca JT, Nelson D, Nicoll MP, Connor V, Efstathiou S. 2016. Analyses of herpes simplex virus type 1 latency and reactivation at the single cell level using fluorescent reporter mice. J Gen Virol 97:767-777.
11. Spear PG, Longnecker R. 2003. Herpesvirus entry: an update. J Virol 77:10179-85.
12. Karasneh GA, Shukla D. 2011. Herpes simplex virus infects most cell types in vitro: clues to its success. Virol J 8:481.
13. Thompson RL, Sawtell NM. 2001. Herpes simplex virus type 1 latency-associated transcript gene promotes neuronal survival. J Virol 75:6660-75.
14. Baringer JR, Swoveland P. 1973. Recovery of herpes-simplex virus from human trigeminal ganglions. N Engl J Med 288:648-50.
15. Baringer JR, Pisani P. 1994. Herpes simplex virus genomes in human nervous system tissue analyzed by polymerase chain reaction. Ann Neurol 36:823-9.
16. Richter ER, Dias JK, Gilbert JE, 2nd, Atherton SS. 2009. Distribution of herpes simplex virus type 1 and varicella zoster virus in ganglia of the human head and neck. J Infect Dis 200:1901-6.
17. Warren KG, Brown SM, Wroblewska Z, Gilden D, Koprowski H, Subak-Sharpe J. 1978. Isolation of latent herpes simplex virus from the superior cervical and vagus ganglions of human beings. N Engl J Med 298:1068-9.

18. James SH, Sheffield JS, Kimberlin DW. 2014. Mother-to-Child Transmission of Herpes Simplex Virus. J Pediatric Infect Dis Soc 3 Suppl 1:S19-23.
19. Looker KJ, Magaret AS, May MT, Turner KM, Vickerman P, Gottlieb SL, Newman LM. 2015. Global and Regional Estimates of Prevalent and Incident Herpes Simplex Virus Type 1 Infections in 2012. PLoS One 10:e0140765.
20. Ramchandani M, Kong M, Tronstein E, Selke S, Mikhaylova A, Magaret A, Huang ML, Johnston C, Corey L, Wald A. 2016. Herpes Simplex Virus Type 1 Shedding in Tears and Nasal and Oral Mucosa of Healthy Adults. Sex Transm Dis 43:756-760.
21. Miller CS, Danaher RJ. 2008. Asymptomatic shedding of herpes simplex virus (HSV) in the oral cavity. Oral Surg Oral Med Oral Pathol Oral Radiol Endod 105:43-50.
22. Johnston C, Magaret A, Son H, Stern M, Rathbun M, Renner D, Szpara M, Gunby S, Ott M, Jing L, Campbell VL, Huang ML, Selke S, Jerome KR, Koelle DM, Wald A. 2022. Viral Shedding 1 Year Following First-Episode Genital HSV-1 Infection. JAMA 328:1730-1739.
23. Whitley RJ, Roizman B. 2001. Herpes simplex virus infections. Lancet 357:1513-8.
24. Lairson DR, Begley CE, Reynolds TF, Wilhelmus KR. 2003. Prevention of herpes simplex virus eye disease: a cost-effectiveness analysis. Arch Ophthalmol 121:108-12.
25. McCormick I, James C, Welton NJ, Mayaud P, Turner KME, Gottlieb SL, Foster A, Looker KJ. 2022. Incidence of Herpes Simplex Virus Keratitis and Other Ocular Disease: Global Review and Estimates. Ophthalmic Epidemiol 29:353-362.
26. Nagel MA, Choe A, Traktinskiy I, Gilden D. 2015. Burning mouth syndrome due to herpes simplex virus type 1. BMJ Case Rep 2015.
27. Gonzales GR. 1992. Postherpes simplex type 1 neuralgia simulating postherpetic neuralgia. J Pain Symptom Manage 7:320-3.
28. Valyi-Nagy T, Rathore JS, Rakic AM, Rathore RS, Jain P, Slavin KV. 2017. Herpes Simplex Virus Type 1 Human Cervical Dorsal Root Ganglionitis. Case Rep Neurol 9:188-194.
29. Sasaki A, Takasaki I, Andoh T, Shiraki K, Takeshima H, Takahata H, Kuraishi Y. 2008. Nociceptin-receptor deficiency prevents postherpetic pain without effects on acute herpetic pain in mice. Neuroreport 19:83-6.
30. Takasaki I, Sasaki A, Andoh T, Nojima H, Shiraki K, Kuraishi Y. 2002. Effects of analgesics on delayed postherpetic pain in mice. Anesthesiology 96:1168-74.
31. Takasaki I, Nojima H, Shiraki K, Sugimoto Y, Ichikawa A, Ushikubi F, Narumiya S, Kuraishi Y. 2005. Involvement of cyclooxygenase-2 and EP3 prostaglandin receptor in acute herpetic but not postherpetic pain in mice. Neuropharmacology 49:283-92.
32. Takasaki I, Andoh T, Nitta M, Takahata H, Nemoto H, Shiraki K, Nojima H, Kuraishi Y. 2000. Pharmacological and immunohistochemical characterization of a mouse model of acute herpetic pain. Jpn J Pharmacol 83:319-26.
33. Andoh T, Shiraki K, Kurokawa M, Kuraishi Y. 1995. Paresthesia induced by cutaneous infection with herpes simplex virus in rats. Neurosci Lett 190:101-4.
34. Theil D, Derfuss T, Paripovic I, Herberger S, Meinl E, Schueler O, Strupp M, Arbusow V, Brandt T. 2003. Latent herpesvirus infection in human trigeminal ganglia causes chronic immune response. Am J Pathol 163:2179-84.
35. Srinivasan R, Fink DJ, Glorioso JC. 2008. HSV vectors for gene therapy of chronic pain. Curr Opin Mol Ther 10:449-55.

36. Steiner I, Benninger F. 2013. Update on herpes virus infections of the nervous system. Curr Neurol Neurosci Rep 13:414.
37. Duarte LF, Farias MA, Alvarez DM, Bueno SM, Riedel CA, Gonzalez PA. 2019. Herpes Simplex Virus Type 1 Infection of the Central Nervous System: Insights Into Proposed Interrelationships With Neurodegenerative Disorders. Front Cell Neurosci 13:46.
38. Bradshaw MJ, Venkatesan A. 2016. Herpes Simplex Virus-1 Encephalitis in Adults: Pathophysiology, Diagnosis, and Management. Neurotherapeutics 13:493-508.
39. Armien AG, Hu S, Little MR, Robinson N, Lokensgard JR, Low WC, Cheeran MC. 2010. Chronic cortical and subcortical pathology with associated neurological deficits ensuing experimental herpes encephalitis. Brain Pathol 20:738-50.
40. Riancho J, Delgado-Alvarado M, Sedano MJ, Polo JM, Berciano J. 2013. Herpes simplex encephalitis: clinical presentation, neurological sequelae and new prognostic factors. Ten years of experience. Neurol Sci 34:1879-81.
41. Misra UK, Tan CT, Kalita J. 2008. Viral encephalitis and epilepsy. Epilepsia 49 Suppl 6:13-8.
42. Protto V, Marcocci ME, Miteva MT, Piacentini R, Li Puma DD, Grassi C, Palamara AT, De Chiara G. 2022. Role of HSV-1 in Alzheimer's disease pathogenesis: A challenge for novel preventive/therapeutic strategies. Curr Opin Pharmacol 63:102200.
43. Piacentini R, De Chiara G, Li Puma DD, Ripoli C, Marcocci ME, Garaci E, Palamara AT, Grassi C. 2014. HSV-1 and Alzheimer's disease: more than a hypothesis. Front Pharmacol 5:97.
44. Mielcarska MB, Skowronska K, Wyzewski Z, Toka FN. 2021. Disrupting Neurons and Glial Cells Oneness in the Brain-The Possible Causal Role of Herpes Simplex Virus Type 1 (HSV-1) in Alzheimer's Disease. Int J Mol Sci 23.
45. Marcocci ME, Napoletani G, Protto V, Kolesova O, Piacentini R, Li Puma DD, Lomonte P, Grassi C, Palamara AT, De Chiara G. 2020. Herpes Simplex Virus-1 in the Brain: The Dark Side of a Sneaky Infection. Trends Microbiol 28:808-820.
46. Mancuso R, Sicurella M, Agostini S, Marconi P, Clerici M. 2019. Herpes simplex virus type 1 and Alzheimer's disease: link and potential impact on treatment. Expert Rev Anti Infect Ther 17:715-731.
47. Cairns DM, Itzhaki RF, Kaplan DL. 2022. Potential Involvement of Varicella Zoster Virus in Alzheimer's Disease via Reactivation of Quiescent Herpes Simplex Virus Type 1. J Alzheimers Dis 88:1189-1200.
48. Itzhaki RF, Lin WR, Shang D, Wilcock GK, Faragher B, Jamieson GA. 1997. Herpes simplex virus type 1 in brain and risk of Alzheimer's disease. Lancet 349:241-4.
49. Linard M, Letenneur L, Garrigue I, Doize A, Dartigues JF, Helmer C. 2020. Interaction between APOE4 and herpes simplex virus type 1 in Alzheimer's disease. Alzheimers Dement 16:200-208.
50. Albaret MA, Textoris J, Dalzon B, Lambert J, Linard M, Helmer C, Hacot S, Ghayad SE, Ferreol M, Mertani HC, Diaz JJ. 2023. HSV-1 cellular model reveals links between aggresome formation and early step of Alzheimer's disease. Transl Psychiatry 13:86.
51. Napoletani G, Protto V, Marcocci ME, Nencioni L, Palamara AT, De Chiara G. 2021. Recurrent Herpes Simplex Virus Type 1 (HSV-1) Infection Modulates Neuronal Aging Marks in In Vitro and In Vivo Models. Int J Mol Sci 22.

52. Piacentini R, Civitelli L, Ripoli C, Marcocci ME, De Chiara G, Garaci E, Azzena GB, Palamara AT, Grassi C. 2011. HSV-1 promotes Ca2+ -mediated APP phosphorylation and Abeta accumulation in rat cortical neurons. Neurobiol Aging 32:2323 e13-26.
53. Civitelli L, Marcocci ME, Celestino I, Piacentini R, Garaci E, Grassi C, De Chiara G, Palamara AT. 2015. Herpes simplex virus type 1 infection in neurons leads to production and nuclear localization of APP intracellular domain (AICD): implications for Alzheimer's disease pathogenesis. J Neurovirol 21:480-90.
54. Savitz J, Yolken RH. 2023. Therapeutic Implications of the Microbial Hypothesis of Mental Illness. Curr Top Behav Neurosci 61:315-351.
55. Prasad KM, Eack SM, Keshavan MS, Yolken RH, Iyengar S, Nimgaonkar VL. 2013. Antiherpes virus-specific treatment and cognition in schizophrenia: a test-of-concept randomized double-blind placebo-controlled trial. Schizophr Bull 39:857-66.
56. Sadowski LA, Upadhyay R, Greeley ZW, Margulies BJ. 2021. Current Drugs to Treat Infections with Herpes Simplex Viruses-1 and -2. Viruses 13.
57. de Miranda P, Whitley RJ, Blum MR, Keeney RE, Barton N, Cocchetto DM, Good S, Hemstreet GP, 3rd, Kirk LE, Page DA, Elion GB. 1979. Acyclovir kinetics after intravenous infusion. Clin Pharmacol Ther 26:718-28.
58. Barber KE, Wagner JL, Stover KR. 2019. Impact of Obesity on Acyclovir-Induced Nephrotoxicity. Open Forum Infect Dis 6:ofz121.
59. Yalcinkaya R, Oz FN, Kaman A, Aydin Teke T, Yasar Durmus S, Celikkaya E, Tanir G. 2021. Factors associated with acyclovir nephrotoxicity in children: data from 472 pediatric patients from the last 10 years. Eur J Pediatr 180:2521-2527.
60. Powell-Doherty RD, Abbott ARN, Nelson LA, Bertke AS. 2020. Amyloid-beta and p-Tau Anti-Threat Response to Herpes Simplex Virus 1 Infection in Primary Adult Murine Hippocampal Neurons. J Virol 94.
61. Anton-Vazquez V, Mehra V, Mbisa JL, Bradshaw D, Basu TN, Daly ML, Mufti GJ, Pagliuca A, Potter V, Zuckerman M. 2020. Challenges of aciclovir-resistant HSV infection in allogeneic bone marrow transplant recipients. J Clin Virol 128:104421.
62. Morfin F, Thouvenot D. 2003. Herpes simplex virus resistance to antiviral drugs. J Clin Virol 26:29-37.
63. Roizman B, Whitley RJ, Lopez C. 1993. The Human herpesviruses. Raven Press, New York.
64. Madavaraju K, Koganti R, Volety I, Yadavalli T, Shukla D. 2020. Herpes Simplex Virus Cell Entry Mechanisms: An Update. Front Cell Infect Microbiol 10:617578.
65. Reske A, Pollara G, Krummenacher C, Chain BM, Katz DR. 2007. Understanding HSV-1 entry glycoproteins. Rev Med Virol 17:205-15.
66. Arii J, Kawaguchi Y. 2018. The Role of HSV Glycoproteins in Mediating Cell Entry. Adv Exp Med Biol 1045:3-21.
67. Musarrat F, Chouljenko V, Kousoulas KG. 2021. Cellular and Viral Determinants of HSV-1 Entry and Intracellular Transport towards Nucleus of Infected Cells. J Virol 95.
68. Richards AL, Sollars PJ, Pitts JD, Stults AM, Heldwein EE, Pickard GE, Smith GA. 2017. The pUL37 tegument protein guides alpha-herpesvirus retrograde axonal transport to promote neuroinvasion. PLoS Pathog 13:e1006741.

69. Villanueva-Valencia JR, Tsimtsirakis E, Evilevitch A. 2021. Role of HSV-1 Capsid Vertex-Specific Component (CVSC) and Viral Terminal DNA in Capsid Docking at the Nuclear Pore. Viruses 13.
70. Liu YT, Jih J, Dai X, Bi GQ, Zhou ZH. 2019. Cryo-EM structures of herpes simplex virus type 1 portal vertex and packaged genome. Nature 570:257-261.
71. McElwee M, Vijayakrishnan S, Rixon F, Bhella D. 2018. Structure of the herpes simplex virus portal-vertex. PLoS Biol 16:e2006191.
72. Sekine E, Schmidt N, Gaboriau D, O'Hare P. 2017. Spatiotemporal dynamics of HSV genome nuclear entry and compaction state transitions using bioorthogonal chemistry and super-resolution microscopy. PLoS Pathog 13:e1006721.
73. Copeland AM, Newcomb WW, Brown JC. 2009. Herpes simplex virus replication: roles of viral proteins and nucleoporins in capsid-nucleus attachment. J Virol 83:1660-8.
74. Pasdeloup D, Blondel D, Isidro AL, Rixon FJ. 2009. Herpesvirus capsid association with the nuclear pore complex and viral DNA release involve the nucleoporin CAN/Nup214 and the capsid protein pUL25. J Virol 83:6610-23.
75. Lentine AF, Bachenheimer SL. 1990. Intracellular organization of herpes simplex virus type 1 DNA assayed by staphylococcal nuclease sensitivity. Virus Res 16:275-92.
76. Pignatti PF, Cassai E. 1980. Analysis of herpes simplex virus nucleoprotein complexes extracted from infected cells. J Virol 36:816-28.
77. Leinbach SS, Summers WC. 1980. The structure of herpes simplex virus type 1 DNA as probed by micrococcal nuclease digestion. J Gen Virol 51:45-59.
78. Varnum SM, Streblow DN, Monroe ME, Smith P, Auberry KJ, Pasa-Tolic L, Wang D, Camp DG, 2nd, Rodland K, Wiley S, Britt W, Shenk T, Smith RD, Nelson JA. 2004. Identification of proteins in human cytomegalovirus (HCMV) particles: the HCMV proteome. J Virol 78:10960-6.
79. Johannsen E, Luftig M, Chase MR, Weicksel S, Cahir-McFarland E, Illanes D, Sarracino D, Kieff E. 2004. Proteins of purified Epstein-Barr virus. Proc Natl Acad Sci U S A 101:16286-91.
80. Bechtel JT, Winant RC, Ganem D. 2005. Host and viral proteins in the virion of Kaposi's sarcoma-associated herpesvirus. J Virol 79:4952-64.
81. Kent JR, Zeng PY, Atanasiu D, Gardner J, Fraser NW, Berger SL. 2004. During lytic infection herpes simplex virus type 1 is associated with histones bearing modifications that correlate with active transcription. J Virol 78:10178-86.
82. Conn KL, Hendzel MJ, Schang LM. 2008. Linker histones are mobilized during infection with herpes simplex virus type 1. J Virol 82:8629-46.
83. Conn KL, Hendzel MJ, Schang LM. 2011. Core histones H2B and H4 are mobilized during infection with herpes simplex virus 1. J Virol 85:13234-52.
84. Herrera FJ, Triezenberg SJ. 2004. VP16-dependent association of chromatin-modifying coactivators and underrepresentation of histones at immediate-early gene promoters during herpes simplex virus infection. J Virol 78:9689-96.
85. Lacasse JJ, Schang LM. 2010. During lytic infections, herpes simplex virus type 1 DNA is in complexes with the properties of unstable nucleosomes. J Virol 84:1920-33.
86. Osterrieder N, Wallaschek N, Kaufer BB. 2014. Herpesvirus Genome Integration into Telomeric Repeats of Host Cell Chromosomes. Annu Rev Virol 1:215-35.

87. Fan D, Wang M, Cheng A, Jia R, Yang Q, Wu Y, Zhu D, Zhao X, Chen S, Liu M, Zhang S, Ou X, Mao S, Gao Q, Sun D, Wen X, Liu Y, Yu Y, Zhang L, Tian B, Pan L, Chen X. 2020. The Role of VP16 in the Life Cycle of Alphaherpesviruses. Front Microbiol 11:1910.
88. Dembowski JA, Dremel SE, DeLuca NA. 2017. Replication-Coupled Recruitment of Viral and Cellular Factors to Herpes Simplex Virus Type 1 Replication Forks for the Maintenance and Expression of Viral Genomes. PLoS Pathog 13:e1006166.
89. Ahmad I, Wilson DW. 2020. HSV-1 Cytoplasmic Envelopment and Egress. Int J Mol Sci 21.
90. Remillard-Labrosse G, Lippe R. 2011. In vitro nuclear egress of herpes simplex virus type 1 capsids. Methods 55:153-9.
91. Bigalke JM, Heldwein EE. 2016. Nuclear Exodus: Herpesviruses Lead the Way. Annu Rev Virol 3:387-409.
92. Owen DJ, Crump CM, Graham SC. 2015. Tegument Assembly and Secondary Envelopment of Alphaherpesviruses. Viruses 7:5084-114.
93. Suzich JB, Cuddy SR, Baidas H, Dochnal S, Ke E, Schinlever AR, Babnis A, Boutell C, Cliffe AR. 2021. PML-NB-dependent type I interferon memory results in a restricted form of HSV latency. EMBO Rep 22:e52547.
94. Cook SD, Paveloff MJ, Doucet JJ, Cottingham AJ, Sedarati F, Hill JM. 1991. Ocular herpes simplex virus reactivation in mice latently infected with latency-associated transcript mutants. Invest Ophthalmol Vis Sci 32:1558-61.
95. Vicetti Miguel RD, Sheridan BS, Harvey SA, Schreiner RS, Hendricks RL, Cherpes TL. 2010. 17-beta estradiol promotion of herpes simplex virus type 1 reactivation is estrogen receptor dependent. J Virol 84:565-72.
96. Sawtell NM, Thompson RL. 1992. Rapid in vivo reactivation of herpes simplex virus in latently infected murine ganglionic neurons after transient hyperthermia. J Virol 66:2150-6.
97. Shimeld C, Whiteland JL, Nicholls SM, Easty DL, Hill TJ. 1996. Immune cell infiltration in corneas of mice with recurrent herpes simplex virus disease. J Gen Virol 77 (Pt 5):977-85.
98. Whitford AL, Clinton CA, Lane Kennedy EB, Dochnal SA, Suzich JB, Cliffe AR. 2022. Herpes Simplex Virus Reactivation Induced Ex Vivo Involves a DLK-Dependent but Histone Demethylase-Independent Wave of Lytic Gene Expression. bioRxiv doi:10.1101/2022.02.25.481951:2022.02.25.481951.
99. Cliffe AR, Arbuckle JH, Vogel JL, Geden MJ, Rothbart SB, Cusack CL, Strahl BD, Kristie TM, Deshmukh M. 2015. Neuronal Stress Pathway Mediating a Histone Methyl/Phospho Switch Is Required for Herpes Simplex Virus Reactivation. Cell Host Microbe 18:649-58.
100. Messer HG, Jacobs D, Dhummakupt A, Bloom DC. 2015. Inhibition of H3K27me3-specific histone demethylases JMJD3 and UTX blocks reactivation of herpes simplex virus 1 in trigeminal ganglion neurons. J Virol 89:3417-20.
101. Du T, Zhou G, Roizman B. 2011. HSV-1 gene expression from reactivated ganglia is disordered and concurrent with suppression of latency-associated transcript and miRNAs. Proc Natl Acad Sci U S A 108:18820-4.
102. Valtcheva MV, Copits BA, Davidson S, Sheahan TD, Pullen MY, McCall JG, Dikranian K, Gereau RWt. 2016. Surgical extraction of human dorsal root ganglia from organ donors and preparation of primary sensory neuron cultures. Nat Protoc 11:1877-88.

103. Camarena V, Kobayashi M, Kim JY, Roehm P, Perez R, Gardner J, Wilson AC, Mohr I, Chao MV. 2010. Nature and duration of growth factor signaling through receptor tyrosine kinases regulates HSV-1 latency in neurons. Cell Host Microbe 8:320-30.
104. Ives AM, Bertke AS. 2017. Stress Hormones Epinephrine and Corticosterone Selectively Modulate Herpes Simplex Virus 1 (HSV-1) and HSV-2 Productive Infections in Adult Sympathetic, but Not Sensory, Neurons. J Virol 91.
105. Wilcox CL, Smith RL, Freed CR, Johnson EM, Jr. 1990. Nerve growth factor-dependence of herpes simplex virus latency in peripheral sympathetic and sensory neurons in vitro. J Neurosci 10:1268-75.
106. Wilcox CL, Johnson EM, Jr. 1988. Characterization of nerve growth factor-dependent herpes simplex virus latency in neurons in vitro. J Virol 62:393-9.
107. Kobayashi M, Kim JY, Camarena V, Roehm PC, Chao MV, Wilson AC, Mohr I. 2012. A primary neuron culture system for the study of herpes simplex virus latency and reactivation. J Vis Exp doi:10.3791/3823.
108. Linderman JA, Kobayashi M, Rayannavar V, Fak JJ, Darnell RB, Chao MV, Wilson AC, Mohr I. 2017. Immune Escape via a Transient Gene Expression Program Enables Productive Replication of a Latent Pathogen. Cell Rep 18:1312-1323.
109. Cuddy SR, Schinlever AR, Dochnal S, Seegren PV, Suzich J, Kundu P, Downs TK, Farah M, Desai BN, Boutell C, Cliffe AR. 2020. Neuronal hyperexcitability is a DLK-dependent trigger of herpes simplex virus reactivation that can be induced by IL-1. Elife 9.
110. Colgin MA, Smith RL, Wilcox CL. 2001. Inducible cyclic AMP early repressor produces reactivation of latent herpes simplex virus type 1 in neurons in vitro. J Virol 75:2912-20.
111. De Regge N, Van Opdenbosch N, Nauwynck HJ, Efstathiou S, Favoreel HW. 2010. Interferon alpha induces establishment of alphaherpesvirus latency in sensory neurons in vitro. PLoS One 5.
112. Hu HL, Shiflett LA, Kobayashi M, Chao MV, Wilson AC, Mohr I, Huang TT. 2019. TOP2beta-Dependent Nuclear DNA Damage Shapes Extracellular Growth Factor Responses via Dynamic AKT Phosphorylation to Control Virus Latency. Mol Cell 74:466-480 e4.
113. Halford WP, Schaffer PA. 2001. ICP0 is required for efficient reactivation of herpes simplex virus type 1 from neuronal latency. J Virol 75:3240-9.
114. Pourchet A, Modrek AS, Placantonakis DG, Mohr I, Wilson AC. 2017. Modeling HSV-1 Latency in Human Embryonic Stem Cell-Derived Neurons. Pathogens 6.
115. Thellman NM, Botting C, Madaj Z, Triezenberg SJ. 2017. An Immortalized Human Dorsal Root Ganglion Cell Line Provides a Novel Context To Study Herpes Simplex Virus 1 Latency and Reactivation. J Virol 91.
116. Edwards TG, Bloom DC. 2019. Lund Human Mesencephalic (LUHMES) Neuronal Cell Line Supports Herpes Simplex Virus 1 Latency In Vitro. J Virol 93.
117. Dochnal S, Merchant HY, Schinlever AR, Babnis A, Depledge DP, Wilson AC, Cliffe AR. 2022. DLK-Dependent Biphasic Reactivation of Herpes Simplex Virus Latency Established in the Absence of Antivirals. J Virol 96:e0050822.
118. Bertke AS, Swanson SM, Chen J, Imai Y, Kinchington PR, Margolis TP. 2011. A5-positive primary sensory neurons are nonpermissive for productive infection with herpes simplex virus 1 in vitro. J Virol 85:6669-77.

119. Dochnal SA, Francois AK, Cliffe AR. 2021. De Novo Polycomb Recruitment: Lessons from Latent Herpesviruses. Viruses 13.
120. Wang QY, Zhou C, Johnson KE, Colgrove RC, Coen DM, Knipe DM. 2005. Herpesviral latency-associated transcript gene promotes assembly of heterochromatin on viral lytic-gene promoters in latent infection. Proc Natl Acad Sci U S A 102:16055-9.
121. Cliffe AR, Garber DA, Knipe DM. 2009. Transcription of the herpes simplex virus latency-associated transcript promotes the formation of facultative heterochromatin on lytic promoters. J Virol 83:8182-90.
122. Cliffe AR, Coen DM, Knipe DM. 2013. Kinetics of facultative heterochromatin and polycomb group protein association with the herpes simplex viral genome during establishment of latent infection. mBio 4.
123. Kwiatkowski DL, Thompson HW, Bloom DC. 2009. The polycomb group protein Bmi1 binds to the herpes simplex virus 1 latent genome and maintains repressive histone marks during latency. J Virol 83:8173-81.
124. Nicoll MP, Hann W, Shivkumar M, Harman LE, Connor V, Coleman HM, Proenca JT, Efstathiou S. 2016. The HSV-1 Latency-Associated Transcript Functions to Repress Latent Phase Lytic Gene Expression and Suppress Virus Reactivation from Latently Infected Neurons. PLoS Pathog 12:e1005539.
125. Loubiere V, Martinez AM, Cavalli G. 2019. Cell Fate and Developmental Regulation Dynamics by Polycomb Proteins and 3D Genome Architecture. Bioessays 41:e1800222.
126. Petracovici A, Bonasio R. 2021. Distinct PRC2 subunits regulate maintenance and establishment of Polycomb repression during differentiation. Mol Cell doi:10.1016/j.molcel.2021.03.038.
127. Kang SJ, Chun T. 2020. Structural heterogeneity of the mammalian polycomb repressor complex in immune regulation. Exp Mol Med 52:1004-1015.
128. Blackledge NP, Farcas AM, Kondo T, King HW, McGouran JF, Hanssen LLP, Ito S, Cooper S, Kondo K, Koseki Y, Ishikura T, Long HK, Sheahan TW, Brockdorff N, Kessler BM, Koseki H, Klose RJ. 2014. Variant PRC1 complex-dependent H2A ubiquitylation drives PRC2 recruitment and polycomb domain formation. Cell 157:1445-1459.
129. Piunti A, Shilatifard A. 2021. The roles of Polycomb repressive complexes in mammalian development and cancer. Nat Rev Mol Cell Biol 22:326-345.
130. Connelly KE, Dykhuizen EC. 2017. Compositional and functional diversity of canonical PRC1 complexes in mammals. Biochim Biophys Acta Gene Regul Mech 1860:233-245.
131. Laugesen A, Hojfeldt JW, Helin K. 2019. Molecular Mechanisms Directing PRC2 Recruitment and H3K27 Methylation. Mol Cell 74:8-18.
132. Yu JR, Lee CH, Oksuz O, Stafford JM, Reinberg D. 2019. PRC2 is high maintenance. Genes Dev 33:903-935.
133. Cao R, Wang L, Wang H, Xia L, Erdjument-Bromage H, Tempst P, Jones RS, Zhang Y. 2002. Role of histone H3 lysine 27 methylation in Polycomb-group silencing. Science 298:1039-43.
134. Cao R, Zhang Y. 2004. SUZ12 is required for both the histone methyltransferase activity and the silencing function of the EED-EZH2 complex. Mol Cell 15:57-67.
135. Chammas P, Mocavini I, Di Croce L. 2020. Engaging chromatin: PRC2 structure meets function. Br J Cancer 122:315-328.

136. Oksuz O, Narendra V, Lee CH, Descostes N, LeRoy G, Raviram R, Blumenberg L, Karch K, Rocha PP, Garcia BA, Skok JA, Reinberg D. 2018. Capturing the Onset of PRC2-Mediated Repressive Domain Formation. Mol Cell 70:1149-1162 e5.
137. Ferrari KJ, Scelfo A, Jammula S, Cuomo A, Barozzi I, Stutzer A, Fischle W, Bonaldi T, Pasini D. 2014. Polycomb-dependent H3K27me1 and H3K27me2 regulate active transcription and enhancer fidelity. Mol Cell 53:49-62.
138. Hojfeldt JW, Laugesen A, Willumsen BM, Damhofer H, Hedehus L, Tvardovskiy A, Mohammad F, Jensen ON, Helin K. 2018. Accurate H3K27 methylation can be established de novo by SUZ12-directed PRC2. Nat Struct Mol Biol 25:225-232.
139. van Mierlo G, Veenstra GJC, Vermeulen M, Marks H. 2019. The Complexity of PRC2 Subcomplexes. Trends Cell Biol 29:660-671.
140. Kloet SL, Makowski MM, Baymaz HI, van Voorthuijsen L, Karemaker ID, Santanach A, Jansen P, Di Croce L, Vermeulen M. 2016. The dynamic interactome and genomic targets of Polycomb complexes during stem-cell differentiation. Nat Struct Mol Biol 23:682-690.
141. Beringer M, Pisano P, Di Carlo V, Blanco E, Chammas P, Vizan P, Gutierrez A, Aranda S, Payer B, Wierer M, Di Croce L. 2016. EPOP Functionally Links Elongin and Polycomb in Pluripotent Stem Cells. Mol Cell 64:645-658.
142. Liefke R, Karwacki-Neisius V, Shi Y. 2016. EPOP Interacts with Elongin BC and USP7 to Modulate the Chromatin Landscape. Mol Cell 64:659-672.
143. Conway E, Jerman E, Healy E, Ito S, Holoch D, Oliviero G, Deevy O, Glancy E, Fitzpatrick DJ, Mucha M, Watson A, Rice AM, Chammas P, Huang C, Pratt-Kelly I, Koseki Y, Nakayama M, Ishikura T, Streubel G, Wynne K, Hokamp K, McLysaght A, Ciferri C, Di Croce L, Cagney G, Margueron R, Koseki H, Bracken AP. 2018. A Family of Vertebrate-Specific Polycombs Encoded by the LCOR/LCORL Genes Balance PRC2 Subtype Activities. Mol Cell 70:408-421 e8.
144. Cooper S, Grijzenhout A, Underwood E, Ancelin K, Zhang T, Nesterova TB, Anil-Kirmizitas B, Bassett A, Kooistra SM, Agger K, Helin K, Heard E, Brockdorff N. 2016. Jarid2 binds mono-ubiquitylated H2A lysine 119 to mediate crosstalk between Polycomb complexes PRC1 and PRC2. Nat Commun 7:13661.
145. Sanulli S, Justin N, Teissandier A, Ancelin K, Portoso M, Caron M, Michaud A, Lombard B, da Rocha ST, Offer J, Loew D, Servant N, Wassef M, Burlina F, Gamblin SJ, Heard E, Margueron R. 2015. Jarid2 Methylation via the PRC2 Complex Regulates H3K27me3 Deposition during Cell Differentiation. Mol Cell 57:769-783.
146. Son J, Shen SS, Margueron R, Reinberg D. 2013. Nucleosome-binding activities within JARID2 and EZH1 regulate the function of PRC2 on chromatin. Genes Dev 27:2663-77.
147. Kasinath V, Beck C, Sauer P, Poepsel S, Kosmatka J, Faini M, Toso D, Aebersold R, Nogales E. 2021. JARID2 and AEBP2 regulate PRC2 in the presence of H2AK119ub1 and other histone modifications. Science 371.
148. Youmans DT, Gooding AR, Dowell RD, Cech TR. 2021. Competition between PRC2.1 and 2.2 subcomplexes regulates PRC2 chromatin occupancy in human stem cells. Mol Cell 81:488-501 e9.
149. Fursova NA, Blackledge NP, Nakayama M, Ito S, Koseki Y, Farcas AM, King HW, Koseki H, Klose RJ. 2019. Synergy between Variant PRC1 Complexes Defines Polycomb-Mediated Gene Repression. Mol Cell 74:1020-1036 e8.

150. Margueron R, Li G, Sarma K, Blais A, Zavadil J, Woodcock CL, Dynlacht BD, Reinberg D. 2008. Ezh1 and Ezh2 maintain repressive chromatin through different mechanisms. Mol Cell 32:503-18.
151. Stojic L, Jasencakova Z, Prezioso C, Stutzer A, Bodega B, Pasini D, Klingberg R, Mozzetta C, Margueron R, Puri PL, Schwarzer D, Helin K, Fischle W, Orlando V. 2011. Chromatin regulated interchange between polycomb repressive complex 2 (PRC2)-Ezh2 and PRC2-Ezh1 complexes controls myogenin activation in skeletal muscle cells. Epigenetics Chromatin 4:16.
152. Al-Raawi D, Jones R, Wijesinghe S, Halsall J, Petric M, Roberts S, Hotchin NA, Kanhere A. 2019. A novel form of JARID2 is required for differentiation in lineage-committed cells. EMBO J 38.
153. von Schimmelmann M, Feinberg PA, Sullivan JM, Ku SM, Badimon A, Duff MK, Wang Z, Lachmann A, Dewell S, Ma'ayan A, Han MH, Tarakhovsky A, Schaefer A. 2016. Polycomb repressive complex 2 (PRC2) silences genes responsible for neurodegeneration. Nat Neurosci 19:1321-30.
154. Gao Z, Zhang J, Bonasio R, Strino F, Sawai A, Parisi F, Kluger Y, Reinberg D. 2012. PCGF homologs, CBX proteins, and RYBP define functionally distinct PRC1 family complexes. Mol Cell 45:344-56.
155. Fischle W, Wang Y, Jacobs SA, Kim Y, Allis CD, Khorasanizadeh S. 2003. Molecular basis for the discrimination of repressive methyl-lysine marks in histone H3 by Polycomb and HP1 chromodomains. Genes Dev 17:1870-81.
156. Min J, Zhang Y, Xu RM. 2003. Structural basis for specific binding of Polycomb chromodomain to histone H3 methylated at Lys 27. Genes Dev 17:1823-8.
157. Moussa HF, Bsteh D, Yelagandula R, Pribitzer C, Stecher K, Bartalska K, Michetti L, Wang J, Zepeda-Martinez JA, Elling U, Stuckey JI, James LI, Frye SV, Bell O. 2019. Canonical PRC1 controls sequence-independent propagation of Polycomb-mediated gene silencing. Nat Commun 10:1931.
158. Garcia E, Marcos-Gutierrez C, del Mar Lorente M, Moreno JC, Vidal M. 1999. RYBP, a new repressor protein that interacts with components of the mammalian Polycomb complex, and with the transcription factor YY1. EMBO J 18:3404-18.
159. Tavares L, Dimitrova E, Oxley D, Webster J, Poot R, Demmers J, Bezstarosti K, Taylor S, Ura H, Koide H, Wutz A, Vidal M, Elderkin S, Brockdorff N. 2012. RYBP-PRC1 complexes mediate H2A ubiquitylation at polycomb target sites independently of PRC2 and H3K27me3. Cell 148:664-78.
160. Farcas AM, Blackledge NP, Sudbery I, Long HK, McGouran JF, Rose NR, Lee S, Sims D, Cerase A, Sheahan TW, Koseki H, Brockdorff N, Ponting CP, Kessler BM, Klose RJ. 2012. KDM2B links the Polycomb Repressive Complex 1 (PRC1) to recognition of CpG islands. Elife 1:e00205.
161. Ren X, Kerppola TK. 2011. REST interacts with Cbx proteins and regulates polycomb repressive complex 1 occupancy at RE1 elements. Mol Cell Biol 31:2100-10.
162. Lagarou A, Mohd-Sarip A, Moshkin YM, Chalkley GE, Bezstarosti K, Demmers JA, Verrijzer CP. 2008. dKDM2 couples histone H2A ubiquitylation to histone H3 demethylation during Polycomb group silencing. Genes Dev 22:2799-810.

163. Blackledge NP, Fursova NA, Kelley JR, Huseyin MK, Feldmann A, Klose RJ. 2020. PRC1 Catalytic Activity Is Central to Polycomb System Function. Mol Cell 77:857-874 e9.
164. Tamburri S, Lavarone E, Fernandez-Perez D, Conway E, Zanotti M, Manganaro D, Pasini D. 2020. Histone H2AK119 Mono-Ubiquitination Is Essential for Polycomb-Mediated Transcriptional Repression. Mol Cell 77:840-856 e5.
165. Zhou W, Zhu P, Wang J, Pascual G, Ohgi KA, Lozach J, Glass CK, Rosenfeld MG. 2008. Histone H2A monoubiquitination represses transcription by inhibiting RNA polymerase II transcriptional elongation. Mol Cell 29:69-80.
166. Stock JK, Giadrossi S, Casanova M, Brookes E, Vidal M, Koseki H, Brockdorff N, Fisher AG, Pombo A. 2007. Ring1-mediated ubiquitination of H2A restrains poised RNA polymerase II at bivalent genes in mouse ES cells. Nat Cell Biol 9:1428-35.
167. Di Croce L, Helin K. 2013. Transcriptional regulation by Polycomb group proteins. Nat Struct Mol Biol 20:1147-55.
168. Illingworth RS. 2019. Chromatin folding and nuclear architecture: PRC1 function in 3D. Curr Opin Genet Dev 55:82-90.
169. Morey L, Aloia L, Cozzuto L, Benitah SA, Di Croce L. 2013. RYBP and Cbx7 define specific biological functions of polycomb complexes in mouse embryonic stem cells. Cell Rep 3:60-9.
170. Klauke K, Radulovic V, Broekhuis M, Weersing E, Zwart E, Olthof S, Ritsema M, Bruggeman S, Wu X, Helin K, Bystrykh L, de Haan G. 2013. Polycomb Cbx family members mediate the balance between haematopoietic stem cell self-renewal and differentiation. Nat Cell Biol 15:353-62.
171. Plys AJ, Davis CP, Kim J, Rizki G, Keenen MM, Marr SK, Kingston RE. 2019. Phase separation of Polycomb-repressive complex 1 is governed by a charged disordered region of CBX2. Genes Dev 33:799-813.
172. Tsuboi M, Kishi Y, Yokozeki W, Koseki H, Hirabayashi Y, Gotoh Y. 2018. Ubiquitination-Independent Repression of PRC1 Targets during Neuronal Fate Restriction in the Developing Mouse Neocortex. Dev Cell 47:758-772 e5.
173. Frohlich J, Grundhoff A. 2020. Epigenetic control in Kaposi sarcoma-associated herpesvirus infection and associated disease. Semin Immunopathol 42:143-157.
174. Gunther T, Grundhoff A. 2010. The epigenetic landscape of latent Kaposi sarcoma-associated herpesvirus genomes. PLoS Pathog 6:e1000935.
175. Toth Z, Maglinte DT, Lee SH, Lee HR, Wong LY, Brulois KF, Lee S, Buckley JD, Laird PW, Marquez VE, Jung JU. 2010. Epigenetic analysis of KSHV latent and lytic genomes. PLoS Pathog 6:e1001013.
176. Toth Z, Brulois K, Lee HR, Izumiya Y, Tepper C, Kung HJ, Jung JU. 2013. Biphasic euchromatin-to-heterochromatin transition on the KSHV genome following de novo infection. PLoS Pathog 9:e1003813.
177. Jha HC, Lu J, Verma SC, Banerjee S, Mehta D, Robertson ES. 2014. Kaposi's sarcoma-associated herpesvirus genome programming during the early stages of primary infection of peripheral blood mononuclear cells. mBio 5.
178. Sun R, Tan X, Wang X, Wang X, Yang L, Robertson ES, Lan K. 2017. Epigenetic Landscape of Kaposi's Sarcoma-Associated Herpesvirus Genome in Classic Kaposi's Sarcoma Tissues. PLoS Pathog 13:e1006167.

179. Toth Z, Papp B, Brulois K, Choi YJ, Gao SJ, Jung JU. 2016. LANA-Mediated Recruitment of Host Polycomb Repressive Complexes onto the KSHV Genome during De Novo Infection. PLoS Pathog 12:e1005878.
180. Gunther T, Frohlich J, Herrde C, Ohno S, Burkhardt L, Adler H, Grundhoff A. 2019. A comparative epigenome analysis of gammaherpesviruses suggests cis-acting sequence features as critical mediators of rapid polycomb recruitment. PLoS Pathog 15:e1007838.
181. Hopcraft SE, Pattenden SG, James LI, Frye S, Dittmer DP, Damania B. 2018. Chromatin remodeling controls Kaposi's sarcoma-associated herpesvirus reactivation from latency. PLoS Pathog 14:e1007267.
182. Murata T, Kondo Y, Sugimoto A, Kawashima D, Saito S, Isomura H, Kanda T, Tsurumi T. 2012. Epigenetic histone modification of Epstein-Barr virus BZLF1 promoter during latency and reactivation in Raji cells. J Virol 86:4752-61.
183. Ramasubramanyan S, Osborn K, Flower K, Sinclair AJ. 2012. Dynamic chromatin environment of key lytic cycle regulatory regions of the Epstein-Barr virus genome. J Virol 86:1809-19.
184. Woellmer A, Arteaga-Salas JM, Hammerschmidt W. 2012. BZLF1 governs CpG-methylated chromatin of Epstein-Barr Virus reversing epigenetic repression. PLoS Pathog 8:e1002902.
185. Ichikawa T, Okuno Y, Sato Y, Goshima F, Yoshiyama H, Kanda T, Kimura H, Murata T. 2018. Regulation of Epstein-Barr Virus Life Cycle and Cell Proliferation by Histone H3K27 Methyltransferase EZH2 in Akata Cells. mSphere 3.
186. Imai K, Kamio N, Cueno ME, Saito Y, Inoue H, Saito I, Ochiai K. 2014. Role of the histone H3 lysine 9 methyltransferase Suv39 h1 in maintaining Epsteinn-Barr virus latency in B95-8 cells. FEBS J 281:2148-58.
187. Vargas-Ayala RC, Jay A, Manara F, Maroui MA, Hernandez-Vargas H, Diederichs A, Robitaille A, Sirand C, Ceraolo MG, Romero-Medina MC, Cros MP, Cuenin C, Durand G, Le Calvez-Kelm F, Mundo L, Leoncini L, Manet E, Herceg Z, Gruffat H, Accardi R. 2019. Interplay between the Epigenetic Enzyme Lysine (K)-Specific Demethylase 2B and Epstein-Barr Virus Infection. J Virol 93.
188. Abraham CG, Kulesza CA. 2013. Polycomb repressive complex 2 silences human cytomegalovirus transcription in quiescent infection models. J Virol 87:13193-205.
189. Gan X, Wang H, Yu Y, Yi W, Zhu S, Li E, Liang Y. 2017. Epigenetically repressing human cytomegalovirus lytic infection and reactivation from latency in THP-1 model by targeting H3K9 and H3K27 histone demethylases. PLoS One 12:e0175390.
190. Rossetto CC, Tarrant-Elorza M, Pari GS. 2013. Cis and trans acting factors involved in human cytomegalovirus experimental and natural latent infection of CD14 (+) monocytes and CD34 (+) cells. PLoS Pathog 9:e1003366.
191. Lee SH, Albright ER, Lee JH, Jacobs D, Kalejta RF. 2015. Cellular defense against latent colonization foiled by human cytomegalovirus UL138 protein. Sci Adv 1:e1501164.
192. Cliffe AR, Coen DM, Knipe DM. 2013. Kinetics of facultative heterochromatin and polycomb group protein association with the herpes simplex viral genome during establishment of latent infection. mBio 4:e00590-12-e00590-12.
193. Knipe DM, Cliffe A. 2008. Chromatin control of herpes simplex virus lytic and latent infection. Nat Rev Microbiol 6:211-21.

194. Proenca JT, Coleman HM, Connor V, Winton DJ, Efstathiou S. 2008. A historical analysis of herpes simplex virus promoter activation in vivo reveals distinct populations of latently infected neurones. J Gen Virol 89:2965-2974.
195. Sawtell NM. 1997. Comprehensive quantification of herpes simplex virus latency at the single-cell level. J Virol 71:5423-31.
196. Slobedman B, Efstathiou S, Simmons A. 1994. Quantitative analysis of herpes simplex virus DNA and transcriptional activity in ganglia of mice latently infected with wild-type and thymidine kinase-deficient viral strains. J Gen Virol 75 (Pt 9):2469-74.
197. Javier RT, Stevens JG, Dissette VB, Wagner EK. 1988. A herpes simplex virus transcript abundant in latently infected neurons is dispensable for establishment of the latent state. Virology 166:254-7.
198. Steiner I, Spivack JG, Lirette RP, Brown SM, MacLean AR, Subak-Sharpe JH, Fraser NW. 1989. Herpes simplex virus type 1 latency-associated transcripts are evidently not essential for latent infection. EMBO J 8:505-11.
199. Stevens JG, Wagner EK, Devi-Rao GB, Cook ML, Feldman LT. 1987. RNA complementary to a herpesvirus alpha gene mRNA is prominent in latently infected neurons. Science 235:1056-9.
200. Umbach JL, Kramer MF, Jurak I, Karnowski HW, Coen DM, Cullen BR. 2008. MicroRNAs expressed by herpes simplex virus 1 during latent infection regulate viral mRNAs. Nature 454:780-3.
201. Bloom DC, Giordani NV, Kwiatkowski DL. 2010. Epigenetic regulation of latent HSV-1 gene expression. Biochim Biophys Acta 1799:246-56.
202. Amelio AL, McAnany PK, Bloom DC. 2006. A chromatin insulator-like element in the herpes simplex virus type 1 latency-associated transcript region binds CCCTC-binding factor and displays enhancer-blocking and silencing activities. J Virol 80:2358-68.
203. Chen Q, Lin L, Smith S, Huang J, Berger SL, Zhou J. 2007. CTCF-dependent chromatin boundary element between the latency-associated transcript and ICP0 promoters in the herpes simplex virus type 1 genome. J Virol 81:5192-201.
204. Kubat NJ, Amelio AL, Giordani NV, Bloom DC. 2004. The herpes simplex virus type 1 latency-associated transcript (LAT) enhancer/rcr is hyperacetylated during latency independently of LAT transcription. J Virol 78:12508-18.
205. Kubat NJ, Tran RK, McAnany P, Bloom DC. 2004. Specific histone tail modification and not DNA methylation is a determinant of herpes simplex virus type 1 latent gene expression. J Virol 78:1139-49.
206. Bloom DC. 2004. HSV LAT and neuronal survival. Int Rev Immunol 23:187-98.
207. Shen W, Sa e Silva M, Jaber T, Vitvitskaia O, Li S, Henderson G, Jones C. 2009. Two small RNAs encoded within the first 1.5 kilobases of the herpes simplex virus type 1 latency-associated transcript can inhibit productive infection and cooperate to inhibit apoptosis. J Virol 83:9131-9.
208. Chen SH, Kramer MF, Schaffer PA, Coen DM. 1997. A viral function represses accumulation of transcripts from productive-cycle genes in mouse ganglia latently infected with herpes simplex virus. J Virol 71:5878-84.

209. Garber DA, Schaffer PA, Knipe DM. 1997. A LAT-associated function reduces productive-cycle gene expression during acute infection of murine sensory neurons with herpes simplex virus type 1. J Virol 71:5885-93.
210. Perng GC, Jones C, Ciacci-Zanella J, Stone M, Henderson G, Yukht A, Slanina SM, Hofman FM, Ghiasi H, Nesburn AB, Wechsler SL. 2000. Virus-induced neuronal apoptosis blocked by the herpes simplex virus latency-associated transcript. Science 287:1500-3.
211. Trotman JB, Braceros KCA, Cherney RE, Murvin MM, Calabrese JM. 2021. The control of polycomb repressive complexes by long noncoding RNAs. Wiley Interdiscip Rev RNA doi:10.1002/wrna.1657:e1657.
212. Lanfranca MP, Mostafa HH, Davido DJ. 2014. HSV-1 ICP0: An E3 Ubiquitin Ligase That Counteracts Host Intrinsic and Innate Immunity. Cells 3:438-54.
213. Wilcox DR, Longnecker R. 2016. The Herpes Simplex Virus Neurovirulence Factor gamma34.5: Revealing Virus-Host Interactions. PLoS Pathog 12:e1005449.
214. Davidovich C, Cech TR. 2015. The recruitment of chromatin modifiers by long noncoding RNAs: lessons from PRC2. RNA 21:2007-22.
215. Almeida M, Bowness JS, Brockdorff N. 2020. The many faces of Polycomb regulation by RNA. Curr Opin Genet Dev 61:53-61.
216. Long Y, Hwang T, Gooding AR, Goodrich KJ, Rinn JL, Cech TR. 2020. RNA is essential for PRC2 chromatin occupancy and function in human pluripotent stem cells. Nat Genet 52:931-938.
217. Balas MM, Hartwick EW, Barrington C, Roberts JT, Wu SK, Bettcher R, Griffin AM, Kieft JS, Johnson AM. 2021. Establishing RNA-RNA interactions remodels lncRNA structure and promotes PRC2 activity. Sci Adv 7.
218. Beltran M, Tavares M, Justin N, Khandelwal G, Ambrose J, Foster BM, Worlock KB, Tvardovskiy A, Kunzelmann S, Herrero J, Bartke T, Gamblin SJ, Wilson JR, Jenner RG. 2019. G-tract RNA removes Polycomb repressive complex 2 from genes. Nat Struct Mol Biol 26:899-909.
219. Rossetto CC, Tarrant-Elorza M, Verma S, Purushothaman P, Pari GS. 2013. Regulation of viral and cellular gene expression by Kaposi's sarcoma-associated herpesvirus polyadenylated nuclear RNA. J Virol 87:5540-53.
220. Withers JB, Li ES, Vallery TK, Yario TA, Steitz JA. 2018. Two herpesviral noncoding PAN RNAs are functionally homologous but do not associate with common chromatin loci. PLoS Pathog 14:e1007389.
221. Vanni EAH, Foley JW, Davison AJ, Sommer M, Liu D, Sung P, Moffat J, Zerboni L, Arvin AM. 2020. The latency-associated transcript locus of herpes simplex virus 1 is a virulence determinant in human skin. PLoS Pathog 16:e1009166.
222. Pintacuda G, Wei G, Roustan C, Kirmizitas BA, Solcan N, Cerase A, Castello A, Mohammed S, Moindrot B, Nesterova TB, Brockdorff N. 2017. hnRNPK Recruits PCGF3/5-PRC1 to the Xist RNA B-Repeat to Establish Polycomb-Mediated Chromosomal Silencing. Mol Cell 68:955-969 e10.
223. Kim JY, Mandarino A, Chao MV, Mohr I, Wilson AC. 2012. Transient reversal of episome silencing precedes VP16-dependent transcription during reactivation of latent HSV-1 in neurons. PLoS Pathog 8:e1002540.

224. Hu HL, Srinivas KP, Wang S, Chao MV, Lionnet T, Mohr I, Wilson AC, Depledge DP, Huang TT. 2022. Single-cell transcriptomics identifies Gadd45b as a regulator of herpesvirus-reactivating neurons. EMBO Rep 23:e53543.
225. Gehani SS, Agrawal-Singh S, Dietrich N, Christophersen NS, Helin K, Hansen K. 2010. Polycomb group protein displacement and gene activation through MSK-dependent H3K27me3S28 phosphorylation. Mol Cell 39:886-900.
226. Lau PN, Cheung P. 2011. Histone code pathway involving H3 S28 phosphorylation and K27 acetylation activates transcription and antagonizes polycomb silencing. Proc Natl Acad Sci U S A 108:2801-6.
227. Palomer E, Carretero J, Benvegnu S, Dotti CG, Martin MG. 2016. Neuronal activity controls Bdnf expression via Polycomb de-repression and CREB/CBP/JMJD3 activation in mature neurons. Nat Commun 7:11081.
228. Cliffe AR. 2019. DNA Damage Meets Neurotrophin Signaling: A Delicate Balancing AKT to Maintain Virus Latency. Mol Cell 74:411-413.
229. Besirli CG, Johnson EM, Jr. 2003. JNK-independent activation of c-Jun during neuronal apoptosis induced by multiple DNA-damaging agents. J Biol Chem 278:22357-66.
230. Bjorkblom B, Ostman N, Hongisto V, Komarovski V, Filen JJ, Nyman TA, Kallunki T, Courtney MJ, Coffey ET. 2005. Constitutively active cytoplasmic c-Jun N-terminal kinase 1 is a dominant regulator of dendritic architecture: role of microtubule-associated protein 2 as an effector. J Neurosci 25:6350-61.
231. Malik AN, Vierbuchen T, Hemberg M, Rubin AA, Ling E, Couch CH, Stroud H, Spiegel I, Farh KK, Harmin DA, Greenberg ME. 2014. Genome-wide identification and characterization of functional neuronal activity-dependent enhancers. Nat Neurosci 17:1330-9.
232. Su Y, Shin J, Zhong C, Wang S, Roychowdhury P, Lim J, Kim D, Ming GL, Song H. 2017. Neuronal activity modifies the chromatin accessibility landscape in the adult brain. Nat Neurosci 20:476-483.
233. Sawtell NM, Thompson RL. 2004. Comparison of herpes simplex virus reactivation in ganglia in vivo and in explants demonstrates quantitative and qualitative differences. J Virol 78:7784-94.
234. Yanez AA, Harrell T, Sriranganathan HJ, Ives AM, Bertke AS. 2017. Neurotrophic Factors NGF, GDNF and NTN Selectively Modulate HSV1 and HSV2 Lytic Infection and Reactivation in Primary Adult Sensory and Autonomic Neurons. Pathogens 6.
235. Catez F, Picard C, Held K, Gross S, Rousseau A, Theil D, Sawtell N, Labetoulle M, Lomonte P. 2012. HSV-1 genome subnuclear positioning and associations with host-cell PML-NBs and centromeres regulate LAT locus transcription during latency in neurons. PLoS Pathog 8:e1002852.
236. DeLeon M, Covenas R, Chadi G, Narvaez JA, Fuxe K, Cintra A. 1994. Subpopulations of primary sensory neurons show coexistence of neuropeptides and glucocorticoid receptors in the rat spinal and trigeminal ganglia. Brain Res 636:338-42.
237. Gold MS, Dastmalchi S, Levine JD. 1997. Alpha 2-adrenergic receptor subtypes in rat dorsal root and superior cervical ganglion neurons. Pain 69:179-90.
238. Lallemend F, Ernfors P. 2012. Molecular interactions underlying the specification of sensory neurons. Trends Neurosci 35:373-81.

239. Singh N, Tscharke DC. 2020. Herpes Simplex Virus Latency Is Noisier the Closer We Look. J Virol 94.
240. Bloom DC. 2016. Alphaherpesvirus Latency: A Dynamic State of Transcription and Reactivation. Adv Virus Res 94:53-80.
241. Speck PG, Simmons A. 1991. Divergent molecular pathways of productive and latent infection with a virulent strain of herpes simplex virus type 1. J Virol 65:4001-5.
242. Speck PG, Simmons A. 1992. Synchronous appearance of antigen-positive and latently infected neurons in spinal ganglia of mice infected with a virulent strain of herpes simplex virus. J Gen Virol 73 (Pt 5):1281-5.
243. Proenca JT, Coleman HM, Nicoll MP, Connor V, Preston CM, Arthur J, Efstathiou S. 2011. An investigation of herpes simplex virus promoter activity compatible with latency establishment reveals VP16-independent activation of immediate-early promoters in sensory neurones. J Gen Virol 92:2575-2585.
244. Maillet S, Naas T, Crepin S, Roque-Afonso AM, Lafay F, Efstathiou S, Labetoulle M. 2006. Herpes simplex virus type 1 latently infected neurons differentially express latency-associated and ICP0 transcripts. J Virol 80:9310-21.
245. Tzeng NS, Chung CH, Lin FH, Chiang CP, Yeh CB, Huang SY, Lu RB, Chang HA, Kao YC, Yeh HW, Chiang WS, Chou YC, Tsao CH, Wu YF, Chien WC. 2018. Anti-herpetic Medications and Reduced Risk of Dementia in Patients with Herpes Simplex Virus Infections-a Nationwide, Population-Based Cohort Study in Taiwan. Neurotherapeutics 15:417-429.
246. Letenneur L, Peres K, Fleury H, Garrigue I, Barberger-Gateau P, Helmer C, Orgogozo JM, Gauthier S, Dartigues JF. 2008. Seropositivity to herpes simplex virus antibodies and risk of Alzheimer's disease: a population-based cohort study. PLoS One 3:e3637.
247. De Chiara G, Piacentini R, Fabiani M, Mastrodonato A, Marcocci ME, Limongi D, Napoletani G, Protto V, Coluccio P, Celestino I, Li Puma DD, Grassi C, Palamara AT. 2019. Recurrent herpes simplex virus-1 infection induces hallmarks of neurodegeneration and cognitive deficits in mice. PLoS Pathog 15:e1007617.
248. Itzhaki RF. 2014. Herpes simplex virus type 1 and Alzheimer's disease: increasing evidence for a major role of the virus. Front Aging Neurosci 6:202.
249. Koelle DM, Magaret A, Warren T, Schellenberg GD, Wald A. 2010. APOE genotype is associated with oral herpetic lesions but not genital or oral herpes simplex virus shedding. Sex Transm Infect 86:202-6.
250. Steel AJ, Eslick GD. 2015. Herpes Viruses Increase the Risk of Alzheimer's Disease: A Meta-Analysis. J Alzheimers Dis 47:351-64.
251. Readhead B, Haure-Mirande JV, Funk CC, Richards MA, Shannon P, Haroutunian V, Sano M, Liang WS, Beckmann ND, Price ND, Reiman EM, Schadt EE, Ehrlich ME, Gandy S, Dudley JT. 2018. Multiscale Analysis of Independent Alzheimer's Cohorts Finds Disruption of Molecular, Genetic, and Clinical Networks by Human Herpesvirus. Neuron 99:64-82 e7.
252. Lopatko Lindman K, Hemmingsson ES, Weidung B, Brannstrom J, Josefsson M, Olsson J, Elgh F, Nordstrom P, Lovheim H. 2021. Herpesvirus infections, antiviral treatment, and the risk of dementia-a registry-based cohort study in Sweden. Alzheimers Dement (N Y) 7:e12119.

253. Honess RW, Roizman B. 1974. Regulation of herpesvirus macromolecular synthesis. I. Cascade regulation of the synthesis of three groups of viral proteins. J Virol 14:8-19.
254. Honess RW, Roizman B. 1975. Regulation of herpesvirus macromolecular synthesis: sequential transition of polypeptide synthesis requires functional viral polypeptides. Proc Natl Acad Sci U S A 72:1276-80.
255. Monier K, Armas JC, Etteldorf S, Ghazal P, Sullivan KF. 2000. Annexation of the interchromosomal space during viral infection. Nat Cell Biol 2:661-5.
256. Kutluay SB, Doroghazi J, Roemer ME, Triezenberg SJ. 2008. Curcumin inhibits herpes simplex virus immediate-early gene expression by a mechanism independent of p300/CBP histone acetyltransferase activity. Virology 373:239-47.
257. Kutluay SB, Triezenberg SJ. 2009. Regulation of histone deposition on the herpes simplex virus type 1 genome during lytic infection. J Virol 83:5835-45.
258. Oh J, Fraser NW. 2008. Temporal association of the herpes simplex virus genome with histone proteins during a lytic infection. J Virol 82:3530-7.
259. Cliffe AR, Knipe DM. 2008. Herpes simplex virus ICP0 promotes both histone removal and acetylation on viral DNA during lytic infection. J Virol 82:12030-8.
260. Liang Y, Vogel JL, Arbuckle JH, Rai G, Jadhav A, Simeonov A, Maloney DJ, Kristie TM. 2013. Targeting the JMJD2 histone demethylases to epigenetically control herpesvirus infection and reactivation from latency. Sci Transl Med 5:167ra5.
261. Liang Y, Vogel JL, Narayanan A, Peng H, Kristie TM. 2009. Inhibition of the histone demethylase LSD1 blocks alpha-herpesvirus lytic replication and reactivation from latency. Nat Med 15:1312-7.
262. Narayanan A, Ruyechan WT, Kristie TM. 2007. The coactivator host cell factor-1 mediates Set1 and MLL1 H3K4 trimethylation at herpesvirus immediate early promoters for initiation of infection. Proc Natl Acad Sci U S A 104:10835-40.
263. Wysocka J, Myers MP, Laherty CD, Eisenman RN, Herr W. 2003. Human Sin3 deacetylase and trithorax-related Set1/Ash2 histone H3-K4 methyltransferase are tethered together selectively by the cell-proliferation factor HCF-1. Genes Dev 17:896-911.
264. Dremel SE, DeLuca NA. 2019. Herpes simplex viral nucleoprotein creates a competitive transcriptional environment facilitating robust viral transcription and host shut off. Elife 8.
265. Cliffe AR, Wilson AC. 2017. Restarting Lytic Gene Transcription at the Onset of Herpes Simplex Virus Reactivation. J Virol 91.
266. Steiner I, Spivack JG, Deshmane SL, Ace CI, Preston CM, Fraser NW. 1990. A herpes simplex virus type 1 mutant containing a nontransinducing Vmw65 protein establishes latent infection in vivo in the absence of viral replication and reactivates efficiently from explanted trigeminal ganglia. J Virol 64:1630-8.
267. Wilson AC, Mohr I. 2012. A cultured affair: HSV latency and reactivation in neurons. Trends Microbiol 20:604-11.
268. Lachmann R. 2003. Herpes simplex virus latency. Expert Rev Mol Med 5:1-14.
269. Cabrera JR, Charron AJ, Leib DA. 2018. Neuronal Subtype Determines Herpes Simplex Virus 1 Latency-Associated-Transcript Promoter Activity during Latency. J Virol 92.
270. Arthur JL, Scarpini CG, Connor V, Lachmann RH, Tolkovsky AM, Efstathiou S. 2001. Herpes simplex virus type 1 promoter activity during latency establishment,

maintenance, and reactivation in primary dorsal root neurons in vitro. J Virol 75:3885-95.
271. De Clercq E. 2008. The discovery of antiviral agents: ten different compounds, ten different stories. Med Res Rev 28:929-53.
272. De Clercq E, Holy A. 2005. Acyclic nucleoside phosphonates: a key class of antiviral drugs. Nat Rev Drug Discov 4:928-40.
273. Benboudjema L, Mulvey M, Gao Y, Pimplikar SW, Mohr I. 2003. Association of the herpes simplex virus type 1 Us11 gene product with the cellular kinesin light-chain-related protein PAT1 results in the redistribution of both polypeptides. J Virol 77:9192-203.
274. Forrester A, Farrell H, Wilkinson G, Kaye J, Davis-Poynter N, Minson T. 1992. Construction and properties of a mutant of herpes simplex virus type 1 with glycoprotein H coding sequences deleted. J Virol 66:341-8.
275. Hilterbrand AT, Heldwein EE. 2019. Go go gadget glycoprotein!: HSV-1 draws on its sizeable glycoprotein tool kit to customize its diverse entry routes. PLoS Pathog 15:e1007660.
276. Turner A, Bruun B, Minson T, Browne H. 1998. Glycoproteins gB, gD, and gHgL of herpes simplex virus type 1 are necessary and sufficient to mediate membrane fusion in a Cos cell transfection system. J Virol 72:873-5.
277. Chao MV. 2003. Neurotrophins and their receptors: a convergence point for many signalling pathways. Nat Rev Neurosci 4:299-309.
278. van Zeijl M, Fairhurst J, Jones TR, Vernon SK, Morin J, LaRocque J, Feld B, O'Hara B, Bloom JD, Johann SV. 2000. Novel class of thiourea compounds that inhibit herpes simplex virus type 1 DNA cleavage and encapsidation: resistance maps to the UL6 gene. J Virol 74:9054-61.
279. Newcomb WW, Brown JC. 2002. Inhibition of herpes simplex virus replication by WAY-150138: assembly of capsids depleted of the portal and terminase proteins involved in DNA encapsidation. J Virol 76:10084-8.
280. Pesola JM, Zhu J, Knipe DM, Coen DM. 2005. Herpes simplex virus 1 immediate-early and early gene expression during reactivation from latency under conditions that prevent infectious virus production. J Virol 79:14516-25.
281. Hollville E, Romero SE, Deshmukh M. 2019. Apoptotic cell death regulation in neurons. FEBS J 286:3276-3298.
282. Annis RP, Swahari V, Nakamura A, Xie AX, Hammond SM, Deshmukh M. 2016. Mature neurons dynamically restrict apoptosis via redundant premitochondrial brakes. FEBS J 283:4569-4582.
283. Kole AJ, Swahari V, Hammond SM, Deshmukh M. 2011. miR-29b is activated during neuronal maturation and targets BH3-only genes to restrict apoptosis. Genes Dev 25:125-30.
284. Smith RL, Pizer LI, Johnson EM, Jr., Wilcox CL. 1992. Activation of second-messenger pathways reactivates latent herpes simplex virus in neuronal cultures. Virology 188:311-8.

285. Danaher RJ, Jacob RJ, Miller CS. 2003. Herpesvirus quiescence in neuronal cells. V: forskolin-responsiveness of the herpes simplex virus type 1 alpha0 promoter and contribution of the putative cAMP response element. J Neurovirol 9:489-97.
286. Moriya A, Yoshiki A, Kita M, Fushiki S, Imanishi J. 1994. Heat shock-induced reactivation of herpes simplex virus type 1 in latently infected mouse trigeminal ganglion cells in dissociated culture. Arch Virol 135:419-25.
287. Halford WP, Gebhardt BM, Carr DJ. 1996. Mechanisms of herpes simplex virus type 1 reactivation. J Virol 70:5051-60.
288. Kushnir AS, Davido DJ, Schaffer PA. 2010. Role of nuclear factor Y in stress-induced activation of the herpes simplex virus type 1 ICP0 promoter. J Virol 84:188-200.
289. Perng GC, Osorio N, Jiang X, Geertsema R, Hsiang C, Brown D, BenMohamed L, Wechsler SL. 2016. Large Amounts of Reactivated Virus in Tears Precedes Recurrent Herpes Stromal Keratitis in Stressed Rabbits Latently Infected with Herpes Simplex Virus. Curr Eye Res 41:284-91.
290. Shimomura Y, Higaki S, Watanabe K. 2010. Suppression of herpes simplex virus 1 reactivation in a mouse eye model by cyclooxygenase inhibitor, heat shock protein inhibitor, and adenosine monophosphate. Jpn J Ophthalmol 54:187-90.
291. Hill JM, Lukiw WJ, Gebhardt BM, Higaki S, Loutsch JM, Myles ME, Thompson HW, Kwon BS, Bazan NG, Kaufman HE. 2001. Gene expression analyzed by microarrays in HSV-1 latent mouse trigeminal ganglion following heat stress. Virus Genes 23:273-80.
292. Thompson RL, Preston CM, Sawtell NM. 2009. De novo synthesis of VP16 coordinates the exit from HSV latency in vivo. PLoS Pathog 5:e1000352.
293. Patel S, Cohen F, Dean BJ, De La Torre K, Deshmukh G, Estrada AA, Ghosh AS, Gibbons P, Gustafson A, Huestis MP, Le Pichon CE, Lin H, Liu W, Liu X, Liu Y, Ly CQ, Lyssikatos JP, Ma C, Scearce-Levie K, Shin YG, Solanoy H, Stark KL, Wang J, Wang B, Zhao X, Lewcock JW, Siu M. 2015. Discovery of dual leucine zipper kinase (DLK, MAP3K12) inhibitors with activity in neurodegeneration models. J Med Chem 58:401-18.
294. Heinemann B, Nielsen JM, Hudlebusch HR, Lees MJ, Larsen DV, Boesen T, Labelle M, Gerlach LO, Birk P, Helin K. 2014. Inhibition of demethylases by GSK-J1/J4. Nature 514:E1-2.
295. Sawtell NM, Thompson RL. 2016. Herpes simplex virus and the lexicon of latency and reactivation: a call for defining terms and building an integrated collective framework. F1000Res 5.
296. Wang L, Brown JL, Cao R, Zhang Y, Kassis JA, Jones RS. 2004. Hierarchical recruitment of polycomb group silencing complexes. Mol Cell 14:637-46.
297. Chadwick BP, Willard HF. 2003. Barring gene expression after XIST: maintaining facultative heterochromatin on the inactive X. Semin Cell Dev Biol 14:359-67.
298. Tedeschi A, Bradke F. 2013. The DLK signalling pathway--a double-edged sword in neural development and regeneration. EMBO Rep 14:605-14.
299. Karney-Grobe S, Russo A, Frey E, Milbrandt J, DiAntonio A. 2018. HSP90 is a chaperone for DLK and is required for axon injury signaling. Proc Natl Acad Sci U S A 115:E9899-E9908.

300. Summers DW, Frey E, Walker LJ, Milbrandt J, DiAntonio A. 2020. DLK Activation Synergizes with Mitochondrial Dysfunction to Downregulate Axon Survival Factors and Promote SARM1-Dependent Axon Degeneration. Mol Neurobiol 57:1146-1158.
301. Hirai S, Kawaguchi A, Suenaga J, Ono M, Cui DF, Ohno S. 2005. Expression of MUK/DLK/ZPK, an activator of the JNK pathway, in the nervous systems of the developing mouse embryo. Gene Expr Patterns 5:517-23.
302. Matthews SM, Groves IJ, O'Connor CM. 2023. Chromatin control of human cytomegalovirus infection. mBio 14:e0032623.
303. Collins-McMillen D, Buehler J, Peppenelli M, Goodrum F. 2018. Molecular Determinants and the Regulation of Human Cytomegalovirus Latency and Reactivation. Viruses 10.
304. Guo R, Gewurz BE. 2022. Epigenetic control of the Epstein-Barr lifecycle. Curr Opin Virol 52:78-88.
305. Chen HS, Lu F, Lieberman PM. 2013. Epigenetic regulation of EBV and KSHV latency. Curr Opin Virol 3:251-9.
306. Tovey MG, Lenoir G, Begon-Lours J. 1978. Activation of latent Epstein-Barr virus by antibody to human IgM. Nature 276:270-2.
307. Reeves MB, MacAry PA, Lehner PJ, Sissons JG, Sinclair JH. 2005. Latency, chromatin remodeling, and reactivation of human cytomegalovirus in the dendritic cells of healthy carriers. Proc Natl Acad Sci U S A 102:4140-5.
308. Reeves MB, Lehner PJ, Sissons JGP, Sinclair JH. 2005. An in vitro model for the regulation of human cytomegalovirus latency and reactivation in dendritic cells by chromatin remodelling. J Gen Virol 86:2949-2954.
309. Soderberg-Naucler C, Streblow DN, Fish KN, Allan-Yorke J, Smith PP, Nelson JA. 2001. Reactivation of latent human cytomegalovirus in CD14(+) monocytes is differentiation dependent. J Virol 75:7543-54.
310. Taylor-Wiedeman J, Sissons P, Sinclair J. 1994. Induction of endogenous human cytomegalovirus gene expression after differentiation of monocytes from healthy carriers. J Virol 68:1597-604.
311. Dooley AL, O'Connor CM. 2020. Regulation of the MIE Locus During HCMV Latency and Reactivation. Pathogens 9.
312. Hill JM, Garza HH, Jr., Helmy MF, Cook SD, Osborne PA, Johnson EM, Jr., Thompson HW, Green LC, O'Callaghan RJ, Gebhardt BM. 1997. Nerve growth factor antibody stimulates reactivation of ocular herpes simplex virus type 1 in latently infected rabbits. J Neurovirol 3:206-11.
313. Mattila RK, Harila K, Kangas SM, Paavilainen H, Heape AM, Mohr IJ, Hukkanen V. 2015. An investigation of herpes simplex virus type 1 latency in a novel mouse dorsal root ganglion model suggests a role for ICP34.5 in reactivation. J Gen Virol 96:2304-2313.
314. Stevens JG, Cook ML. 1971. Restriction of herpes simplex virus by macrophages. An analysis of the cell-virus interaction. J Exp Med 133:19-38.
315. Wysocka J, Herr W. 2003. The herpes simplex virus VP16-induced complex: the makings of a regulatory switch. Trends Biochem Sci 28:294-304.
316. Fischle W, Wang Y, Allis CD. 2003. Binary switches and modification cassettes in histone biology and beyond. Nature 425:475-9.

317. Fischle W, Tseng BS, Dormann HL, Ueberheide BM, Garcia BA, Shabanowitz J, Hunt DF, Funabiki H, Allis CD. 2005. Regulation of HP1-chromatin binding by histone H3 methylation and phosphorylation. Nature 438:1116-22.
318. Noh KM, Maze I, Zhao D, Xiang B, Wenderski W, Lewis PW, Shen L, Li H, Allis CD. 2015. ATRX tolerates activity-dependent histone H3 methyl/phos switching to maintain repetitive element silencing in neurons. Proc Natl Acad Sci U S A 112:6820-7.
319. Miller BR, Press C, Daniels RW, Sasaki Y, Milbrandt J, DiAntonio A. 2009. A dual leucine kinase-dependent axon self-destruction program promotes Wallerian degeneration. Nat Neurosci 12:387-9.
320. Ghosh AS, Wang B, Pozniak CD, Chen M, Watts RJ, Lewcock JW. 2011. DLK induces developmental neuronal degeneration via selective regulation of proapoptotic JNK activity. J Cell Biol 194:751-64.
321. Welsbie DS, Yang Z, Ge Y, Mitchell KL, Zhou X, Martin SE, Berlinicke CA, Hackler L, Jr., Fuller J, Fu J, Cao LH, Han B, Auld D, Xue T, Hirai S, Germain L, Simard-Bisson C, Blouin R, Nguyen JV, Davis CH, Enke RA, Boye SL, Merbs SL, Marsh-Armstrong N, Hauswirth WW, DiAntonio A, Nickells RW, Inglese J, Hanes J, Yau KW, Quigley HA, Zack DJ. 2013. Functional genomic screening identifies dual leucine zipper kinase as a key mediator of retinal ganglion cell death. Proc Natl Acad Sci U S A 110:4045-50.
322. Miller M. 2009. The importance of being flexible: the case of basic region leucine zipper transcriptional regulators. Curr Protein Pept Sci 10:244-69.
323. Reinke AW, Baek J, Ashenberg O, Keating AE. 2013. Networks of bZIP protein-protein interactions diversified over a billion years of evolution. Science 340:730-4.
324. Deppmann CD, Alvania RS, Taparowsky EJ. 2006. Cross-species annotation of basic leucine zipper factor interactions: Insight into the evolution of closed interaction networks. Mol Biol Evol 23:1480-92.
325. Buschle A, Hammerschmidt W. 2020. Epigenetic lifestyle of Epstein-Barr virus. Semin Immunopathol 42:131-142.
326. Valyi-Nagy T, Deshmane S, Dillner A, Fraser NW. 1991. Induction of cellular transcription factors in trigeminal ganglia of mice by corneal scarification, herpes simplex virus type 1 infection, and explantation of trigeminal ganglia. J Virol 65:4142-52.
327. Gieroba ZJ, Zhu BS, Blessing WW, Wesselingh SL. 1995. Herpes simplex virus induces Fos expression in rat brainstem neurons. Brain Res 675:329-32.
328. Tsuchida K, Chaki H, Takakura T, Kotsubo H, Tanaka T, Aikawa Y, Shiozawa S, Hirono S. 2006. Discovery of nonpeptidic small-molecule AP-1 inhibitors: lead hopping based on a three-dimensional pharmacophore model. J Med Chem 49:80-91.
329. Krishna BA, Wass AB, O'Connor CM. 2020. Activator protein-1 transactivation of the major immediate early locus is a determinant of cytomegalovirus reactivation from latency. Proc Natl Acad Sci U S A 117:20860-20867.
330. Crowder RJ, Freeman RS. 1998. Phosphatidylinositol 3-kinase and Akt protein kinase are necessary and sufficient for the survival of nerve growth factor-dependent sympathetic neurons. J Neurosci 18:2933-43.
331. Yuan Z, Gong S, Luo J, Zheng Z, Song B, Ma S, Guo J, Hu C, Thiel G, Vinson C, Hu CD, Wang Y, Li M. 2009. Opposing roles for ATF2 and c-Fos in c-Jun-mediated neuronal apoptosis. Mol Cell Biol 29:2431-42.

332. Dhanasekaran DN, Reddy EP. 2008. JNK signaling in apoptosis. Oncogene 27:6245-51.
333. Kristiansen M, Menghi F, Hughes R, Hubank M, Ham J. 2011. Global analysis of gene expression in NGF-deprived sympathetic neurons identifies molecular pathways associated with cell death. BMC Genomics 12:551.
334. Deshmane SL, Fraser NW. 1989. During latency, herpes simplex virus type 1 DNA is associated with nucleosomes in a chromatin structure. J Virol 63:943-7.
335. Cohen C, Corpet A, Roubille S, Maroui MA, Poccardi N, Rousseau A, Kleijwegt C, Binda O, Texier P, Sawtell N, Labetoulle M, Lomonte P. 2018. Promyelocytic leukemia (PML) nuclear bodies (NBs) induce latent/quiescent HSV-1 genomes chromatinization through a PML NB/Histone H3.3/H3.3 Chaperone Axis. PLoS Pathog 14:e1007313.
336. Tiwari VK, Stadler MB, Wirbelauer C, Paro R, Schubeler D, Beisel C. 2011. A chromatin-modifying function of JNK during stem cell differentiation. Nat Genet 44:94-100.
337. Workman A, Eudy J, Smith L, da Silva LF, Sinani D, Bricker H, Cook E, Doster A, Jones C. 2012. Cellular transcription factors induced in trigeminal ganglia during dexamethasone-induced reactivation from latency stimulate bovine herpesvirus 1 productive infection and certain viral promoters. J Virol 86:2459-73.
338. Ostler JB, Thunuguntla P, Hendrickson BY, Jones C. 2021. Transactivation of Herpes Simplex Virus 1 (HSV-1) Infected Cell Protein 4 Enhancer by Glucocorticoid Receptor and Stress-Induced Transcription Factors Requires Overlapping Kruppel-Like Transcription Factor 4/Sp1 Binding Sites. J Virol 95.
339. Ostler JB, Jones C. 2021. Stress Induced Transcription Factors Transactivate the Herpes Simplex Virus 1 Infected Cell Protein 27 (ICP27) Transcriptional Enhancer. Viruses 13.
340. Wijesekera N, Hazell N, Jones C. 2022. Independent Cis-Regulatory Modules within the Herpes Simplex Virus 1 Infected Cell Protein 0 (ICP0) Promoter Are Transactivated by Kruppel-like Factor 15 and Glucocorticoid Receptor. Viruses 14.
341. Takahashi K, Yamanaka S. 2006. Induction of pluripotent stem cells from mouse embryonic and adult fibroblast cultures by defined factors. Cell 126:663-76.
342. Soufi A, Garcia MF, Jaroszewicz A, Osman N, Pellegrini M, Zaret KS. 2015. Pioneer transcription factors target partial DNA motifs on nucleosomes to initiate reprogramming. Cell 161:555-568.
343. Fonseca GJ, Tao J, Westin EM, Duttke SH, Spann NJ, Strid T, Shen Z, Stender JD, Sakai M, Link VM, Benner C, Glass CK. 2019. Diverse motif ensembles specify non-redundant DNA binding activities of AP-1 family members in macrophages. Nat Commun 10:414.
344. McLean TI, Bachenheimer SL. 1999. Activation of cJUN N-terminal kinase by herpes simplex virus type 1 enhances viral replication. J Virol 73:8415-26.
345. Zachos G, Clements B, Conner J. 1999. Herpes simplex virus type 1 infection stimulates p38/c-Jun N-terminal mitogen-activated protein kinase pathways and activates transcription factor AP-1. J Biol Chem 274:5097-103.
346. Ashcraft KA, Bonneau RH. 2008. Psychological stress exacerbates primary vaginal herpes simplex virus type 1 (HSV-1) infection by impairing both innate and adaptive immune responses. Brain Behav Immun 22:1231-40.
347. Ashcraft KA, Hunzeker J, Bonneau RH. 2008. Psychological stress impairs the local CD8+ T cell response to mucosal HSV-1 infection and allows for increased pathogenicity via a glucocorticoid receptor-mediated mechanism. Psychoneuroendocrinology 33:951-63.

348. Torres-Berrio A, Estill M, Ramakrishnan A, Kronman H, Patel V, Minier-Toribio A, Issler O, Browne CJ, Parise EM, van der Zee Y, Walker D, Martinez-Rivera FJ, Lardner CK, Cuttoli RD, Russo SJ, Shen L, Sidoli S, Nestler EJ. 2023. Monomethylation of Lysine 27 at Histone 3 Confers Lifelong Susceptibility to Stress. bioRxiv doi:10.1101/2023.05.08.539829.
349. Kronman H, Torres-Berrio A, Sidoli S, Issler O, Godino A, Ramakrishnan A, Mews P, Lardner CK, Parise EM, Walker DM, van der Zee YY, Browne CJ, Boyce BF, Neve R, Garcia BA, Shen L, Pena CJ, Nestler EJ. 2021. Long-term behavioral and cell-type-specific molecular effects of early life stress are mediated by H3K79me2 dynamics in medium spiny neurons. Nat Neurosci 24:667-676.
350. Price AM, Luftig MA. 2015. To be or not IIb: a multi-step process for Epstein-Barr virus latency establishment and consequences for B cell tumorigenesis. PLoS Pathog 11:e1004656.
351. Bhutani M, Polizzotto MN, Uldrick TS, Yarchoan R. 2015. Kaposi sarcoma-associated herpesvirus-associated malignancies: epidemiology, pathogenesis, and advances in treatment. Semin Oncol 42:223-46.
352. Ye F, Lei X, Gao SJ. 2011. Mechanisms of Kaposi's Sarcoma-Associated Herpesvirus Latency and Reactivation. Adv Virol 2011.
353. Washington SD, Musarrat F, Ertel MK, Backes GL, Neumann DM. 2018. CTCF Binding Sites in the Herpes Simplex Virus 1 Genome Display Site-Specific CTCF Occupation, Protein Recruitment, and Insulator Function. J Virol 92.
354. Hou Y, Liu W, Yi X, Yang Y, Su D, Huang W, Yu H, Teng X, Yang Y, Feng W, Zhang T, Gao J, Zhang K, Qiu R, Wang Y. 2020. PHF20L1 as a H3K27me2 reader coordinates with transcriptional repressors to promote breast tumorigenesis. Sci Adv 6:eaaz0356.
355. Skene PJ, Henikoff S. 2017. An efficient targeted nuclease strategy for high-resolution mapping of DNA binding sites. Elife 6.
356. Ertel MK, Cammarata AL, Hron RJ, Neumann DM. 2012. CTCF occupation of the herpes simplex virus 1 genome is disrupted at early times postreactivation in a transcription-dependent manner. J Virol 86:12741-59.
357. Kreso A, van Galen P, Pedley NM, Lima-Fernandes E, Frelin C, Davis T, Cao L, Baiazitov R, Du W, Sydorenko N, Moon YC, Gibson L, Wang Y, Leung C, Iscove NN, Arrowsmith CH, Szentgyorgyi E, Gallinger S, Dick JE, O'Brien CA. 2014. Self-renewal as a therapeutic target in human colorectal cancer. Nat Med 20:29-36.
358. Akita N, Okada R, Mukae K, Sugino RP, Takenobu H, Chikaraishi K, Ochiai H, Yamaguchi Y, Ohira M, Koseki H, Kamijo T. 2022. Polycomb group protein BMI1 protects neuroblastoma cells against DNA damage-induced apoptotic cell death. Exp Cell Res 422:113412.
359. Shukla S, Ying W, Gray F, Yao Y, Simes ML, Zhao Q, Miao H, Cho HJ, Gonzalez-Alonso P, Winkler A, Lund G, Purohit T, Kim E, Zhang X, Ray JM, He S, Nikolaidis C, Ndoj J, Wang J, Jaremko L, Jaremko M, Ryan RJH, Guzman ML, Grembecka J, Cierpicki T. 2021. Small-molecule inhibitors targeting Polycomb repressive complex 1 RING domain. Nat Chem Biol 17:784-793.
360. Zhu Y, Dong L, Wang C, Hao K, Wang J, Zhao L, Xu L, Xia Y, Jiang Q, Qin J. 2022. Functional redundancy among Polycomb complexes in maintaining the pluripotent state of embryonic stem cells. Stem Cell Reports 17:1198-1214.

361. Pasini D, Bracken AP, Jensen MR, Lazzerini Denchi E, Helin K. 2004. Suz12 is essential for mouse development and for EZH2 histone methyltransferase activity. EMBO J 23:4061-71.
362. Lotharius J, Brundin P. 2002. Impaired dopamine storage resulting from alpha-synuclein mutations may contribute to the pathogenesis of Parkinson's disease. Hum Mol Genet 11:2395-407.
363. Lotharius J, Falsig J, van Beek J, Payne S, Dringen R, Brundin P, Leist M. 2005. Progressive degeneration of human mesencephalic neuron-derived cells triggered by dopamine-dependent oxidative stress is dependent on the mixed-lineage kinase pathway. J Neurosci 25:6329-42.
364. Yao B, Christian KM, He C, Jin P, Ming GL, Song H. 2016. Epigenetic mechanisms in neurogenesis. Nat Rev Neurosci 17:537-49.
365. Richly H, Rocha-Viegas L, Ribeiro JD, Demajo S, Gundem G, Lopez-Bigas N, Nakagawa T, Rospert S, Ito T, Di Croce L. 2010. Transcriptional activation of polycomb-repressed genes by ZRF1. Nature 468:1124-8.
366. Glancy E, Wang C, Tuck E, Healy E, Amato S, Neikes HK, Mariani A, Mucha M, Vermeulen M, Pasini D, Bracken AP. 2023. PRC2.1- and PRC2.2-specific accessory proteins drive recruitment of different forms of canonical PRC1. Mol Cell 83:1393-1411 e7.
367. Fan H, Lu J, Guo Y, Li D, Zhang ZM, Tsai YH, Pi WC, Ahn JH, Gong W, Xiang Y, Allison DF, Geng H, He S, Diao Y, Chen WY, Strahl BD, Cai L, Song J, Wang GG. 2020. BAHCC1 binds H3K27me3 via a conserved BAH module to mediate gene silencing and oncogenesis. Nat Genet 52:1384-1396.
368. Yu M, Mazor T, Huang H, Huang HT, Kathrein KL, Woo AJ, Chouinard CR, Labadorf A, Akie TE, Moran TB, Xie H, Zacharek S, Taniuchi I, Roeder RG, Kim CF, Zon LI, Fraenkel E, Cantor AB. 2012. Direct recruitment of polycomb repressive complex 1 to chromatin by core binding transcription factors. Mol Cell 45:330-43.
369. Soh TK, Davies CTR, Muenzner J, Hunter LM, Barrow HG, Connor V, Bouton CR, Smith C, Emmott E, Antrobus R, Graham SC, Weekes MP, Crump CM. 2020. Temporal Proteomic Analysis of Herpes Simplex Virus 1 Infection Reveals Cell-Surface Remodeling via pUL56-Mediated GOPC Degradation. Cell Rep 33:108235.
370. Zhu S, Viejo-Borbolla A. 2021. Pathogenesis and virulence of herpes simplex virus. Virulence 12:2670-2702.
371. Smith MC, Boutell C, Davido DJ. 2011. HSV-1 ICP0: paving the way for viral replication. Future Virol 6:421-429.
372. Gu H, Zheng Y, Roizman B. 2013. Interaction of herpes simplex virus ICP0 with ND10 bodies: a sequential process of adhesion, fusion, and retention. J Virol 87:10244-54.
373. Chelbi-Alix MK, de The H. 1999. Herpes virus induced proteasome-dependent degradation of the nuclear bodies-associated PML and Sp100 proteins. Oncogene 18:935-41.
374. Gu H, Zheng Y. 2016. Role of ND10 nuclear bodies in the chromatin repression of HSV-1. Virol J 13:62.
375. Jan Fada B, Reward E, Gu H. 2021. The Role of ND10 Nuclear Bodies in Herpesvirus Infection: A Frenemy for the Virus? Viruses 13.

376. Everett RD, Rechter S, Papior P, Tavalai N, Stamminger T, Orr A. 2006. PML contributes to a cellular mechanism of repression of herpes simplex virus type 1 infection that is inactivated by ICP0. J Virol 80:7995-8005.
377. Sijm A, Atlasi Y, van der Knaap JA, Wolf van der Meer J, Chalkley GE, Bezstarosti K, Dekkers DHW, Doff WAS, Ozgur Z, van IWFJ, Demmers JAA, Verrijzer CP. 2022. USP7 regulates the ncPRC1 Polycomb axis to stimulate genomic H2AK119ub1 deposition uncoupled from H3K27me3. Sci Adv 8:eabq7598.
378. Boutell C, Canning M, Orr A, Everett RD. 2005. Reciprocal activities between herpes simplex virus type 1 regulatory protein ICP0, a ubiquitin E3 ligase, and ubiquitin-specific protease USP7. J Virol 79:12342-54.
379. Everett RD, Meredith M, Orr A, Cross A, Kathoria M, Parkinson J. 1997. A novel ubiquitin-specific protease is dynamically associated with the PML nuclear domain and binds to a herpesvirus regulatory protein. EMBO J 16:1519-30.
380. Machida YJ, Machida Y, Vashisht AA, Wohlschlegel JA, Dutta A. 2009. The deubiquitinating enzyme BAP1 regulates cell growth via interaction with HCF-1. J Biol Chem 284:34179-88.
381. Sowa ME, Bennett EJ, Gygi SP, Harper JW. 2009. Defining the human deubiquitinating enzyme interaction landscape. Cell 138:389-403.
382. Misaghi S, Ottosen S, Izrael-Tomasevic A, Arnott D, Lamkanfi M, Lee J, Liu J, O'Rourke K, Dixit VM, Wilson AC. 2009. Association of C-terminal ubiquitin hydrolase BRCA1-associated protein 1 with cell cycle regulator host cell factor 1. Mol Cell Biol 29:2181-92.
383. Yu H, Mashtalir N, Daou S, Hammond-Martel I, Ross J, Sui G, Hart GW, Rauscher FJ, 3rd, Drobetsky E, Milot E, Shi Y, Affar el B. 2010. The ubiquitin carboxyl hydrolase BAP1 forms a ternary complex with YY1 and HCF-1 and is a critical regulator of gene expression. Mol Cell Biol 30:5071-85.
384. Erecinska M, Silver IA. 2001. Tissue oxygen tension and brain sensitivity to hypoxia. Respir Physiol 128:263-76.
385. Sun X, Volobouеva LA, Stary CM, Giffard RG. 2015. Physiologically normal 5% O2 supports neuronal differentiation and resistance to inflammatory injury in neural stem cell cultures. J Neurosci Res 93:1703-12.
386. De Filippis L, Delia D. 2011. Hypoxia in the regulation of neural stem cells. Cell Mol Life Sci 68:2831-44.
387. Storch A, Paul G, Csete M, Boehm BO, Carvey PM, Kupsch A, Schwarz J. 2001. Long-term proliferation and dopaminergic differentiation of human mesencephalic neural precursor cells. Exp Neurol 170:317-25.
388. Studer L, Csete M, Lee SH, Kabbani N, Walikonis J, Wold B, McKay R. 2000. Enhanced proliferation, survival, and dopaminergic differentiation of CNS precursors in lowered oxygen. J Neurosci 20:7377-83.
389. Filice F, Blum W, Lauber E, Schwaller B. 2019. Inducible and reversible silencing of the Pvalb gene in mice: An in vitro and in vivo study. Eur J Neurosci 50:2694-2706.
390. Watson ZL, Washington SD, Phelan DM, Lewin AS, Tuli SS, Schultz GS, Neumann DM, Bloom DC. 2018. In Vivo Knockdown of the Herpes Simplex Virus 1 Latency-Associated Transcript Reduces Reactivation from Latency. J Virol 92.

391. Bertke AS, Patel A, Krause PR. 2007. Herpes simplex virus latency-associated transcript sequence downstream of the promoter influences type-specific reactivation and viral neurotropism. J Virol 81:6605-13.
392. Goswami P, Ives AM, Abbott ARN, Bertke AS. 2022. Stress Hormones Epinephrine and Corticosterone Selectively Reactivate HSV-1 and HSV-2 in Sympathetic and Sensory Neurons. Viruses 14.
393. Sturzl M, Gaus D, Dirks WG, Ganem D, Jochmann R. 2013. Kaposi's sarcoma-derived cell line SLK is not of endothelial origin, but is a contaminant from a known renal carcinoma cell line. Int J Cancer 132:1954-8.
394. Tachibana M, Sugimoto K, Fukushima T, Shinkai Y. 2001. Set domain-containing protein, G9a, is a novel lysine-preferring mammalian histone methyltransferase with hyperactivity and specific selectivity to lysines 9 and 27 of histone H3. J Biol Chem 276:25309-17.
395. Fong KW, Zhao JC, Lu X, Kim J, Piunti A, Shilatifard A, Yu J. 2022. PALI1 promotes tumor growth through competitive recruitment of PRC2 to G9A-target chromatin for dual epigenetic silencing. Mol Cell 82:4611-4626 e7.
396. Cooper S, Dienstbier M, Hassan R, Schermelleh L, Sharif J, Blackledge NP, De Marco V, Elderkin S, Koseki H, Klose R, Heger A, Brockdorff N. 2014. Targeting polycomb to pericentric heterochromatin in embryonic stem cells reveals a role for H2AK119u1 in PRC2 recruitment. Cell Rep 7:1456-1470.
397. Leeb M, Pasini D, Novatchkova M, Jaritz M, Helin K, Wutz A. 2010. Polycomb complexes act redundantly to repress genomic repeats and genes. Genes Dev 24:265-76.
398. Puschendorf M, Terranova R, Boutsma E, Mao X, Isono K, Brykczynska U, Kolb C, Otte AP, Koseki H, Orkin SH, van Lohuizen M, Peters AH. 2008. PRC1 and Suv39h specify parental asymmetry at constitutive heterochromatin in early mouse embryos. Nat Genet 40:411-20.
399. Saksouk N, Barth TK, Ziegler-Birling C, Olova N, Nowak A, Rey E, Mateos-Langerak J, Urbach S, Reik W, Torres-Padilla ME, Imhof A, Dejardin J, Simboeck E. 2014. Redundant mechanisms to form silent chromatin at pericentromeric regions rely on BEND3 and DNA methylation. Mol Cell 56:580-94.
400. Abdouh M, Hanna R, El Hajjar J, Flamier A, Bernier G. 2016. The Polycomb Repressive Complex 1 Protein BMI1 Is Required for Constitutive Heterochromatin Formation and Silencing in Mammalian Somatic Cells. J Biol Chem 291:182-97.
401. Sabbattini P, Sjoberg M, Nikic S, Frangini A, Holmqvist PH, Kunowska N, Carroll T, Brookes E, Arthur SJ, Pombo A, Dillon N. 2014. An H3K9/S10 methyl-phospho switch modulates Polycomb and Pol II binding at repressed genes during differentiation. Mol Biol Cell 25:904-15.
402. Leib DA, Bogard CL, Kosz-Vnenchak M, Hicks KA, Coen DM, Knipe DM, Schaffer PA. 1989. A deletion mutant of the latency-associated transcript of herpes simplex virus type 1 reactivates from the latent state with reduced frequency. J Virol 63:2893-900.
403. Brown JC. 2007. High G+C Content of Herpes Simplex Virus DNA: Proposed Role in Protection Against Retrotransposon Insertion. Open Biochem J 1:33-42.

404. Naik NG, Nguyen TH, Roberts L, Fischer LT, Glickman K, Golas G, Papp B, Toth Z. 2020. Epigenetic factor siRNA screen during primary KSHV infection identifies novel host restriction factors for the lytic cycle of KSHV. PLoS Pathog 16:e1008268.
405. Kim DJ, Khoury-Hanold W, Jain PC, Klein J, Kong Y, Pope SD, Ge W, Medzhitov R, Iwasaki A. 2020. RUNX Binding Sites Are Enriched in Herpesvirus Genomes, and RUNX1 Overexpression Leads to Herpes Simplex Virus 1 Suppression. J Virol 94.
406. Dahlke C, Maul K, Christalla T, Walz N, Schult P, Stocking C, Grundhoff A. 2012. A microRNA encoded by Kaposi sarcoma-associated herpesvirus promotes B-cell expansion in vivo. PLoS One 7:e49435.
407. Wood CD, Carvell T, Gunnell A, Ojeniyi OO, Osborne C, West MJ. 2018. Enhancer Control of MicroRNA miR-155 Expression in Epstein-Barr Virus-Infected B Cells. J Virol 92.
408. Poepsel S, Kasinath V, Nogales E. 2018. Cryo-EM structures of PRC2 simultaneously engaged with two functionally distinct nucleosomes. Nat Struct Mol Biol 25:154-162.
409. Albright ER, Kalejta RF. 2016. Canonical and Variant Forms of Histone H3 Are Deposited onto the Human Cytomegalovirus Genome during Lytic and Latent Infections. J Virol 90:10309-10320.
410. Frasson I, Nadai M, Richter SN. 2019. Conserved G-Quadruplexes Regulate the Immediate Early Promoters of Human Alphaherpesviruses. Molecules 24.
411. Artusi S, Nadai M, Perrone R, Biasolo MA, Palu G, Flamand L, Calistri A, Richter SN. 2015. The Herpes Simplex Virus-1 genome contains multiple clusters of repeated G-quadruplex: Implications for the antiviral activity of a G-quadruplex ligand. Antiviral Res 118:123-31.
412. Biswas B, Kandpal M, Jauhari UK, Vivekanandan P. 2016. Genome-wide analysis of G-quadruplexes in herpesvirus genomes. BMC Genomics 17:949.
413. Dietrich N, Lerdrup M, Landt E, Agrawal-Singh S, Bak M, Tommerup N, Rappsilber J, Sodersten E, Hansen K. 2012. REST-mediated recruitment of polycomb repressor complexes in mammalian cells. PLoS Genet 8:e1002494.
414. Du T, Zhou G, Khan S, Gu H, Roizman B. 2010. Disruption of HDAC/CoREST/REST repressor by dnREST reduces genome silencing and increases virulence of herpes simplex virus. Proc Natl Acad Sci U S A 107:15904-9.
415. Zhou G, Du T, Roizman B. 2013. HSV carrying WT REST establishes latency but reactivates only if the synthesis of REST is suppressed. Proc Natl Acad Sci U S A 110:E498-506.
416. Spivack JG, Fraser NW. 1987. Detection of herpes simplex virus type 1 transcripts during latent infection in mice. J Virol 61:3841-7.
417. Wang Z, Qiu H, He J, Liu L, Xue W, Fox A, Tickner J, Xu J. 2020. The emerging roles of hnRNPK. J Cell Physiol 235:1995-2008.
418. Chen X, Xie R, Gu P, Huang M, Han J, Dong W, Xie W, Wang B, He W, Zhong G, Chen Z, Huang J, Lin T. 2019. Long Noncoding RNA LBCS Inhibits Self-Renewal and Chemoresistance of Bladder Cancer Stem Cells through Epigenetic Silencing of SOX2. Clin Cancer Res 25:1389-1403.
419. Koren S, Walenz BP, Berlin K, Miller JR, Bergman NH, Phillippy AM. 2017. Canu: scalable and accurate long-read assembly via adaptive k-mer weighting and repeat separation. Genome Res 27:722-736.

420. Vaser R, Sovic I, Nagarajan N, Sikic M. 2017. Fast and accurate de novo genome assembly from long uncorrected reads. Genome Res 27:737-746.
421. Li H, Handsaker B, Wysoker A, Fennell T, Ruan J, Homer N, Marth G, Abecasis G, Durbin R, Genome Project Data Processing S. 2009. The Sequence Alignment/Map format and SAMtools. Bioinformatics 25:2078-9.
422. Quinlan AR, Hall IM. 2010. BEDTools: a flexible suite of utilities for comparing genomic features. Bioinformatics 26:841-2.
423. Hahne F, Ivanek R. 2016. Visualizing Genomic Data Using Gviz and Bioconductor. Methods Mol Biol 1418:335-51.
424. Lawrence M, Huber W, Pages H, Aboyoun P, Carlson M, Gentleman R, Morgan MT, Carey VJ. 2013. Software for computing and annotating genomic ranges. PLoS Comput Biol 9:e1003118.
425. Malin SA, Davis BM, Molliver DC. 2007. Production of dissociated sensory neuron cultures and considerations for their use in studying neuronal function and plasticity. Nat Protoc 2:152-60.
426. Riccio RE, Park SJ, Longnecker R, Kopp SJ. 2019. Characterization of Sex Differences in Ocular Herpes Simplex Virus 1 Infection and Herpes Stromal Keratitis Pathogenesis of Wild-Type and Herpesvirus Entry Mediator Knockout Mice. mSphere 4.
427. D GH, Kelley DR, Tenen D, Bernstein B, Rinn JL. 2016. Widespread RNA binding by chromatin-associated proteins. Genome Biol 17:28.
428. Stewart SA, Dykxhoorn DM, Palliser D, Mizuno H, Yu EY, An DS, Sabatini DM, Chen IS, Hahn WC, Sharp PA, Weinberg RA, Novina CD. 2003. Lentivirus-delivered stable gene silencing by RNAi in primary cells. RNA 9:493-501.
429. McFarlane S, Orr A, Roberts APE, Conn KL, Iliev V, Loney C, da Silva Filipe A, Smollett K, Gu Q, Robertson N, Adams PD, Rai TS, Boutell C. 2019. The histone chaperone HIRA promotes the induction of host innate immune defences in response to HSV-1 infection. PLoS Pathog 15:e1007667.
430. Alandijany T, Roberts APE, Conn KL, Loney C, McFarlane S, Orr A, Boutell C. 2018. Distinct temporal roles for the promyelocytic leukaemia (PML) protein in the sequential regulation of intracellular host immunity to HSV-1 infection. PLoS Pathog 14:e1006769.
431. Burman LG, Mauro VP. 2012. Analysis of rRNA processing and translation in mammalian cells using a synthetic 18S rRNA expression system. Nucleic Acids Res 40:8085-98.